



This work is protected by copyright and other intellectual property rights and duplication or sale of all or part is not permitted, except that material may be duplicated by you for research, private study, criticism/review or educational purposes. Electronic or print copies are for your own personal, non-commercial use and shall not be passed to any other individual. No quotation may be published without proper acknowledgement. For any other use, or to quote extensively from the work, permission must be obtained from the copyright holder/s.

## CHAPTER 4. MINERALOGY AND PHASE CHEMISTRY OF THE BASIC AND INTERMEDIATE IGNEOUS ROCKS

### 4.1. INTRODUCTION

In Chapters 2 and 3 detailed descriptions of the various formations of the Fishguard Volcanic Group were presented. This Chapter will deal with more specific aspects of the minerals present within the volcanic and intrusive rocks, paying particular attention to their chemical compositions. However, only the basic and intermediate rocks will be discussed here, as the widest range of minerals and mineral compositions are found within these rocks. Both primary igneous and secondary alteration phases are present within these basic and intermediate rocks and they will be dealt with separately below. The compositions of minerals analysed are listed in Appendix 2, along with a recalculation of atomic proportions. The chemical analyses of the minerals listed in Appendix 2 were obtained using a Geoscan Mark II electron-microprobe. Further information on this technique is included at the beginning of the Appendix.

### 4.2. DESCRIPTION OF THE PRIMARY IGNEOUS PHASES

From petrographical examinations and a consideration of whole-rock major and trace element geochemistry, it is possible to deduce that the original mineralogy of the basic and intermediate igneous rocks described here was dominated by plagioclase feldspar and clinopyroxene with minor ore which becomes abundant in the more fractionated rocks, and possibly olivine within some of the least fractionated rocks. However, this primary mineralogy has subsequently been affected by various alteration processes. The only primary phase which is generally unaffected by such



alteration is clinopyroxene, although even this mineral has been locally altered, such as in the Llech Dafad Intrusion (Fig. 5 ), where it shows marginal replacement by an amphibole of hornblende composition.

Clinopyroxene is also sometimes replaced by chlorite in a number of lavas, for example in sample 422.

#### 4.2.1. CLINOPYROXENE

Clinopyroxene is found within almost all of the basic igneous rocks collected and, since it is largely unaffected by alteration, has proved suitable for a more detailed study. This has largely taken the form of an investigation into the morphology and chemistry of clinopyroxene in relation to the cooling history of the rock in question. This naturally depends upon whether the magma reached the surface and erupted as a lava flow, or whether it failed to reach the surface, now being seen as a high level intrusion. Not only are the intrusions such as Garn Fawr, Llech Dafad, and Llanwnda (Fig. 5 ) examples of high level sheets, but so are the intrusions present within the volcanic pile of the Fishguard Volcanic Group. These latter sheets intruded close to the sea-water rock interface (see Chapter 2).

When the magma intruded at a high level, cooling rates were naturally slower than for the surface lava flows and it is this contrasted history which produces much of the morphological and chemical variation which has been observed. However, interesting compositions and textural forms are seen in a number of thick sheets which intruded the volcanic pile. All these forms and chemical variations are discussed below.

##### 4.2.1.1. DESCRIPTION OF CLINOPYROXENES FROM BASIC INTRUSIONS WITHIN THE OLDER SEDIMENTARY STRATA

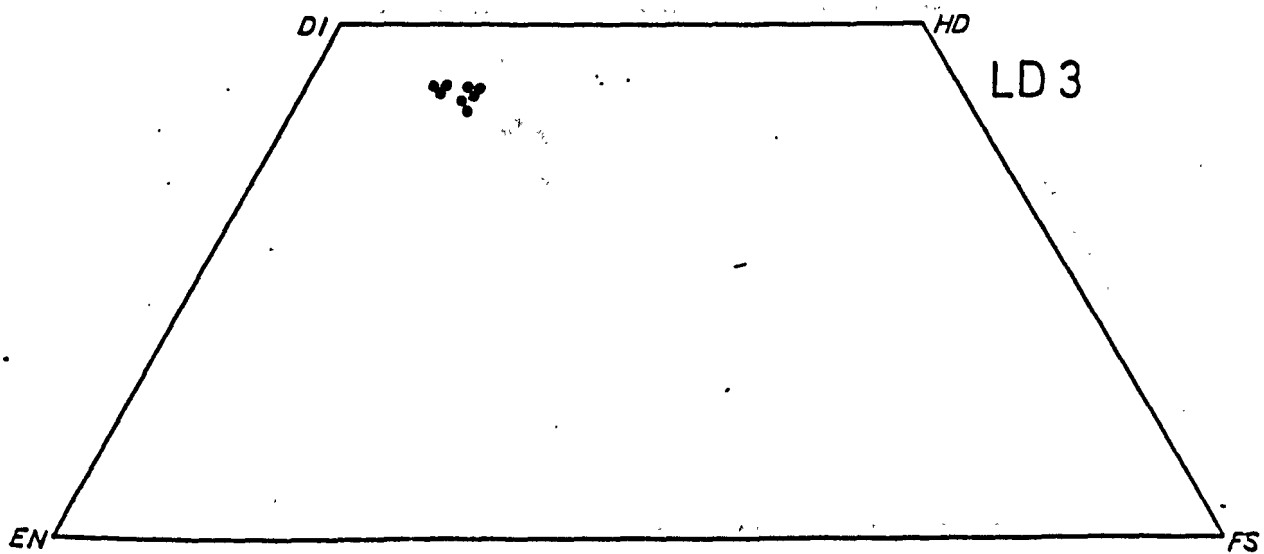
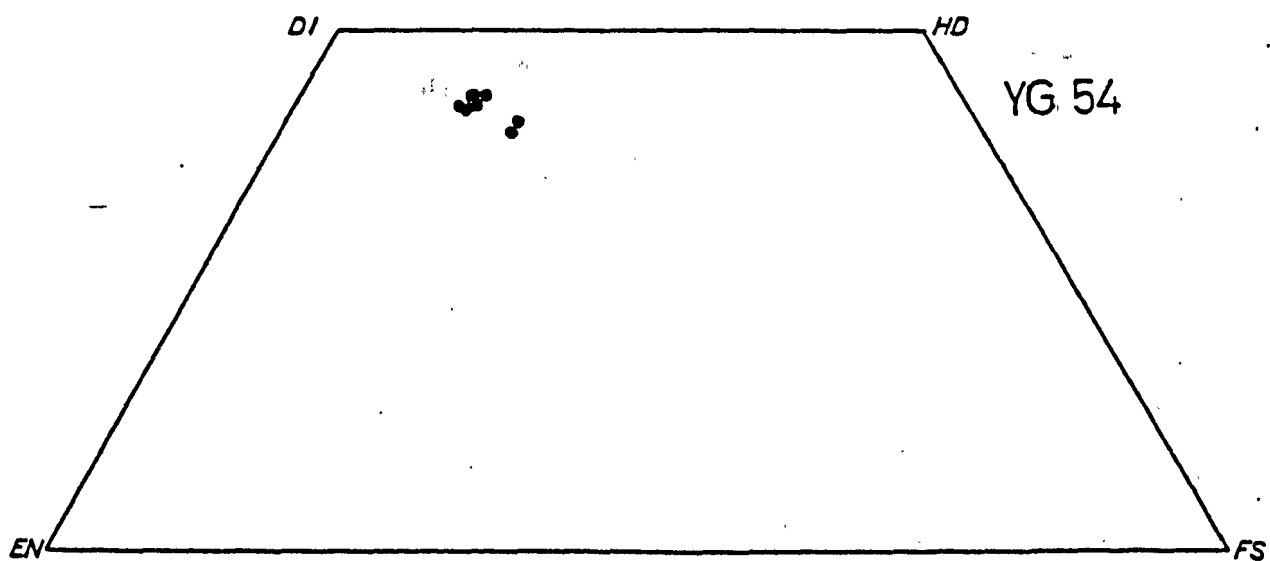
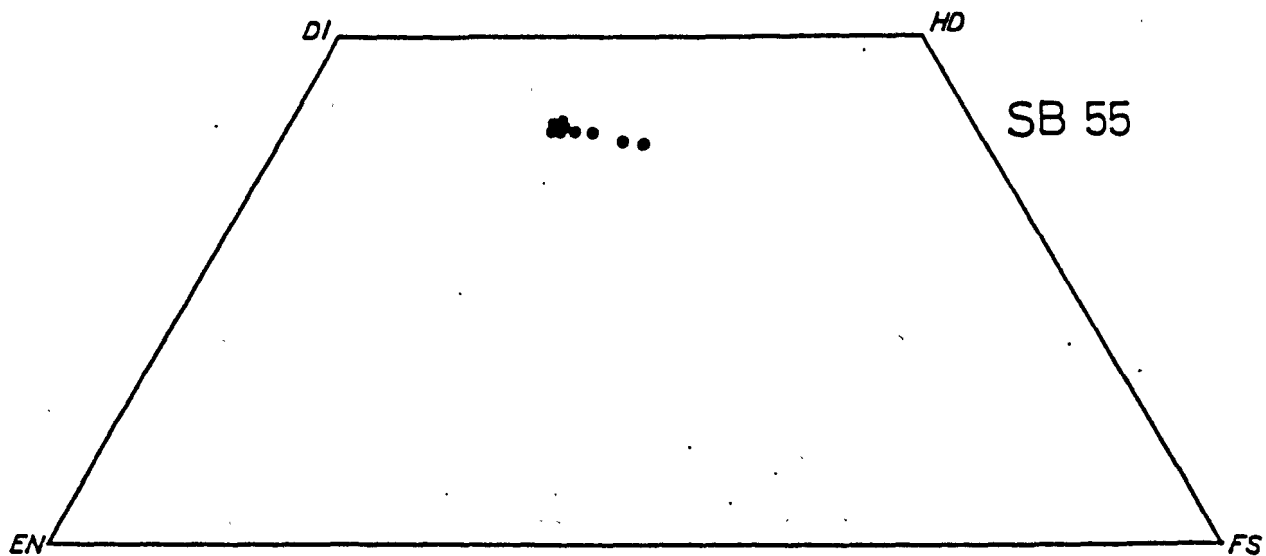
This section deals with the nature of clinopyroxenes from

intrusions which occur within the sedimentary strata which underlie the Fishguard Volcanic Group.

As discussed earlier (S.2.2.2.2.) and by Rowbotham and Bevins (1978), clinopyroxenes present within the intrusive basic igneous rocks show a variety of textural forms. Predominantly, they occur as large, colourless, chemically homogenous, irregular crystals, ophitically enclosing plagioclase crystals (Fig. 44). In other cases, as for example within parts of the Llanwnda Gabbro, they occur as discrete, colourless, euhedral, chemically zoned crystals, which commonly exhibit twinning (Fig. 41). Transitions between these two textural types may also be found, with an ophitic texture changing laterally into areas characterized by discrete isolated crystals of plagioclase and clinopyroxene, within the area of a single thin section. Small clusters of clinopyroxene are occasionally observed and may represent the early separation and accumulation of clinopyroxene from the melt. Alternatively, the accumulations may have resulted from synneusis.

Within this group, samples from the Llanwnda (LG4, LG7, LG6), Y Garn (YG54), Llech Dafad (LD3) and Treseissylt (SB55) intrusions (Fig. 5) have been analysed. The chemical compositions of these samples in the Di-Hd-En-Fs quadrilateral diagram is illustrated in Figures 141a - f. Figure 142 shows the overall variation displayed by these analyses. Only a limited chemical range is generally observed between clinopyroxene crystals within individual samples from each intrusion. However, individual crystals may show considerable variation from their core to their rim. The rims are generally enriched in iron in comparison with the core and a corresponding depletion in magnesium and calcium is recorded. This variation is well displayed in analyses from samples LG6 and LG7 (from the Llanwnda Gabbro) reflecting the build up

FIG. 141a to f. Composition of clinopyroxenes in the Di-Hd-En-Fs quadrilateral from samples collected from intrusions of the Fishguard area.



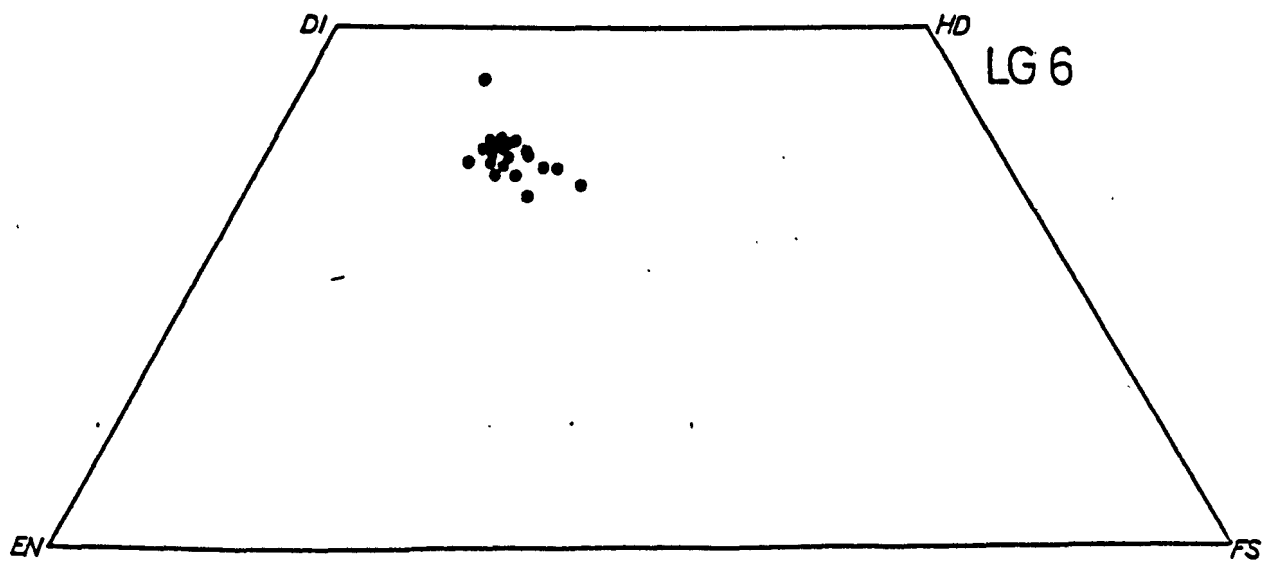
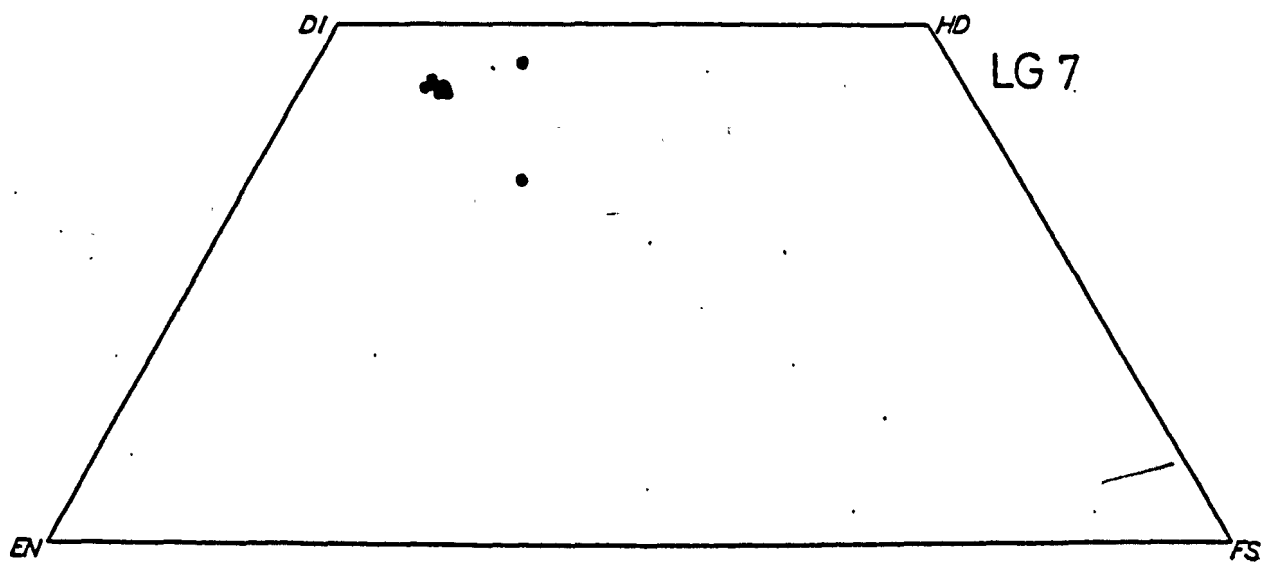
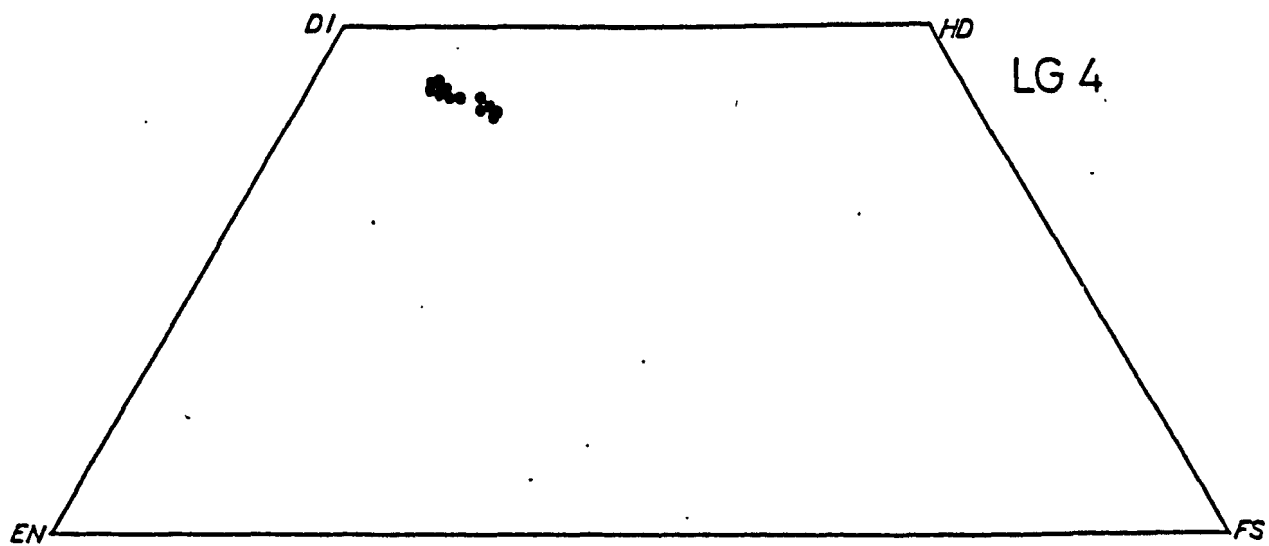
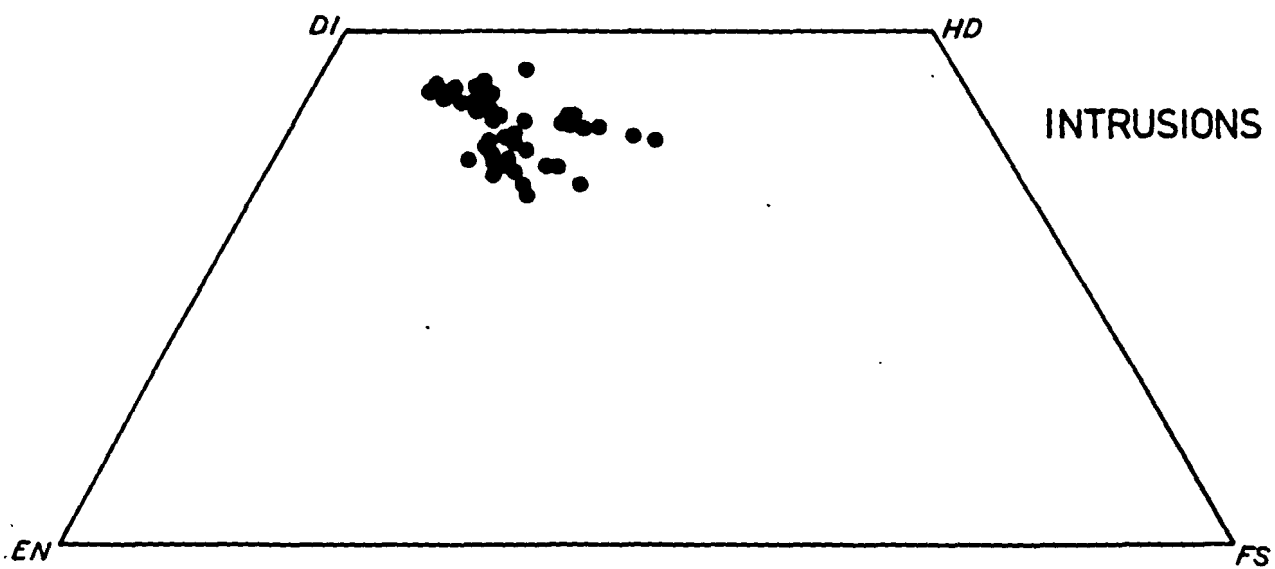




FIG. 142. Overall variation shown by clinopyroxenes within intrusions from the Fishguard area.



of iron in the residual liquid. The overall chemical variation displayed between samples is also one of iron enrichment. The most iron-enriched clinopyroxenes are found within sample LG6.

It is considered likely that three major variation trends in clinopyroxene compositions are exhibited by basic magmas during equilibrium crystallization:

- (i) the calcic augite-calcic ferroaugite-hedenbergite trend, as seen in the Shiant Isles sill (Gibb, 1973) and probably typical of moderately undersaturated magmas;
- (ii) the augite-ferroaugite trend, as seen in tholeiitic intrusions, such as Skaergaard (Wager and Brown, 1967); and
- (iii) the salite-ferrosalite-aegirine trend, displayed by strongly undersaturated alkaline magmas, as, for example, the Shonkin Sag Laccolith (Nash and Wilkinson, 1970).

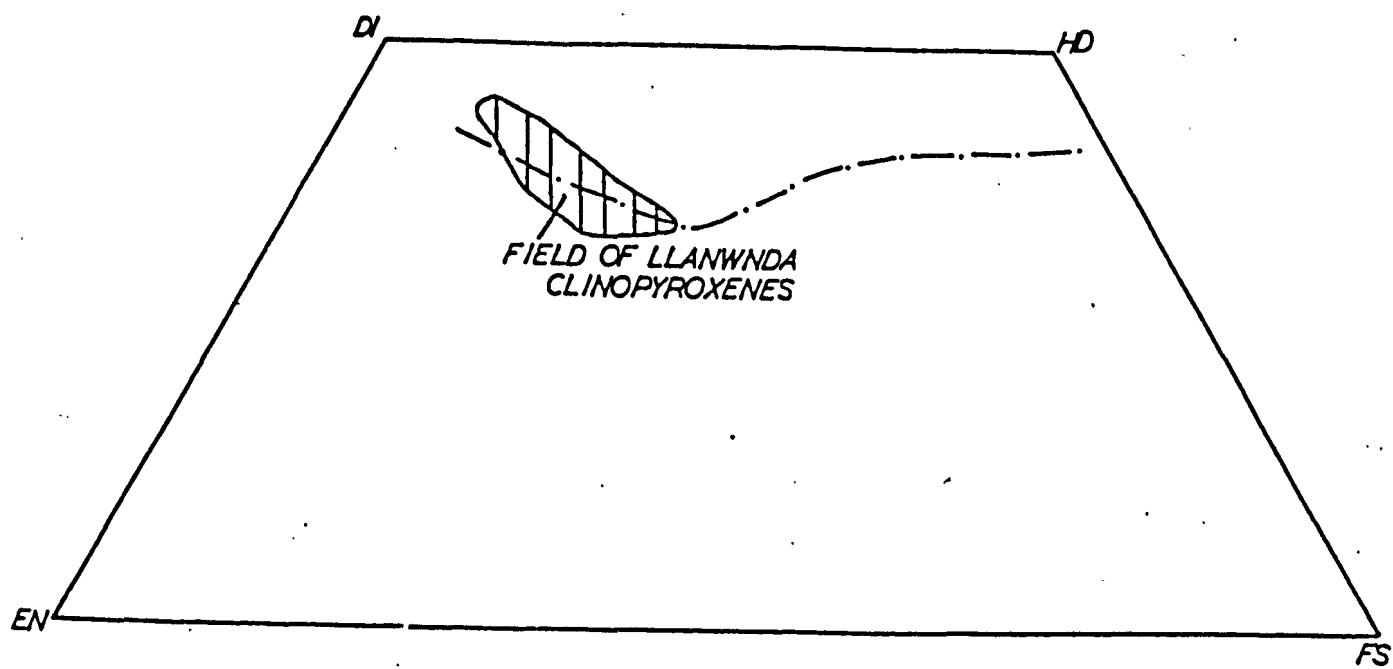
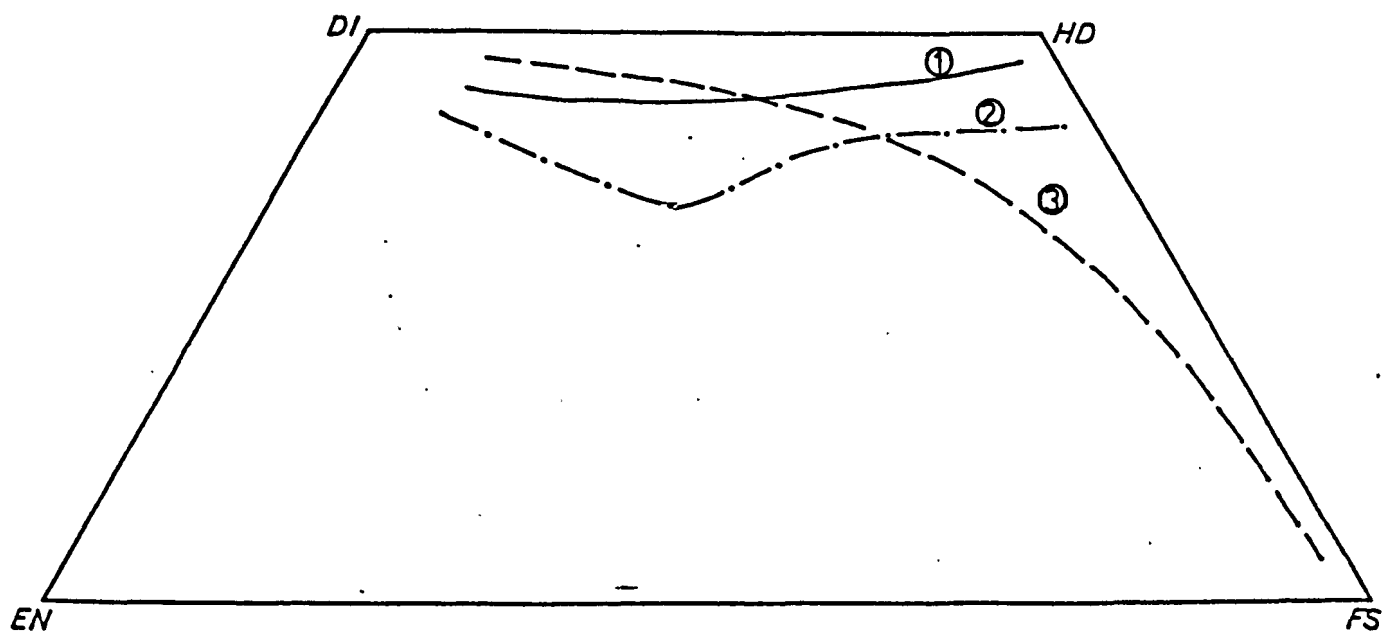
These three trends are illustrated in Figure 143. In the case of the Skaergaard example, only the calcium-rich clinopyroxenes have been plotted.

Figure 144 shows the Skaergaard tholeiitic trend along with that displayed by the Llanwnda intrusion (the Llanwnda samples were collected in a vertical sequence through the intrusion). A position close to the Skaergaard trend is seen for the Llanwnda analyses, with a relatively rapid iron enrichment. These analyses clearly reflect a near equilibrium crystallization history for the Pembrokeshire analyses, which offers marked contrast with the evidence obtained from the lavas, as outlined below (Section 4.2.1.2.).



FIG. 143. Three variation trends of clinopyroxenes exhibited by basic magmas. See text for description of these trends.

FIG. 144. Variation displayed by clinopyroxenes within the Llanwnda Intrusion compared to that within the Skaergaard Intrusion.



Kushiro (1960) and Le Bas (1962) have attempted to relate the concentration of  $Al^{total}$  and Ti in clinopyroxenes to the nature of the parental magma. However, Gibb (1973) argued that this correlation cannot be justified. He showed how Al and Ti contents of the clinopyroxenes vary with differentiation, whilst Barberi et al. (1971) argued that the presence of tholeiitic-type clinopyroxenes in rocks of a mildly alkalic nature from the Afar region was related to the physical conditions of crystallization, with  $fO_2$  (oxygen fugacity) being particularly important. However, when the North Pembrokeshire intrusions are plotted on a 'Le Bas-type' diagram (Fig.158), they plot within the tholeiitic field, which is in agreement with whole-rock major and trace element chemical evidence, as outlined below (S.5.5.). Thus it would appear that in this particular case, that is equilibrium crystallization of a tholeiitic melt, the divisions suggested by Le Bas (1962) may be justified.

Clinopyroxenes were analysed from rocks showing varying degrees of fractionation and with the possible change of melt composition, a sympathetic change in clinopyroxene compositions may also be recognized. This aids in assessing the petrogenetic history of the rocks.

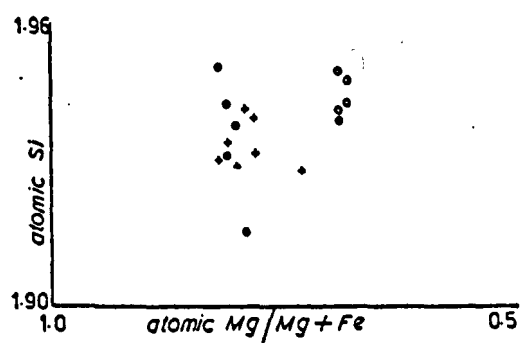
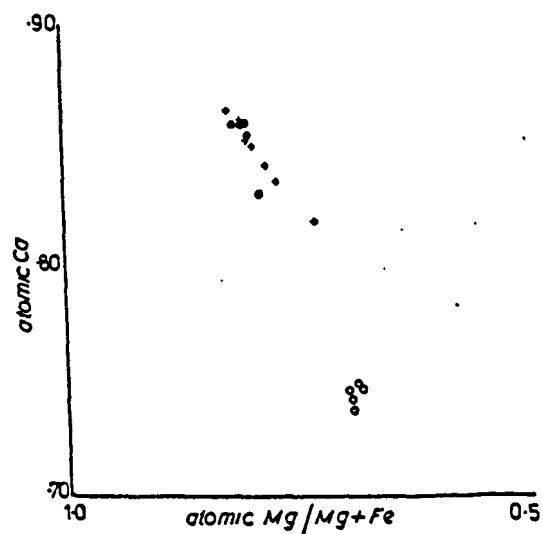
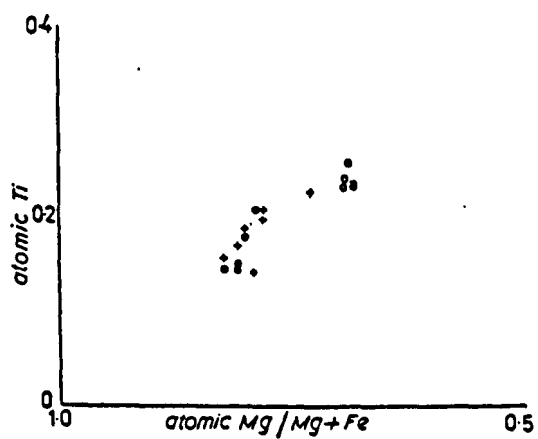
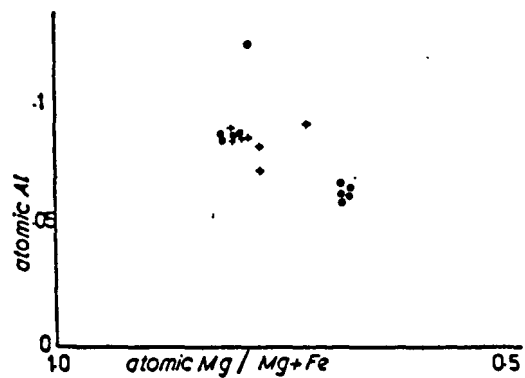
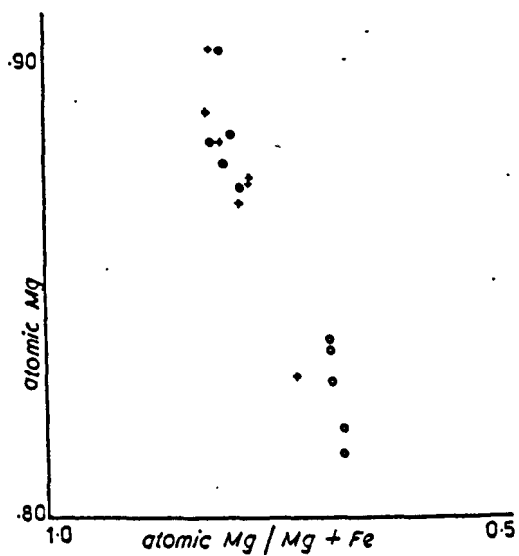
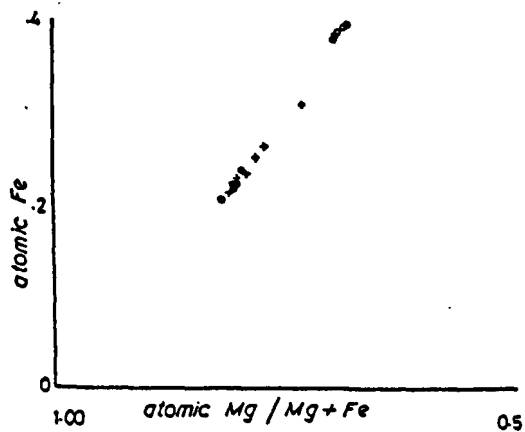
Samples LG4, LG7 and LG6 (from the Llanwnda gabbro) were analysed and appear to display a range of compositions, with LG6 being the most iron-enriched. This may suggest that LG6 is more fractionated than LG4 and LG7, a contention supported by the whole-rock chemistry. An analysis of LG6 is listed in Appendix 1 and shows high whole-rock concentrations of  $SiO_2$  (about 51%), as well as relatively high contents of incompatible elements. Within the clinopyroxene analyses, an overall increase in atomic Fe, Ti, Na, and Mn is seen from LG7, through LG4, to LG6, with a concomitant decrease in the concentrations of Ca, Al, and Mg. These

variations (except for Na and Mn) are illustrated in Figures 145a - f where the elements are plotted against an index of differentiation (atomic  $Mg/(Mg + Fe)$ ). The decrease in Ca and Mg probably monitor the removal of clinopyroxene from the melt, whilst increases in the contents of Fe, Mn, and Ti in the clinopyroxenes reflect increased concentrations of these elements in the melt. This probably results from the fact that only minor amounts of ore were being precipitated. The variations described here are typical of liquids of tholeiitic affinities.

Analyses from samples YG54 (Y Garn) and SB55 (Treseissyllt) show significant differences to those samples described above. YG54 appears to have higher  $Al^{cpx}$  and lower  $Si^{cpx}$  contents. This probably results from the fact that the melt from which the clinopyroxenes crystallized was higher in aluminium compared with the liquid from which clinopyroxenes of LG7 and LG4 crystallized. However, due to the lack of available whole-rock analyses this cannot be verified. Analyses from LD3 (Llech Dafad) appear similar in most respects to those of LG4 and LG7.

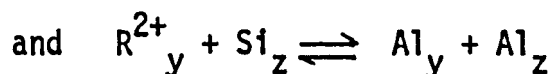
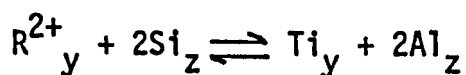
SB55 contains clinopyroxenes which have high Si, moderately high Fe and Mn, and low Mg, Al, and Ti. These concentrations are thought to be due to the fact that the liquid from which these clinopyroxenes crystallized was a fractionated liquid which had undergone removal of a small amount of an iron-titanium oxide, along with the removal of significant amounts of plagioclase and clinopyroxene. These suggestions are supported by major and trace element whole-rock chemistry which confirm the fractionated nature of the liquid (see analysis of sample SB55, Appendix 1).

FIGS. 145a to f. Variations in atomic proportions of elements plotted against an index of differentiation (atomic  $\text{Mg}/\text{Mg} + \text{Fe}$ ) for clinopyroxenes from the Llanwnda Intrusion.



It is possible, from the variations displayed within these clinopyroxenes, to make some deductions regarding the nature of the elemental substitutions which were operative.

Figure 146 illustrates a plot of  $Al^Z$  against Ti (where  $Al^Z$  represents tetrahedral aluminium) for the Llanwnda clinopyroxene analyses. In this diagram it can be seen that the ratio of  $Al^Z$  : Ti changes from approximately 4 : 1 in LG4 and LG7 to 3 : 1 and even 2 : 1 in LG6. Al in the Z sites and Ti in the Y sites are thought to enter clinopyroxenes by the following coupled substitutions:-



where  $y = M(1)$  [octahedral sites]

$z = T$  [tetrahedral sites]

$x = M(2)$  [6-8 coordination sites]

and  $R^{2+}$  represents a divalent cation.

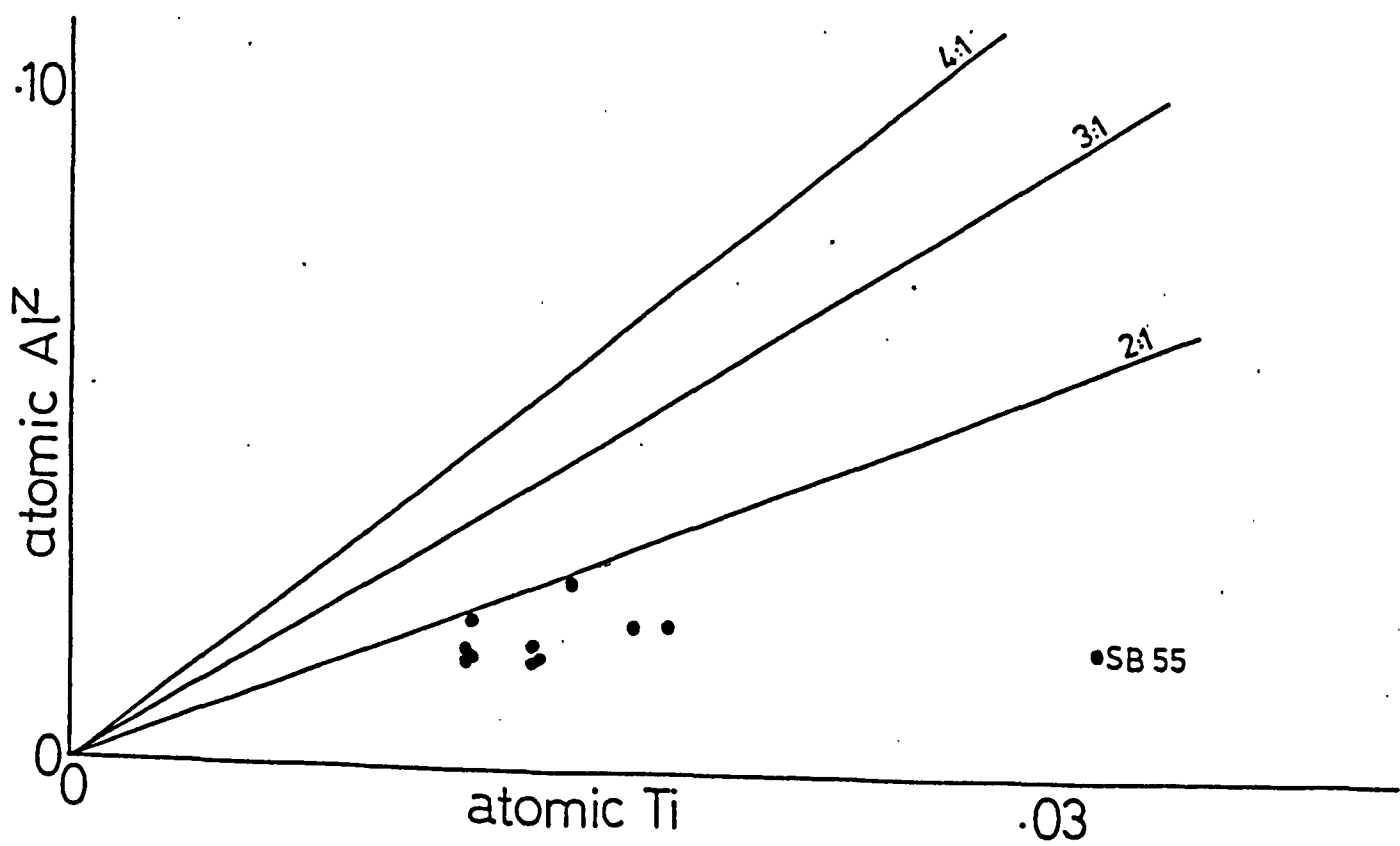
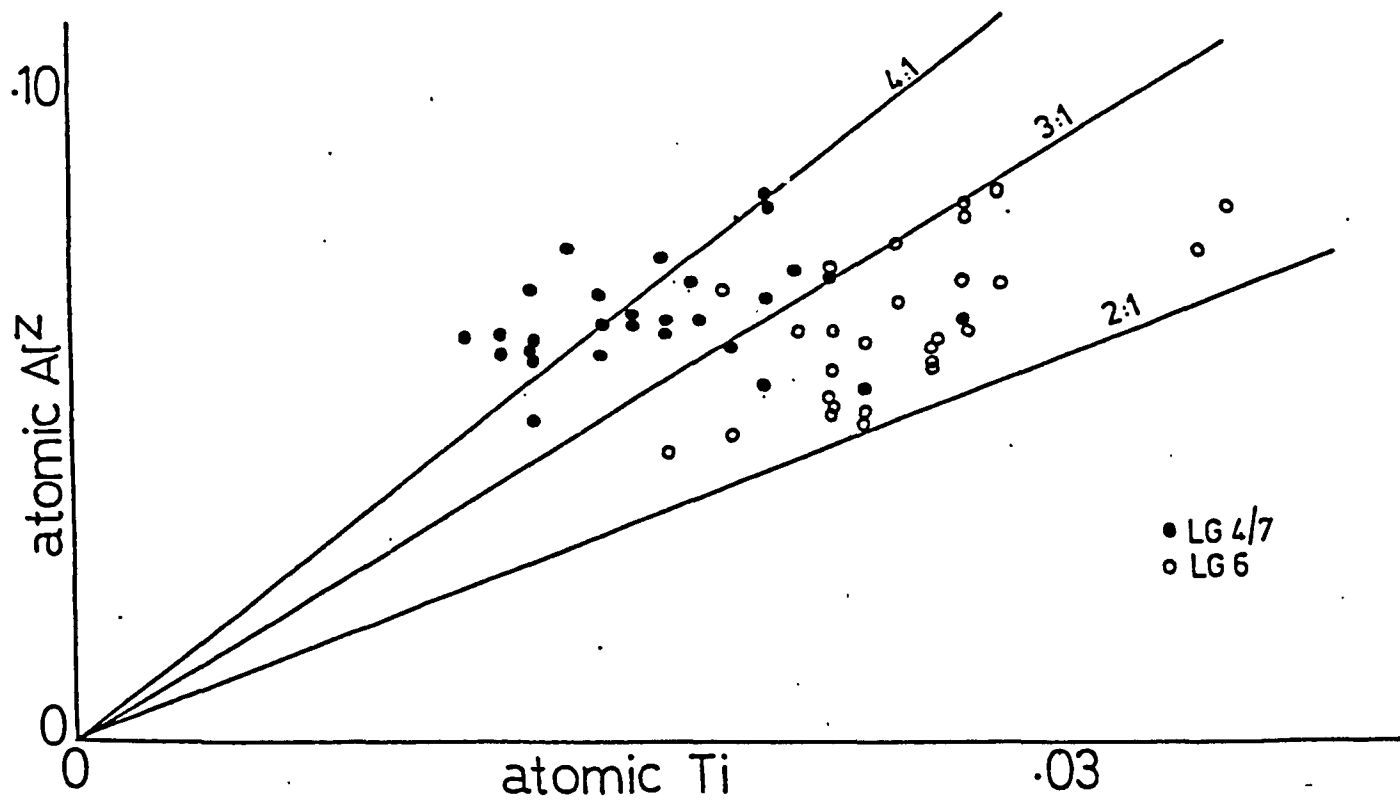
In clinopyroxenes, the following site occupancy normally occurs

T or Z [tetrahedral]	M(1) [octahedral]	M(2) [6-8 coord.]
Si	Al	Mg
Al	Fe <sup>3+</sup>	Fe <sup>2+</sup>
	Cr <sup>3+</sup>	Mn
	Ti <sup>4+</sup>	Ca
	Mg	Na
	Fe <sup>2+</sup>	
	Mn	

FIG. 146. Atomic  $Al^Z$  vs Ti for clinopyroxenes from samples LG4, LG7 ..  
and LG6.

FIG. 147. Atomic  $Al^Z$  vs Ti for clinopyroxenes from sample SB55.





In LG4 and LG7 clinopyroxenes, it is thought that both of these substitutions are important, whilst in LG6, the former is dominant. As a result,  $Al^{2+}$  contents are constant, whilst Ti concentration increases. Thus LG4 and LG7 clinopyroxenes contain significant amounts of the molecules  $R^{2+}AlSiAlO_6$  (Tschermak's molecule) and  $R^{2+}TiSiAlO_6$ , whilst the clinopyroxenes from LG6 only contain the latter. Once again this is related to changing liquid compositions, with Ti increasing in concentration and Al declining due to the precipitation of plagioclase. SB55 shows very low concentrations of Ti and  $Al^{2+}$ , as would be anticipated from the evidence outlined above. This is illustrated in Figure 147, where the low Al contents are reflected by ratios of  $Al^{2+} : Ti$  in less than 2 : 1.

Compositional zoning is present within a number of rocks examined from the basic intrusions. It is particularly well developed in euhedral crystals in sample LG7 from the Llanwnda Gabbro. The most pronounced chemical variations identified are a rise in iron content and a decrease in magnesium from the core to the rim of individual crystals. Slight variations are also recorded for calcium and aluminium, which both decrease from core to rim, and in titanium and silica, which increase from core to rim. These variations correspond to those recorded between individual samples of the intrusions analysed, and is no doubt a response to changing liquid composition. Little or no zoning is observed within the large, ophitic clinopyroxenes from samples LD3 or YG54. Simple twinning is common within the discrete, euhedral crystals of LG4 and LG7. It occurs on both (100) and (001) planes.

#### 4.2.1.2. DESCRIPTION OF CLINOPYROXENES FROM PILLOWED LAVAS

Six pillow lava samples were selected for a study of their clinopyroxene compositions and were chosen in order to examine a maximum range of clinopyroxene compositions. Sample locations for the analysed specimens are recorded in Appendix 3. Two groups are clearly discernible within the population of analyses:

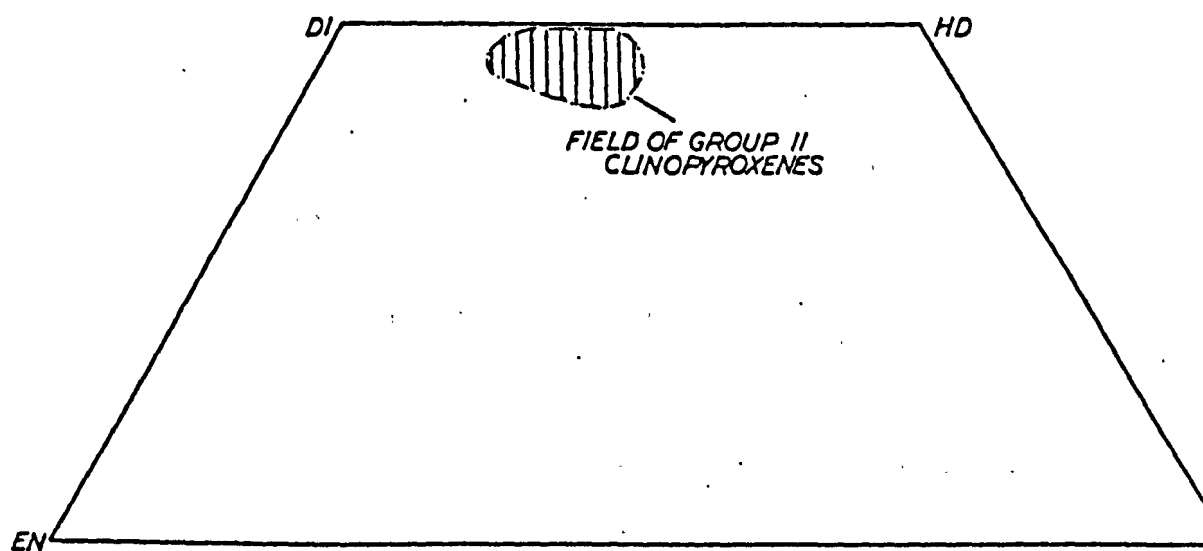
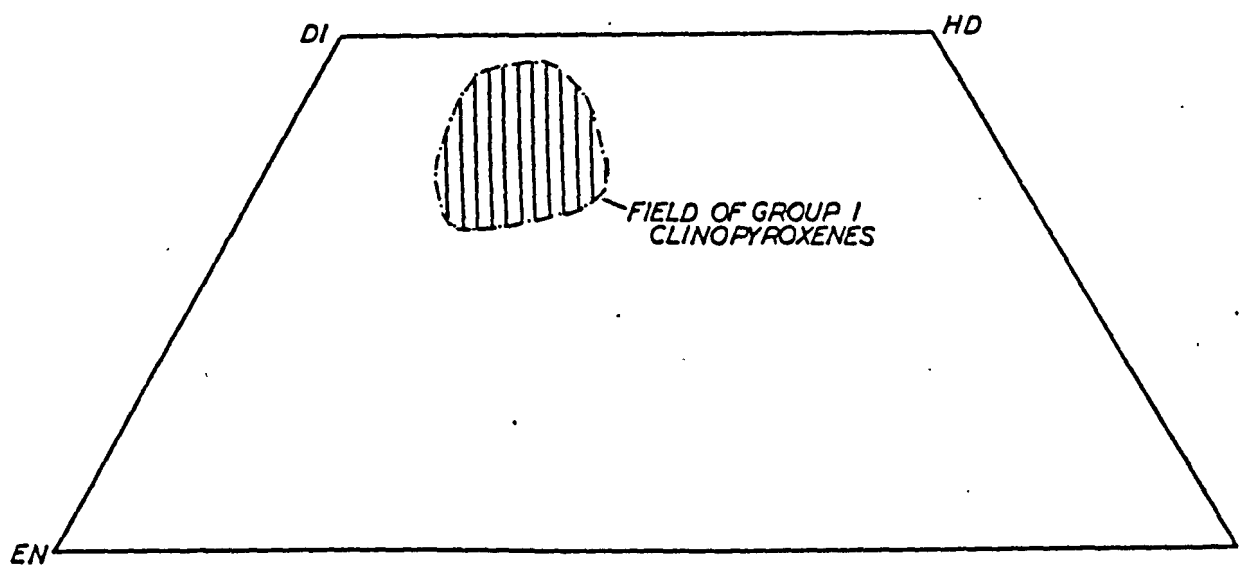
- (i) A group showing a wide scatter of clinopyroxene compositions, falling principally within the augite field in the Di-Hd-En-Fs quadrilateral (Fig.148)(following the classification of Poldervaart and Hess, 1951). They occur as colourless to slightly coloured phenocrysts and groundmass crystals and comprise samples SBC5, SBC1, SB23, SB13, and SB31; and
- (ii) A group which shows a limited range of compositions with all the analyses falling within the salite field and plotting close to the Di-Hd tie line (Fig.149). These clinopyroxenes occur as strongly-coloured crystals in samples SB60 and SB63, and they exhibit a variety of textures, as described below.

##### (i) Group 1 clinopyroxenes

The clinopyroxenes of this group are colourless to slightly coloured crystals present as microphenocrysts, phenocrysts and groundmass crystals. Euhedral to subhedral, zoned, microphenocrysts and phenocrysts are abundant within samples SBC5 and SB31 and are set within a fine-grained groundmass composed of spherulitic intergrowths of clinopyroxene and plagioclase. Sample SBC1 is aphyric, wholly composed of a very

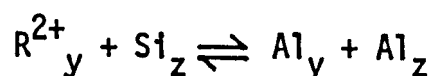
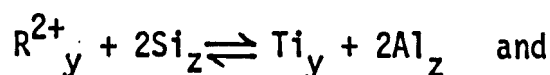
FIG. 148. Field of variation shown by clinopyroxenes of group 1.

FIG. 149. Field of variation shown by clinopyroxenes of group 11.



fine-grained intergrowth of plagioclase and clinopyroxene. SB23 is coarser grained than all the other group 1 samples, with an intersertal texture. SB13 contains rare phenocrysts of clinopyroxene, set within a fine-grained groundmass composed essentially of plagioclase feldspar.

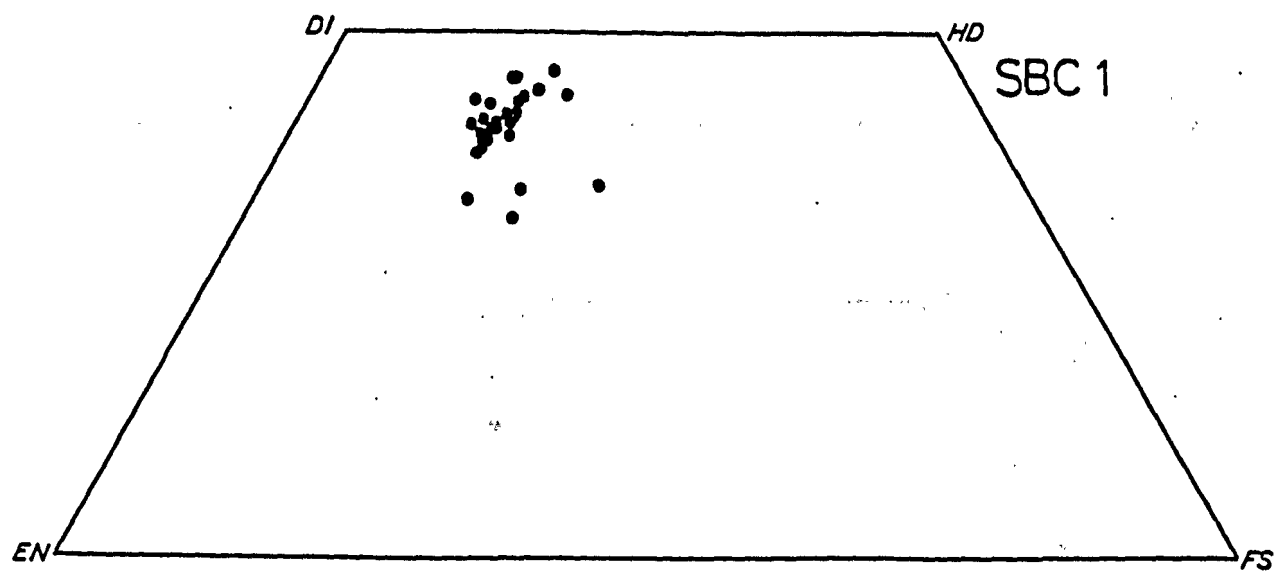
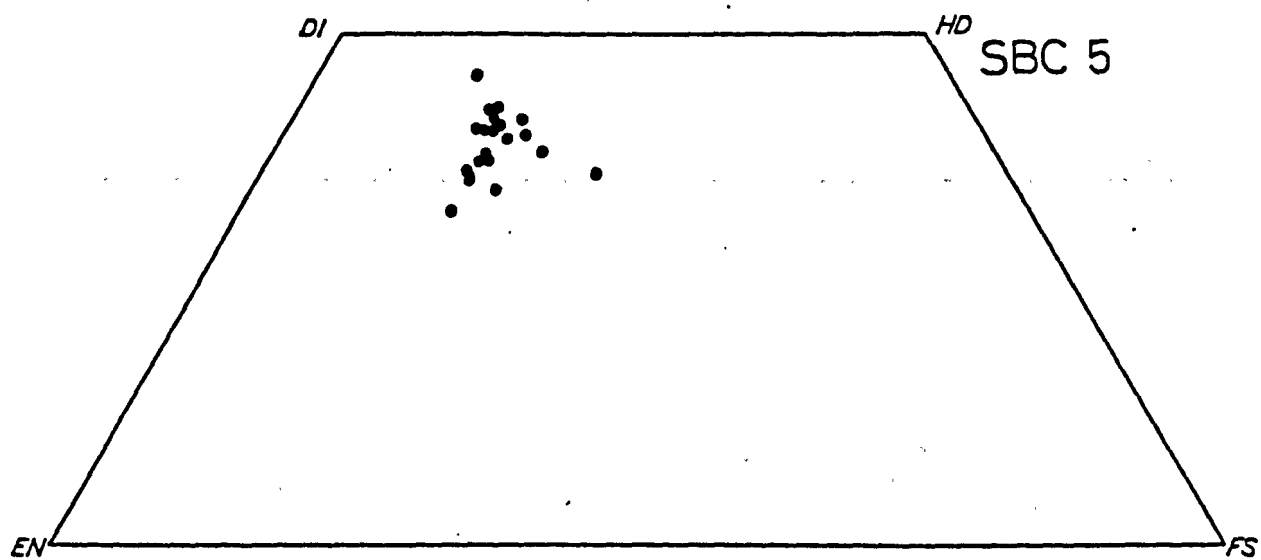
Figures 150 to e show these clinopyroxene analyses plotted on the Di-Hd-En-Fs quadrilateral diagram and illustrate the wide variation in Mg-Fe-Ca solid solution present within each rock sample. However, little variation between samples exists, despite the possible variation in extent of differentiation between these samples (see Appendix 1). This group of samples contain higher  $Al^{cpx}$  and  $Ti^{cpx}$  contents than the intrusive samples described above, whilst  $Si^{cpx}$  contents are slightly lower.  $Ca^{cpx}$ ,  $Mg^{cpx}$ , and  $Fe^{cpx}$  contents, as stated above, are highly variable. An  $Al^{IV}$  vs Ti ratio of approximately 3 : 1 is typical for these clinopyroxenes (Fig. 151) and suggests, once again, the presence of octahedral aluminium in Y sites, indicating substitutions of the form outlined above, i.e.



producing high contents of the molecules  $R^{2+}TiAl_2O_6$  and  $R^{2+}Al_2SiO_6$ .

The increased amount of Al, substituting for Si in the z sites accounts for the decreased  $Si^{cpx}$  contents of these samples. Varying degrees of the above substitutions between crystals within individual samples appear to be present, resulting in a variation trend parallel to the Di-En tie line (see Fig. 150) and is due to an interrelationship between Ti and Mg. A second variation identified results from the iron-enrichment of rims of microphenocrysts.  $Fe^{2+}$  and  $Mn^{2+}$  replace  $Mg^{2+}$  in

FIGS. 150a to e. Composition of clinopyroxenes from samples SBC5, SBC1, SB31, SB23, and SB13 plotted on the Di-Hd-En-Fs quadrilateral.





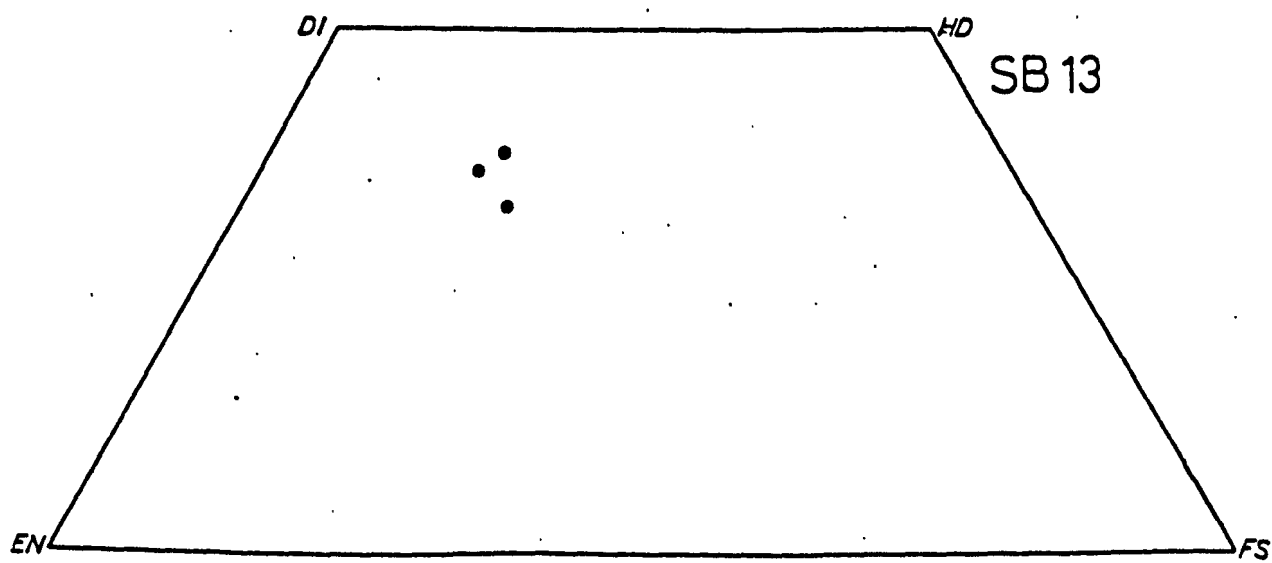
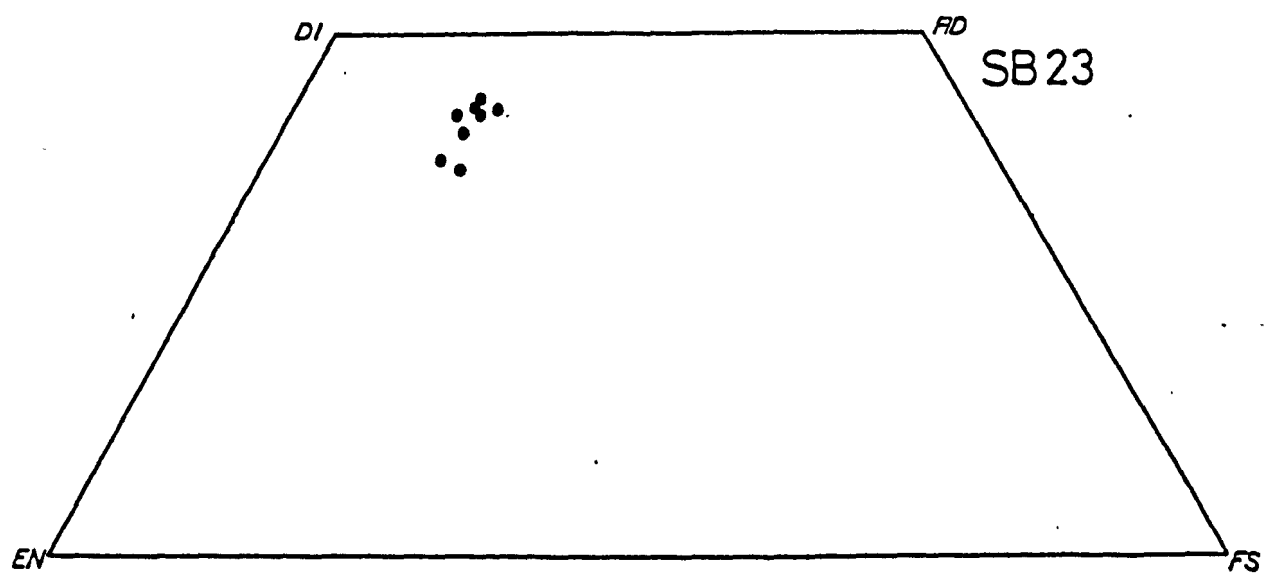
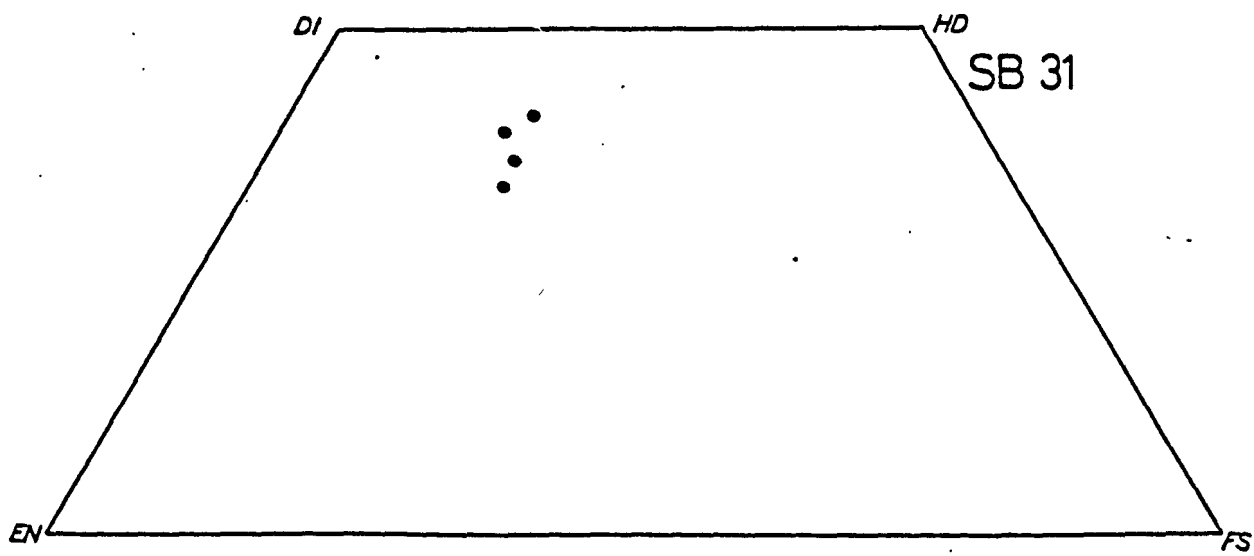
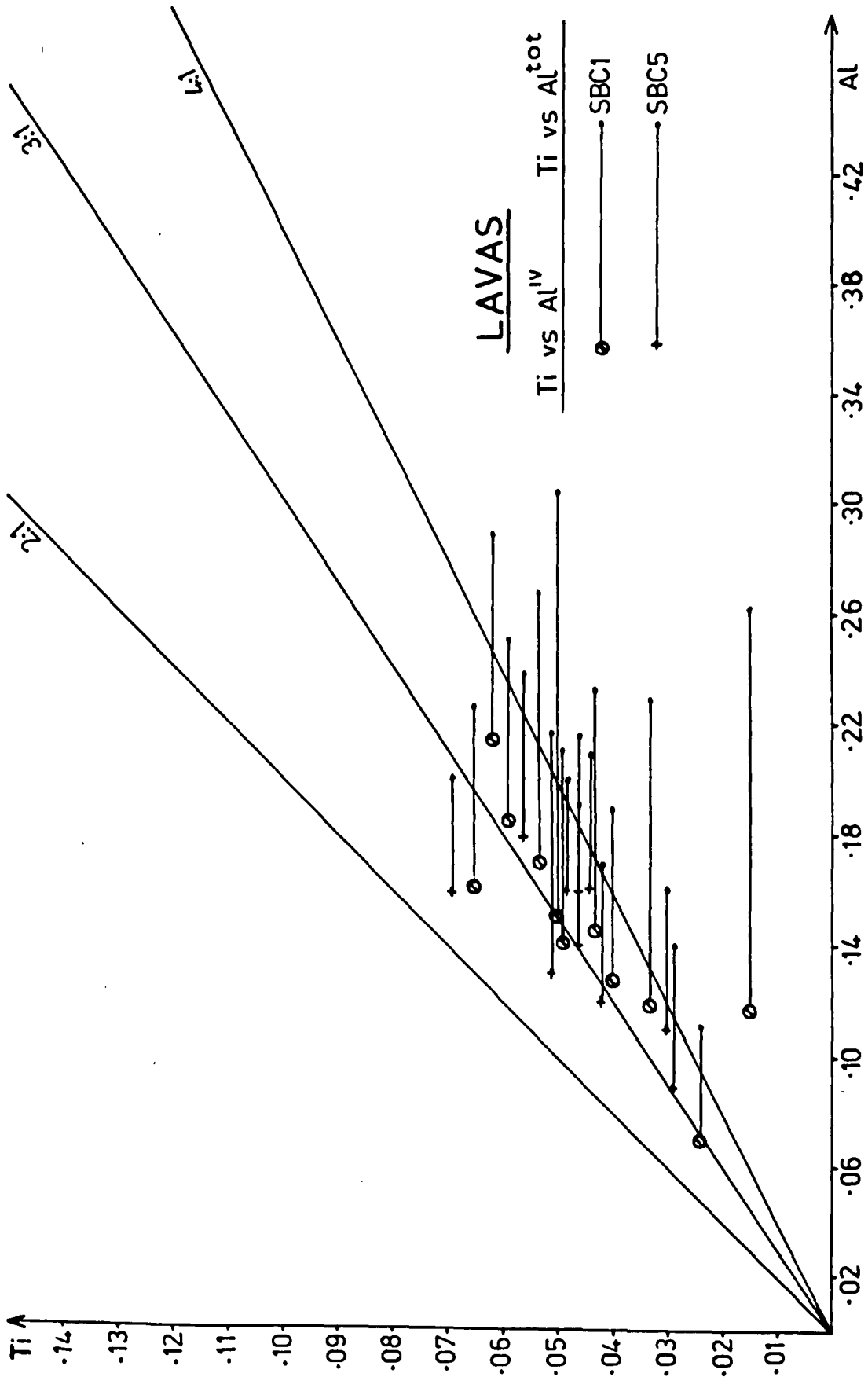
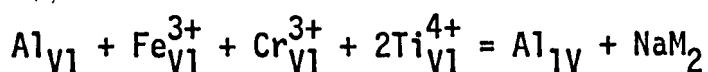


FIG. 151. Atomic Al vs Ti for clinopyroxenes from samples SBC1 and SBC5.



the y sites and consequently a trend towards the Fs corner of the quadrilateral is produced.

Minor amounts of Na are found within clinopyroxenes of this group, being present in the x sites, substituting for Ca and forming a small proportion of possibly the jadeite molecule ( $\text{NaAlSi}_2\text{O}_6$ ) or more probably the aegirine molecule ( $\text{NaFe}^{3+}\text{Si}_2\text{O}_6$ ). However, the quantity of  $\text{Fe}^{3+}$  present within these crystals cannot be directly obtained from microprobe analyses. Papike et al. (1974) suggested that a rough estimate of  $\text{Fe}^{3+}$  may be made by solving the following equation:



This method of  $\text{Fe}^{3+}$  determination assumes:

- (i) Fe is the only element with a variable valency state;
- (ii) each analysis is 'good' and complete, (see below); and
- (iii) stoichiometry requirements are met.

The tests for superior analyses are:

- (i) The sum of  $\text{Si} + \text{Al}^{\text{IV}}$  must =  $2 \pm 0.02$  atoms per 6 oxygens.
- (ii) The octahedral cations ( $\text{Mn}, \text{Fe}^{2+}, \text{Fe}^{3+}, \text{Mg}, \text{Ti}, \text{Cr}, \text{Al}$ ) must sum to  $>0.98$ .
- (iii) Excess octahedral cations (those greater than 1.0 atoms necessary to fill the M1 site) plus calcium must be less than 1.02.
- (iv) The M2 site occupancy must =  $1.0 \pm 0.02$ .
- (v) The charge balance equation must be balanced to 0.02 or less of a charge.

From this it can be clearly seen that high Na contents are correlated with high  $\text{Fe}^{3+}$ , both probably present within the acmite molecule. The higher  $\text{Fe}^{3+}$  contents of these clinopyroxenes could be related to the fact that this group comprises analyses from pillow lavas erupted subaqueously, where the  $\text{Fe}^{3+}/\text{Fe}^{2+}$  ratio of the liquid will be higher than in the case of the intrusions.

(ii) Group 2 clinopyroxenes

The second group of clinopyroxenes, represented by analyses from samples SB60 and SB63, show a very limited compositional range, with all analyses falling close to the Di-Hd tie line on the pyroxene quadrilateral diagram (Fig.152). Titanium contents of these pyroxenes are much higher than within the pyroxenes described above, with up to 4wt%  $\text{TiO}_2$ . These are true titanaugites in the sense of Yagi and Onuma (1967), that is with >2wt%  $\text{TiO}_2$ . The high Ti values are reflected by high contents of the  $\text{R}^{2+}\text{Ti}^{4+}\text{Al}_2\text{O}_6$  molecule. Hence, although Al contents of the titanaugites are slightly greater than those of Group 1 clinopyroxenes described above, the amount of  $\text{Al}^{\text{VI}}$  is relatively reduced, with most of the available Al entering the above molecule, instead of the  $\text{R}^{2+}\text{AlSiAlO}_6$  molecule, as in the Group 1 clinopyroxenes. This is illustrated in Figure153.  $\text{Cr}^{3+}$ , particularly abundant in SB60 clinopyroxenes, is presumably present within  $\text{R}^{2+}\text{CrSiAlO}_6$  molecules. Na may be present with  $\text{Fe}^{3+}$  in the component  $\text{NaFe}^{3+}\text{Si}_2\text{O}_6$ , whilst  $\text{Fe}^{3+}$  may also occur as  $\text{CaFe}^{3+}\text{SiAlO}_6$  (Kushiro, 1962).

As a result of high  $\text{Ti}^{\text{cpx}}$  contents,  $\text{Mg}^{\text{cpx}}$  is low in these clinopyroxenes, accounting for the analyses falling close to the Di-Hd tie line on the pyroxene quadrilateral diagram. The coupled substitution  $\text{R}^{2+} + \text{Si} \rightleftharpoons \text{Ti} + \text{Al}$  (where  $\text{R}^{2+}$  is chiefly  $\text{Mg}^{2+}$ ), discussed above, also

**FIGS. 152a and b. Clinopyroxene compositions from samples SB63 and SB60 plotted on the Di-Hd-En-Fs quadrilateral.**

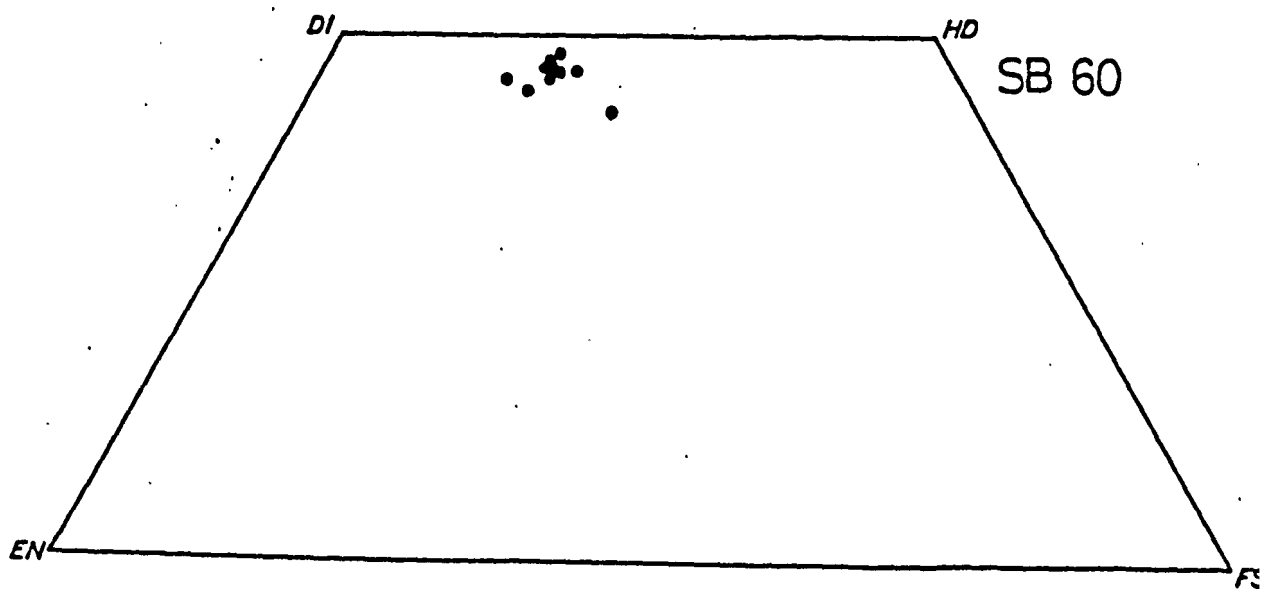
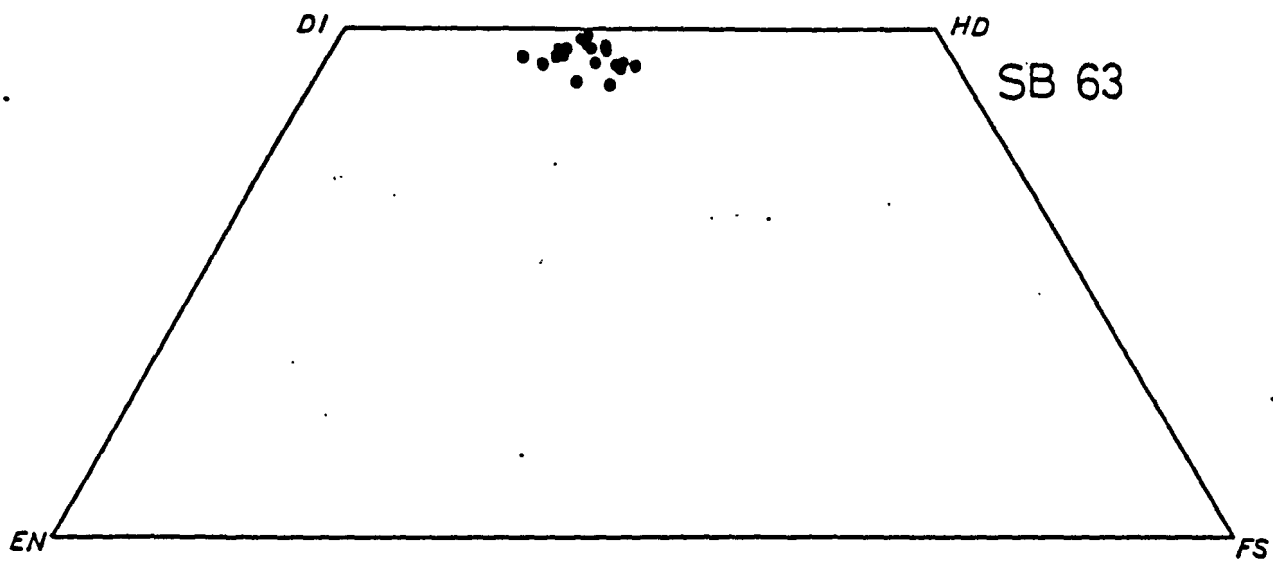
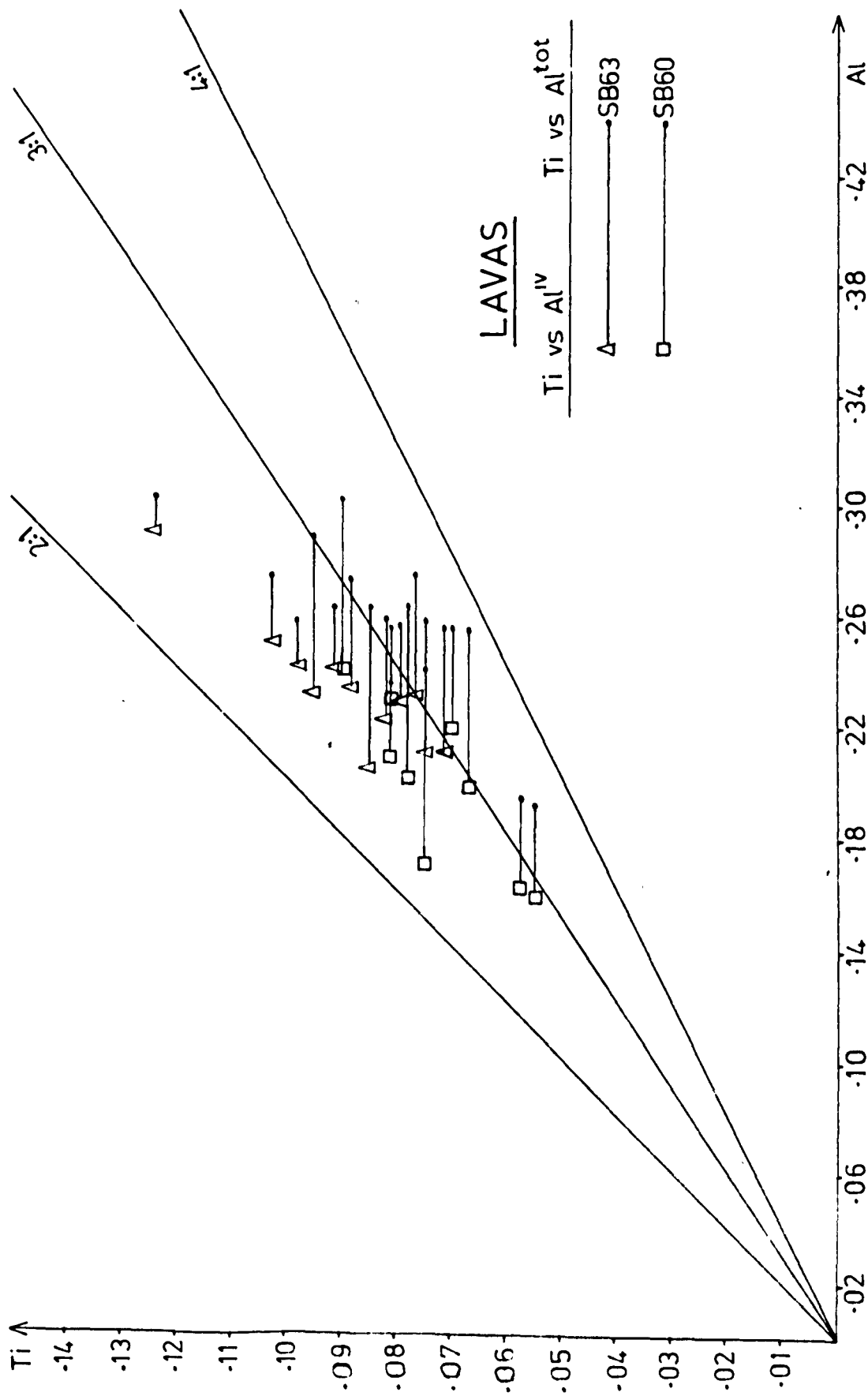


FIG. 153. Atomic Al vs Ti for clinopyroxenes from samples SB60 and SB63.





accounts for the low Si contents. The relationship between Mg and Ti is illustrated in Figure 154, and the interdependence of these elements is clearly visible. The dominant trend apparent from the Di-Hd-En-Fs diagram is parallel to the Di-Hd tie line, i.e. constant Ca, with  $\text{Mg} \rightleftharpoons \text{Fe}$ .

Clinopyroxenes of this group have a high proportion of 'other' components (Papike et al., 1974), and are dominated by the TAl component.

#### 4.2.1.3. DESCRIPTION OF CLINOPYROXENES FROM INTRUSIVE SHEETS WITHIN THE FISHGUARD VOLCANIC GROUP

Within the volcanic pile of the Fishguard Volcanic Group, a large number of intrusive sheets can be identified. These are interpreted as being magmas which have failed to reach the surface (sea-water-rock interface). However, they appear to be contemporaneous with the extrusive vulcanicity of the Fishguard Volcanic Group (see Chapter 2). These sheets probably had a cooling history which was intermediate, in terms of the rate of cooling, between the lavas, which suffered rapid cooling, and the thick intrusive sheets within the underlying sediments, which display evidence of relatively slow, equilibrium crystallization cooling conditions. This is suggested by the textural evidence from certain sheets (e.g. samples from SB51 and SB27), which contain skeletal clinopyroxenes. A sample from one of these sheets was studied, but it is not known how typical these results are.

In the analysed sample (SB27), clinopyroxene crystallized later than plagioclase and is present as large, tabular, slightly-coloured crystals. On the Di-Hd-En-Fs quadrilateral diagram (Fig. 155) the analyses fall close to the Di-Hd tie line, a consequence of their moderate Ti contents, and plot within the salite field. A correlation

FIG. 154. Atomic Mg vs atomic Ti for clinopyroxenes from samples SB60 and SB63.

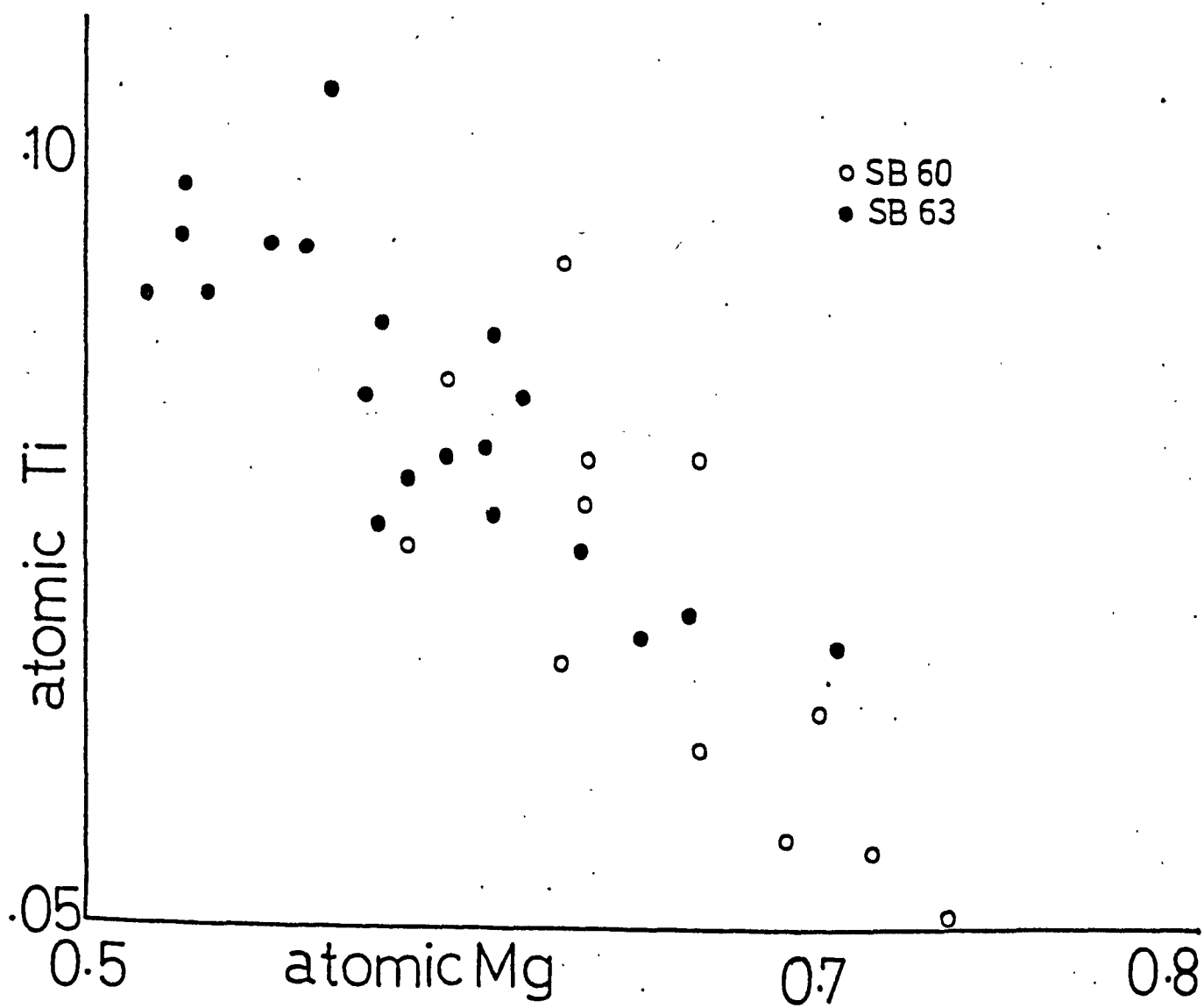
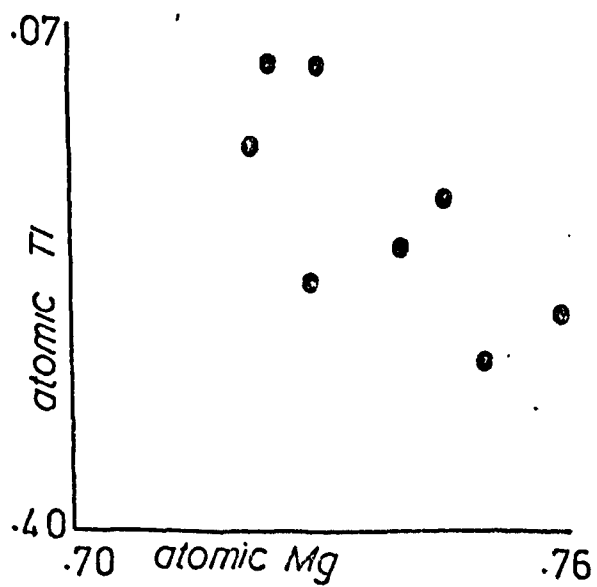
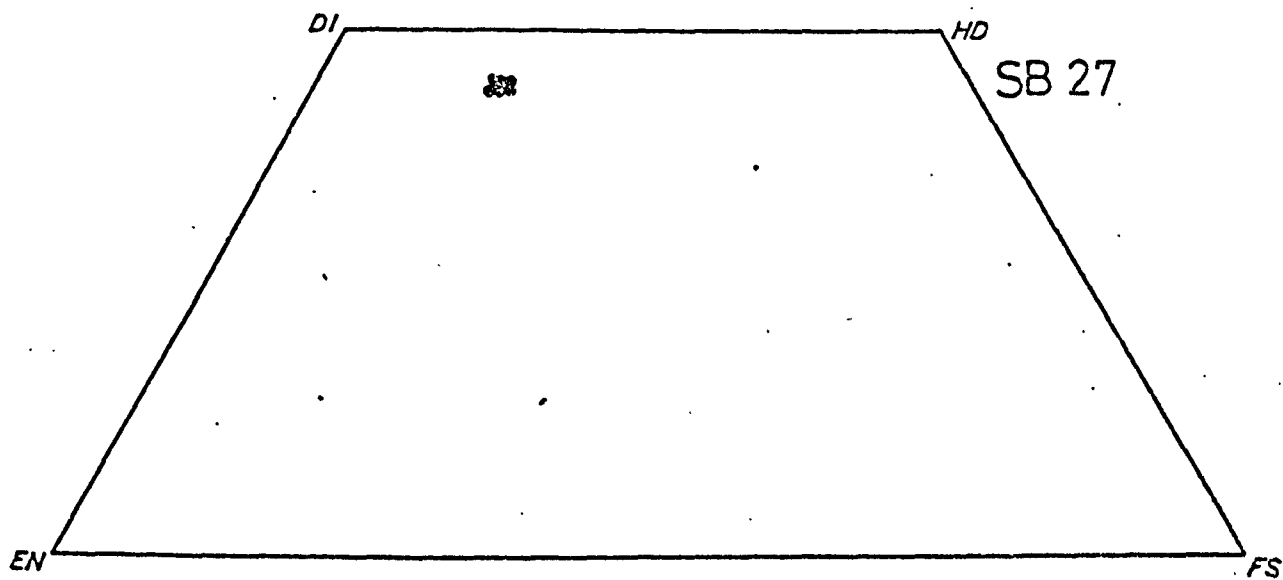
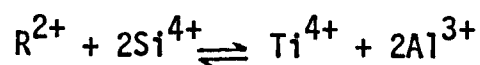


FIG. 155. Clinopyroxene compositions from sample SB27 plotted on the Di-Hd-En-Fs quadrilateral.

FIG. 156. Atomic Mg vs atomic Ti for clinopyroxenes from sample SB27.



of Ti with Mg (Fig.156) suggests, once again, that the coupled substitution



is responsible for the observed compositions.

#### 4.2.1.4. THE RELATIONSHIP BETWEEN CLINOPYROXENE COMPOSITION AND CRYSTALLIZATION HISTORY

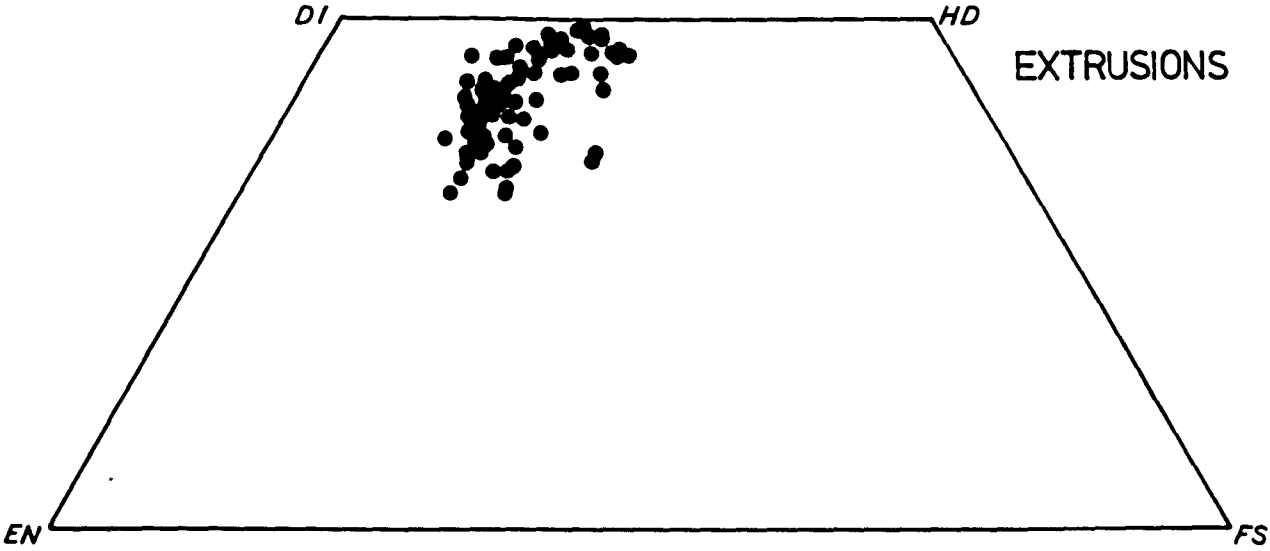
The concentrations of  $TiO_2$  in Group 2 clinopyroxenes are higher than in Group 1 clinopyroxenes, which in turn are higher than those from the intrusions of Llanwnda, Garn Fawr etc. As emphasized above, it is thought that the substitution  $R^{2+} + 2Si^{4+} \rightleftharpoons Ti^{4+} + 2Al^{3+}$  has been operative. As a result variable Mg and Si contents in the clinopyroxenes analysed were produced. In the more Ti-rich clinopyroxenes (Group 2 S.4.2.1.3.), most of the aluminium present is in tetrahedral sites with only limited octahedral aluminium. Thus on Al vs Ti diagram, only a limited spread between  $Al^{IV}$  and  $Al^{tot}$  is seen (Fig.153). In contrast, Group 1 clinopyroxenes have lower concentrations of Ti, and less aluminium present in tetrahedral sites. Consequently  $Al^{VI}$  contents are higher (Fig. 151).

Clearly, the entry of Ti into the crystal lattice is of major importance in determining the chemistry of the clinopyroxenes analysed here. It is important, therefore, to examine the possible factors controlling the entry of Ti into clinopyroxene.

Figure 157 illustrates the spread of all of the clinopyroxene analyses from the lava samples analysed, and shows two major chemical variations:

FIG. 157. Di-Hd-En-Fs diagram showing composition of clinopyroxenes from lavas of the Fishguard Volcanic Group.





(i) a trend of iron-enrichment, which is parallel to the iron-enrichment shown by clinopyroxenes from the intrusions (Fig. 144), and is related to changing liquid composition during crystallization of the sample in question; and

(ii) a trend parallel to the Di-En tie line, i.e. one of constant iron contents, but varying Ca-Mg relationships.

A similar trend to the latter was described by Lofgren et al. (1974) during crystallization experiments on quartz-normative lunar basalts. In their experiments, the greater the degree of supercooling the liquid suffered or the faster the cooling rate, the more Ca-Fe-Al-Ti rich and Mg-Si poor were the clinopyroxenes which subsequently crystallized from that liquid. In the experiments of Lofgren et al. (op. cit.), extreme Ti enrichments were observed in some crystals at specific rates of cooling. Thus, it appears most likely that the variation in the crystal chemistry observed for the clinopyroxenes described above is related to variable cooling rates and/or degrees of supercooling. Further support for this contention is provided by petrographical evidence. The most Ca, Ti rich clinopyroxene bearing lavas analysed from the Fishguard area (SB60, SB63) exhibit a range of textures which conform with textures developed either during rapid cooling or from supercooled liquids.

With moderate to high degrees of supercooling and/or rapid cooling, an increased amount of 'other' components (i.e. other than quadrilateral components), particularly Ti and Al, are incorporated into the clinopyroxene crystal lattice. This entry is probably governed by the rates of diffusion. When crystallization is rapid, the removal of 'other' components away from the crystal/liquid interface is not efficient enough to prevent some of these elements entering the lattice.

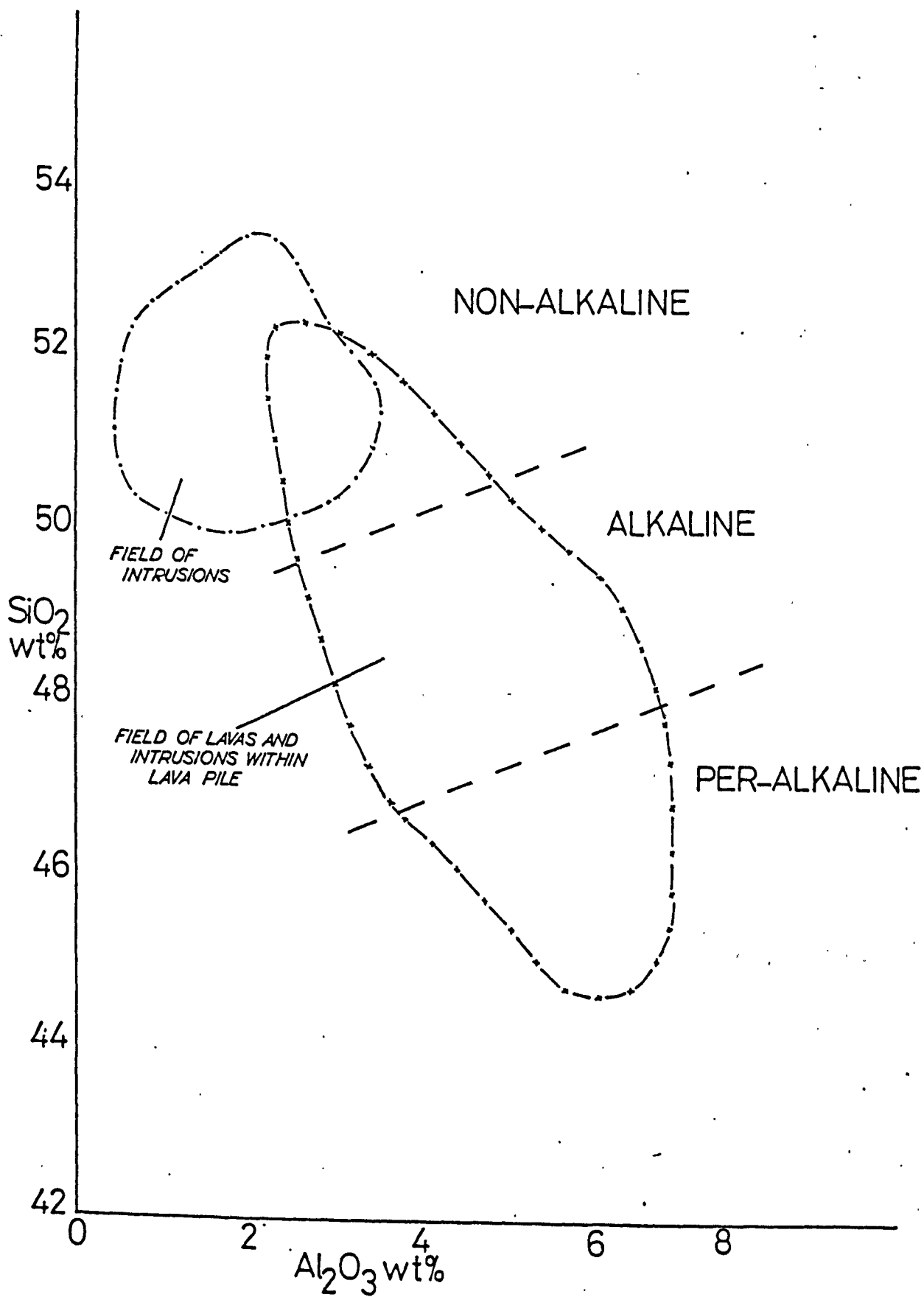
The incorporation of these elements into the clinopyroxene lattice produces compositions typical of clinopyroxenes from undersaturated melts. This could, therefore, explain other occurrences of Ti-rich pyroxenes in basalts of tholeiitic affinity as, for example, described by Mevel and Velde (1976) and Baragar et al. (1977). Therefore, the crystallization history of a liquid has important consequences for the chemistry of the phases contained and will be important if any deductions are attempted to be made from the phase chemistry. One such case is where attempts are made to identify the magmatic affinity of altered basic rocks from the composition of the metastable clinopyroxenes. This is discussed more fully below.

#### 4.2.1.5. CLINOPYROXENE COMPOSITION AS AN INDICATOR OF MAGMATIC AFFINITY

It has been suggested by a number of workers (e.g. Kushiro, 1960, Le Bas, 1962) that the composition of clinopyroxenes is directly related to the nature of the melt from which they crystallized. This has recently been extended in a reverse manner by, for example, Vallance (1974b) and Nisbet and Pearce (1977), who suggest that within altered basic igneous rocks the nature of the magma may be discerned by examining the compositions of the clinopyroxenes if they are in an unaltered state. This may be the case for clinopyroxenes which have crystallized under equilibrium or near equilibrium crystallization conditions but for crystallization under disequilibrium conditions, as for example during rapid cooling or in supercooled liquids, the composition is dependent upon additional factors to that of liquid composition (e.g. diffusion rates). Experimental work demonstrates that varying compositions result from different cooling histories of the same liquid (Lofgren et al., 1974). During disequilibrium crystallization, relatively large amounts of 'other' components are incorporated into the

crystal lattice (see S.4.2.1.4.). On Figure 158, a  $\text{SiO}_2\text{-Al}_2\text{O}_3$  diagram after Le Bas (1962), all the analyses of clinopyroxenes from the lavas of the Fishguard Volcanic Group and associated intrusions are plotted together. The three fields discriminated by Le Bas (1962) are marked and are supposedly occupied by clinopyroxenes from tholeiitic, alkaline, and peralkaline magmas. Clearly, the clinopyroxenes analysed in this study occupy all three fields. Those which crystallized under equilibrium conditions (i.e. those from the thick intrusions within the underlying sedimentary strata) fall within the tholeiitic field and it is suggested that the melt from which they crystallized was tholeiitic in nature. However, the remainder of the analyses, from the lava samples and the intrusive sheets within the volcanic pile, clearly owe their compositions to factors other than solely melt composition, as they plot across the alkaline and peralkaline fields. These findings are in keeping with those of Gibb (1973). Recently, Nisbet and Pearce (1977) attempted to show the possibilities of using clinopyroxene compositions in identifying the magmatic affinity of spilitic rocks by using a method of discriminant analysis. They produced discriminant function diagrams in addition to the oxide plots  $\text{Na}_2\text{O-TiO}_2\text{-MnO}$  and  $\text{SiO}_2\text{-TiO}_2$ , suggesting that significant variations in clinopyroxenes from different melts could be determined utilising these plots. However, for the reason described above, it is considered that these diagrams must be used with extreme caution. Evidence of equilibrium or near-equilibrium crystallization conditions would appear to be critical before deductions are made concerning the nature of the melt from which the particular clinopyroxenes crystallized.

FIG. 158.  $\text{SiO}_2^{\text{cpx}}$  vs  $\text{Al}_2\text{O}_3^{\text{epx}}$ , showing variation displayed by intrusions and lavas within the Fishguard area. Fields of non-alkaline, alkaline, and per-alkaline after Le Bas (1962).



#### 4.2.2. PLAGIOCLASE FELDSPAR

Several analyses of plagioclase feldspar have been determined but these will be discussed more fully below, along with the secondary mineral phases because all of the rock samples show varying degrees of albitization. The highest An content recorded was An<sub>38</sub>. However, higher contents in samples not analysed are suggested by extinction angle measurements using the Michel-Levy method. Using this method, labradorite compositions were recorded in a number of samples, and these may well represent pristine plagioclase crystals. Occasionally, zoning is still identifiable and is taken to be an original chemical zoning produced during initial crystallization. Clearly, in these rocks plagioclase feldspar has not been completely altered. The fact that high anorthite bearing feldspars are locally preserved argues in favour of albite being of a secondary origin in the more altered rocks, which has important bearings on the origin of 'spilites' and meta-basites.

#### 4.3. DESCRIPTION OF THE SECONDARY PHASES

The igneous rocks of the Fishguard Volcanic Group and the surrounding strata have been affected by varying degrees of alteration. The timing of this alteration is difficult to determine and it appears likely that different processes have operated at various times. Thus, an initial sea-water alteration in the pillowed lavas may in fact have been subsequently overprinted by the effects of a regional metamorphic episode. As a result, the primary igneous mineral assemblage has largely been replaced by secondary minerals (see Chapter 2).

##### 4.3.1. PLAGIOCLASE FELDSPAR

As stated in S.4.2.2. a number of plagioclase analyses have been made, as well as estimations of compositions from extinction angles.

From these estimations, a wide variation within and between samples is recorded. These feldspars have suffered albitization, with the introduction of Na and Si at the expense of Ca and, to a lesser extent, Al. This process, however, has not been uniform and accounts for the variable feldspar compositions recorded. Microprobe analyses of a very limited number of samples show a range from  $\text{Ab}_{99}\text{An}_1$ , (in sample SB23) to  $\text{Ab}_{62}\text{An}_{38}$  (in SB27).

#### 4.3.2. PUMPELLYITE

As reported above (in Chapter 2) and by Bevins (1978), pumpellyite has been identified for the first time in the Ordovician igneous rocks of South Wales.

Pumpellyite occurs both within the basic and intermediate lavas of the Fishguard Volcanic Group and the basic and intermediate intrusions of the Fishguard area. It shows a number of characteristic forms:

- (i) as discrete, euhedral crystals associated with prehnite, and occurring in alteration veins (Fig. 53);
- (ii) as radiating needles, occurring within vesicles, associated with quartz and/or chlorite (Fig. 54);
- (iii) poorly formed, spongy crystals, replacing plagioclase feldspar (Fig. 52); and
- (iv) in small crystalline aggregates in the groundmass of lavas or intrusions.

It occurs most commonly replacing feldspar and is best developed within the intrusive rocks.



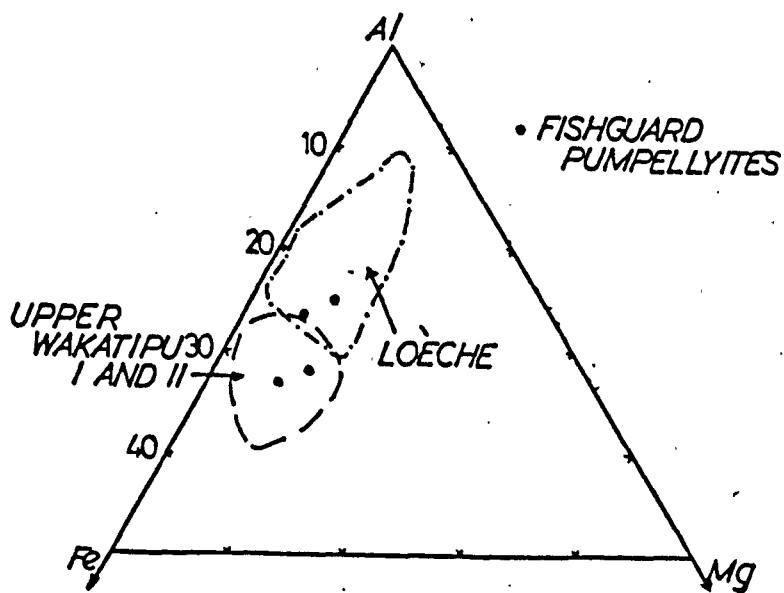
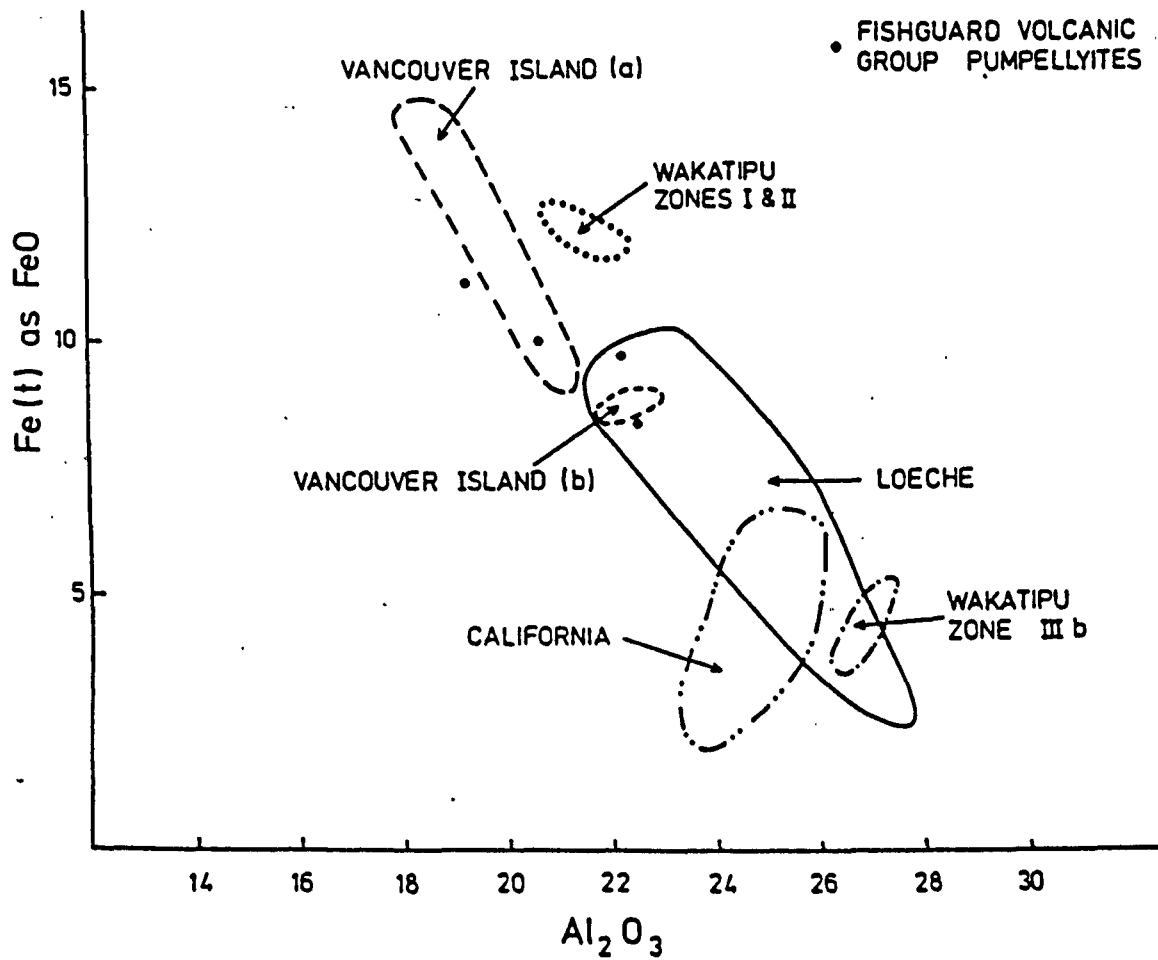
Five analyses of pumpellyite have been determined (see Appendix 2). Four of these (two from SB55 and two from YG54) show a limited spread in composition, whilst the fifth shows a significantly different composition and probably represents the analysis of a pumpellyite-chlorite intergrowth.

Generally, pumpellyite possesses a moderate to strong pleochroism from blue/green or green to colourless. This colour can be related to the moderate iron contents present (8-12% FeO). In one sample, however, (SBR11) a strong brown to greeny brown to colourless pleochroic scheme is present. Zen (1974) reported similar pleochroism in pumpellyites from Jonestown, Pennsylvania and showed this to be due to a high iron content. The Fishguard example occurs in a rock which is relatively fractionated and the high iron content of the pumpellyite may be the result of the high  $\text{Fe}^*/\text{Fe}^* + \text{Mg}$  ratio of the whole rock (where  $\text{Fe}^*$  = total iron).

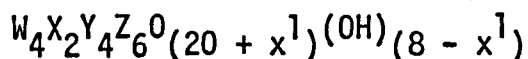
Several workers have noted a tendency for a decreasing depth of colour of pumpellyites (and also epidotes) with increasing metamorphic grade (e.g. Bishop, 1972; Kawachi, 1975). This corresponds to a decrease in the contents of Fe and, as a result of substitution, an increase in Al. When compared with other occurrences of pumpellyite in low-grade metamorphic environments (Fig.159), it can be seen that the Fishguard pumpellyites are relatively high in iron and correspond closely with analyses of pumpellyites from the Karmutsen Volcanic Group, Vancouver Island (Kuniyoshi and Liou, 1976; Surdam, 1969), which belong to the prehnite-pumpellyite facies grade of metamorphism. However, care must be exercised, as whole-rock compositions probably also control the phase chemistry as does the availability of a growth site for the secondary phase.

FIG. 159. Fe(t) as FeO vs  $Al_2O_3$  for pumpellyites of the Fishguard area. Other fields after; Vancouver Island (a), Surdam (1969); Vancouver Island (b), Kuniyoshi and Liou (1975); Wakatipu, Kawachi (1975); Loèche, Coombs et al. (1976); California, Ernst et al. (1970).

FIG. 160. Al : Fe : Mg diagram for pumpellyites of the Fishguard area. Fields for Wakatipu after Kawachi (1975) and Loèche after Coombs et al. (1976).



Coombs et al. (1976) reported an ideal formula of pumpellyite to be:



where W = Ca, Mn

X = (Mg, Fe<sup>2+</sup>, Mn)<sub>2 - x<sup>1</sup></sub>(Fe<sup>3+</sup>, Al)<sub>x<sup>1</sup></sub>

Y = Fe<sup>3+</sup>, Al

Z = Si

This contrasts with a generally assumed idealized pumpellyite formula of Ca<sub>4</sub>(Mg, Fe<sup>2+</sup>)Al<sub>5</sub>Si<sub>6</sub>O<sub>21</sub>(OH)<sub>7</sub>. The latter formula assumes 7OH to be present which Coombs et al. (1976) suggest may be erroneous. When the Fishguard pumpellyites are recalculated on either basis it becomes clear that considerable Fe<sup>3+</sup> is present. This is shown by the fact that Σ(Mg + Fe<sup>2+</sup> + Mn), which is generally in the X sites, is usually in the range 0.71 to 1.55 (Passaglia and Gottardi, 1973), whilst Σ(Mg + Fe(total) + Mn) ranges from 1.55 to 1.85 in the Fishguard pumpellyites, the excess presumably being Fe<sup>3+</sup>. The exact amount, however, is indeterminable, as Fe<sup>3+</sup> may be present in either the X sites or the Y sites. The recalculations made in this study are on the basis of 16 cations and assume that the Y sites are occupied by as much Al as possible. In three of the analyses there is sufficient Al to fill the Y site, but in one there is not sufficient and the remainder must be occupied by Fe<sup>3+</sup>. Figure 160 shows the Fishguard pumpellyites plotted on an Al : Fe\* : Mg triangular diagram (where Fe\* is total iron as FeO). The Fishguard analyses fall within the field of ferriferous pumpellyites (according to the classification of Passaglia and Gottardi, 1973), similar to pumpellyites from Upper Wakatipu zones I and II (Kawachi, 1975), Vancouver Island (Surdam, 1969), the Olympic Peninsula (Glassley, 1975)

and Jonestown (Zen, 1974), all of which occur in rocks metamorphosed within the prehnite-pumpellyite facies. It is suggested, therefore, that the rocks of the Fishguard area in which pumpellyite, with or without prehnite, has been identified, belong to the prehnite-pumpellyite facies (see Chapter 7). During the course of the present study, pumpellyite has also been identified from other areas in South Wales. Its presence in meta-volcanic rocks of Arenig age from Treffgarne has been detected by x-ray diffraction. In thin section, it appears to be present as very small, colourless crystals associated with quartz and clinozoisite in thin veins. It appears to be very low in iron. Preliminary investigations of the dolerites of the Prescelly Hills area reveal the presence of pumpellyite in a number of intrusions, but its abundance is somewhat reduced compared to the Fishguard area. The Sealyham volcanic lavas also contain pumpellyite, along with other secondary phases, such as epidote and prehnite.

It is thought likely that the mineral described by Reed (1895, p. 187) and suggested as belonging to the epidote family, was in fact pumpellyite.

#### 4.3.3. CHLORITE

Chlorite is ubiquitously developed within the igneous rocks of the Fishguard area and is one of the most abundant secondary phases present. Ten analyses of chlorites are presented in Appendix 2, along with atomic recalculations of the analyses on the basis of 36 O, OH. This recalculation assumes an ideal composition  $Y_{12}Z_6O_{20}OH_{16}$

where  $Y = Al, Fe^{2+}, Fe^{3+}, Mg, Mn$

$Z = Si, Al$

$\text{SiO}_2$  and  $\text{Al}_2\text{O}_3$  contents are relatively constant in comparison with the variation displayed by  $\text{FeO}(\text{total})$  and  $\text{MgO}$ . Various workers, for example Iwasaki (1963) have suggested that the  $\text{Fe}^{2+}$  content of chlorites varies with metamorphic grade. Kawachi (1975), however, demonstrated a relationship between  $\Sigma\text{Fe}/\Sigma\text{Fe} + \text{Mg}_{\text{chlorite}}$  and  $\Sigma\text{Fe}/\Sigma\text{Fe} + \text{Mg}_{\text{whole-rock}}$  and suggested that the whole-rock composition probably controls chlorite composition to a large extent. Figure 161 shows  $\Sigma\text{Fe}/\Sigma\text{Fe} + \text{Mg}_{\text{whole-rock}}$  against  $\Sigma\text{Fe}/\Sigma\text{Fe} + \text{Mg}_{\text{chlorite}}$  for chlorites from the groundmass of certain Fishguard samples. Clearly, a correlation between these two variables is also present here, suggesting that chlorite composition cannot be used to determine the grade of metamorphism. However analyses of chlorites from vesicles fall well away from the 1 : 1 relationship seen for the groundmass chlorites.

The co-variation of octahedral Fe and Mg suggests that iron is largely in the ferrous state. The aluminium ions are divided between tetrahedral and octahedral sites, with enough Al being allotted to the tetrahedral sites to counter the deficiency of Si ions. Theoretically, to balance the negative charge created by this tetrahedral substitution ( $\text{Al}_{3+} \rightleftharpoons \text{Si}_{4+}$ ), a similar number of trivalent ions must enter the octahedral sites. In only two analyses is this relationship seen, whilst in all others, an excess of trivalent aluminium cations are present. This is in keeping with the findings of other workers (e.g. Foster, 1962; Von Rahden and Von Rahden, 1972). The analysed specimens (except those from SB48) are plotted on Figure 162 which is based upon the classification of Hey (1954). Four of the specimens are pycnochlorites, three are brunsivigites and one is a diabantite. The dominant variation in composition (i.e. the variation of Fe and accordingly Mg) is clearly demonstrated.

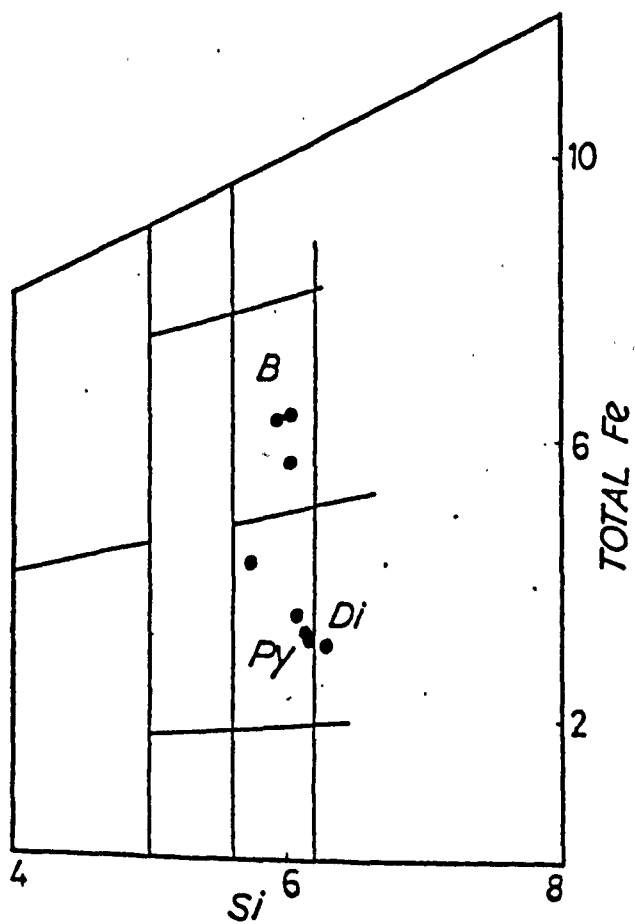
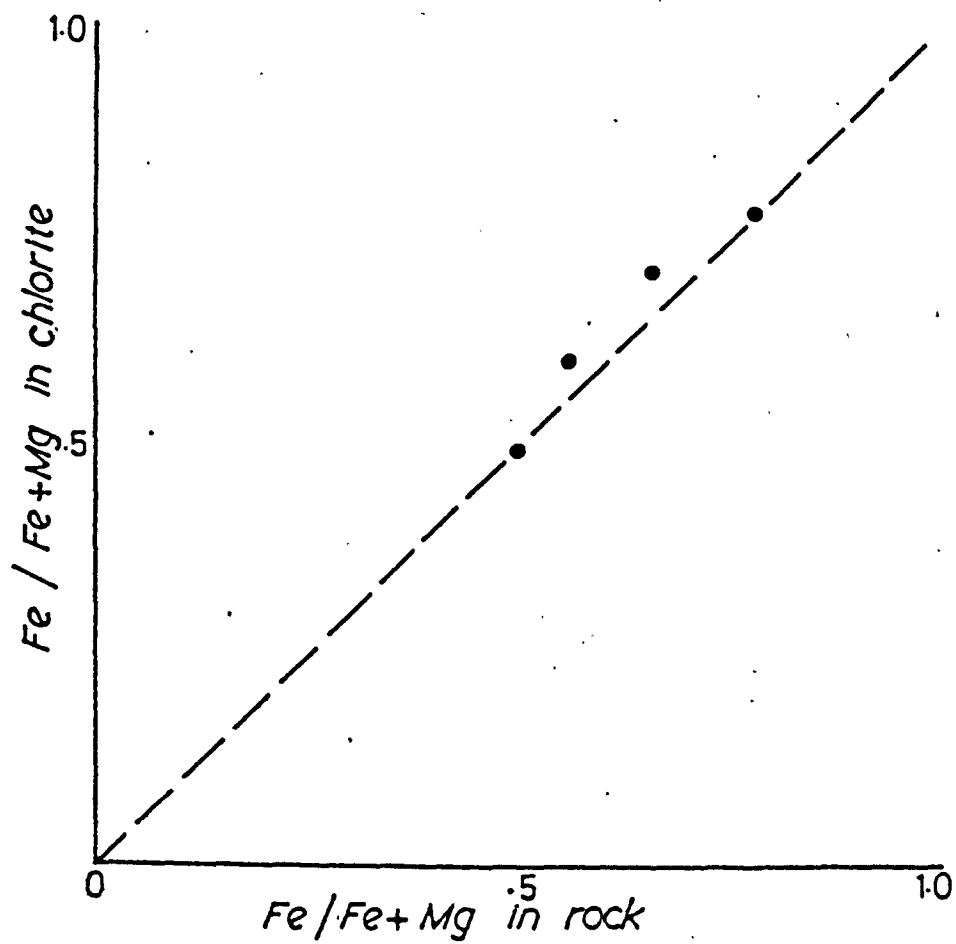
FIG. 161.  $\text{Fe}/\text{Fe} + \text{Mg}^{\text{chl}}$  vs  $\text{Fe}/\text{Fe} + \text{Mg}^{\text{w.r.}}$  for chlorites of the Fishguard area.

FIG. 162. Chlorites of the Fishguard area plotted on an Si vs total Fe diagram. Fields after Hey (1954),

B = Brunsvigite.

Py = Pycnochlorite.

D = Diabantite.





#### 4.3.4. STILPNOMELANE

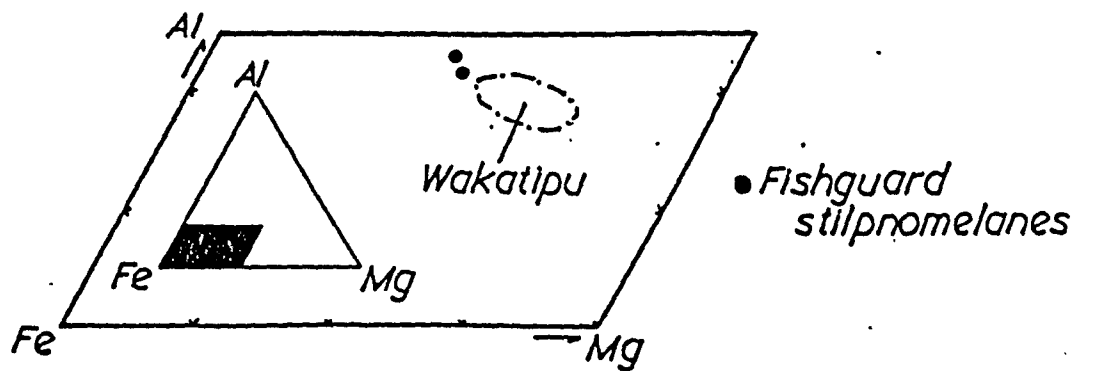
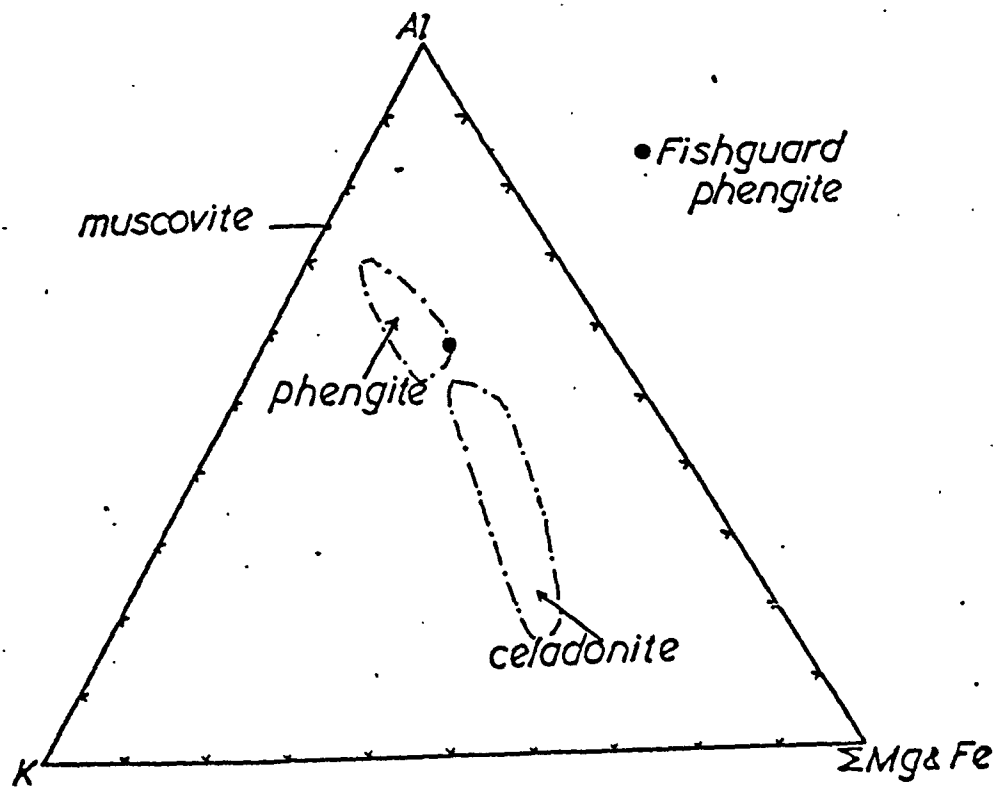
Although not common, stilpnomelane occurs sporadically throughout the igneous rocks of the Fishguard area, locally reaching very high proportions. It has also been identified within rocks of the St. David's Head Intrusion, to the west of Fishguard (Roach, 1969). This identification was confirmed during the present study by the author using x-ray diffractometry. It is typically brown in colour and is considered to be ferristilpnomelane, ferrostilpnomelane only rarely being identified. Two analyses of stilpnomelane are presented in Appendix 2, with recalculations on the basis of 4 Si cations. Compared with analyses reported recently by Chauvel (1973), these analyses are seen to be typical ferristilpnomelanes, although  $K_2O$  is possibly slightly higher than average. Kawachi (1975) noted the tendency for stilpnomelane to occur in rocks with high Fe/Fe + Mg ratio. The analysed samples are from SB55, which also has a high Fe/Fe + Mg whole-rock ratio (0.78) and belongs to group II (see Chapter 5). The analyses presented here compare closely with stilpnomelanes from Wakatipu (Kawachi, 1975), although the Fishguard examples are lower in magnesium (see Fig. 164). However, both the Fishguard samples and those from Wakatipu are higher in Mg compared with analyses reported by Zen (1974) from Jonestown, Pennsylvania. All the other major chemical constituents are of comparable atomic proportions between these three areas. As all these areas have suffered prehnite-pumpellyite facies metamorphism, stilpnomelane is undoubtedly metamorphic in origin in the rocks of the Fishguard area.

#### 4.3.5. EPIDOTE

Epidote is common in all the basic igneous rocks of the study area. It generally occurs within the groundmass of slightly altered lavas and

FIG. 163. Al : K :  $\Sigma$ Mg + Fe diagram, showing phengite from the Porth Maen Melyn isolated-pillow breccia.

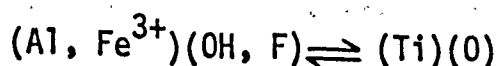
FIG. 164. Al : Fe : Mg diagram, showing Fishguard stilpnomelanes. Field for Wakatipu after Kawachi (1975).



dolerites, but also forms stout, euhedral crystals surrounded by and in apparent equilibrium with chlorite. In most cases it possesses a yellow to colourless pleochroism, suggesting moderate iron contents (pistacitic epidote). A number of analyses have been determined (Appendix 2) and these show the presence of moderate amounts of the molecule  $\text{Ca}_2\text{Fe}_3\text{Si}_3\text{O}_{12}(\text{OH})$  (26% in the case of epidote from SBC1). A number of workers have suggested a correlation between the grade of metamorphism and epidote iron content. Kawachi (1975) reported a considerable decrease in iron content and increase in Al content with increasing grade, whilst Coombs et al. (1976) suggested that lower iron contents with advancing metamorphism may be due to declining  $f\text{O}_2$ . This is discussed in more detail below (Chapter 7). In comparison with the epidotes of the Fishguard area, those occurring in dolerites from the Prescelly Hills appear to be clinozoisites. This may reflect slight changes in the conditions of metamorphism. Some of these Prescelly epidotes show strong chemical zoning, changing from Fe-rich cores to Fe-poor rims. Such a zonation may be the result of prograde metamorphism, producing iron-rich epidote at the early, low grade stage and then iron-poor rims as the grade increased. Such a history has been reported by Brown (1967).

#### 4.3.6. SPHENE

Sphene is typically present in small, granular aggregates, scattered throughout the altered basic igneous rocks. It may also occur as pseudomorphs after the titanium-rich component of titanomagnetites, in which the iron-rich component is largely unaltered. One analysis of sphene is reported in Appendix 2. This sample is moderately enriched in Al and Fe, which according to Sahama (1946) substitute for Ti:



The Ti content of the analysed specimen is correspondingly low, suggesting that the above substitution may well have occurred. Boles and Coombs (1977) suggest that this substitution is characteristic of sphenes from very low grade metamorphic rocks. Aluminium sphene ('grothite') has been recorded from other meta-volcanic and pyroclastic rocks, for example the Permo-Carboniferous spilites of Northern France (Morre-Biot, 1970) and the Taveyanne Formation, Loèche, Switzerland (Coombs et al., 1976).

#### 4.3.7. PHENGITIC MUSCOVITE

Phengitic muscovite forms the matrix of the rhyodacitic isolated-pillow breccias of Porth Maen Melyn (see Chapter 2). It appears to have been formed as a result of the alteration of glassy rhyodacite lava, at the margins of the pillowed masses and probably results from metasomatic exchange between the lava and K-rich fluids. The mica is a 2m polymorph and its cell dimensions have been calculated by x-ray diffractometry, which are  $a^0 = 5.215$ ,  $b^0 = 9.024$ ,  $c^0 = 19.93$ . These values correspond closely with the cell dimensions reported by Güven (1971). When compared with normal K-rich micas, the most notable difference occurs in the ' $b^0$ ' values, as typical muscovite has the following cell dimensions:  $a^0 = 5.191$ ,  $b^0 = 9.008$ ,  $c^0 = 20.047$ . Fettes et al. (1976) have recently attempted to use the  $b$  value as a geobarometer for low grade metamorphic rocks. A chemical analysis was made of a mineral separate of this phengitic mica and the result is reported in Appendix 2. It was analysed by wet chemical methods. Unfortunately, although the mica was easily separated from the quartz and feldspar present within the isolated-pillow breccia, the small sphene granules, which are pervasive throughout the mica flakes, could not effectively be removed. This probably accounts for the relatively high CaO and  $TiO_2$  contents of the analysis when compared with

other phengite analyses. Fortunately, however, these two oxides are not major or even important components of phengite and accordingly have not been included in the atomic recalculation. From the triangular diagram  $Al : K : \Sigma Mg + Fe^{2+} + Fe^{3+}$ , it can be seen that this sample has a high celadonite component due to the high iron content (Fig. 164). It also plots close to phengites from other low grade (prehnite-pumpellyite and pumpellyite-actinolite facies) metamorphic areas, and is a characteristic mineral of these low grades. However, this occurrence in the Fishguard Volcanic Group is unique, other white micas, which are developed within the pelites of the Fishguard area are colourless and presumably more normal, iron-free muscovites.

A deficiency in Si cations necessary for the tetrahedral sites is present, suggesting that Al is present within the tetrahedral layer, a feature typical of micas within the muscovite-celadonite solid solution series. The octahedral sites are occupied by Al, Fe (both  $Fe^{2+}$  and  $Fe^{3+}$ ), and Mg, whilst Na and K represent the interlayer cations. Compositionally, this sample is close to two of the celadonite analyses reported by Boles and Coombs (1975) from zeolite-facies metamorphosed Triassic tuffs of the Hokonui Hills, New Zealand. The zeolites present, principally heulandite and celadonite, represent the alteration products of andesitic and dacitic volcanic glasses. If the phengite described here is an alteration product of volcanic glass, then considerable chemical exchange occurred during alteration, i.e. losses in  $SiO_2$  and  $Na_2O$  and additions of  $FeO$ ,  $MgO$ ,  $Al_2O_3$ , and  $K_2O$ .

It is thought likely that the phengite described here is that mineral which Thomas and Thomas (1956, p. 300) identified as phlogopite.

#### 4.3.8. ORE

Although no analyses of the ore phase present within the various igneous rocks of the Fishguard area were determined, certain deductions may be made from petrological observations. In most of the lavas, an ore phase is only present in minor amounts, although certain rocks, such as sample SB44, an intrusive sheet, have comparatively high ore contents. In these cases the ore appears to be an homogeneous Fe-Ti bearing phase. However, a halo of sphene is commonly developed around the ore phase and clearly represents the outward migration and local fixing of Ti. In some of the more slowly cooled, larger intrusive sheets, certain horizons show the presence of unmixed ilmenite and magnetite. The magnetite, present as thin bars within the crystals, is unaltered, whilst the host ilmenite has altered to sphene. The primary unmixing occurred during slow cooling, whilst the production of sphene was probably metamorphic in origin. Similar alteration has been observed by Zen (1974) and Kuniyoshi and Liou (1976).

#### 4.3.9. AMPHIBOLE

Amphibole is locally developed within the igneous rocks of the Fishguard area, although generally it only forms a very small modal proportion. The most abundant occurrence of amphibole is within the Llech Dafad Intrusion. Within this sheet, ophitic clinopyroxene appears to be mantled by a blue-green hornblende. A number of analyses of these calcic-amphiboles from the Llech Dafad Intrusion have been made (Appendix 2) and of particular importance is the high Al content. Amphiboles from low-grade metamorphic terrains are generally poor in Al (i.e. actinolitic) and this suggests that the amphiboles analysed here

may be the result of deuteric alteration, during initial cooling. However, colourless, fibrous amphiboles (probably actinolitic and of metamorphic origin) are seen in a number of rocks within the Fishguard area. A third variety of amphibole identified occurs in small alteration patches in clinopyroxene crystals from the slowly cooled intrusive sheets, such as the Llanwnda Intrusion. This amphibole is brown in colour and strongly pleochroic, and has recently been identified as kaersutite (Rowbotham, pers. comm.).

#### 4.3.10. PREHNITE

Prehnite occurs in many of the basic igneous rocks of the Fishguard area, as well as from other areas of North Pembrokeshire (Roach, 1969). Eight analyses from sample YG54 were determined and are listed in Appendix 2. Very little compositional variation is displayed by these analyses. Prehnite has an ideal formula  $\text{Ca}_2(\text{Al}, \text{Fe}^{3+})_2\text{Si}_3\text{O}_{10}(\text{OH})_2$  and in the samples reported here, there is approximately 10 mole percent  $\text{Ca}_2\text{Fe}_2\text{Si}_3\text{O}_{10}(\text{OH})_2$ . This gives an approximate formula of  $\text{Ca}_2\text{Fe}_{0.25}\text{Al}_{1.75}\text{Si}_3\text{O}_{10}(\text{OH})_2$ . The analyses reported here are similar to certain prehnites from the Karmutsen Volcanic Group (Surdam, 1969), although they do not show the range displayed by the Karmutsen prehnites.



## CHAPTER 5. WHOLE-ROCK GEOCHEMISTRY

### 5.1. INTRODUCTION

89 samples from the Fishguard Volcanic Group were collected and analysed by x-ray fluorescence techniques for major elements ( $\text{SiO}_2$ ,  $\text{TiO}_2$ , total iron,  $\text{MgO}$ ,  $\text{MnO}$ ,  $\text{CaO}$ ,  $\text{Na}_2\text{O}$ ,  $\text{K}_2\text{O}$ , and  $\text{P}_2\text{O}_5$ ) and a number of trace elements (including Ba, Cr, Nb, Ni, Rb, Sc, Sr, V, Y, Zr and the Rare Earth Elements). These analyses are tabulated in Appendix 1, along with a brief description of analytical techniques and an estimation of the precision and accuracy of the methods employed. A small number of analyses of volcanic and volcanoclastic rocks from other parts of North Pembrokeshire (Treffgarne, Llanrian, Abercastle and Sealyham) were also determined.

Also included, for comparative purposes, in this work are 29 unpublished major and trace element analyses from other intrusive bodies of the North Pembrokeshire region, determined by Roach, Floyd and Rea (1972).

### 5.2. PROBLEMS OF INTERPRETATION OF THE GEOCHEMICAL DATA

From a consideration of the present phase assemblage within the basic igneous rocks of the Fishguard area, it is clear that they have suffered secondary alteration. Much work has been undertaken on the geochemistry of altered basic igneous rocks. Initially this was restricted to the significance of major element concentrations (for example, Vallance, 1960, 1965, 1969) but more recently, in an attempt to interpret the tectonic setting of ancient volcanic suites, attention has been focussed on the significance of minor and trace element values (e.g. Cann, 1969; Pearce and Cann, 1971, 1973; Floyd and Winchester,

1975, 1978 and Winchester and Floyd, 1976, 1977). It is thus necessary to examine the results obtained in this study in the light of information provided by the above works. The major elements will be dealt with first, followed by consideration of the minor and trace elements.

### 5.3. CHEMICAL AND MINERALOGICAL EFFECTS OF ALTERATION

In Chapter 2 it was shown that the basic to intermediate igneous rocks of this area have a mineralogy similar to that of rocks termed 'spilites'. The strict definition of the term 'spilite' appears confused, but is used here in the sense of Vallance (1974a) who states that spilites are analagous to normal basalts but differ in the fact that they are composed largely of mineral phases of the greenschist facies, such as albite, chlorite, epidote, calcite etc. It is not believed, however, that greenschist facies metamorphism is necessary for the formation of spilitic assemblages; indeed the Fishguard Volcanic Group and associated rocks appear to have been metamorphosed within the prehnite-pumpellyite facies (see Chapter 7) and Coombs (1974) recognized the production of a spilitic assemblage under zeolite facies metamorphic conditions. A variety of low-grade alteration processes, all involving hydrolysis and ionic exchange, can in fact be responsible for the production of rocks bearing a spilitic assemblage (see below). Before discussing the chemical effects of these processes, it is necessary to consider the evidence for spilites and similar rocks as representing the alteration products of basaltic magma, as much controversy has existed in the past as to their origin.

It has been suggested that spilites are the direct cooling of a magma of spilitic composition (e.g. Benson, 1915; Amstutz, 1948,

1950; etc.), whilst, as stated above, it is also argued that they represent the alteration products of a normal basalt, either due to the effects of autolysis or low-grade metamorphism. A review of the spilite controversy is provided by Amstutz (1974).

Probably the strongest argument against a parental magma of spilitic composition is the non-recognition of spilitic magmas amongst contemporary volcanic piles (other than those of the ocean-floor), whereas most other ancient volcanic rocks have modern analogues.

Considerable debate has existed, however, on the feasibility of an initial water-rich magma crystallizing primary albite and chlorite (Rittmann, 1958; Amstutz, 1968). Experimental work in the basalt-water system (Yoder and Tilley, 1962) showed that water in this system, in the necessary amounts, produced hornblende as a primary phase, offering contrast to the rocks themselves where clinopyroxene is the chief mafic phase identified, with olivine commonly retrogressed and pseudomorphed. In addition, Fawcett and Yoder (1966) showed that the highest temperature at which chlorite is stable is  $700^{\circ}\text{C}$  at 2kb  $\text{pH}_2\text{O}$ , whereas pyroxenes present in spilites have compositions identical to those found in basalts, with liquidus temperatures in excess of  $1000^{\circ}\text{C}$ . Clearly, these two phases are not the products of simultaneous crystallization. Yoder (1967) proposed the existence of a 'spilite reaction', namely

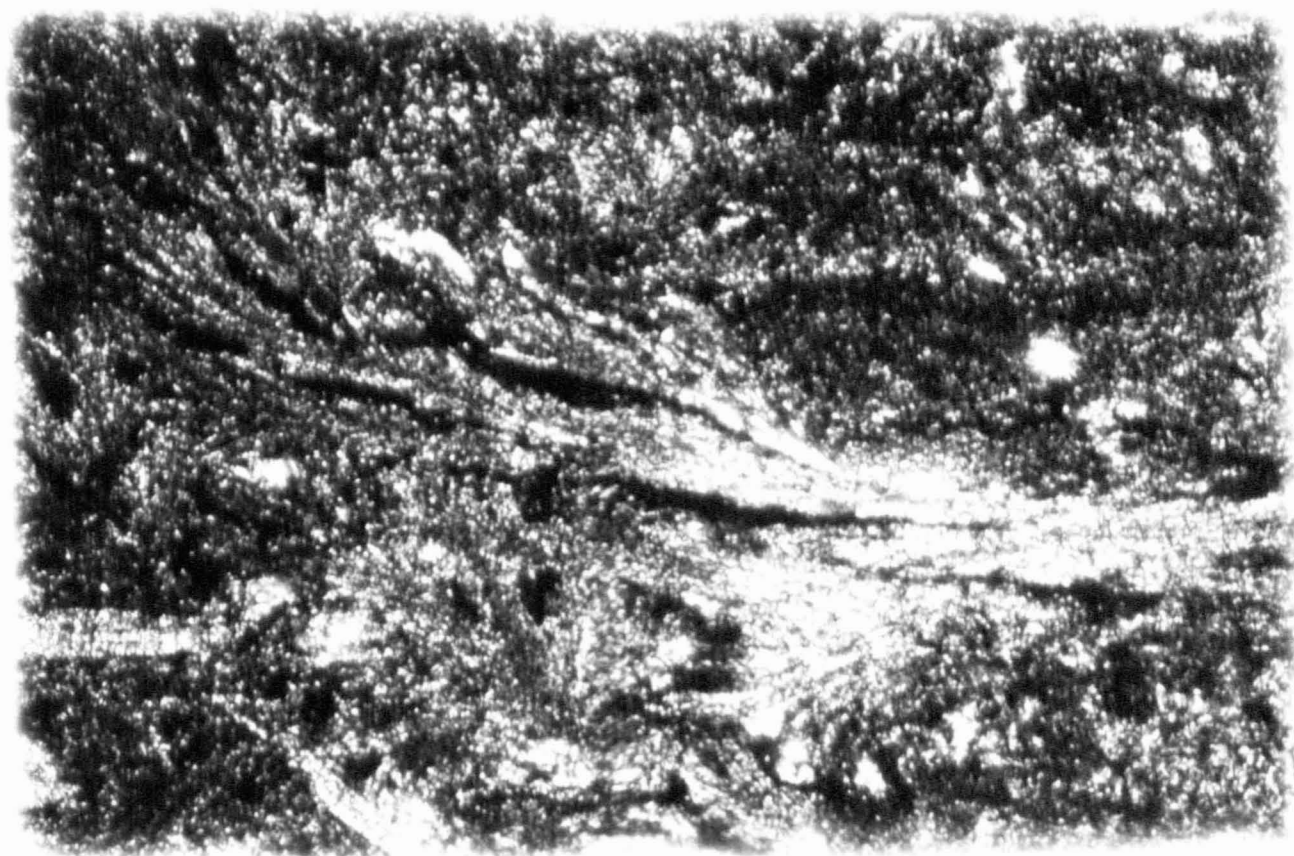


Coombs (1974) argued, however, that textures in spilitic rocks are incompatible with this reaction, a suggestion supported by observations of textures within the Fishguard Volcanic Group. Figures 165a and b.

FIGS. 165a and b. Complex, fan spherulitic intergrowths of plagioclase feldspar and clinopyroxene. Strumble Head Volcanic Formation. PPL.

a) x100.

b) x100.



illustrate evidence for the simultaneous crystallization of augite and plagioclase feldspar, producing a complex fan spherulite. The plagioclase, now albitic in composition, is assumed to have resulted from the alteration of a more calcic member, whilst the clinopyroxene represents a relict primary phase. Further, in the reaction described above, diopside represents a product of the reaction, belonging to the 'spilite assemblage'. Clearly this is not so, as evidence from the Fishguard Volcanic Group clearly demonstrates that it is primary in origin (evidence outlined above, in Chapters 2 and 4, as well as the fact that clinopyroxene itself is locally replaced by hornblende and even chlorite (Figs. 47 and 45)). As mentioned above, the feldspar observed within spilites is albitic in composition. However, reactions during alteration processes producing spilitic assemblages are slow and equilibrium is not always attained. This commonly results in assemblages showing a range of feldspar compositions, with the local preservation of calcic members. From microprobe analysis, sample SB27 shows feldspars of composition around  $An_{30-40}$ , whilst sample SB23 has pure albite. Clearly the albitization process has proceeded further in SB23. More lately plagioclase of labradoritic compositions have been detected (author's own unpublished analyses). The low Ca feldspars are clearly of secondary origin.

The evidence suggests that spilites are derived from basalts as a result of secondary alteration processes. Vallance (1969) emphasised the similarity in chemistry between 225 spilites and 1996 basalts, compiled by Manson (1968). The means of these compilations are shown in table 2, below. The similarity between basalt and spilite for most elements is striking. Significant differences exist in  $CaO$ ,  $Na_2O$ ,

TABLE 2

	Average of 1996 basalts (compiled by Manson, 1968)	Average of 225 spilites (after Vallance, 1969)
$\text{SiO}_2$	49.2	49.0
$\text{Al}_2\text{O}_3$	15.8	15.4
$\text{Fe}_2\text{O}_3$	3.0	4.1
$\text{FeO}$	8.0	6.1
$\text{MnO}$	0.17	0.18
$\text{MgO}$	6.6	5.3
$\text{CaO}$	10.0	7.6
$\text{Na}_2\text{O}$	2.7	4.1
$\text{K}_2\text{O}$	1.0	1.1
$\text{H}_2\text{O}^+$	0.9	3.2
$\text{CO}_2$	-	2.4
$\text{TiO}_2$	1.9	1.5
$\text{P}_2\text{O}_5$	0.33	0.30

and  $H_2O^+$  concentrations, but these may be readily explained by processes of alteration (hydration and albitization).

Vallance (1974b) provided evidence from the Deccan Basalts for the derivation of a spilitic lava from a tholeiitic parent due to alteration effects. The Bhoiwada profile, Vallance suggested, represents one flow unit, the lower part of which was erupted subaqueously and the upper part subaerially. Due to sea-water alteration effects, the lower part has been altered and a spilitic mineral assemblage produced, with coincident chemical readjustments. The upper part, unaltered in nature and representing the parent for the spilite, is a typical Deccan Basalt tholeiite. This ideal picture does, however, possess certain difficulties, as outlined by Floyd (1977).

Pyroxenes, present within many spilitic rocks, also place severe constraints upon their mode of origin. It is generally considered (for example, by Vallance, 1974a; Nisbet and Pearce, 1977; Rowbotham and Bevins, 1978; Bevins, this work) that pyroxenes in spilites represent metastable relict phases. In the Bhoiwada section (see above), Vallance (1974b) illustrated the similarity of pyroxene compositions from the basalt and the spilite. The pyroxenes are augites and Vallance (op. cit.) concluded that they must have crystallized with a calcic plagioclase feldspar, which is now pseudomorphed by albite within the spilitic rocks. Similar conclusions are reached in this study from a consideration of the compositions of pyroxenes analysed from the altered basalts and dolerites (see Chapter 4). Nearly all the pyroxenes have typical igneous compositions. Recently, Nisbet and Pearce (1977) have used pyroxene compositions in altered basic igneous



rocks to discriminate between magma types. However, this extension to magma type discrimination is criticised by Rowbotham and Bevins (1978).

It is possible to envisage a simple model for the derivation of spilites from basalts. This relates the characteristic chemical composition of spilites with the secondary phases which are developed within them. Albite is almost ubiquitously developed and hydrous phases are also common. A model of albitization of the plagioclase feldspar, resulting in a net loss of calcium from the system, coupled with an increase in sodium, can be pictured. The development of hydrous phases such as chlorite, serpentine or amphibole would account for increased  $H_2O^+$  contents, whilst some of the calcium and aluminium, liberated from the feldspar may be fixed in calcium-aluminium silicates, such as prehnite, pumpellyite or epidote.

Nearly all of the above mentioned phases are present within basic rocks of the Fishguard area and it is considered that the Fishguard Volcanic Group represents a suite of basic, intermediate and acid lavas and associated intrusions which have suffered alteration. It is now pertinent to examine the processes which may have been responsible for this alteration.

#### 5.3.1. ALTERATION PROCESSES

Three principal processes have been attributed to the production of spilites and other metabasalts, namely sea-water alteration, hydrothermal alteration, and low-grade metamorphism (either burial or regional). Metamorphism has long been suggested as a possible cause

of spilitization, whilst the other two processes have received increased attention in recent years, principally due to the extensive programme of the Deep Sea Drilling Project. Complex models relating to the alteration of the oceanic basement have lately been described (for example Spooner and Fyfe, 1973).

#### 5.3.1.1. BASALT - SEA-WATER INTERACTION

Basalts drilled and dredged from the ocean basins have been seen, in many cases, to be extensively altered. Here the principal cause of alteration is the interaction between sea-water and the solidified basaltic lava. Scott and Hajash (1976) reviewed the processes of basaltic pillow lava alteration put forward recently by workers such as Melson and Van Andel (1966), S. R. Hart (1969), R. A. Hart (1970), Matthews (1971), Melson (1973), Thompson (1973) etc. The picture is necessarily complicated by the fact that the pillows possess initial textural differences within the body, from a glassy outer crust to crystalline core. However, two basic types of alteration have been identified; firstly a high temperature process which occurs immediate upon eruption, followed by a low temperature (halmyrolitic) alteration, after the initial cooling. Thompson (1973) attempted to identify which part of a pillow body is more representative of the initial magma composition, either the glassy crust or the crystalline interior. He concluded that initially the glassy crust remained unaltered and acted as a closed system, whereas the crystalline pillow interior was initially exposed to high temperature fluids and later to low temperature fluids along the radial joint pattern which commonly develops in pillowed lava. Thus, he suggested that in young basalts the glass from the outer crust is more representative of original composition. However, as soon as palagonitization starts to occur then

the chemical composition of the glass is rapidly altered and the situation becomes reversed with the 'relatively' fresh interiors being closer to the original composition.

Obviously it becomes difficult to monitor all the chemical changes related to the alteration of pillow cores and rims by these two processes, although it is generally agreed that certain elements are more susceptible to alteration than others (see below).

#### 5.3.1.2. HYDROTHERMAL ALTERATION

Extensive investigations of obducted ophiolite complexes and other ultramafic masses (e.g. Troodos, Othris Mountains, E. Liguira) have revealed the presence of altered basic and ultrabasic components, commonly cross-cut by thick hydrothermal veins. Spooner and Fyfe (1973) envisaged a sub-seafloor geothermal system involving the circulation of large amounts of heated sea-water through the system. Large volumes of water, penetrating down to depths of 2km or more are considered to take part in a convective cycle with water temperatures reaching a maximum temperature in the E. Liguira complex of approximately  $370^{\circ} \pm 30^{\circ}\text{C}$ . This type of system is thought to be responsible for the generation of metabasaltic rocks dredged from the ocean floors, such as described by Melson et al. (1968), Cann (1969, 1971) and Miyashiro et al. (1971).

#### 5.3.1.3. LOW-GRADE METAMORPHISM

Spilites and meta-basalts commonly appear in the stratigraphical column associated with metasediments and metavolcaniclastic rocks showing mineralogical and textural evidence of reconstitution under low-grade metamorphic conditions. Secondary minerals present within the

volcanic rocks may also be identified within the sedimentary horizons (as for example the occurrence of pumpellyite in sediments associated with Ordovician metavolcanics at Builth Wells, Wales).

There is little doubt in these cases that the origin of the spilitic lava is due to metamorphic alteration. Chemical alteration during metamorphism depends primarily upon the mineralogical reconstitution which occurs, which itself is largely governed by the primary mineralogy and texture of the lava concerned. Considerable complexities occur in pillowed lava bodies, due to local variations in texture and mineralogy, as described in more detail later. Although phases such as chlorite, calcite and albite are ubiquitously developed at low grades of metamorphism and their distribution is governed by the factors described above, other minerals are more restricted by variables such as pressure, temperature, partial pressure of  $H_2O$ ,  $CO_2$ , etc. Most important amongst these are prehnite, pumpellyite and actinolite and which have been used to suggest pressure and temperature conditions prevalent during the metamorphic episode.

This particular process of spilite formation has gained much support from Coombs (1974), Smith (1968) and others, and it is suggested as being the principal process concerned in the production of metabasalts within the Fishguard Volcanic Group. However, it is possible that the rocks may have been altered by either of the two processes outlined above, prior to subsequent burial and metamorphism, which have now erased evidence of earlier alteration processes.

## 5.3.2. CHEMICAL EFFECTS OF THE PRINCIPAL TYPES OF ALTERATION

The processes outlined above produce a redistribution of the elements related to the breakdown of the primary igneous mineral assemblage and the development of secondary phases. As the processes differ in nature, different chemical trends are produced depending upon the process involved. The greatest contrast appears between initial submarine weathering and metamorphism (either produced by a sub-seafloor geothermal system or by regional metamorphism with burial). Relative mobilities of major elements are shown in Table 3 below. Of critical importance, naturally, is the degree of alteration which the rocks have suffered.

TABLE 3

	<u>Initial submarine</u> <u>weathering</u>	<u>metamorphism</u>	
$\text{SiO}_2$	loss	loss or gain	data from
$\text{TiO}_2$	immobile	immobile	Pearce (1975),
$\text{Al}_2\text{O}_3$	immobile	slight loss	Cann (1969),
$\text{FeO}$	loss	loss	Miyashiro <u>et al.</u>
$\text{Fe}_2\text{O}_3$	gain	gain	(1971),
$\text{MgO}$	loss	gain	R. A. Hart
$\text{CaO}$	loss	loss	(1973), Melson
$\text{Na}_2\text{O}$	gain	gain	and Van Andel
$\text{K}_2\text{O}$	gain	loss	(1966), Hart
			(1970),
			Matthews (1971).

These mobilities are, of course, generalizations, and trends opposite to those outlined above are to be found in the literature. For example, Wood et al. (1976) found an overall loss in MgO concentrations in basalts from Eastern Iceland which have undergone low-grade metamorphism (Zeolite facies). The picture is also somewhat more complex for pillow lava sequences, where primary textures and mineralogy appear to govern alteration patterns. Mevel (1975) emphasized this control over chemical zonation observed in pillow lavas from the French Alps; a similar control has been operative in the Fishguard Volcanic Group lava pile.

In Appendix 1 are listed chemical analyses of core and rim samples from six pillows from the Fishguard Volcanic Group. The original glassy crust has been lost from these pillows, presumably early in their history, with fragments often being identified within the interpillow material when present. The rim thus represents the outermost zone of the pillow which had a crystalline nature upon consolidation; equivalent to the 'zone spherolitique' of pillows from Les Gets (Mevel, 1975). The rims of the Fishguard pillows generally show quench textures, including spherulites of plagioclase, with minor clinopyroxene. In the core regions, which display evidence of crystallization conditions which were closer to equilibrium, clinopyroxene has a higher modal abundance. Thus this original mineralogical contrast, which was governed principally by rates of cooling (presently shown by textural contrasts) produced original chemical inhomogeneities. With metamorphism and recrystallization, the development of secondary phases has necessarily been governed by available sites, and thus a chemical zonation has been preserved.

Naturally, each pillow varied in size and consequently in cooling history. Some pillows were chilled very quickly by contact with seawater, whereas others were rapidly buried by other pillows or were larger entities, allowing a slower cooling history. It is felt this may be a cause of the lack of uniform trends between core and rim samples. Increases in  $\text{Na}_2\text{O}$  and  $\text{Al}_2\text{O}_3$  contents in rim samples are fairly constant, however, and this possibly reflects the albitization of the high modal plagioclase contents of the pillow margins. Although albitization releases aluminium, it is likely that it is fixed locally, along with liberated Ca, in hydrated calcium aluminium silicates, such as epidote, prehnite, and pumpellyite, all of which are found within the basic igneous rocks of the Fishguard area. Calcium values are generally lower in the rims of the analysed pillows, as might be expected.

In an attempt to bring uniformity to the analysed rocks, only pillow cores were analysed in the belief that they possibly represent liquids which have suffered crystallization under conditions closer to equilibrium than more marginal zones. However, it is obvious that chemical complexities have been introduced as a result of secondary processes and due consideration of the likely effects of these processes must be made before the chemical variations identified may be related to igneous processes.

As far as possible, only the freshest material was collected for analysis. Smith (1968) described an alteration sequence produced during burial metamorphism of Ordovician lavas in New South Wales, in which the colour of the lava changed with increased alteration from grey, through grey/green to yellow/green. In view of this, 'grey'



material was, as far as possible, collected. Indeed, petrographic examination clearly shows that the 'grey' material contains lesser amounts of secondary minerals. In a number of cases, however, altered material was collected with a view to examining the effects of the presence of these phases on the whole-rock chemistry. Samples SB15, SB58, and SB59 are samples which are heavily carbonated, the effects of which are discussed below.

#### 5.3.2.1. MAJOR ELEMENT RESULTS

The possible effects of alteration upon the chemistry of the rocks in question will be dealt with under two headings, namely rocks <64%  $\text{SiO}_2$  and rocks with >64%  $\text{SiO}_2$ . The rocks of the Fishguard area have been divided into four groups (groups i-iv below), based upon silica concentrations. This is described in more detail below (section 5.4.).

##### (i) Rocks with <64% $\text{SiO}_2$

In an attempt to identify chemical changes produced as a result of alteration various elemental plots have been utilised. One such plot (used, for example, by Hattori et al., 1972; R. A. Hart, 1973; Floyd, 1976; Coish, 1977) is that of water content or total volatile content against major element concentrations. When major element concentrations of the basic (group 1) and intermediate (group 2) members of the Fishguard Volcanic Group and high level intrusives are plotted against total volatiles, few significant correlations are observed. However, certain points appear worthy of explanation. Firstly, a negative correlation between  $\text{Na}_2\text{O}$  and total volatiles is present. An identical correlation has previously been

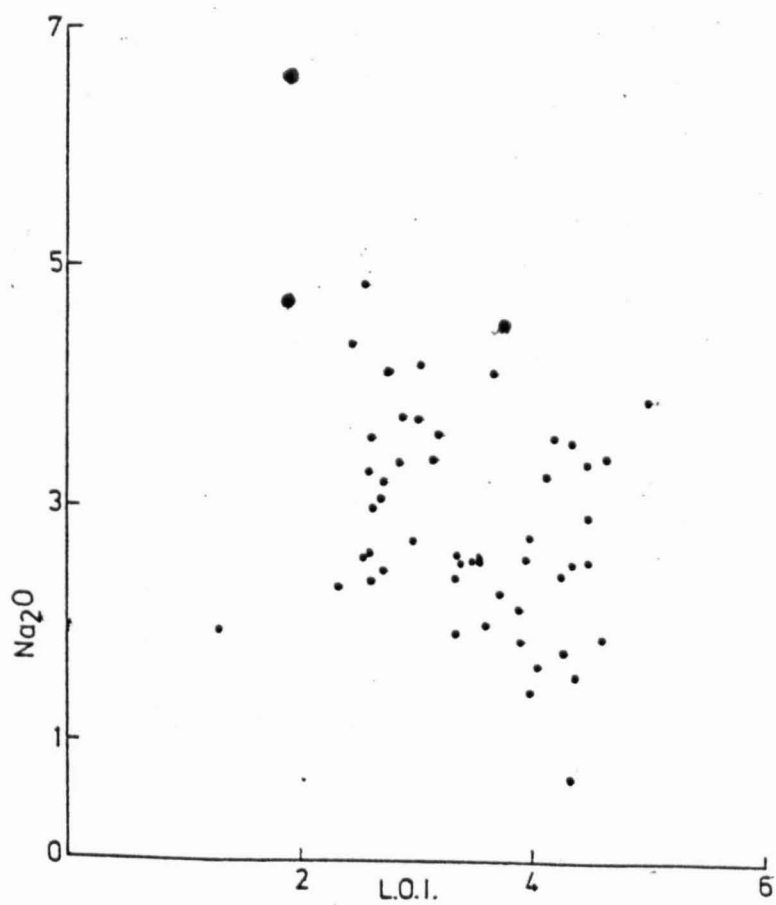
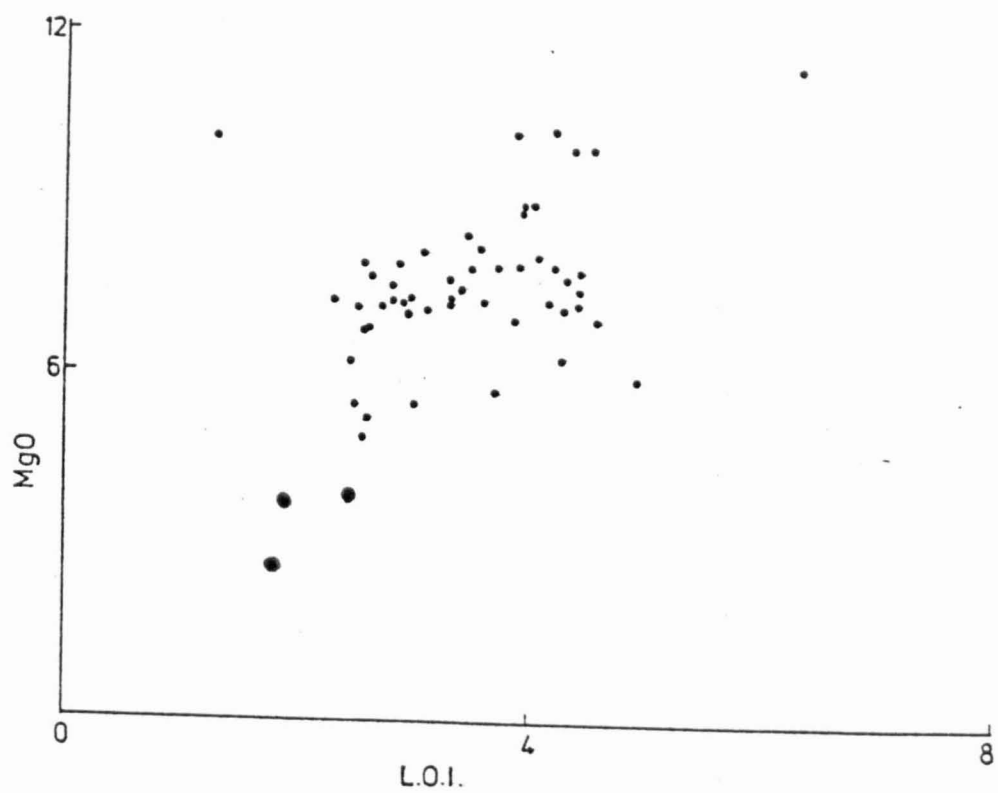


observed by Hattori et al. (1972), who attributed it to leaching during hydration, and also by Coish (1977) who suggested that it was due to the introduction of Na-free hydrous phases. This latter cause may well be responsible for the observed trend in the Fishguard Volcanic Group rocks, as a slight positive correlation between MgO and total volatiles is also present (see Fig. 166). Group 2 rocks have lower modal properties of mafic minerals, whilst they have higher proportions of feldspar, when compared with group 1 rocks. The feldspar in these rocks would initially have been more Ab rich than group 1 rocks, and upon alteration even more sodium would have been introduced due to the availability of abundant sites. However, the development of secondary, hydrous phases, which generally replace mafics, would be restricted. A small amount of the calcium liberated during albitization may be fixed in phases such as pumpellyite, but the possibility of the formation of phases such as chlorite, actinolite etc. is restricted. Group 1 rocks, however, show lesser increases in sodium, due to lower amounts of modal feldspar, whilst secondary hydrous phases, such as chlorite, allow relatively large amounts of water to be incorporated. These variations are shown in Figure 167. Clearly not all the variation is produced as a result of these factors, as no consideration of calcite formation is considered.

Another method of identifying possible alteration effects is to plot major element concentrations against a so-called 'immobile' element. Zirconium has previously been used for this purpose (for example by Wood et al., 1976; Coish, 1977), based upon evidence (e.g. Cann, 1970; Pearce and Cann, 1971) that this element is relatively immobile during low-grade alteration processes. If the element which is plotted against Zr is expected to show any significant correlation

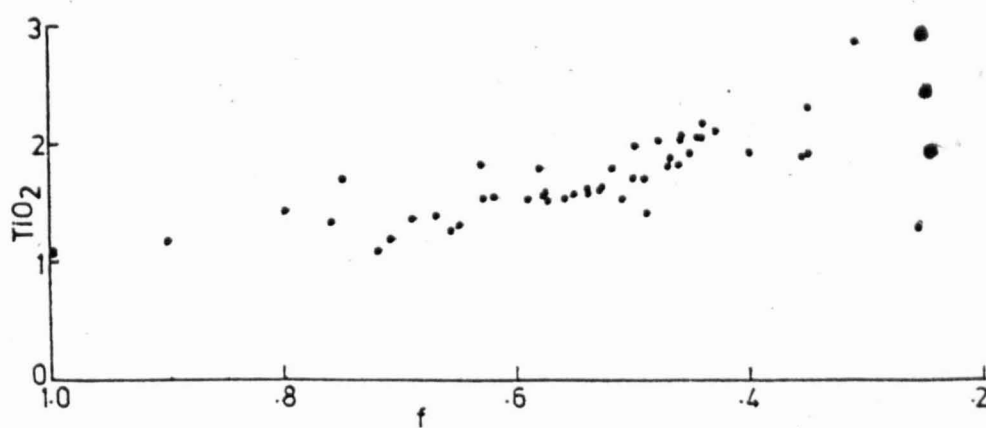
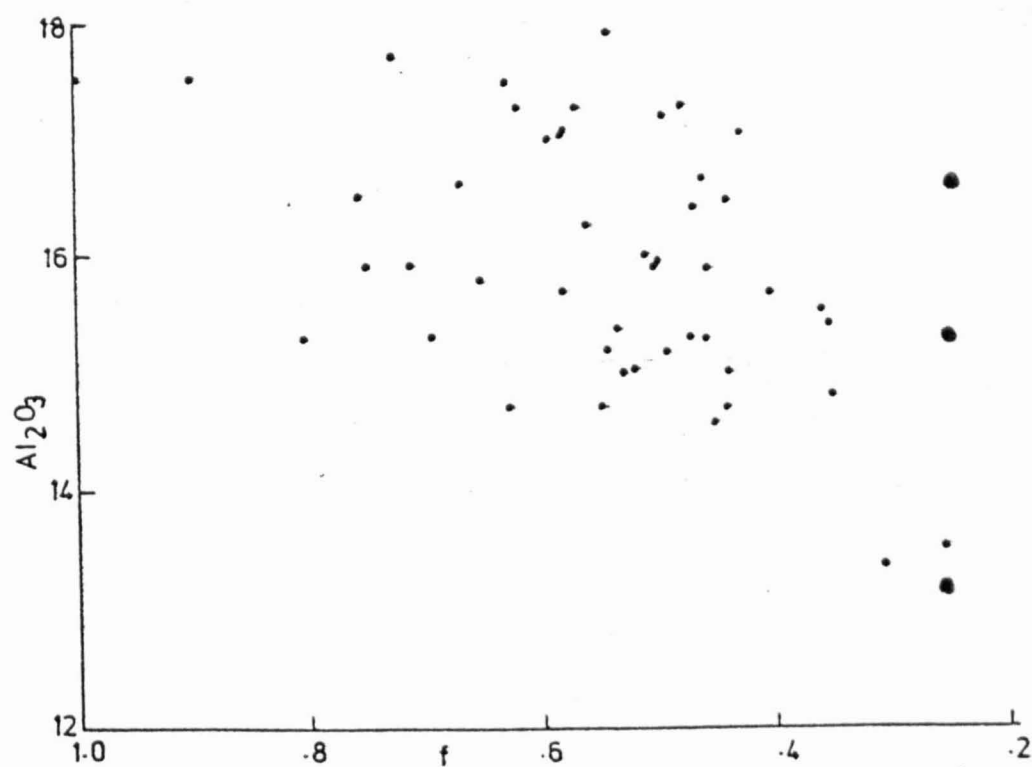
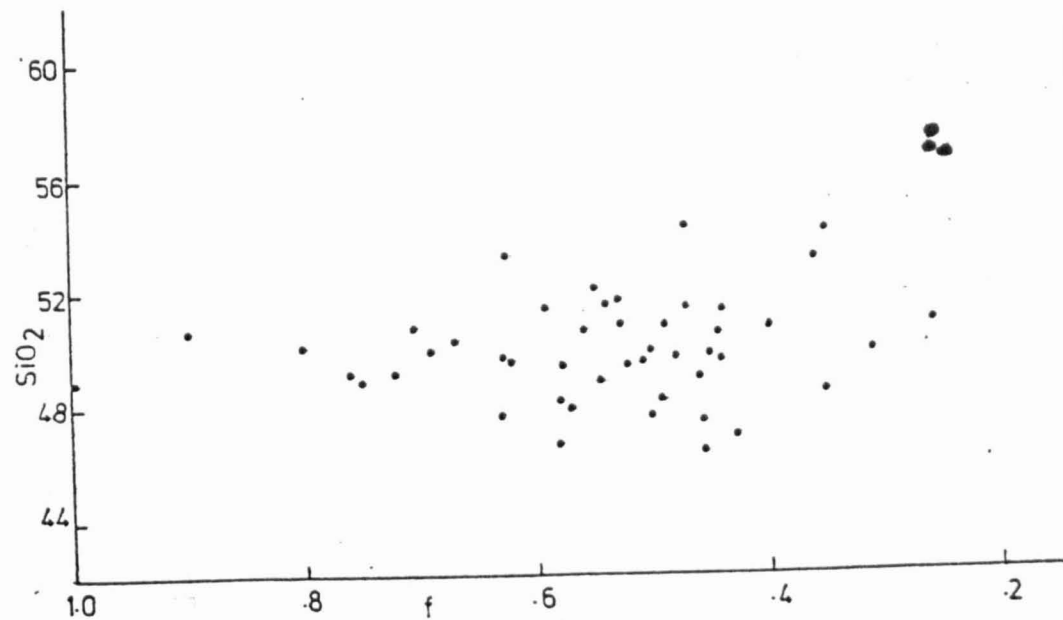
FIG. 166.  $MgO$  vs L.O.I. (loss on ignition) for group 1 and group 2 rocks.  
(Small dots are group 1 rocks, large dots are group 2 rocks).

FIG. 167.  $Na_2O$  vs L.O.I. for group 1 and group 2 rocks.  
(Small dots are group 1 rocks, large dots are group 2 rocks).

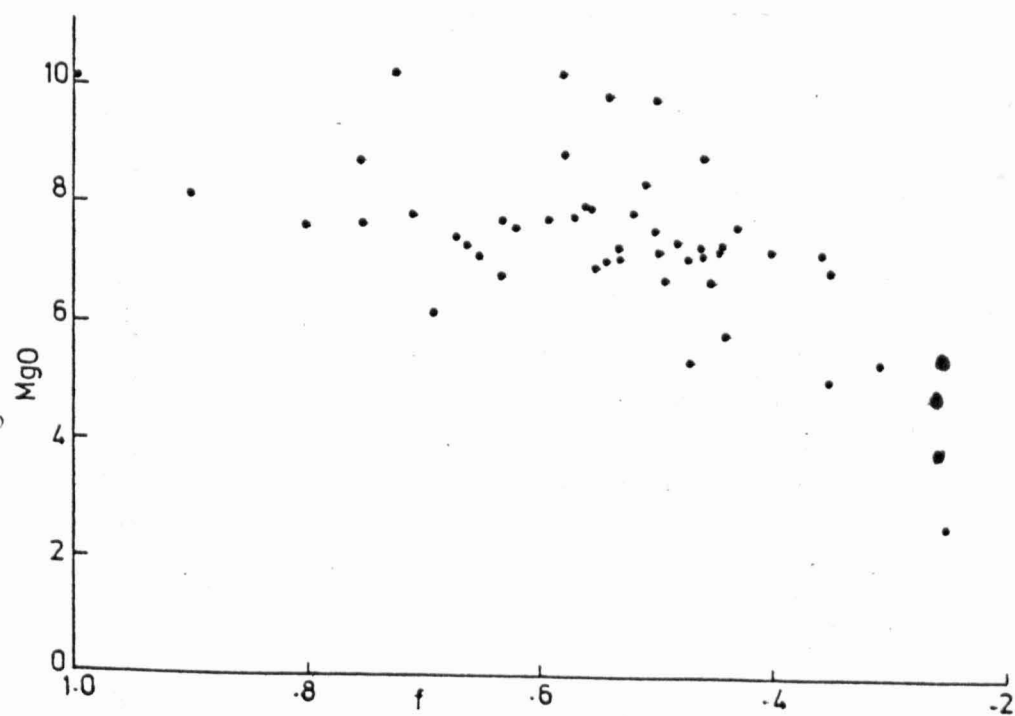
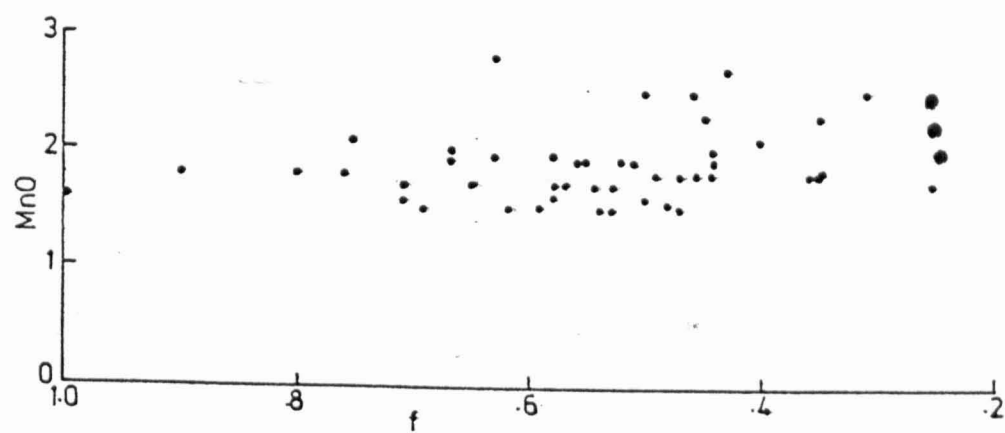
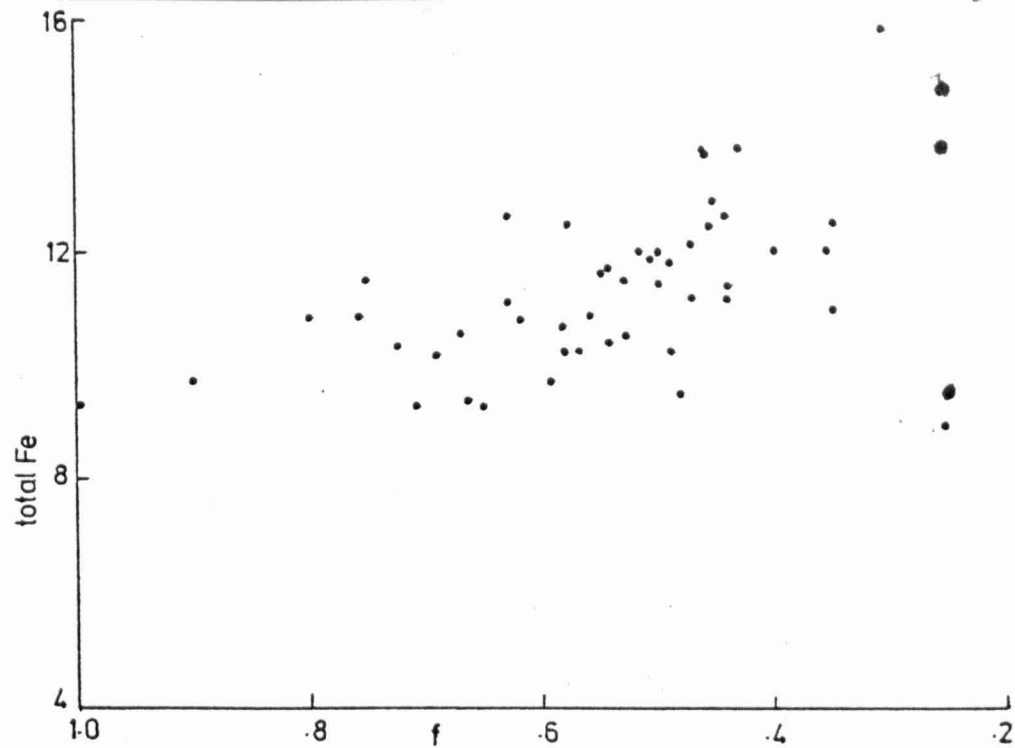


then this will be preserved if the abundances are not significantly altered. In the present work this approach is slightly modified. Major elements are plotted against 'f', where 'f' is equal to the amount of residual liquid remaining and is determined from  $C_i^0/C_i^L$ , where  $C_i^0$  is equal to the concentration of an incompatible trace element i in the original melt (in this case Zr) and  $C_i^L$  is the concentration of trace element i in the derived liquid. A fuller explanation of the derivation of this ratio and the justification of its use here is given below (Chapter 6). As will be shown later, the basic to intermediate rocks of the Fishguard Volcanic Group represent a suite of rocks generated by fractional crystallization. Thus 'f', in this case, can be used to monitor chemical changes during the evolutionary history of the liquid and consequently it is possible to see if any significant deviations from the expected variations are present.

Figure 168 shows the variation of major element values plotted against 'f' (where 'f' is taken as representing an index of differentiation) for the group 1 and 2 rocks of the Fishguard area. Particularly clear in this Figure is the good positive correlation between 'f' and  $P_2O_5$  and  $TiO_2$ . These are considered to represent original correlations and is in agreement with other work which suggests that these two oxide values commonly closely reflect original values in altered basic igneous rocks (e.g. Pearce and Cann, 1971). Other correlations are seen for MnO, Fe (total) and MgO against 'f'. The fact that iron and magnesium values appear relatively unaltered suggests that  $Fe/Fe + Mg$  (where Fe = total iron) may also be used as a differentiation index for this suite. Figure 169 illustrates a relatively good positive correlation between 'f' and  $Fe/Fe + Mg$ .



FIGS. 168a to j. 'f' vs major element values for group 1 and group 2 rocks. (Small dots are group 1 rocks, large dots are group 2 rocks).



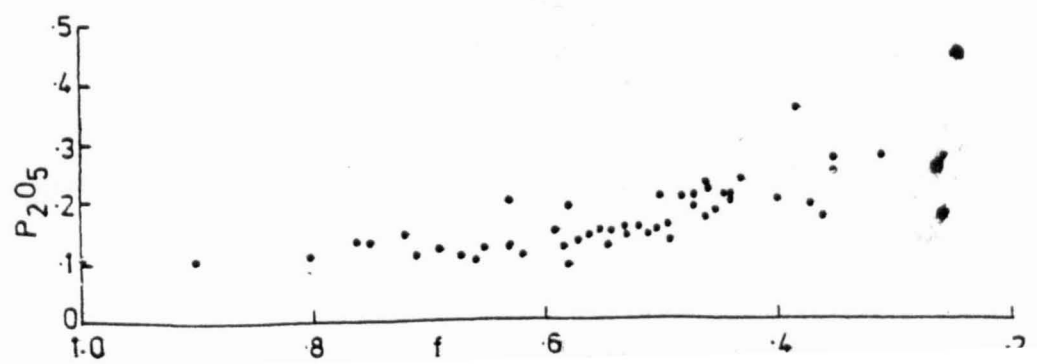
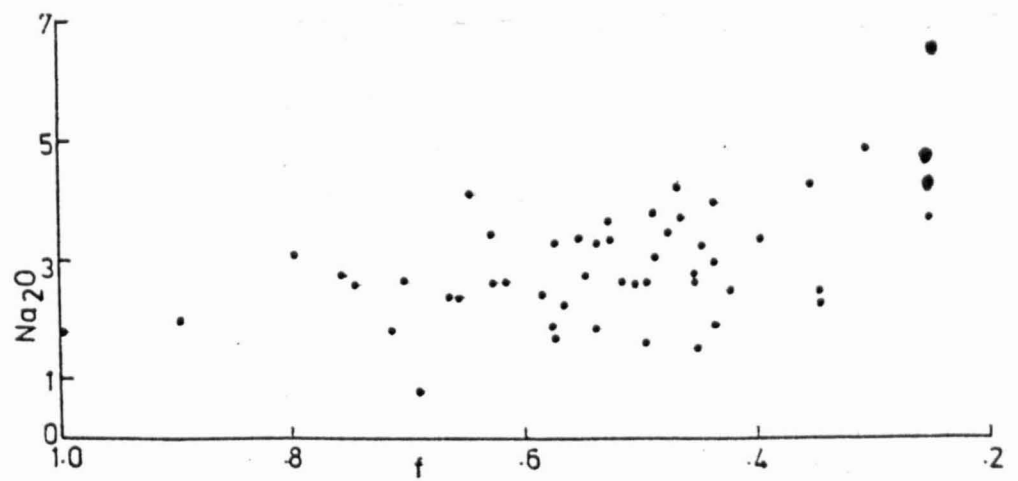
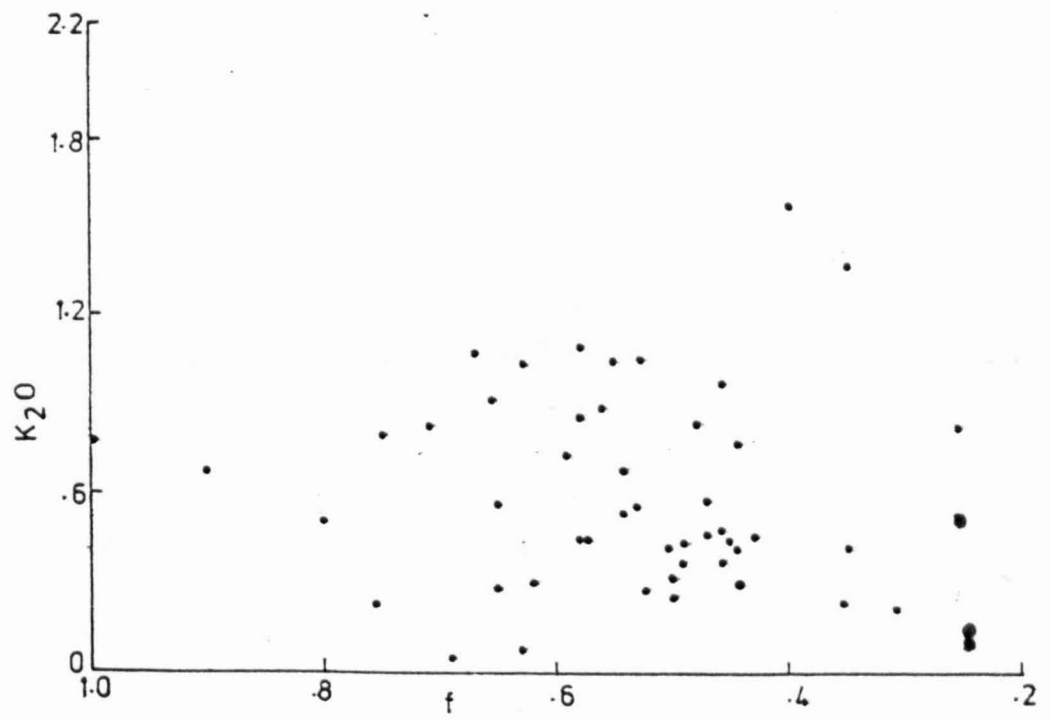
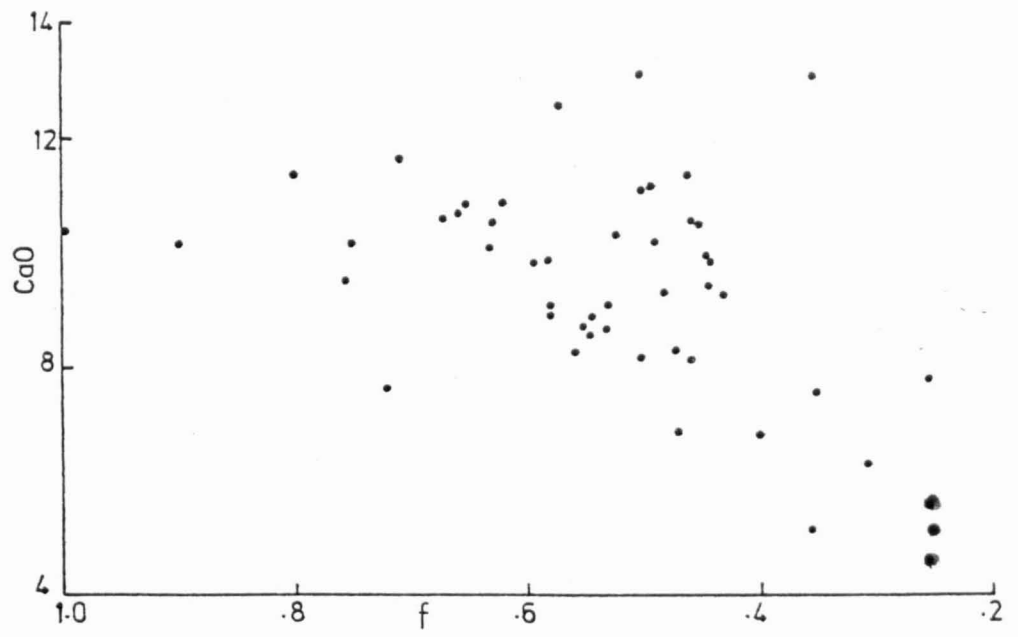
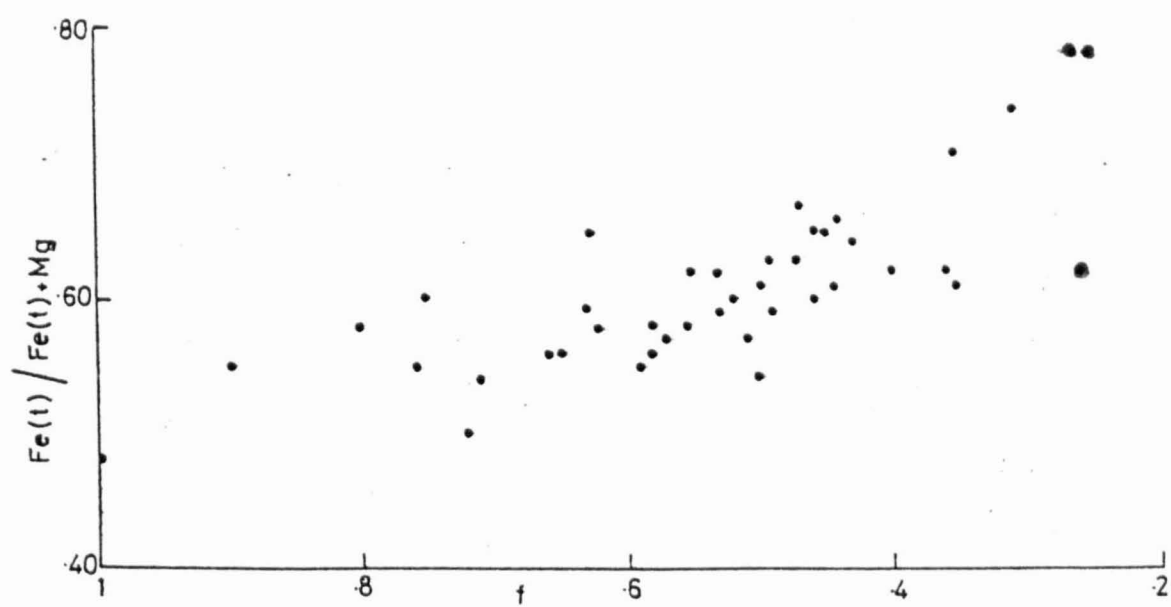




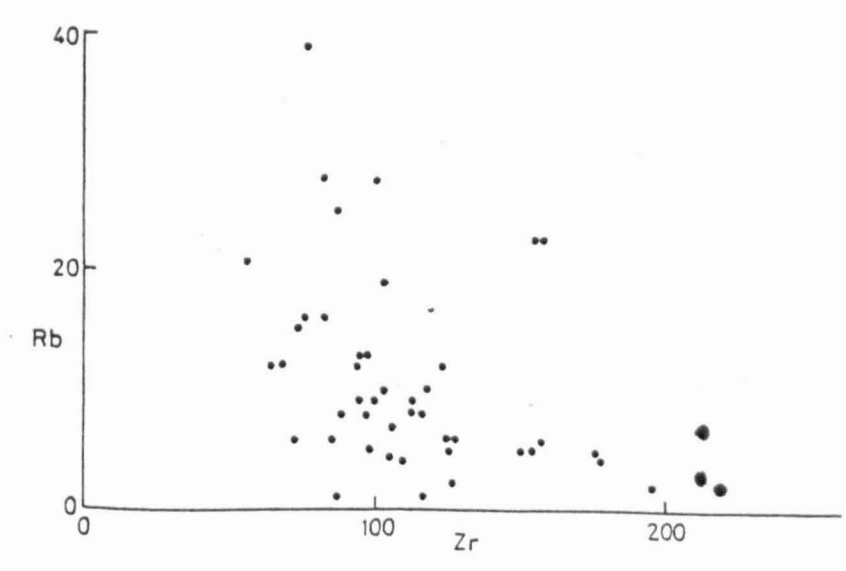
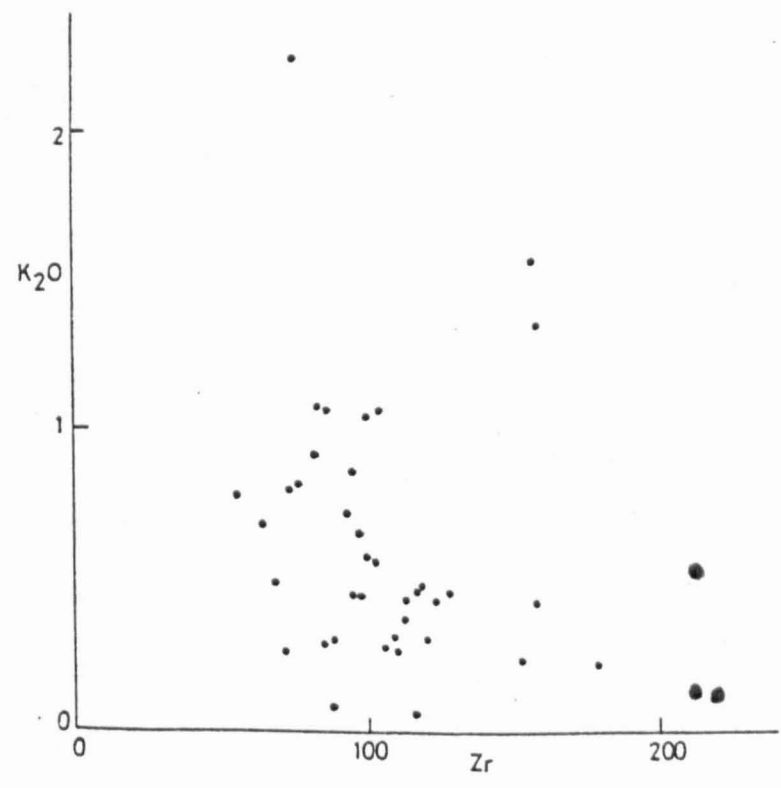
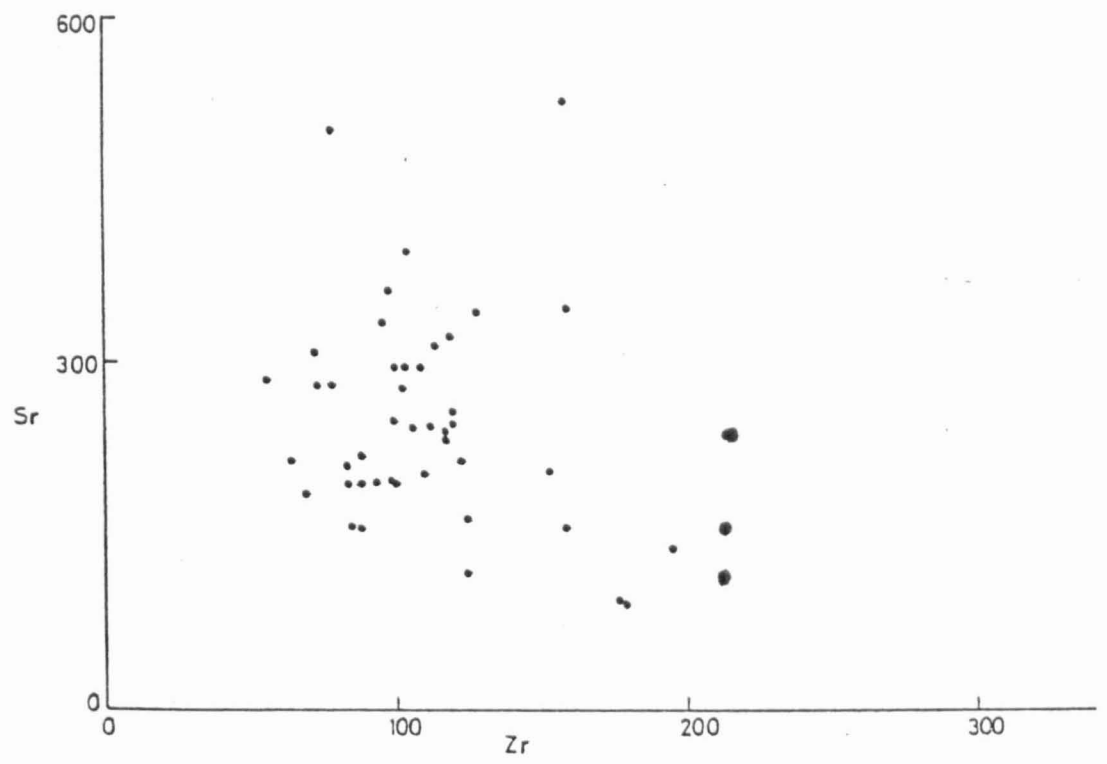
FIG. 169. 'f' vs  $\text{Fe}(t)/\text{Fe}(t) + \text{Mg}$ , where  $\text{Fe}(t)$  = total iron as  $\text{Fe}_2\text{O}_3$ , for rocks of group 1 and group 2.  
(Small dots are group 1 rocks, large dots are group 2 rocks).



Weaker correlations can be observed for  $\text{SiO}_2$ ,  $\text{Al}_2\text{O}_3$ ,  $\text{CaO}$  and  $\text{Na}_2\text{O}$  and it is thought that these also are the result of igneous processes.  $\text{K}_2\text{O}$  versus 'f' shows considerable scatter (Fig.170) and is probably the result of alteration. The mobility of potassium has been emphasised by many workers (for example, S. R. Hart, 1969). Sr and Rb both show considerable scatter, when plotted against Zr (Fig.170) and are also considered to have suffered alteration.

From a consideration of these correlations it is possible to interpret the processes of alteration which have taken place and this may be tested against petrographical evidence. Weak correlations between 'f' and  $\text{CaO}$ ,  $\text{Al}_2\text{O}_3$ ,  $\text{Na}_2\text{O}$ , and  $\text{SiO}_2$  may possibly reflect varying modal proportion of feldspar, but more probably are the result of varying degrees of albitization. During this process  $\text{Na}_2\text{O}$  and  $\text{SiO}_2$  are increased within the feldspar, whilst  $\text{CaO}$  and  $\text{Al}_2\text{O}_3$  are lost. As stated elsewhere (Chapter 4), albitization has variably affected the rocks of the Fishguard area, with An-rich feldspars preserved in certain rocks (e.g. LG7), whilst pure albite is found in others. The scatter of  $\text{K}_2\text{O}$  values probably reflects the production of varying amounts of sericite or clay minerals. The correlation of 'f' with  $\text{Fe}^*$ ,  $\text{TiO}_2$ ,  $\text{MnO}$  and to a lesser extent  $\text{MgO}$  all suggest little alteration of these values, probably reflecting that the major mafic phases, clinopyroxene and ore are generally unaltered. Although the primary iron-titanium phase has been leached of titanium, this is fixed locally in sphene and leucoxene. The possibility of the former presence of another mafic phase (olivine) will be discussed below.

FIGS. 170a to c. Sr,  $K_2O$ , Rb vs Zr for rocks of group 1 and group 2.  
(Small dots are group 1 rocks, large dots are group 2 rocks).



In conclusion, it can be said that values obtained for Fe, Mg, Ti, Mn, and P appear to reflect original values. Si, Ca, Al, and Na have been modified to varying degrees, although even these still retain an overall variation suggestive of magmatic processes, whilst K appears to have been affected in such a way as to render it of no value in a petrogenetic interpretation of these rocks.

(ii) Rocks with  $>64\% \text{SiO}_2$

It is more difficult to discuss possible alteration effects on these rocks as, in recent years, less attention has been focussed on rocks of this composition. Intermediate to acid lavas of the Fishguard area were only sparsely phenocrystic upon eruption and crystallized rapidly to produce glassy flows, which subsequently devitrified. The rhyolites presently show variable  $\text{K}_2\text{O}$  and  $\text{Na}_2\text{O}$  concentrations and appear to have suffered alkali metasomatism, similar to that described by Hughes et al. (1971) in rhyolites from Newfoundland. The rhyodacites and dacites exposed at Porth Maen Melyn show a comparatively limited range in composition (see Appendix 1), with  $\text{K}_2\text{O}$  contents showing the greatest variability. The presence of abundant mica in the isolated-pillow breccias (Bevins and Roach, in press) suggests considerable potassium metasomatism.

#### 5.3.2.2. TRACE ELEMENT RESULTS

A number of trace element determinations were made within rocks from the Fishguard area. These are tabulated in Appendix 1, along with an account of the accuracy and precision of these results. If any of the trace element values determined are to be used in an attempt to understand the petrogenetic processes responsible for the generation and

evolution of the Fishguard magmas, then it must first be established whether values recorded during the present study represent original values or if they have been subsequently modified during alteration processes, such as low-grade metamorphism.

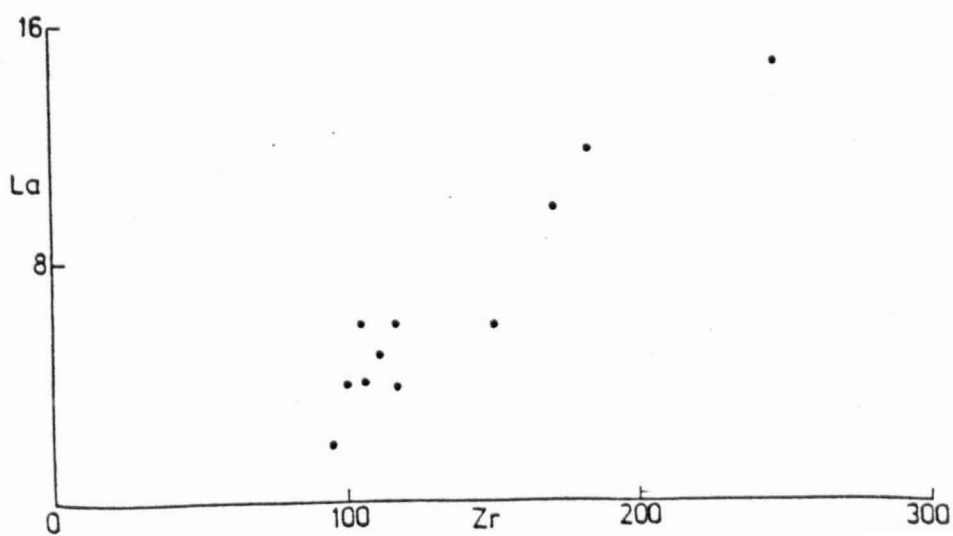
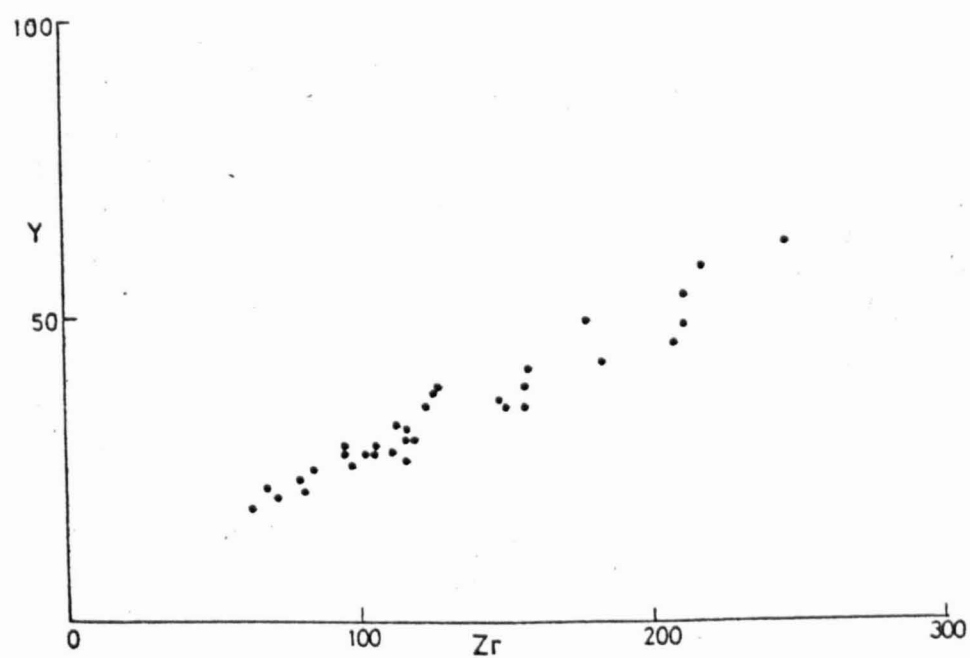
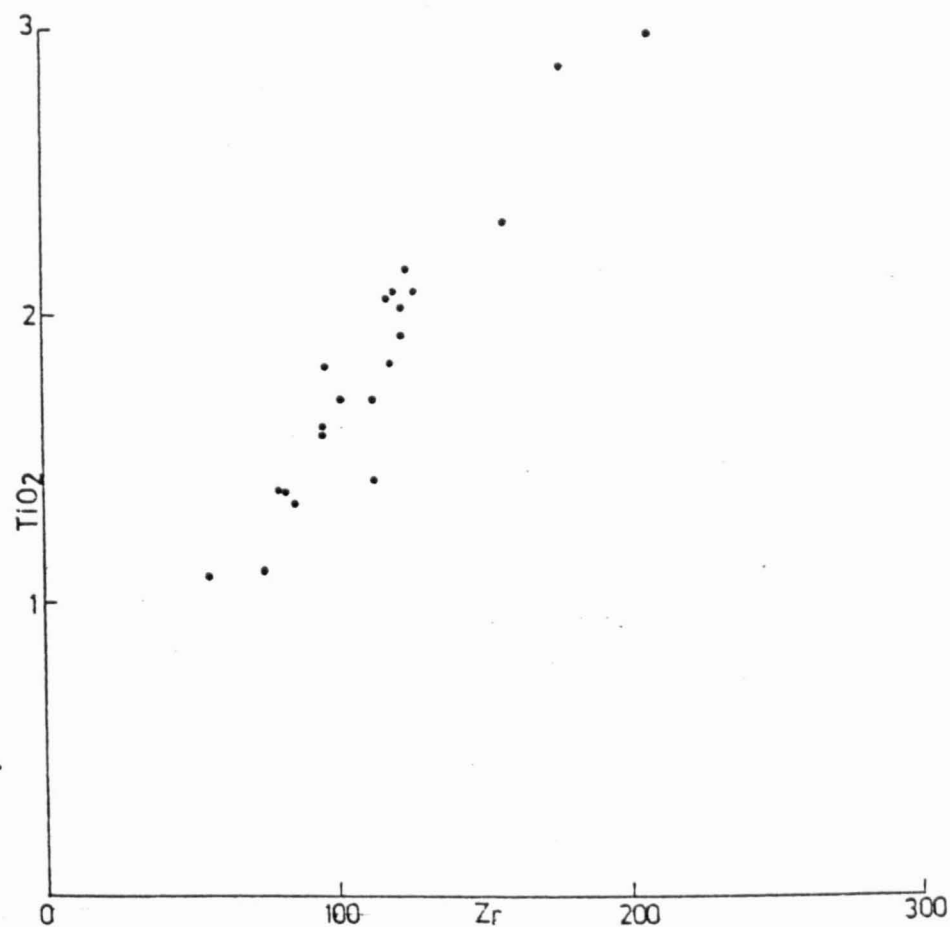
The idea that certain trace elements were immobile was first suggested by Cann (1969). He noticed that certain trace element concentrations in fresh and altered basaltic rocks were similar enough for the differences to be the result of experimental error and that they were therefore largely unaffected by alteration processes. In recent years, many models have been developed in order to determine the tectonic setting of ancient magmatic suites (for example, Pearce and Cann, 1971 and 1973; Floyd and Winchester, 1975; Furnes et al., 1976) and these models assume that certain minor and trace elements are 'immobile' during alteration processes. Zr, Ti, Y, Nb, and P are generally regarded as the most stable elements, whilst the rare earth elements are also considered to be relatively immobile (see Floyd, 1977). 'Immobile' trace elements have also been utilised to determine magma type of ancient volcanic rocks, as well as determining the degree of fractionation of such rocks. Sr and K have also been used in discriminatory diagrams, but it is here considered unlikely that present values in the Fishguard lavas and intrusions are in any way representative of original concentrations. This conclusion was also reached by Smith and Smith (1976) for Sr and K contents in Ordovician lavas from Cleifden, Australia. Positive linear correlations between element pairs from amongst Zr, Y, Nb, Nd, La, and Ce have been identified in many magmatic suites, (for example, Gregory Rift lavas, Scael and Weaver, 1971; Afar Depression lavas,

Treuil and Varet, 1973) and are due to the build up of these incompatible elements in the residual liquid during low-pressure fractional crystallization. It was also pointed out by Treuil and Varet (1973) that such a correlation may be produced by varying degrees of partial melting of the same source material. However, at this stage the exact process is not important, only that such a correlation is a primary chemical characteristic of the lavas in question. Figures 171 and 172 show strong colinear relationships between various incompatible elements and Zr for rocks of groups 1 and 2. Within groups 3 and 4, however, most of these elements are no longer incompatible due to the crystallization of phases such as zircon and apatite, and as a result study of the appropriate analyses in Appendix 1 shows that the strong linear correlations are no longer present. The significance of these results will be discussed later; the fact is clear that these correlations are primary chemical characteristics which appear to have been largely unaffected by secondary processes.

The transition elements, in contrast, are not incompatible elements, but are preferentially incorporated into major silicate lattices as a result of their affinity for octahedral co-ordination sites. Thus the behaviour of these elements in igneous processes is largely governed by the particular silicate phases precipitated at the time of crystallization, since certain elements are strongly concentrated in particular phases, for example Ni in olivine, Cr, V, and Sc in pyroxene, Cr in spinel, Cr, V, and Ti in oxide. Thus, in order to be able to interpret transition metal concentrations of altered basic igneous rocks, it is important to have an understanding



FIGS. 171a to c.  $\text{TiO}_2$ , Y, and La vs Zr for rocks of group 1 and group 2.



FIGS. 172a to d.  $P_2O_5$ , Nb, Nd, and Ce vs Zr for rocks of group 1  
and group 2.

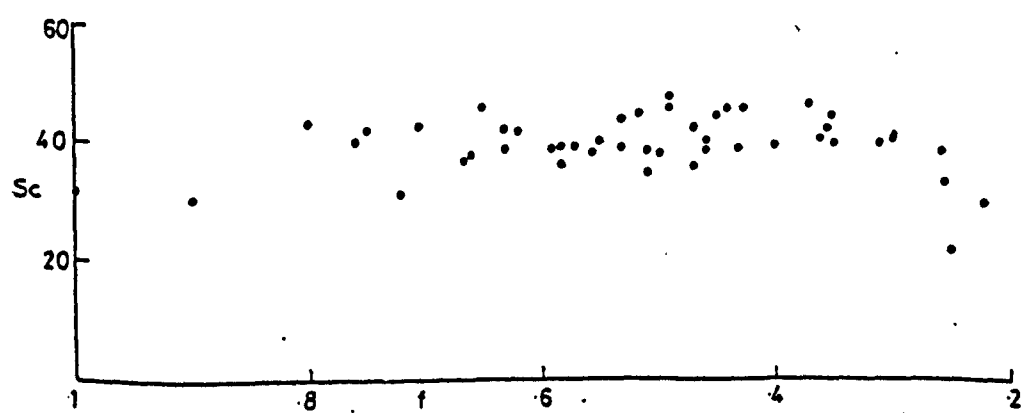
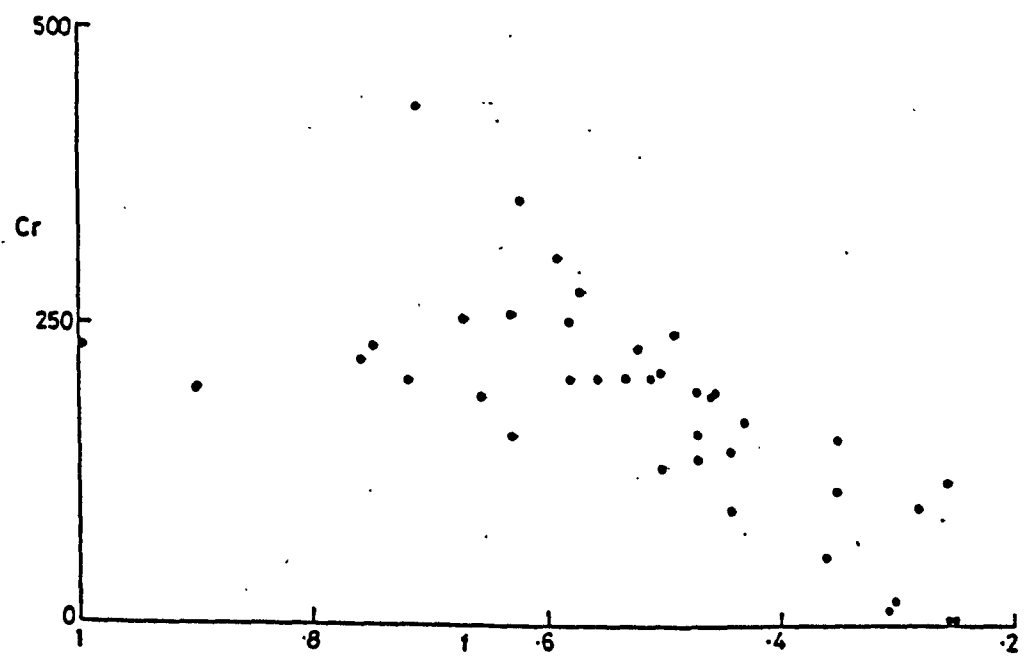
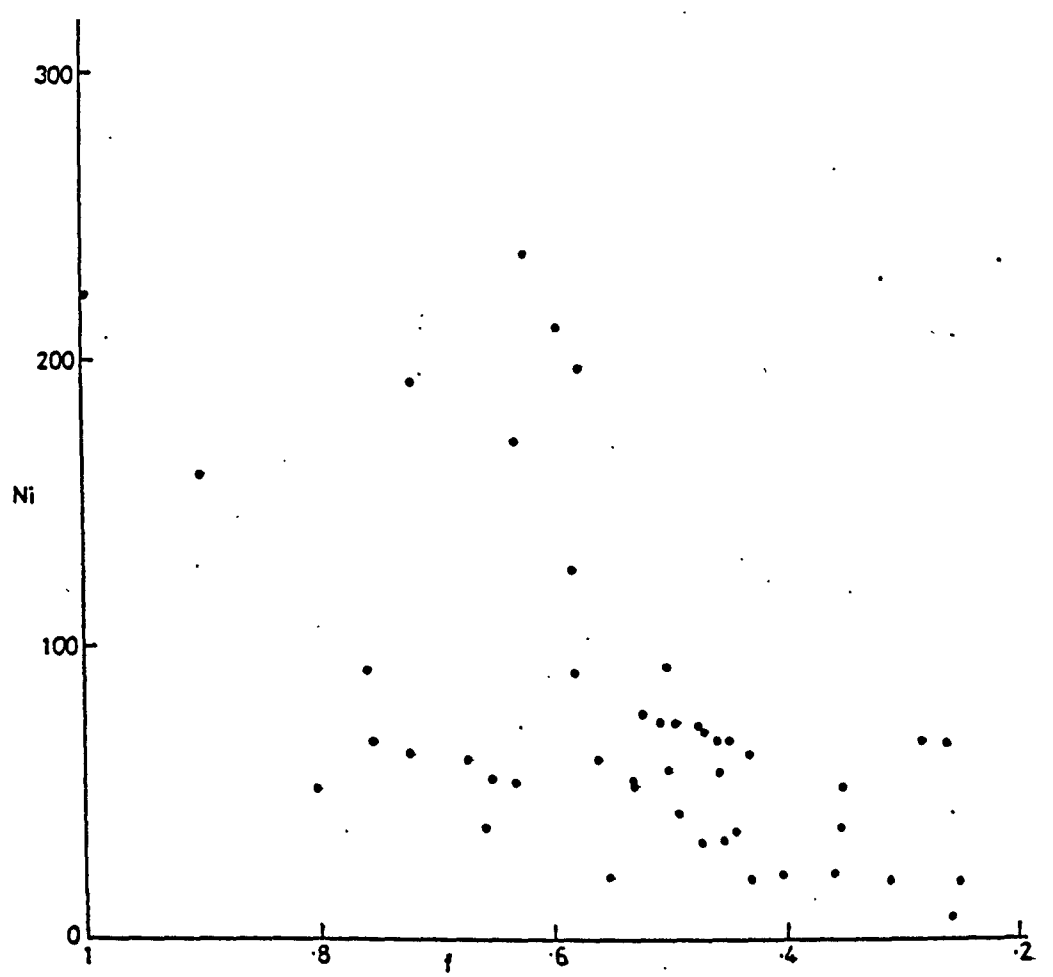


of the processes which have been operative during the evolution of the suite of rocks. Consequently, during low-pressure crystal fractionation processes involving olivine, pyroxene and an oxide phase, all of the important transition elements may be expected to diminish. In Figures 173 and 174, it can be seen that for rocks of groups 1 and 2 of the Fishguard area Ni and Cr decline with increasing 'f' (i.e. with differentiation), whilst Ti and V rise initially but behave erratically after approximately  $f = 0.40$ . Sc is apparently constant through to  $f \approx 0.35$ , after which it declines. These patterns are interpreted as being primary and the significance of these variations are discussed in Chapter 6.

The alkalis and alkaline earths (K, Rb, and Sr) are generally considered to be mobile during alteration processes (Pearce, 1975) and plots of these elements against zirconium for the rocks of the Fishguard area show a considerable scatter of points (Fig. 170) despite the fact that significant correlations are commonly seen in unaltered rocks. It is thus suggested that these elements have been mobile and that their present variable concentrations in rocks of the Fishguard area are secondary in origin and of no value in determining the petrogenesis of the magma suite.

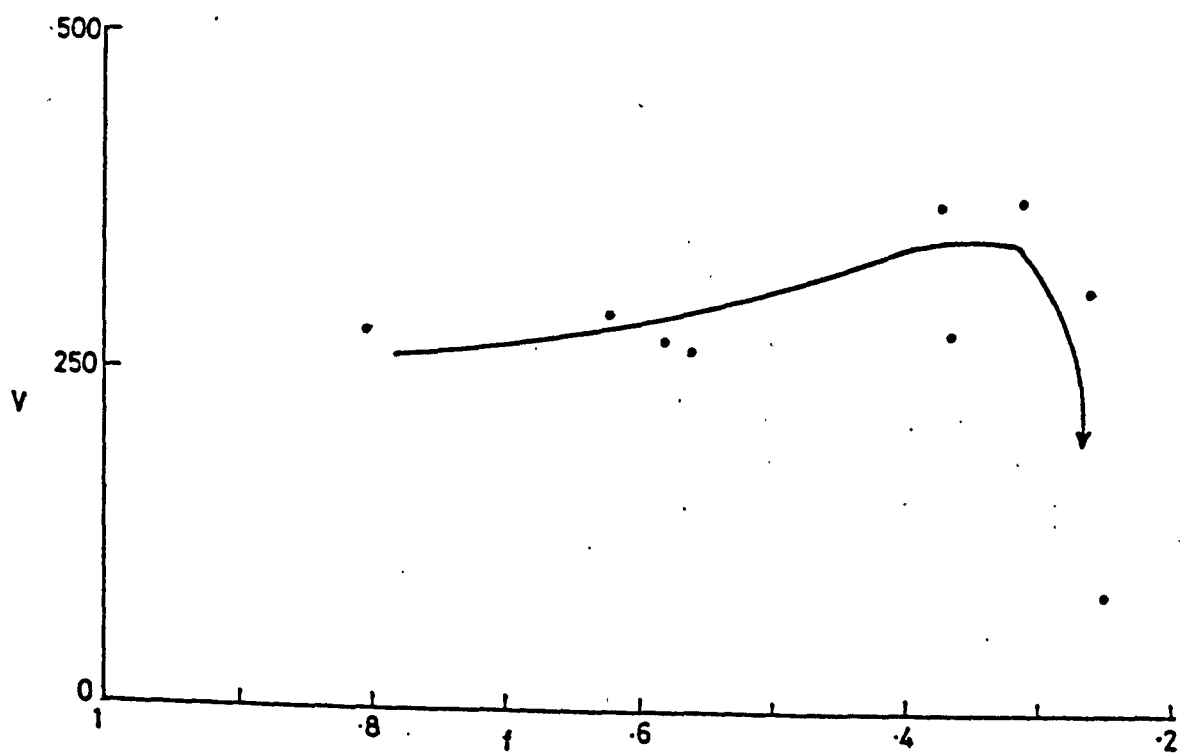
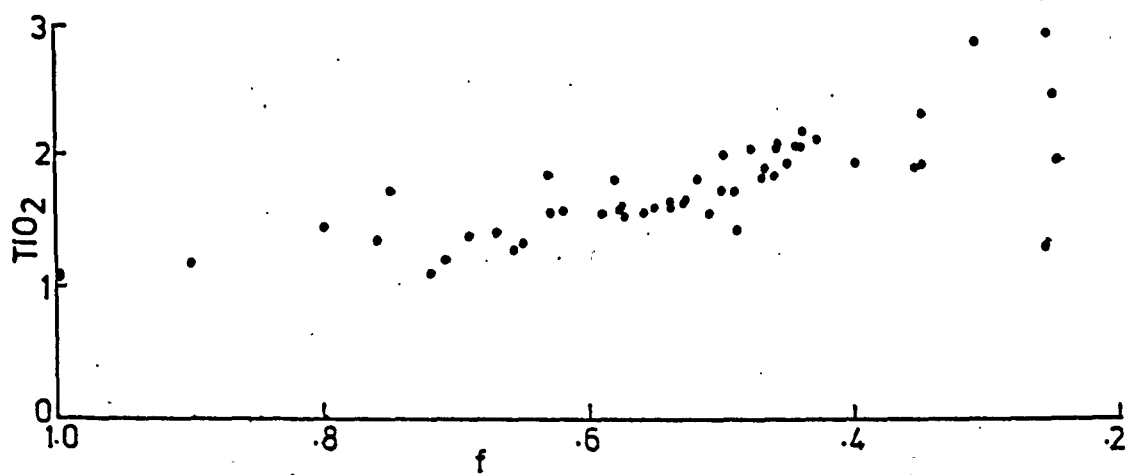
It is also possible to use petrographic evidence to determine which trace elements are mobile and which are relatively immobile during alteration. For example, in altered lavas in which the feldspar is albitized and calcium is liberated, it is likely that Sr will be very mobile. Smith and Smith (1976) showed in lavas from Cliefden that a correlation existed between high Sr values and the modal proportion of epidote. They also showed a significant correlation between high  $K_2O$  concentrations and high modal proportions of albite,

FIGS. 173a to c. Ni, Cr, and Sc vs 'f' for group 1 and group 2 rocks.



FIGS. 174a to c.  $TiO_2$  and V vs 'f' for group 1 and group 2 rocks.





a relationship not identified within the rocks studied here. Mobility of the transition elements is dependent upon whether the host silicate phases suffer alteration. Commonly clinopyroxene is a relict phase in metabasalts and thus the Cr and Sc present within clinopyroxene will most probably be retained. However, chromium is also contained within spinel, a phase rarely identified in metabasalts and possibly also the ore phase. Olivine is similarly susceptible to alteration and accordingly Ni values must be interpreted with caution. Ti, Cr, Sc, and V are found in the ore phase when present. In the rocks of the Fishguard area this was probably a Ti-bearing Fe ore with the Fe component relict, whereas the Ti has been subsequently liberated. However, leucoxene or sphene are generally the secondary stable residual phases produced and can be identified pseudomorphing or rimming the primary ore phase. Thus although this element has been mobile, the movement of Ti has commonly been on the millimetre scale and whole-rock values of Ti appear to be largely unaffected.

The location of incompatible elements in basic to intermediate rocks is somewhat more difficult to determine. Eales and Robey (1976) demonstrated that in certain differentiated Karroo rocks, Zr was present within opaque oxides, iron-magnesium silicates, and to a certain extent also within the mesostasis. Nb was found to be concentrated in a titaniferous opaque phase, where, presumably,  $\text{Nb}^{5+}$  substitutes for  $\text{Ti}^{4+}$ . Y had low concentrations in all phases, with no distinct correlation between  $\text{Y}^{3+}$  and  $\text{Ca}^{2+}$ , as might have been expected. Walker (1969) arrived at similar conclusions with regard to Y, but suggested that  $\text{Zr}^{4+}$  substituted most easily for  $\text{Ti}^{4+}$  and  $\text{Fe}^{2+}$ , thus, entering the ore phase. If this is so, then it may have important bearings on

zirconium behaviour, particularly in the more evolved members of tholeiitic suites. However, with rocks of the Fishguard area no correlation between Zr concentration and the onset of ore fractionation is observed.

Four clinopyroxene mineral separates were analysed for a number of trace elements (see Appendix 2). The results show high concentrations of Cr, V, and Sc in clinopyroxene. Y is consistently low, in the range 30-40ppm.

More work, however, is clearly needed before the location of certain critical trace elements is known. It may be that many of the incompatible elements are trapped within interstitial liquids or on intergranular surfaces. The availability of sites for entry upon alteration appears critical for the transition elements and the metastable presence of clinopyroxene and pseudomorphing of Ti-Fe ore by leucoxene or sphene and magnetite may well have a significance on whole-rock concentrations of Ti, V, Cr, and Sc.

#### 5.4. CHEMICAL CHARACTERISTICS OF THE FISHGUARD VOLCANIC GROUP

As mentioned in section 5.3.2.1., from a consideration of the  $\text{SiO}_2$  contents of the various rocks analysed from the Fishguard area, four groups of rocks may be arbitrarily discerned. The characteristics of each of these groups will be discussed here, whilst the possible relationships between these groups will be discussed in Chapter 6. The distinction of these four groups is considered justified when other major and trace element concentrations are considered. Distinct breaks in colinear variations are seen, for example, between groups.

#### 5.4.1. GROUP 1. $\text{SiO}_2$ <55%.

This group represents 79% of the rocks analysed and constitutes the majority of the basic lavas of the Strumble Head Volcanic Formation, as well as the co-magmatic intrusive suite. Other chemical characteristics of this group, in comparison with groups 2, 3, and 4 are outlined below (Table 4).

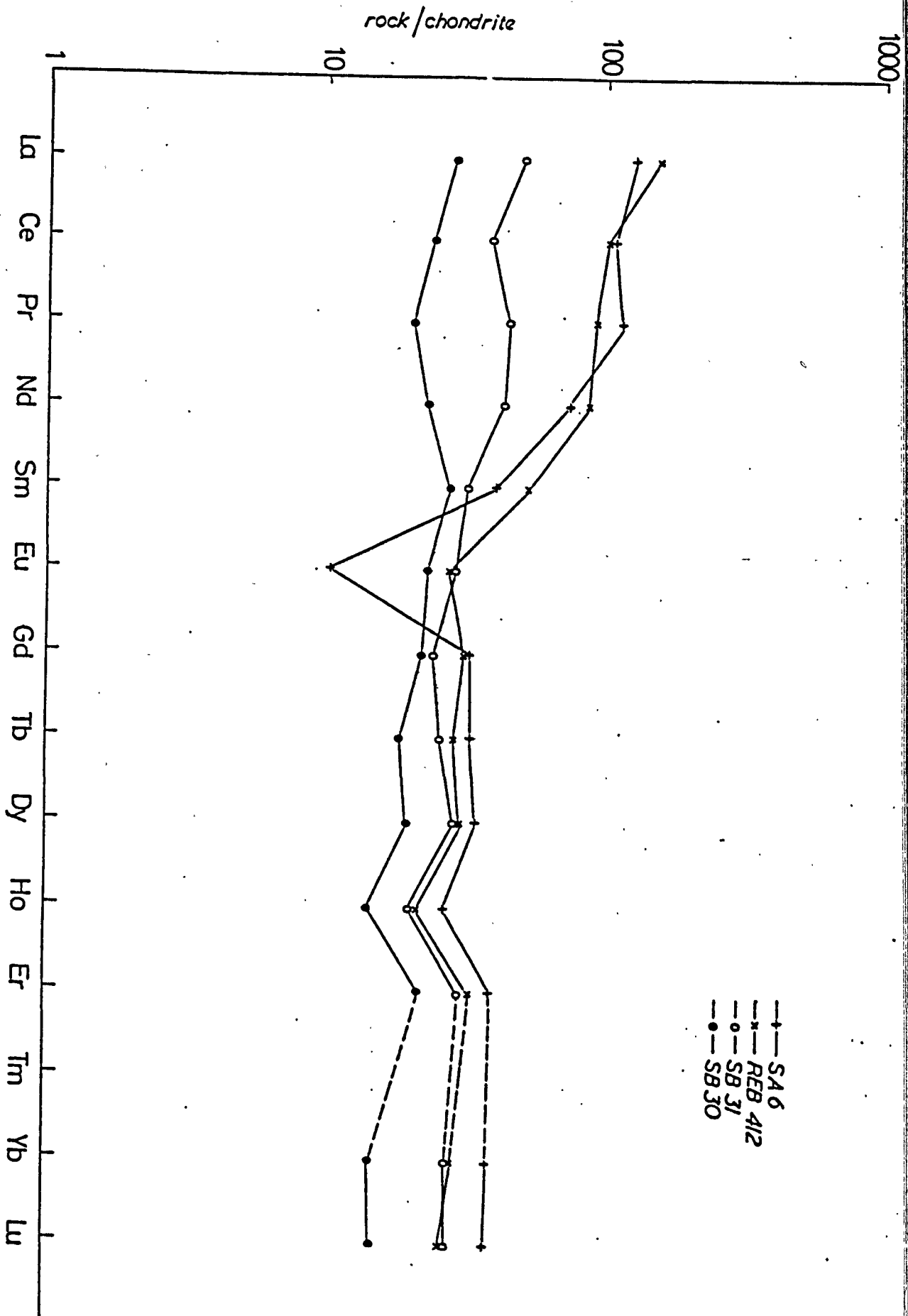
Table 4. Chemical characteristics of group 1 rocks.

Mg	high
Ca	high
Mn	high
Cr	high
Ni	high
V	high
Sc	high
Ti	high

Within the group Ni and Cr show a rapid, progressive depletion with fractionation, whilst Ti, Fe, Mn and the incompatible elements progressively increase. The group possesses a flat REE pattern (Fig. 175, sample SB30).

These elemental concentrations reflect the high mafic modal mineralogy of rocks of this group.

FIG. 175. Normalized REE patterns for samples from the Fishguard  
Volcanic Group.



#### 5.4.2. GROUP 2. $\text{SiO}_2$ 55%-61%.

Representing 5% of the rocks analysed from the Fishguard Volcanic Group, this group appears as basaltic andesite and andesite lavas and intrusives within the Strumble Head Volcanic Formation and surrounding area. Relative to group 1 rocks,  $\text{MgO}$ ,  $\text{CaO}$ , and (generally) Fe (total) concentrations are lower, as are values for Ni, Cr, Sc, V, and Ti. These result from the lower proportion of mafic minerals within this group, whilst high feldspar contents are recorded in high Na values. The group has a flat REE pattern, enriched relative to group 1 rocks (author's unpublished data).

#### 5.4.3. GROUP 3. $\text{SiO}_2$ 62%-71%.

This group represents 8% of rocks analysed. Rocks belonging to this group occur within the dacite-rhyodacite lava flow at Porth Maen Melyn, as well as certain intrusive sheets in the immediate neighbourhood, for example Penbwchddy. The characteristics of this group are outlined in Table 5.

Table 5. Chemical characteristics of group 3 rocks.

Mg low

Fe low

Ti low

Mn low

Ca low

Ni low

Cr low

Sc low

V low

Ti low

Certain incompatible elements have relatively high concentrations (for example, Zr), whilst others (for example, Y) are slightly depleted relative to group 2 rocks. The group possesses a light REE enriched pattern (Fig.175, sample REB412) and shows a slight negative europium anomaly ( $\text{Eu}/\text{Eu}^* = 0.59$ ).

Values in this group are related to high modal proportions of feldspar and correspondingly low concentrations of mafics.

#### 5.4.4. GROUP 4. $\text{SiO}_2 > 71\%$ .

These highly silicic rocks are found only as rhyolitic lavas within the area studied here, where they form part of the Porth Maen Melyn Volcanic Formation, as well as part of the Goodwick Volcanic Formation. Accordingly, most major elements, with exception of  $\text{SiO}_2$ ,  $\text{Al}_2\text{O}_3$ ,  $\text{Na}_2\text{O}$ , and  $\text{K}_2\text{O}$  are of a comparatively low concentration. The alkalis show a wide scatter of values and the rocks are considered to have suffered alkali-metasomatism.

The rocks show a marked depletion in all the transition elements, due to an almost complete absence of mafic minerals. Zr contents are lower than with group 3 rocks, whereas Y is somewhat higher.

The REE element distribution is similar to that for group 3 rocks (Fig.176, sample SA6), but possesses a particularly well developed negative Eu anomaly ( $\text{Eu}/\text{Eu}^* = 0.27$ ); a feature which may be of considerable petrogenetic significance (see Chapter 6).



## 5.5. MAGMATIC CHARACTERISTICS OF THE IGNEOUS ROCKS OF THE FISHGUARD AREA

In this section, the basic igneous rocks of the Fishguard Volcanic Group (group 1 rocks) are plotted on various diagrams. The aim is to show:

- (i) the 'magma type' of these rocks; that is their chemical affinities (nos. 1 to 3); and
- (ii) the possible tectonic setting within which these magmas were generated (nos. 4 and 5).

### 1. $\text{Na}_2\text{O} + \text{K}_2\text{O}/\text{SiO}_2$ (Fig. 176).

This diagram was utilised by MacDonald and Katsura (1964) to discriminate between Hawaiian tholeiitic and alkali rocks. However, as both sodium and potassium are probably mobile during alteration, this diagram is of little use in altered rocks. The rocks of the Fishguard Volcanic Group and associated intrusions straddle the alkalic/subalkalic boundary, but since most of the rocks have suffered albitization, it is likely that, before alteration, most of the rocks would probably have plotted in subalkalic field.

### 2. AFM diagram (Fig. 177), i.e. total iron-MgO- $\text{Na}_2\text{O} + \text{K}_2\text{O}$ .

Once again, this diagram is invalidated if the rocks have been severely altered. However, it has been shown above that Fe and Mg values in the Fishguard Volcanic Group rocks are largely unaltered and the effect of alkali alteration is to pull the trend towards the  $\text{Na}_2\text{O} + \text{K}_2\text{O}$  apex. However, this does not destroy the obvious iron

FIG. 176.  $\text{Na}_2\text{O} + \text{K}_2\text{O}$  vs  $\text{SiO}_2$  diagram for group 1 rocks.

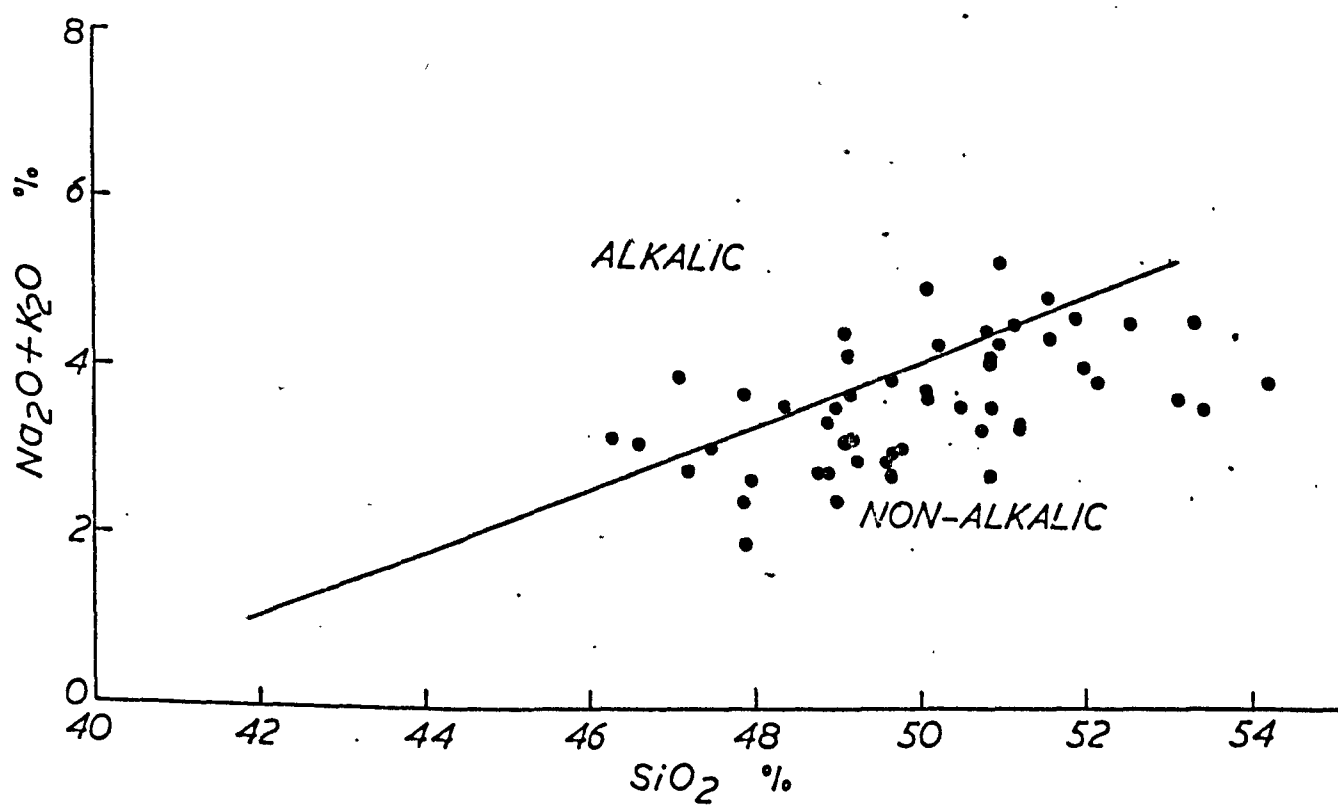
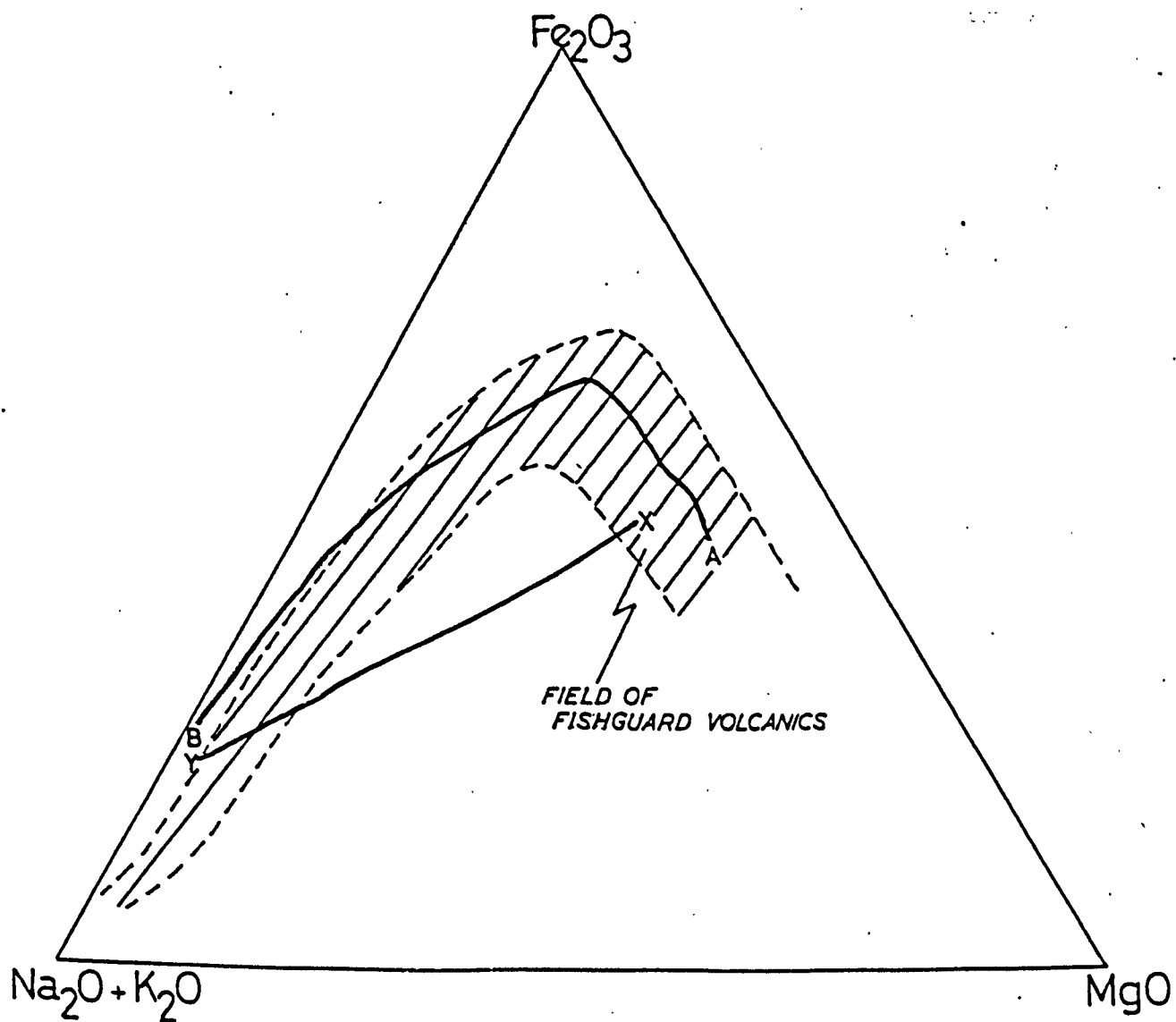
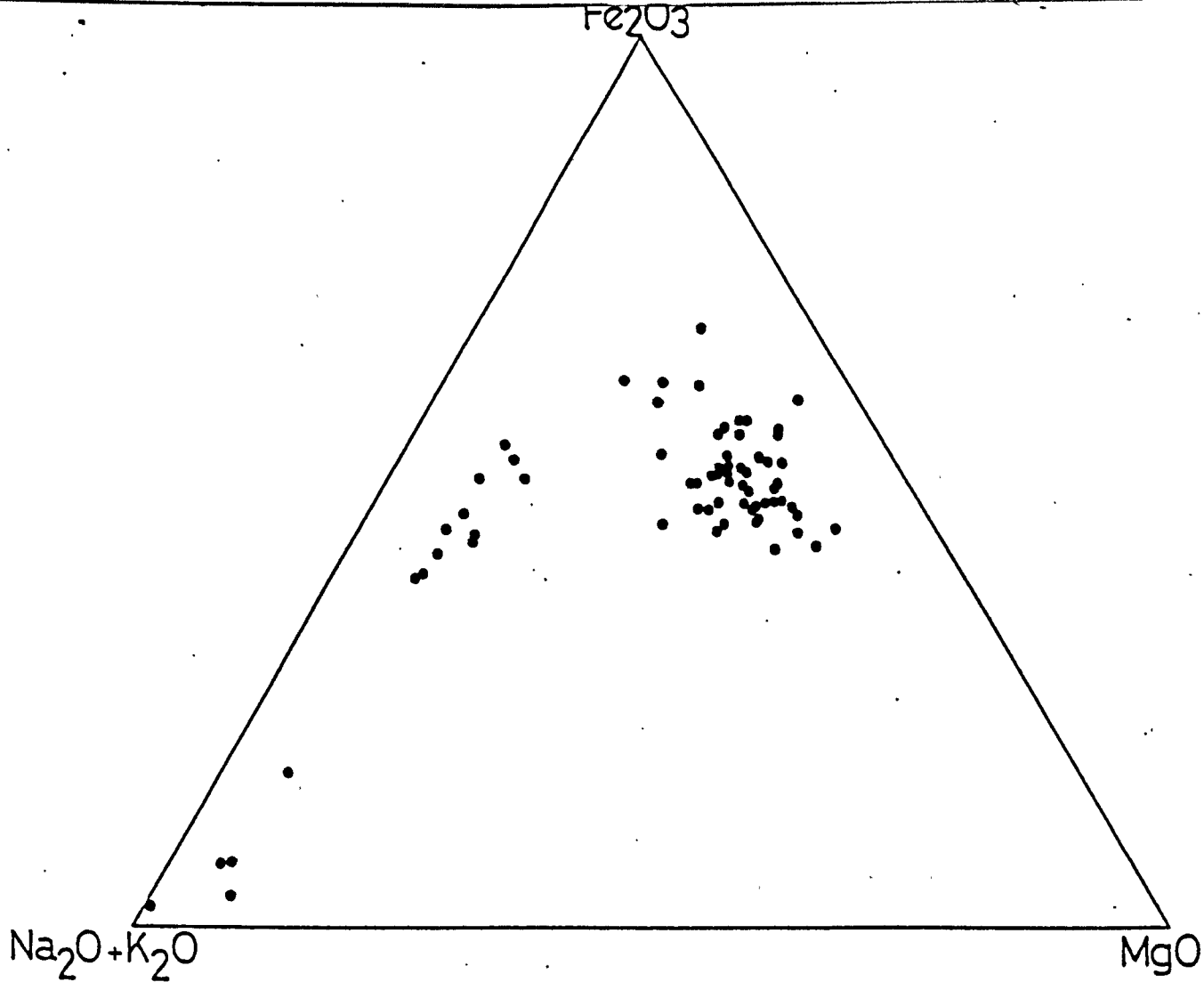


FIG. 177. AFM  $\square(\text{Na}_2\text{O} + \text{K}_2\text{O}) - \text{total Fe as Fe}_2\text{O}_3 - \text{MgO}$  diagram, showing spread of analyses for rocks of the Fishguard Volcanic Group.

FIG. 178. AFM diagram, showing the field of rocks from Fishguard Volcanic Group, compared with trends from Thingmuli, Iceland (A - B) and the Cascades Province, U.S.A. (X - Y). A - B and X - Y from Carmichael et al. (1974).



enrichment trend, illustrated in Figure 177, which is typical of tholeiitic and alkalic magmas. Figure 178 compares the field of Fishguard Volcanics with those of Thingmuli, Iceland, and the Cascades Province, U.S.A. The similarity to the Thingmuli trend is evident. The increase in iron within the basic igneous rocks of the Fishguard area is also demonstrated in Figure 168d, where total iron is plotted against 'f'. Figure 168c shows a similar increase in titanium. However, after the precipitation of an iron-titanium oxide, concentrations of these elements decline and the trend on the AFM is then one of increase in alkalis.

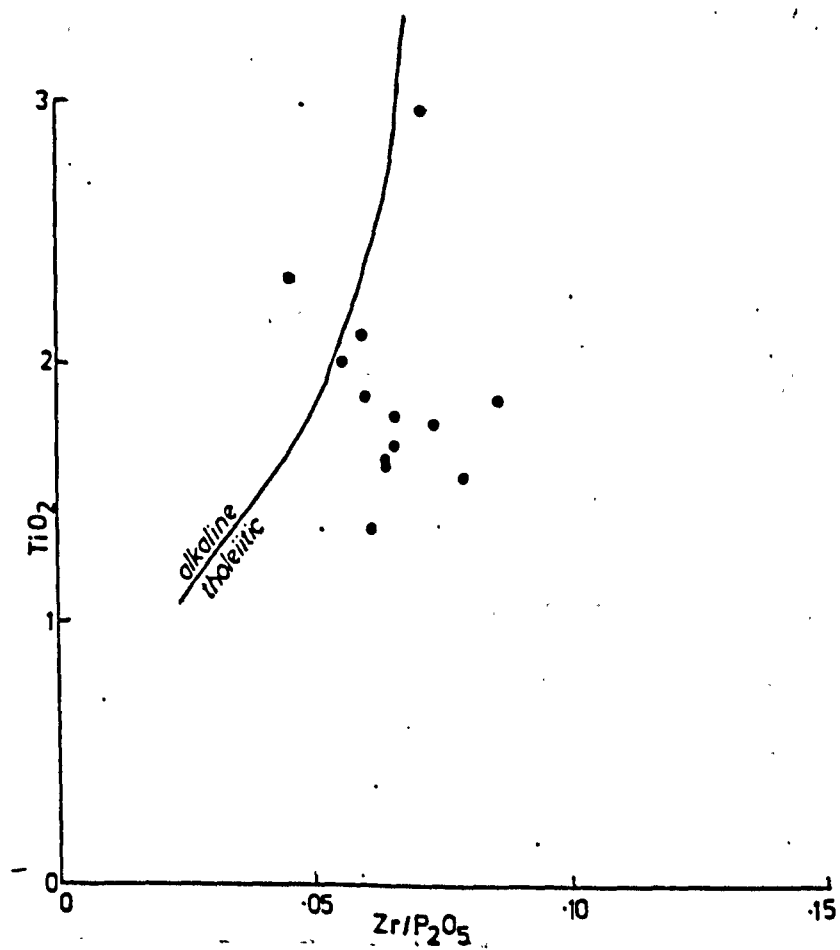
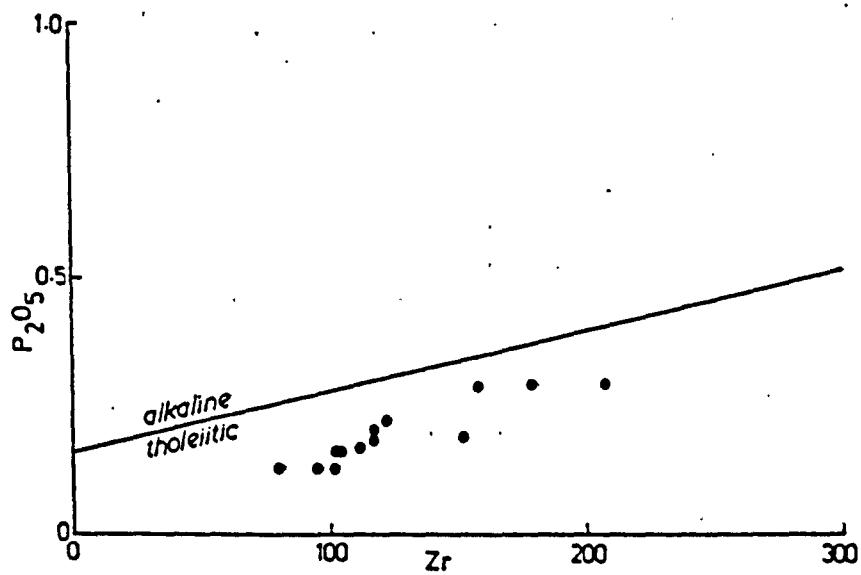
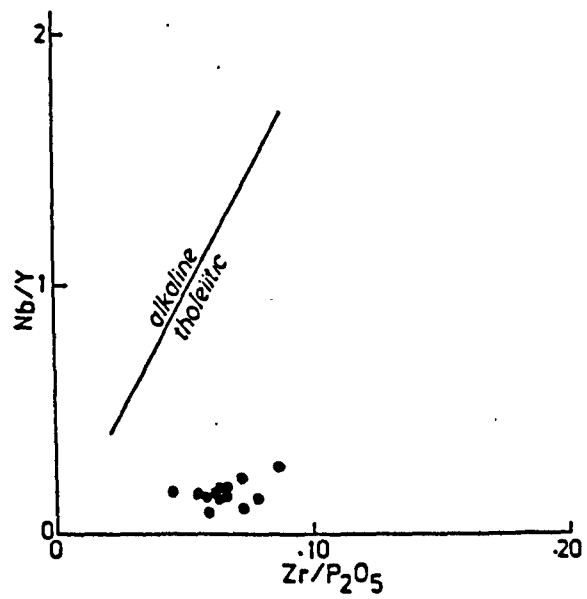
### 3. Binary diagrams of Floyd and Winchester (1975).

In these diagrams various combinations of the relatively immobile elements Ti, Zr, Y, Nb, and P are utilised to discriminate between alkaline and sub-alkaline magmas. Only group 1 rocks with a basaltic mineralogy and having  $\text{SiO}_2$  concentrations between 45% and 52% were plotted. As seen on the Nb/Y against  $\text{Zr/P}_2\text{O}_5$  diagram (Fig. 179) rocks from the Fishguard area plot within the sub-alkaline field. The  $\text{P}_2\text{O}_5$  against Zr diagram (Fig. 180) displays a positive linear correlation between these two elements, with all of the rocks falling within the sub-alkaline field. The  $\text{TiO}_2$  against  $\text{Zr/P}_2\text{O}_5$  diagram (Fig. 181) is possibly one of the most useful discriminatory diagrams, with again the majority of the Fishguard basic rocks falling within the sub-alkaline field. More recently, Winchester and Floyd (1977) have demonstrated the ability to classify complete volcanic suites, including the whole range of differentiation displayed. Using this method, the sub-alkaline nature of the Fishguard suite is emphasized. In addition, it confirms the more differentiated nature of rocks of

FIG. 179. A sample of group 1 analyses plotted on the Nb vs Y diagram with fields after Floyd and Winchester (1975).

FIG. 180. A sample of group 1 analyses plotted on the  $P_2O_5$  vs Zr diagram with fields after Floyd and Winchester (1975).

FIG. 181. A sample of group 1 analyses plotted on the  $TiO_2$  vs  $Zr/P_2O_5$  diagram with fields after Floyd and Winchester (1975).





groups 2 and 3, suggesting that the initial method of classification of these rocks (by  $\text{SiO}_2$  contents) was broadly justified.

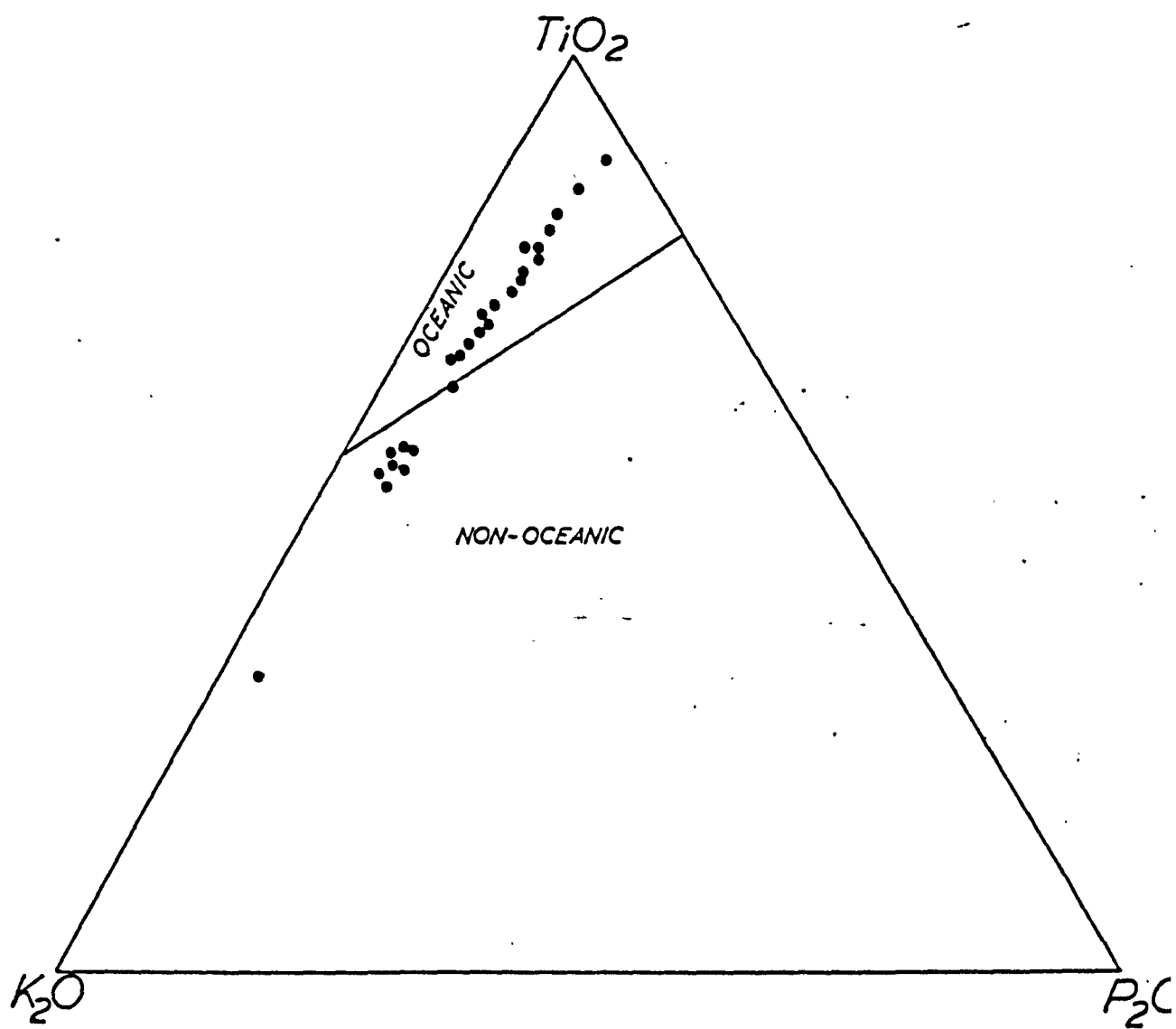
4. The  $\text{TiO}_2$ - $\text{K}_2\text{O}$ - $\text{P}_2\text{O}_5$  diagram (T. H. Pearce et al., 1975).

This diagram attempts to discriminate between oceanic and non-oceanic basalts. Although it has been demonstrated recently that  $\text{TiO}_2$  and  $\text{P}_2\text{O}_5$  are relatively immobile (Floyd and Winchester, 1975), it is well known that  $\text{K}_2\text{O}$  is very susceptible to large increases during alteration and this is well displayed in Figure 182. Pearce et al. (1975) acknowledge this fact, but state that an increase in  $\text{K}_2\text{O}$  tends to transfer all points into their non-oceanic field. Thus, if a metamorphosed basalt plots within the oceanic field, then they suggest it is very likely that it is of oceanic origin. Figure shows the scatter displayed by basic rocks of the Fishguard area and suggests that the Fishguard Volcanic Group may have oceanic affinities. However, the variations of  $\text{K}_2\text{O}$  concentrations are so variable that no significance may be attached to the evidence presented in this diagram.

5. The Ti-Y-Zr, Ti-Zr, Ti-Zr-Sr diagrams of Pearce and Cann (1973).

Once again these diagrams attempt to identify the tectonic setting within which magma suites were generated. The diagrams assume the immobility of these elements during alteration. The strong correlations between Zr and both Ti and Y within the Fishguard basic igneous rocks (Fig. 171) suggest that these elements have not been greatly altered and may be useful discriminants. However, Sr values appear to have been altered, as recognized in other metavolcanic suites

FIG. 182. Group 1 analyses plotted on the  $\text{TiO}_2 - \text{K}_2\text{O} - \text{P}_2\text{O}_5$  diagram. Fields after Pearce et al. (1975).



(for example, Smith and Smith, 1976), although strictly speaking, this plot should be used for less altered basalts (Pearce and Cann, 1973). Figure 184 shows the Ti-Zr-Sr diagram, with rocks of magma group 1 plotted on it. The Ti-Zr ratio is more or less constant throughout, with the scatter produced by Sr variation.

A considerable scatter of points is seen on the Ti-Y-Zr diagram (Fig. 183), straddling the boundary line between the 'ocean-floor basalt' field (field A) and the 'within-plate basalt' field (field C). The scatter present is not likely to be due to differences in the degree of differentiation of the samples as all three elements are largely incompatible within rocks of magma group 1, with low  $D^{\text{bulk}}$  values (approximately  $\geq 0.1$ ). Indeed, there is little variation on this diagram between the position of the most primitive and most fractionated of rocks and the scatter present is most probably due to other factors such as the effects of crystal accumulation, analytical precision, etc.

The Ti-Zr diagram (Fig. 185) once again suggests that the Fishguard basic igneous rocks have ocean-floor affinities. This diagram clearly shows the effects of crystal fractionation in the scatter of points present and perhaps, in certain cases, caution must be exercised when using this plot.

Floyd and Winchester (1975) reported that on the Ti-Zr diagram considerable overlap exists between the magma types. They suggest however (p. 212) that differentiated tholeiitic suites tend to show an increase in both Ti and Zr, whereas differentiated alkali basalt suites (i.e. alkali-basalt  $\rightarrow$  hawaiite  $\rightarrow$  benmoreite) show only an increase in Zr, with Ti remaining nearly constant. This rise in Ti in tholeiitic




FIG. 183. Group 1 analyses plotted on the Ti - Y - Zr diagram,  
after Pearce and Cann (1973).




FIG. 184. Group 1 analyses plotted on the Ti - Zr- Sr diagram,  
after Pearce and Cann (1973).

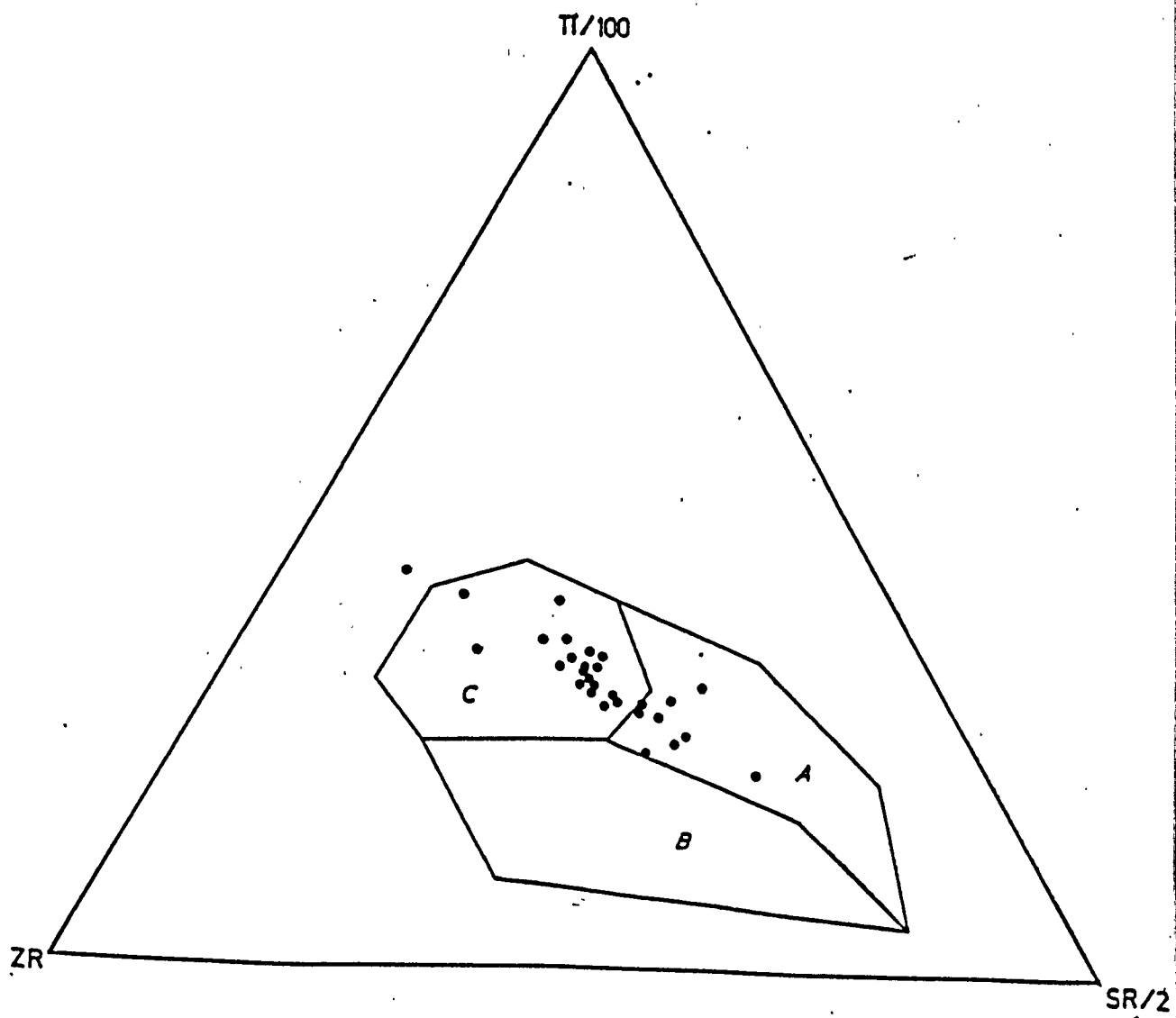
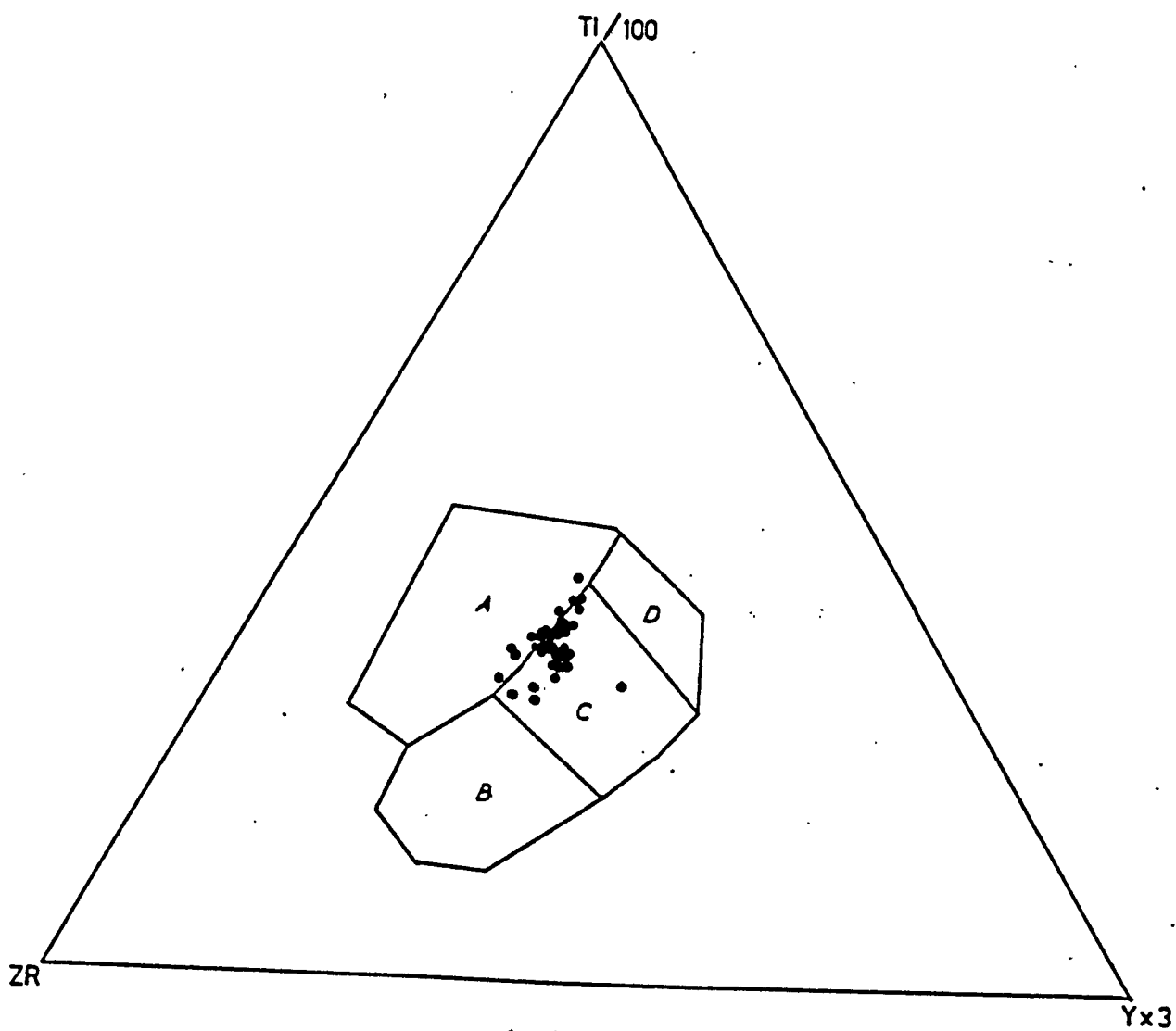
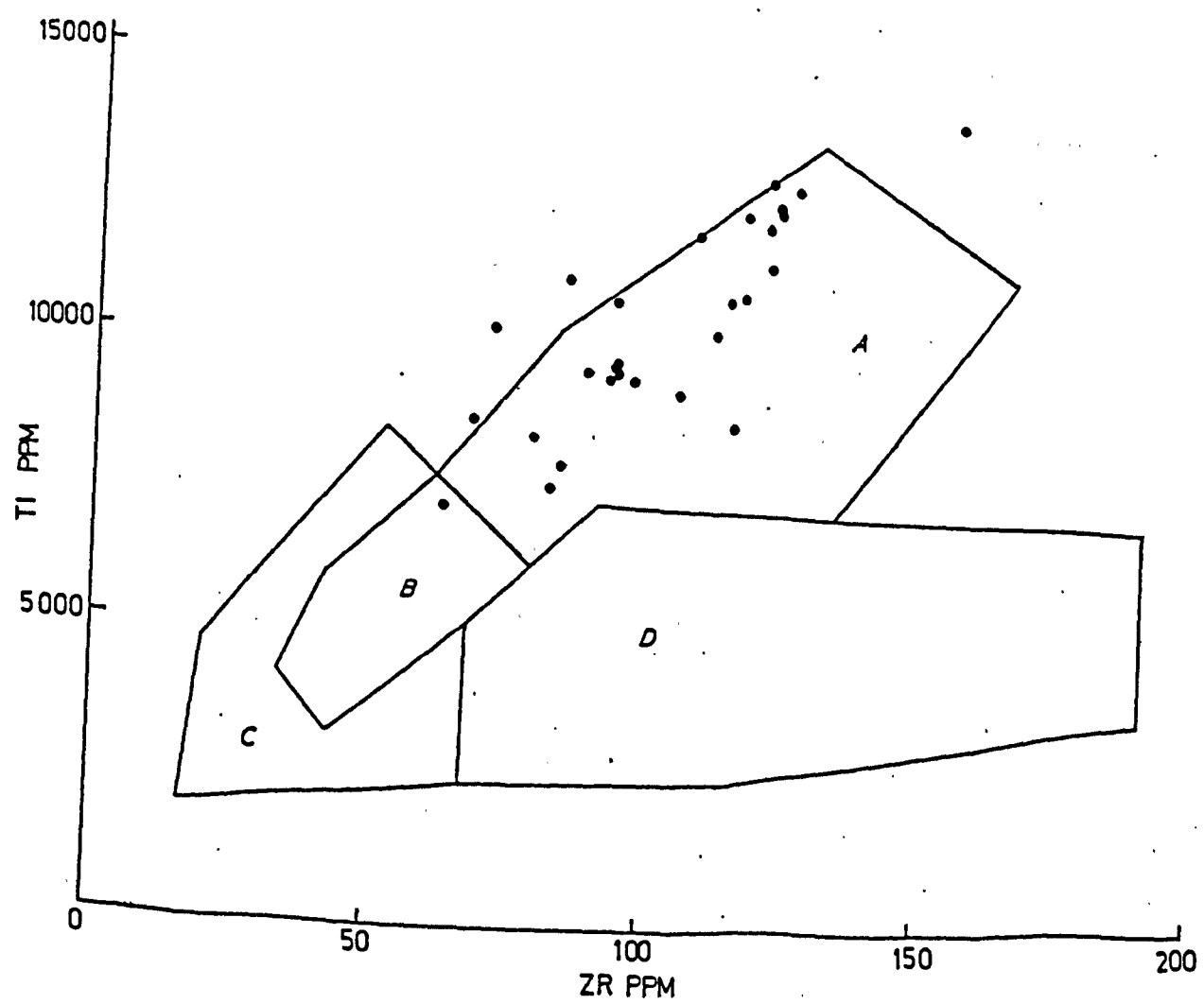


FIG. 185. Group 1 analyses plotted on the Ti - Zr diagram.  
Fields after Pearce and Cann (1973).





suites mirrors the iron enrichment of such suites, as displayed on an AFM diagram. Clearly, if the major elements have been mobile, then this diagram is of considerable use. The metabasic rocks of the Fishguard area display an increase in both Ti and Zr on this diagram, suggesting that the suite is of tholeiitic affinities, which is in agreement with the major element evidence.

In conclusion, from the evidence obtained above, the tholeiitic nature of the basic and intermediate rocks of the Fishguard area is clear. It is difficult, however, to distinguish clearly between rocks of oceanic characteristics and those of continental or within-plate characteristics. Rare-earth element analyses of the Fishguard basic rocks (Fig.175, samples SB30 and SB31) show a flat REE pattern. This, however, assumes immobility of the light REE which may not be a valid assumption (for discussion see, for example, Hellmann and Henderson, 1977; Floyd, 1977). Subsequent light REE enrichment during alteration may be masking an original light REE depletion. The Ti-Zr-Y diagram of Pearce and Cann (1973) shows a scatter of points straddling the 'within-plate' type basalts and the 'ocean-floor' type basalts, which probably reflects a transitional nature for this particular suite, although as stated previously, the scatter may result from other causes, such as analytical precision etc.

## CHAPTER 6. PETROCHEMICAL EVOLUTION

### 6.1. INTRODUCTION

In Chapter 5 four groups were discriminated on a chemical basis, namely Group 1 with  $\text{SiO}_2$  <55%, Group 2 with  $\text{SiO}_2$  55%-61%, Group 3 with  $\text{SiO}_2$  62%-71%, and Group 4 with  $\text{SiO}_2$  >71%. These groups may also be distinguished petrographically (see Chapter 2), although the difference between group 1 and group 2 rocks is difficult to detect, being marked by a reduced modal proportion of mafic minerals. This Chapter will attempt to account for the origin of these four groups, their possible relationships to one another, and also any internal variation to be found within individual groups. As in the previous Chapter, most attention will be devoted to groups 1 and 2, as they represent over 85% of the rock specimens analysed. The origin of magma groups 3 and 4 will be briefly discussed later.

### 6.2. GEOCHEMICAL MODELLING

In this study, it was attempted to explain the origin of chemical variations within the rocks of the Fishguard area by utilizing mathematical models of partial melting and crystal fractionation processes. These will be described here first and their application is given in section 6.3.1.

Linear correlations between pairs of incompatible elements have been previously described in magma suites from East Africa (Weaver et al., 1972), the Afar Depression (Treuil and Varet, 1973) etc. Treuil and Varet (1973) attempted to account for these correlations by extending existing mathematical models of partial melting and fractionation (for example, those of Gast, 1968;

Anderson and Greenland, 1969), to consider the case where  $D_j$  (the solid/liquid mass distribution coefficient of the element  $j$ ) is small relative to 1. A very brief review of these models is pertinent at this stage, including the models developed by Treuil and Varet (1973). These will be discussed under two broad headings, partial melting models and fractional crystallization models.

#### (i) Partial melting

Models for partial melting were formulated by Schilling and Winchester (1967) and Gast (1968) and subsequently simplified by Shaw (1970). Three possible cases exist, the first two of which will be explained in more detail than the third. Firstly there is the possibility of 'incremental melting', where each fraction of melt formed is continuously removed from the residual solid. The general equation for this process is

$$C^L = C^0 \times \frac{1}{D^0} (1 - f)^{\left(\frac{1}{D^0} - 1\right)} \quad (1) \quad \text{(for notations, see table 6)}$$

If the minerals present do not melt in the same proportions, (i.e. nonmodal proportions) as assumed in equation (1), then the equation becomes

$$C^L = C^0 \times \frac{1}{D^0} (1 - Pf)^{\left(\frac{1}{D^0} - 1\right)} \quad (2)$$

In the case of batch melting, continuous equilibrium of the liquid phase with the residual solid is maintained, until removal of that liquid from the solid. General equations for this are

$$c^L = c^0 \times \frac{1}{D_0 + f(1 - D_0)} \quad (3)$$

or where the phases melt in different proportions

$$c^L = c^0 \times \frac{1}{D_0 + f(1 - p)} \quad (4)$$

The third case is where the removal of melt from the residual solid occurs, with collection of this melt in a single chamber where homogenization occurs (O'Hara, 1977). However, this case will not be discussed in detail.

Gast (1968) emphasized the difficulty of removing very small amounts of liquid from a residual solid, and hence suggested that equilibrium 'batch' partial melting was probably the most likely process which occurs in nature, a process similarly considered the most important by Allègre and Minster (1978).

#### (ii) Fractional crystallization

For fractional crystallization, a Rayleigh type law (1896) is commonly followed, with crystallization in a closed, condensed system and assuming equilibrium between the surface of the crystal and the liquid, resulting in the formula

$$\frac{c^L}{c^0} = f^{(D^0 - 1)} \quad (5)$$

Many particular cases of trace element fractionation have been investigated, such as the effects of trapped liquids in cumulates (by Albarede, 1976). However, these specific cases will not be discussed in detail here.

TABLE 6 . NOTATIONS USED IN MATHEMATICAL MODELS

PARTIAL MELTING

$c^L$  = Concentration of a trace element in the liquid.

$c^0$  = Concentration of a trace element in the initial (solid) assemblage.

$f$  = Proportion of liquid.

$D_0$  = Bulk distribution coefficient, where

$$D_0 = X_0^\alpha K^{\alpha/L} + X_0^\beta K^{\beta/L} + \dots$$

where  $X_0^\alpha$  is the initial weight fraction of a phase  $\alpha$  and  $X_0^\beta$  is the initial weight fraction of a phase  $\beta$ , and  $K^{\alpha/L}$  is the solid-liquid distribution coefficient for phase  $\alpha$ ,  $K^{\beta/L}$  is the solid-liquid distribution coefficient for phase  $\beta$ .

$$p = p^\alpha K^{\alpha/L} + p^\beta K^{\beta/L} + \dots$$

where  $p^\alpha$ ,  $p^\beta$  .... are fractions of liquid contributed by each phase during melting.

FRACTIONAL CRYSTALLIZATION

$c^L$  = Concentration of a trace element in the derived liquid.

$c^0$  = Concentration of a trace element in the original liquid.

$f$  = Fraction of liquid remaining.

$D^0$  = Bulk distribution coefficient, where

$$D^0 = X^\alpha K^{\alpha/L} + X^\beta K^{\beta/L} + \dots$$

where  $X^\alpha$  represents the weight fraction of  $\alpha$  in the precipitating phases and  $K^{\alpha/L}$  is the solid/liquid partition coefficient for  $\alpha$ , etc.

In the case of certain elements, notably those with high charges (such as  $\text{Zr}^{4+}$ ,  $\text{Hf}^{4+}$ ,  $\text{La}^{3+}$ ,  $\text{U}^{4+}$ ,  $\text{Th}^{4+}$ ) or those with large ionic radii (e.g.  $\text{Rb}^+$ ,  $\text{K}^+$ ,  $\text{Cs}^+$ ), very low values of  $D$  are realized, and as a result these elements tend to be concentrated in the liquid. The build up in the melt of the latter group (i.e. those with large ionic radii) is explained by the lack of available sites within the early crystallizing phases. As a result, they are more correctly termed 'incompatible elements'. However, the build up of the former group is not explained by such a process. Ringwood (1955) suggested that these elements have a tendency to form complexes in the liquid and as such have a high solubility in the liquid. This group of elements have more recently been called 'hygromagmatophile elements' by Treuil and Varet (1973).

Referring to equations 3 and 5 (the most likely partial melting and fractional crystallization cases), if  $D^{h+} < 0.01$  (where  $D^{h+}$  is the bulk distribution coefficient of a hygromagmatophile element,  $h^+$ ) and the phases melt in the same proportions in the partial melting model, then both the equations simplify to:

$$\frac{C^L}{C^0} = \frac{1}{f} \quad (6)$$

and consequently the patterns produced by these elements during fractional crystallization and partial melting are indistinguishable.

If the concentrations of two such trace elements are plotted on the same diagram, then from

$$\frac{C_X^L}{C_X^0} = \frac{1}{f} = \frac{C_Y^L}{C_Y^0}, \text{ i.e. } C_X^L = \frac{C_Y^L}{C_Y^0} C_X^0 \quad (7)$$

it can be seen that these elements have a linear correlation which passes through the origin (of the form  $y = mx$ ).

However, for a less hygromagmatophile element ( $h^-$ ) where  $0.01 < D^{h^-} < 1$ , then equations 3 and 5 simplify to:

$$C_{h^-}^L = C_{h^-}^0 \frac{1}{D^{h^-} + f} \quad \text{for partial melting, and}$$

$$C_{h^-}^L = C_{h^-}^0 \frac{1}{f} f^{D^{h^-}} \quad \text{for fractional crystallization.}$$

In this case, the patterns produced during partial melting and fractional crystallization are different and the two processes appear distinguishable (see Fig. 186 after Ferrara and Treuil, 1974, Fig. 8). However, the variations between these two curves is only slight and necessitates precise analytical data, such as neutron activation analyses, as obtained by Treuil and Varet (1973) in their case study of the Afar region. Despite this, however, it will be noticed that the variation generated by a fractional crystallization process assumes a straight line, with a positive slope, whilst that produced by a partial melting process flattens out and is curvilinear.

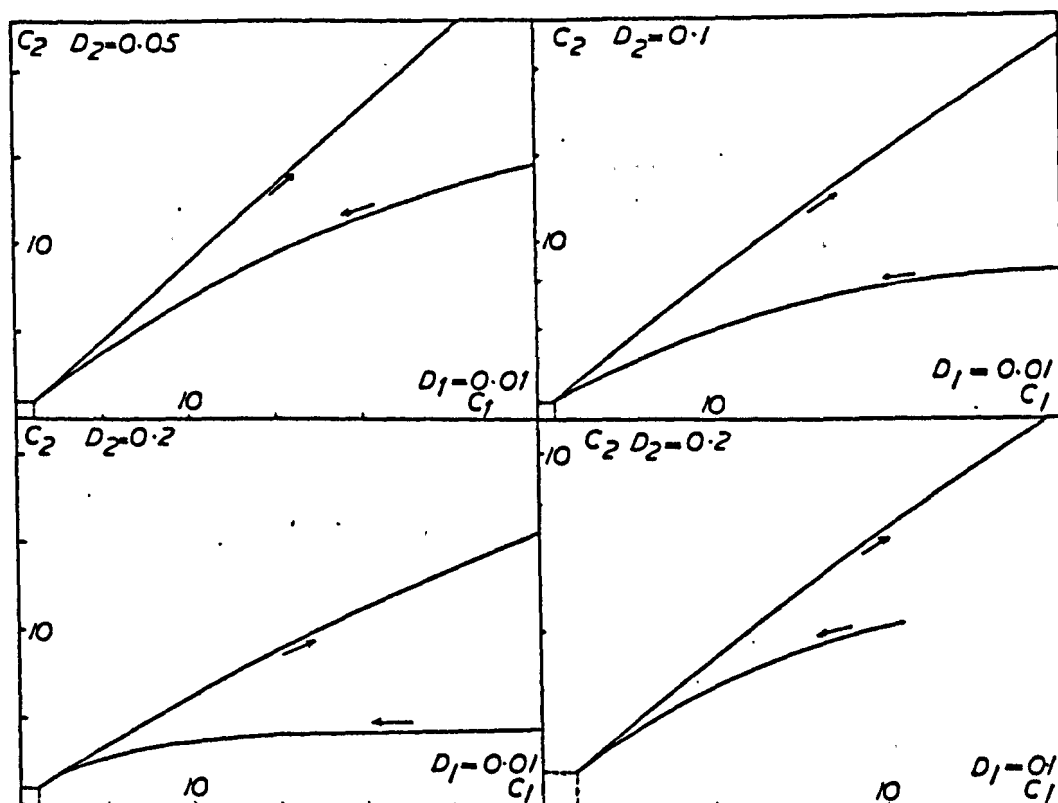
### 6.3. PETROCHEMICAL EVOLUTION OF GROUPS 1 AND 2.

Samples belonging to groups 1 and 2 were collected from a number of occurrences:

- (1) From the lavas of the Strumble Head Volcanic Formation;
- (2) From large intrusive bodies which occur within the Fishguard area, e.g. the Llanwnda Intrusion, the Garn Fawr-Garn Fechan Intrusion etc., and

FIG. 186. Relationship between variation curves for two trace elements  $C_1$  and  $C_2$ , with variable distribution coefficients  $D_1$  and  $D_2$ , during fractional crystallization (upper path) and partial melting (lower path). (After Ferrara and Treuil, 1974, Fig. 8).





- (3) From the many minor intrusive sheets which invade the volcanics of the Fishguard Volcanic Group and also the associated sedimentary horizons underlying, above and within the volcanic pile.

### 6.3.1. GEOCHEMICAL EVIDENCE FOR THE DIVERSITY OF GROUP 1

#### 6.3.1.1. TRACE ELEMENT EVIDENCE

The correlation between element pairs of the group Zr, Y, Nb, Nd, La, Ce, Ti and P are linear and positive. Such variations, it has been suggested above, may result from either partial melting or fractional crystallization if both elements are strongly hygromagmatophile, or fractional crystallization if one of the element pair is strongly hygromagmatophile, whilst the other is only weakly hygromagmatophile. Of the above mentioned elements, Zr is strongly hygromagmatophile in group 1 rocks whilst Ti is probably only weakly hygromatophile (this assumption is tested below). Thus the plot of Zr against Ti (Fig.171a) for rocks of the Fishguard area represents the plot of an  $h^+$  element (strongly hygromatophile) against an  $h^-$  (weakly hygromagmatophile) element. The linear, positive correlation, passing through the origin strongly suggests that the variation present is due to a fractional crystallization process.

Assuming a  $D^{h^+}$  value for Zr of 0.01 within group 1 rocks, then the value of  $D^{h^-}$  for Ti within these rocks may be calculated by taking Zr and Ti concentrations in two samples (SB30 and SB31 are used here) as follows:

$$\text{if } \frac{C_L^{h+}}{C_O^{h+}} = \frac{1}{f} \quad \text{and} \quad C_L^{h-} = C_O^{h-} \cdot f^{(D-1)}$$

$$\text{then } C_L^{h-} = C_O^{h-} \left( \frac{C_O^{h+}}{C_L^{h+}} \right)^{(D-1)}$$

which can then be expressed in the form

$$\text{Log } (C_L^{h-}) = \text{Log } (C_O^{h-}) + (D-1) \text{Log } (C_O^{h+}) - (D-1) \text{Log } (C_L^{h+})$$

The values for Zr and Ti (respectively) in samples SB30 and SB31 (which represent parent and daughter liquids) are:

$$C_O^{h+} = 119 \text{ and } C_L^{h+} = 209$$

$$C_O^{h-} = 1.82 \text{ and } C_L^{h-} = 2.93$$

then by substituting into the above equation, it can be calculated that  $D^{Ti} = 0.15$  and thus conforms with the assumption that Ti is weakly hygromagmatophile in the rocks of group 1 (i.e.  $0.01 < D < 1$ ). Bougault (1977) also deduced that Ti has a low value of D in basaltic systems of similar composition from D.S.D.P. Leg 37.

The fact that analyses of intrusive rocks which occur within the area around Fishguard fall on the same line of liquid descent as that generated by the lavas of the Fishguard Volcanic Group provides evidence for their comagmatic nature, as is suggested by the available field and petrographical information. It becomes clear that the intrusions merely represent a high-level co-eval intrusive suite derived from the same magmatic source as the extrusive rocks.

Further evidence for the origin of the chemical range of igneous rocks of the Fishguard area can be gained when the spread of trace element concentrations outlined above is compared with major element values. If the variation seen were produced by varying degrees of partial melting, then rocks with the highest concentrations of incompatible elements might be expected to show the most primitive major element compositions (e.g. high Mg/Mg + Fe). In contrast, they display features of fractionated liquids, as demonstrated below.

#### 6.3.1.2. MAJOR ELEMENT EVIDENCE

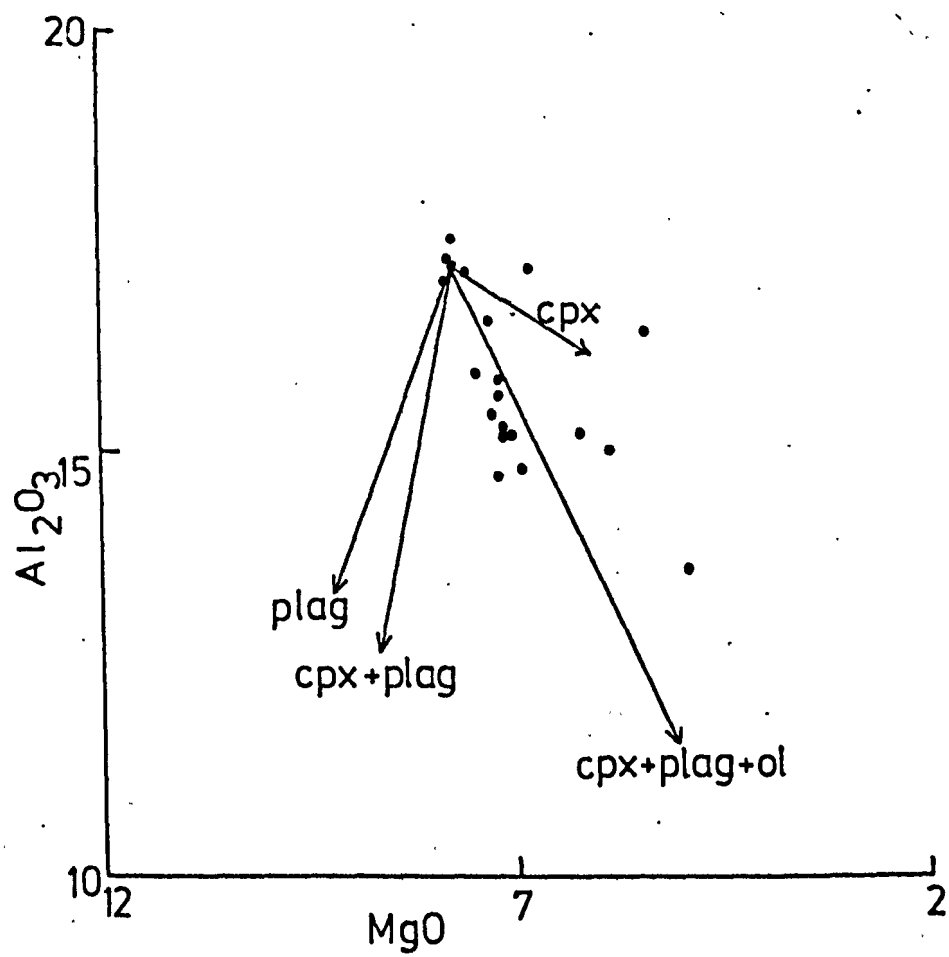
Considerable controversy has existed as to which is the most informative way of presenting geochemical data with a view to illustrating the nature of the variation and identifying the processes responsible for that variation. Wright (1974) suggested that possibly the most useful diagrams were MgO versus major element oxide plots. These diagrams have recently been successfully used for ocean floor basaltic suites, for example by Flower et al. (1977) and by Pearce and Flower (1977). Wright (1974) suggested that diagrams of this form were better than AFM triangular diagrams or the utilization of differentiation indices (such as the Thornton-Tuttle Index or the Kuno Solidification Index) for a number of reasons. The above mentioned diagrams and indices, he claims, only use a proportion of the components of the rock analysis. All major element values must satisfy the model pictured and thus all major elements should be used in the generation of that model. The AFM diagram, in addition, uses varying proportions of major elements depending upon the rock type (for example,  $\Sigma$  AFM components for dacites is only

about 15%, whereas for basalts it is approximately 40%). However, in altered rocks the situation is slightly different. Not all major element concentrations represent original values and thus not all of the variations identified correspond with the original igneous processes. Clearly, therefore, a variety of diagrams must be utilized in order to interpret the petrogenetic history of the rocks.

On an AFM diagram ( $\text{Na}_2\text{O} + \text{K}_2\text{O} - \text{Fe}(\text{total}) - \text{MgO}$ ) group 1 samples show a trend of iron enrichment (Fig.177). This results from the precipitation of a phase or phases which are members of an iron-magnesium solid solution series and in which alkalis are of limited concentrations (in this case, probably clinopyroxene). Thus the AFM diagram appears useful in displaying some of the chemical variation within rocks of the Fishguard area. In addition, the trend of iron-enrichment confirms the tholeiitic affinities of this magma suite, as suggested by other evidence (see Chapter 5).

Further information may be obtained from other diagrams, particularly the  $\text{MgO} - \text{Al}_2\text{O}_3$  plot (Fig.187). This clearly shows a gradual decrease of  $\text{Al}_2\text{O}_3$  and  $\text{MgO}$  concentrations in lavas of group 1. This corresponds very closely with trends displayed by ocean floor basalts fractionating plagioclase + clinopyroxene  $\pm$  olivine and thus it appears that the variation seen within group 1, and probably group 2 also, is related to crystal fractionation, confirming the trace element evidence presented above (6.3.1.1.). The following section will attempt to place constraints upon the nature and proportions of these fractionating phases.

FIG. 187. Plot of  $\text{Al}_2\text{O}_3$  vs  $\text{MgO}$  wt% to show the effects of removal of plagioclase, clinopyroxene + plagioclase, clinopyroxene + plagioclase + olivine, and clinopyroxene from an assumed parental magma.



### 6.3.1.3. EVOLUTION OF GROUP 1

Major and trace element concentrations change consistently between group 1 samples when they are plotted against an index of differentiation, either MgO or 'f' values, where 'f' = residual liquid fraction (see Chapter 5). These 'f' values have been determined assuming sample LD2 as a parental magma for the remainder of the suite. This is justified by the fact that this sample has the lowest concentration of incompatible and hygromagmatophile elements along with the highest MgO/Fe(total). The utilization of 'f' values is in a manner similar to that of Barberi et al., 1975; Minster et al., 1977, etc. Values of 'f' range from 1.00 through to approximately 0.26, although there is overlap in the range 0.28 to 0.26 with rocks of group 2. The regular variations of other elements against these indices suggests a constancy of the bulk distribution coefficients and also physical/chemical parameters during the evolution of this magma group.

Figures 168 to f show a steady increase in Fe(total),  $\text{TiO}_2$ , MnO, and  $\text{P}_2\text{O}_5$  with decreasing 'f', whilst CaO and  $\text{Al}_2\text{O}_3$  show a broad scatter but an overall decrease, as does MgO against 'f'.  $\text{SiO}_2$  remains fairly constant.  $\text{Na}_2\text{O}$  and  $\text{K}_2\text{O}$  concentrations are no doubt altered from their original values and hence will not be considered here. Ni and Cr both decrease very rapidly, whilst V shows a slight increase and Sc remains relatively constant. The incompatible elements all increase systematically (see Figs. 171 to 172) with increasing Zr concentrations.



The decrease of  $\text{Al}_2\text{O}_3$  and  $\text{CaO}$  with differentiation suggests that plagioclase feldspar is probably one of the principal phases involved in the fractionation process, a fact readily confirmed from petrographical examinations of the rocks forming this suite. Cr is partitioned into clinopyroxene, ore and spinel in basaltic liquids. Clinopyroxene and ore are common within most of the rocks of group 1 but spinel was not observed. It is likely, therefore, that the variation in Cr values are due to the removal of clinopyroxene and ore. There is also a marked decrease in Ni concentrations with differentiation and it shows a correlation with  $\text{MgO}$ , suggesting that olivine may also have been a fractionating phase, although probably of minor importance. This can not be borne out, however, as olivine has not been observed in thin section within any of the rocks of the Fishguard area. This may possibly be due to its subsequent alteration, although serpentinous aggregates, which typically pseudomorph olivine were also not observed during the present study. Thus the original presence of olivine remains speculative.

Figure 187 shows vector lines generated by the removal from a parental liquid of plagioclase + clinopyroxene, plagioclase, plagioclase + clinopyroxene + olivine and clinopyroxene. These vectors have been generated using the mathematical mixing model of Wright and Doherty (1970). This model assumes that individual oxides vary linearly between the two liquid compositions under consideration. This is true for small steps in the process and thus variations must be monitored step-wise. The basic premise is that

$$\text{residual liquid} + \text{crystals} = \text{parental liquid.}$$

As can be seen, the observed trend for lavas from group 1 corresponds quite closely with the vector generated by the removal of plagioclase + clinopyroxene  $\pm$  olivine. Actual mathematical calculations on assumed daughter-parent pairs from group 1 analyses not unexpectedly reveal relatively high residuals ( $\Sigma r^2$ , where  $r$  = difference between calculated oxide % and measured oxide %). This is no doubt due to the altered nature of the rocks under investigation. Not only are the analyses reported in this work modified from original values, but so are the phase compositions. Although clinopyroxene phenocryst compositions have been measured, plagioclase feldspar compositions are considerably more albitic than might be expected in nearly all cases, and thus an estimation of original An content must be made. This clearly is not satisfactory. However, despite these limitations, most of the calculations required the removal of clinopyroxene and plagioclase, whilst in some of the more basic rocks, olivine also appeared necessary. Indeed, the estimations of amount of residual liquid bore close correlations with those calculations based upon trace element models (i.e. values of 'f'). It is realized, however, that no conclusions may be drawn from this exercise due to the uncertainties present.

Throughout the rocks of group 1, Ti, Fe and V all increase progressively with decreasing 'f', no doubt due to the absence of an oxide phase on the liquidus. Only in the most fractionated samples (e.g. SB31 at 'f' = 0.26) does an oxide commence to precipitate and is present within the groundmass.

Apatite does not appear on the liquidus of group 1 liquids and consequently phosphorous which has a very low solid/liquid distribution coefficient for any other phase likely to crystallize

from a basaltic liquid, behaves as an incompatible element for group 1 liquids.

Unfortunately no trace element monitor of plagioclase fractionation is preserved as Sr, which has a high affinity for plagioclase (i.e. it has a comparatively high D value) is readily affected during alteration processes.

The chemical variations recorded and the nature of the fractionation process are similar to those of other tholeiitic suites, for example Thingmuli, in Iceland (Carmichael, 1964).

#### 6.3.2. GEOCHEMICAL EVIDENCE FOR THE DIVERSITY OF GROUP 2

This group is composed of a small number of samples with  $\text{SiO}_2$  between 55% and 61%, and correspondingly low 'f' values. However, the fact that they fall on the extended liquid line of descent generated by group 1 basalts suggests that they are directly related. The transition from group 1 and group 2 samples occurs at approximately 'f' = 0.25 (see Appendix 1). Occasional misclassifications are recorded (for example SB33, with 'f' = 0.37) and are considered to be the result of an increase in silica during alteration. Generally this can be verified petrographically.

Rocks of this group show variable concentrations of Ti, Fe, V, and Sc, whilst Ca and Mg concentrations are noticeably reduced over group 1 analyses. Variable contents of the transition elements mentioned above are related to the fractionation of an oxide phase, which is also considered to be responsible for the increased silica values. Ca and Mg are low due to the fact that these rocks represent

liquids derived by extensive fractionation of plagioclase and clinopyroxene, which have removed these elements. Moderate Al concentrations are present due to the high modal proportions of plagioclase within these rocks. Cr and Ni values are low, in agreement with the prior extensive removal of mafic phases. Incompatible element concentrations are increased over group 1 magmas, although phosphorous is variable, no doubt due to the fact that apatite is a liquidus phase in some of these rocks.

Analyses of this group correspond fairly closely with basaltic andesites and icelandites from Thingmuli (Carmichael, 1964) (see Table 7 ). In fact, close similarities exist between the Fishguard Volcanic Group suite and Thingmuli as a whole. Carmichael (op. cit.) concludes that the chemical variation in the suite of lavas from Thingmuli is produced by the fractional crystallization of a primary olivine-tholeiite with the removal of olivine, plagioclase, pyroxene and, in the intermediate and final stages, of an oxide phase. This is in agreement with the conclusions reached here after petrological and geochemical evidence has been examined. Byerly et al. (1976) describe similar compositions in dredged lavas, differentiating from typical ocean floor type basalt through to rhyodacite, by shallow-level fractional crystallization of plagioclase, clinopyroxene and olivine (in the early stages) and plagioclase, clinopyroxene, titanomagnetite and pigeonite in the later stages.

#### 6.4. GEOCHEMICAL EVIDENCE FOR THE ORIGIN OF GROUP 3

Samples forming group three form a tight cluster of analyses, displaying a limited compositional variation. Samples of this group were collected from lavas exposed at Porth Maen Melyn and occurring

TABLE 7

COMPARISON OF VOLCANIC ROCKS FROM FISHGUARD VOLCANIC GROUP WITH THOSE FROM THINGMULI, ICELAND  
(AFTER CARMICHAEL, 1964)

	A		B		C		D	
	1.	SB30	6.	SB31	11.	SB54	14.	SBR11
SiO <sub>2</sub>	47.07	49.2	48.48	51.2	54.11	56.5	60.59	60.3
TiO <sub>2</sub>	1.66	1.82	3.00	2.93	2.65	2.54	1.25	1.34
Al <sub>2</sub> O <sub>3</sub>	14.86	15.3	12.77	13.6	12.64	13.0	15.07	16.1
Fe <sub>2</sub> O <sub>3</sub>	4.08	12.42*	6.97	14.71*	5.27	13.70*	2.31	7.26*
FeO	7.20		8.76		8.07		5.73	
MnO	0.17	0.25	0.25	0.22	0.23	0.24	0.19	0.09
MgO	8.52	7.20	4.76	4.97	3.61	3.85	1.73	4.07
CaO	11.47	11.38	9.20	7.83	7.35	4.76	4.94	3.64
Na <sub>2</sub> O	2.24	2.74	2.91	3.66	3.42	4.50	4.29	5.99
K <sub>2</sub> O	0.20	0.38	0.41	0.84	1.17	0.11	1.59	0.29
P <sub>2</sub> O <sub>5</sub>	0.18	0.18	0.40	0.29	0.50	0.28	0.43	0.32
H <sub>2</sub> O <sup>+</sup>	1.32		0.61		0.56		1.58	
H <sub>2</sub> O <sup>-</sup>	0.93		0.92		0.38		0.26	

1. Olivine tholeiite (olivine normative).

6. Tholeiite (quartz normative).

11. Basaltic-andesite.

14. Andesite (icelandite).

\* Total iron as Fe<sub>2</sub>O<sub>3</sub>

within the Porth Maen Melyn Volcanic Formation, as well as from a number of high-level intrusive sheets, such as Penbwchddy (see Fig. 83). This group is characterized by  $\text{SiO}_2$  between 62% and 71% and low concentrations of Fe and Mg, whilst the alkalis are relatively enriched. Thus, on an AFM diagram (Fig. 177) they fall further towards the alkali apex than samples from group 2. The concentrations of Ni, Cr, Ti, Sc, and V are low, probably due to the fact that these rocks represent liquids from protracted lines of descent. The removal of significant amounts of an oxide phase are responsible for the low values of Ti, Fe, V, and Sc.

It is considered likely that this group was derived from group 2 as a result of fractional crystallization, although the trace element evidence diagnostic of the derivation of group 2 from group 1 (i.e. linear, positive correlations between incompatible element pairs) is no longer present. As can be seen from Figure 183, the Y-Zr line of liquid descent does not pass through the cluster of points representative of group 3 analyses. However, this does not necessarily imply that this magma is not derived from group 2. It may merely reflect that one or both of these elements are no longer incompatible with the phases precipitating. Indeed, apatite appeared as a liquidus phase in rocks of group 2 and thus P was not incompatible in that system. Similarly Ti was readily fractionated by an oxide phase. Y might have been preferentially depleted by apatite. However, in the absence of zircon on the liquidus, zirconium might remain incompatible. When the stage is reached where these 'hygromagmatophile' elements become incorporated into solid phases, then quite clearly other indices of differentiation must be sought. A plot of Zr against  $\text{Fe}/\text{Fe} + \text{Mg}$  (Fig. 189) appears to show a relationship between these two

FIG. 188. Plot of Y vs Zr, showing the spread of analyses for rocks of groups 1 and 2 (dots) compared with those of group 3 (crosses).

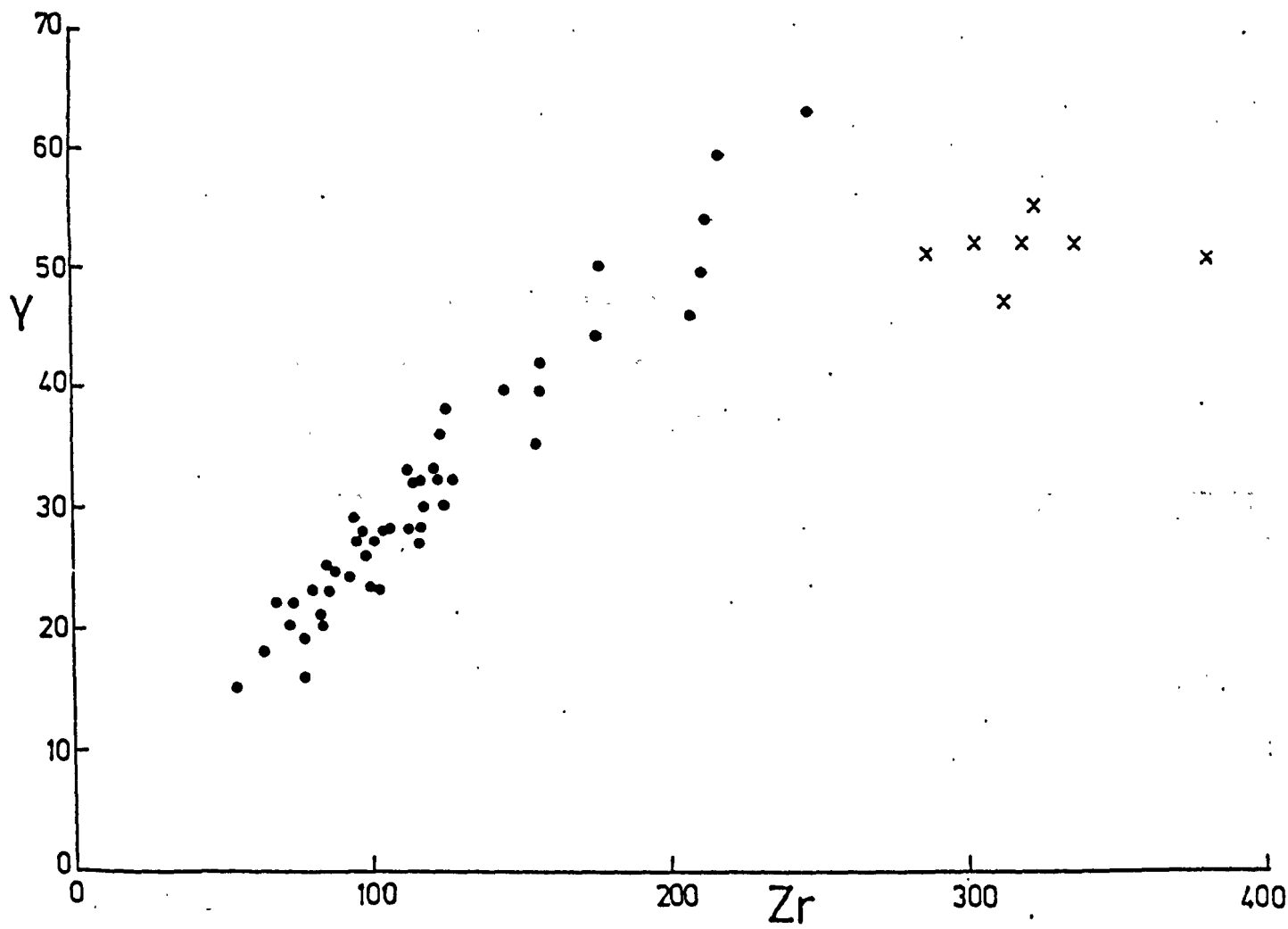
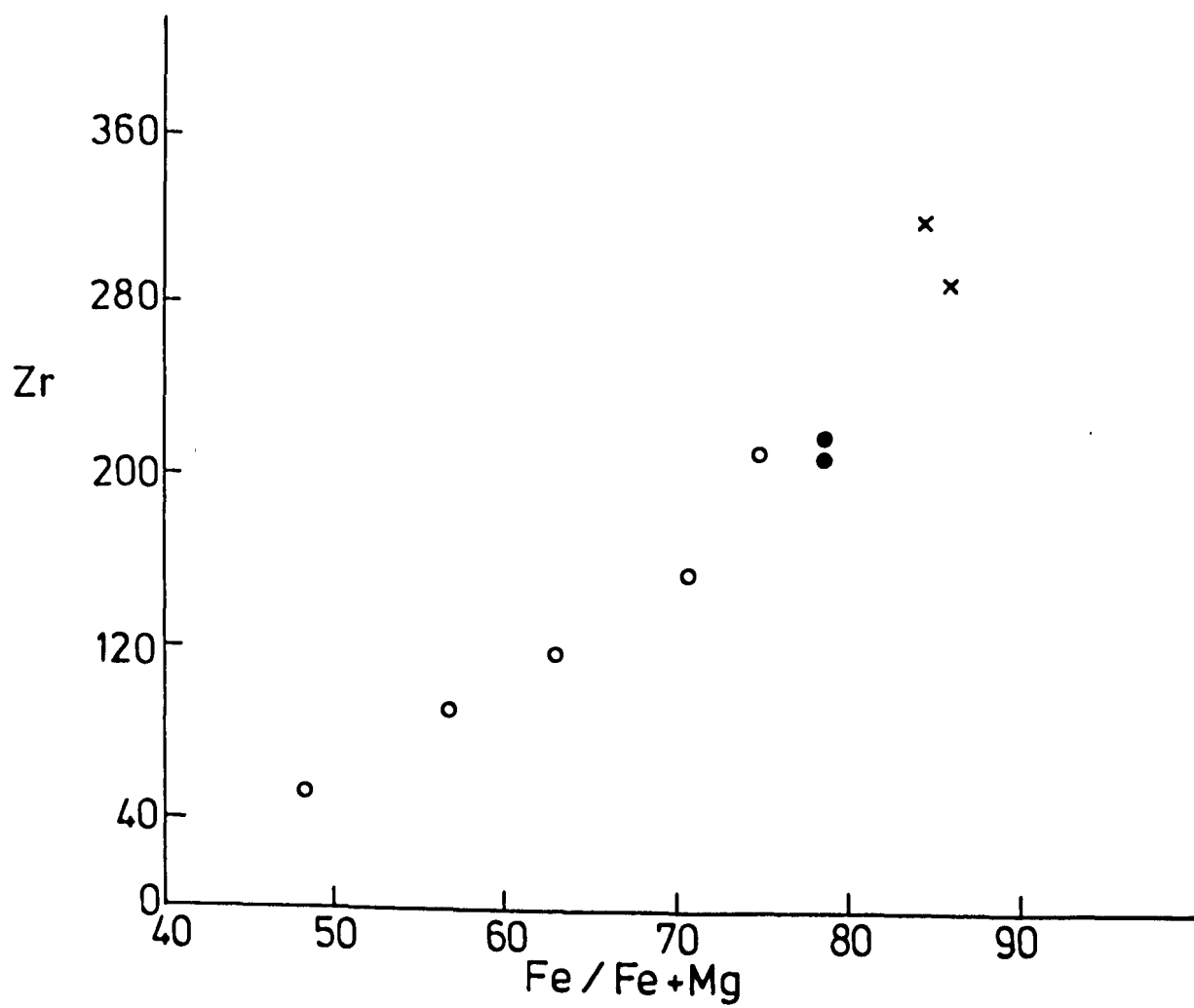




FIG. 189. Zr vs Fe/Fe + Mg (where Fe = total iron as  $\text{Fe}_2\text{O}_3$ ) showing analyses of a number of rocks from group 1 (open circles), group 2 (filled circles) and group 3 (crosses).



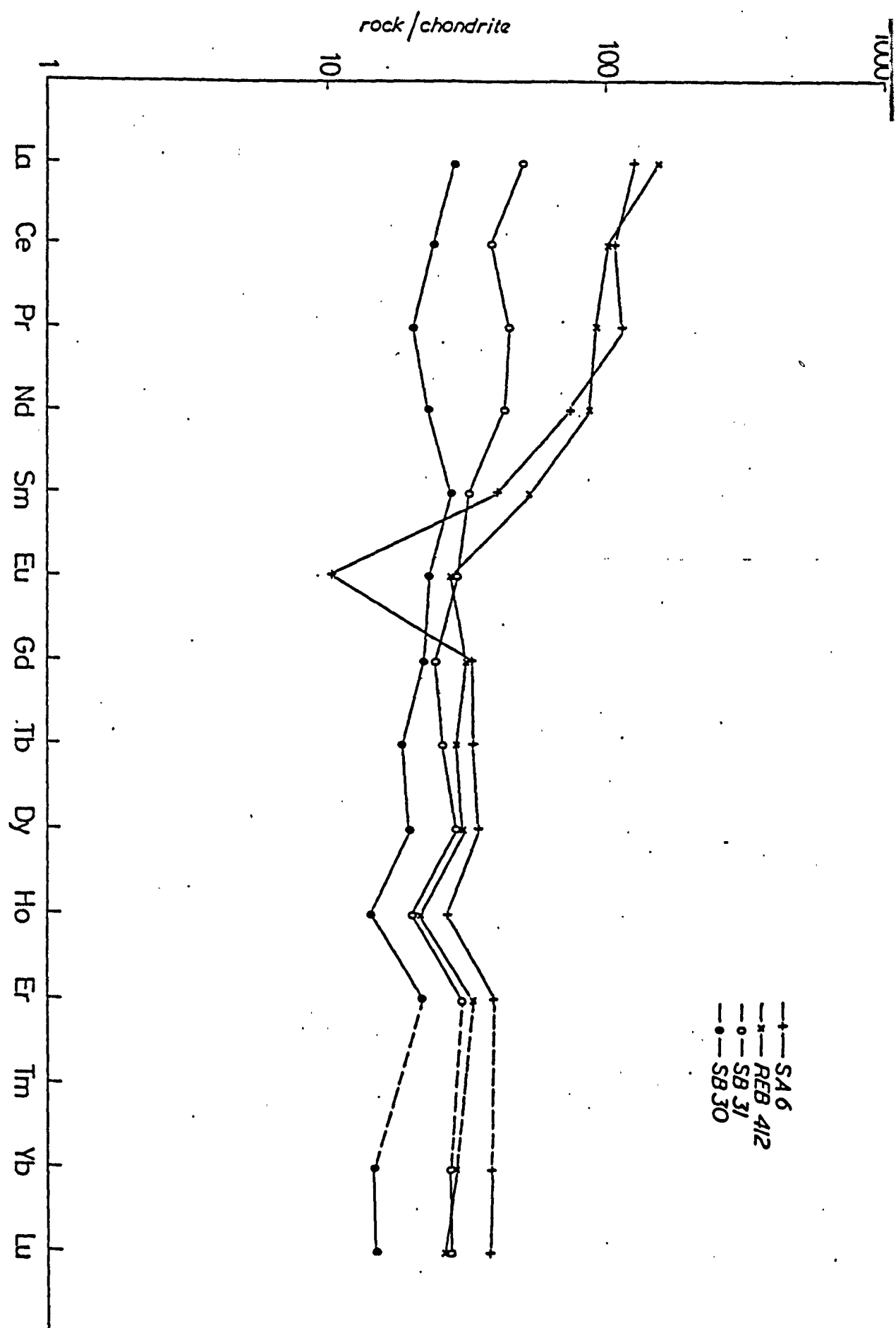
variables and supports the contention that group 3 belongs to the same line of liquid descent. If this is the case, then for this group of rocks  $f \approx 0.15$ .

This magma group shows a slight light rare-earth enrichment (Fig.190) which may be explained by the extensive removal of clinopyroxene which has a higher distribution coefficient for the heavy rare-earth elements. In addition, a slight europium anomaly ( $\text{Eu}/\text{Eu}^* = 0.59$ ) is probably the result of extensive removal of plagioclase feldspar, which has high  $D^{S/L}$  for Eu.

#### 6.5. GEOCHEMICAL EVIDENCE FOR THE ORIGIN OF GROUP 4

Samples of group 4 (those with  $\text{SiO}_2 > 71\%$ ), the most siliceous magmas of the Fishguard area, were collected from rhyolitic lava flows of the Porth Maen Melyn Volcanic Formation and the Goodwick Volcanic Formation. These rocks are of limited compositional range with  $\text{SiO}_2$  and  $\text{Al}_2\text{O}_3$  being the most important components, along with the alkalis. However, there is evidence that alkali-metasomatism has affected these rocks and present concentrations of  $\text{Na}_2\text{O}$  and  $\text{K}_2\text{O}$  in addition to Rb, Sr, and Ba in no way represent original igneous concentrations. However, it is believed that these rhyolites are metaluminous and similar to those described from Iceland (Carmichael, 1964) and California (Carmichael et al., 1974) and are clearly different to pantelleritic and comenditic rocks where  $\text{Al}_2\text{O}_3 < \text{Na}_2\text{O} + \text{K}_2\text{O}$ . This contention is supported by low concentrations of trace elements such as Zr, Nb, La, Ce, etc., all of which are enriched in pantelleritic and comenditic liquids.

FIG. 190. Chondrite normalized rare earth element patterns for rocks of the Fishguard Volcanic Group.



Trace element concentrations are distinctive in comparison with other groups. The REE are relatively enriched compared to groups 1 and 2, particularly the light REE (La, Ce, etc.). The transition elements are almost all below detection limit, typical of such acidic rocks. Nb and Y concentrations are relatively high (approximately 25ppm and 75ppm respectively) whilst Zr is slightly depleted compared with groups 2 and 3. The alkaline earth elements are highly variable and no consistent pattern can be deduced.

The origin of rhyolitic magmas associated with differentiated tholeiitic suites has proved problematical in a number of classic cases (e.g. Karroo, Thingmuli, etc.). In the case study of altered volcanic suites this problem is made even worse by recrystallization and alteration effects. Two principal origins for such acidic magmas are generally forwarded, namely that they represent the liquid derived from a protracted line of liquid descent, or secondly that they represent anatectic crustal melts generated during the rise of the basic magma through continental crust. More recently, Ewart et al. (1977) suggested that the Tertiary rhyolites of the Tweed Volcano, S.E. Queensland represented liquids derived by a fractionation process from a basic parent, but which had suffered contamination due to crustal assimilation during their rise.

The rhyolites of Thingmuli appear to be a clear example of such lavas which have been generated from a basic parent due to a fractional crystallization process. Indeed, in this case no continental crust exists as a possible source for anatectic melting.

Carmichael (1964) suggested that silicic magmas derived from a basic one would precipitate only one feldspar, a sodic plagioclase, in contrast to the two-feldspar bearing rhyolitic magmas which represent magmas from other sources. Unfortunately, in view of subsequent alteration processes, such a distinction may not be used for the Fishguard lavas.

Trace element concentrations in rhyolitic magmas of contrasting origins are not significantly different, despite various attempts by certain workers to use such parameters. Recently, Bruhn et al. (1978) suggested that silicic volcanics from the Tobifera section, north of the Beagle Channel, southernmost Argentina, were derived by crustal melting compared with the calc-alkaline Patagonian Batholith, which displays a variation due to fractional crystallization. In support of this they compare the Tobifera volcanics with analyses of rhyolites from Taupo, New Zealand (Ewart et al., 1968). However, they compare values for elements such as Rb, Sr, and Ba, which are particularly mobile during recrystallization and metamorphism. In addition concentrations of other elements quoted (Zr and Nb) are not significantly different between the suites. Whilst concentrations of Zr are comparable with rhyolitic lavas from Taupo, New Zealand (the origin of which is considered to be partial melting of underlying crust), Nb concentrations are significantly greater within the Fishguard rocks. However, Zr and Nb are greatly enriched in the rhyolitic lavas of Eastern Iceland (Wood, 1978). As would be expected, major element concentrations are roughly similar in all of the above suites. In Figure 190 the rare earth element content of sample SA6, from the Goodwick Volcanic Formation, may be seen.

The overall pattern is broadly similar to that of the rhyodacites and dacites of group 3 (see sample REB412), which it has been suggested were derived from a basic parent through a process of fractional crystallization. In addition, however, a significant europium anomaly exists within this sample ( $\text{Eu}/\text{Eu}^* = 0.27$ ). Such anomalies in granitic and rhyolitic rocks have been taken as evidence for an origin by fractional crystallization due to the high  $D^{S/L}$  between Eu and both plagioclase and K-feldspar (Weill and Drake, 1973), as recently emphasized by Hanson (1978). The removal of large amounts of feldspar depletes the liquid in Eu. The gradual development of an europium anomaly in the series basalt-dacite-rhyolite in the Fishguard rocks suggests that the three rocks may be genetically linked. Similarly an enhancement of normalized distribution patterns from the basalts to the dacites supports this conclusion. However, similar  $\Sigma\text{REE}$  for the dacites and rhyolites may reflect the removal of REE in phases such as apatite and zircon, which may be identified as liquidus phases.

Commonly, volume relationships between rhyolitic and basic magmas are problematical if it is suggested that the rhyolitic magmas represent protracted liquids by crystal fractionation processes. In the Fishguard case it is likely that these liquids would represent considerably less than 15% of the primary melt. However, it is not possible to make volume estimates between basic and acidic magmas in North Pembrokeshire as no idea of the offshore extension of the Fishguard Volcanic Group is presently known.



Another possibility is that the rhyolites represent the product of a period of crustal melting. The existence of sialic crust at a shallow depth is certainly evident, as Pre-Cambrian basement of an acid to intermediate nature is exposed in the St. David's district (Thorpe, 1970).

Thus, whilst the origin of the rhyolitic lavas of this region remains speculative, in the absence of contradictory evidence, it is suggested that, in contrast to popular ideas of Lower Ordovician acidic magmas in Wales (e.g. Hughes, 1972), the Fishguard Volcanic Group rhyolites represent liquids derived by extreme fractionation of a basic parent.

#### 6.6. ORIGINS OF THE PRIMARY MAGMA

The similarity of the more basic members of group 1 rocks to ocean-floor basalts suggests that the Fishguard samples were generated as a result of partial melting within the mantle. The composition of the primary magma will necessarily be dependant, in part, upon the degree of partial melting which has occurred. The remainder of the suite will then have been generated from this primary melt by high-level fractional crystallization.

Recently, many melting models have been put forward based upon rare earth element concentrations in basic rocks, assuming that mantle concentrations mirror those found in chondritic meteorites. However, during the course of this study only a small number of REE element determinations have been made and hence the incompatible elements will be used in an attempt to model partial melting processes.

Calculations of the degree of the partial melting necessary to produce the most primitive magma in group 1 can only, at best, be approximate. However, these studies provide qualitative information which, when used with evidence obtained from other sources, can give an idea of the nature of the processes responsible for the magma suite concerned. Variations in the estimates may be due to the influence of a large number of factors. Firstly, models of the chemical composition of the mantle are very variable and values suggested necessarily depend upon the modal mineralogy envisaged for the starting material (for example, pyrolite of Ringwood (1966); garnet-lherzolite of Kushiro (1973) etc.). Secondly, ideas of magma generation and separation are variable. Menzies (1976) suggested that the separation of a 10% - 30% partial melt liquid from Othris and Lanzo peridotites had occurred, to produce tholeiitic liquids, which had risen to the surface and extruded as surface flows. Various workers (e.g. Green, 1970) seem agreed that ocean-floor basalts with  $Mg/Mg + Fe$  around 0.70 are the result of direct partial melting of mantle material of approximately the same magnitude as suggested by Menzies (1976). It is of note that LD2, one of the most primitive Fishguard magmas, has an  $Mg/Mg + Fe$  ratio of 0.52, and therefore either represents a liquid which was produced by lesser degrees of partial melting than that discussed above, or alternatively represents liquid derived from a more primitive parent (for example by crystal fractionation).

O'Hara et al. (1975) argue, however, that mantle compositions based on nodules in kimberlites from South Africa require extensive crystal fractionation both at high and low pressures to produce the tholeiitic magmas which are seen at the surface. Clearly, until all the variables (mantle composition, mantle and crustal processes etc.) are fully

understood, models of this nature may, at best, be only speculative. Indeed, further complications result from the question whether the mantle has been depleted by previous episodes of melting and is thus inhomogeneous in character. Certainly ocean-floor basalt chemistry suggests the existence of an inhomogeneous mantle under parts of the oceanic crust.

Allègre et al. (1977) and Bougault (1977) have recently outlined a method for determining the chemical composition of the initial melt derived during a partial melting episode of the mantle. Using the partial melting model of Shaw (1970) (equation 1 of section 6.2) it can be shown that  $C^L/C^0$  does not vary greatly with varying 'f' for elements with a high D value, such as Ni (e.g. at 'f' = .10,  $C^L/C^0$  = 0.109; at 'f' = .20,  $C^L/C^0$  = 0.116, during melting of mantle-like peridotite). This is due to the fact that the Ni content of the liquid produced over a wide range of melting (3% - 30%) of peridotite only varies from about 300ppm to 450ppm, assuming an original mantle value of approximately 2400ppm, as used by Allègre et al. (1977), in similar calculations. Bougault (1977) suggests that when 'f' has been calculated for Ni and Cr, initial concentrations of all the other trace elements may be calculated. If an element with a low D is used, then, assuming a mantle value for that element, the degree of partial melting can be deduced. Clearly, however, the assumptions made up to this point in the model are many; too many perhaps to justify its application. Nevertheless, if LD2 is taken as an assumed parent, then from its titanium concentration, about 10% to 15% partial melting is suggested, on condition that this represents a primary liquid, the direct result of

partial melting. It also depends upon an assumed initial Ti mantle value. However, partial melting in this range would produce concentrations of other low partition coefficient elements similar to those seen in LD2, and thus whilst this is only a very approximate estimate, it is probably within the correct range. Assuming chondritic-like values for the rare-earth elements within the mantle, the values recorded for the heavy rare-earth elements agree with this degree of partial melting. The light rare-earth element concentrations, however, suggest considerably lower degrees of melting. This may be due to slight mobility of the light REE during alteration. Certainly, if a low degree of partial melting had occurred, then the concentrations of other relatively incompatible elements (e.g. Zr, Nb, Ti, Y etc.) would be considerably higher than the values recorded.

Thus, whilst it is necessary to consider all the assumptions used in the development of this model, the results appear to confirm the deductions that could be made subjectively. It thus appears that approximately 10% - 15% partial melting of undepleted mantle material occurred during Llanvirn times, generating a liquid of tholeiitic composition. The most 'primitive' magma sampled at the surface today has an  $Mg/(Mg + Fe)$  of 0.52. Subsequent low-pressure fractional crystallization of this melt resulted in the chemical diversity seen within groups 1, 2, and 3, and indeed probably group 4 also.

## CHAPTER 7. METAMORPHISM

### 7.1. INTRODUCTION

There has been little attempt to identify the nature of metamorphism within the Lower Palaeozoic rocks of Wales. Other than on a very local scale, no systematic investigations of mineral assemblages appear to have been undertaken. As a result, an examination of the mineral assemblages of meta-basic rocks from the Fishguard area, as well as from other parts of Wales was made and inferences may be drawn from the assemblages regarding both the local and regional aspects of Caledonian metamorphism. These are discussed, after a brief review of the few previous studies.

The peculiar petrography of the manganiferous horizons of the Harlech Dome was first described in detail by Woodland (1938). He suggested that the present assemblage of biotite, chlorite, sericite, spessartite etc. was the result of metamorphism, and states (in Matley and Wilson, 1946, p. 33) that the rocks belong to 'a zone of metamorphism equivalent to the chlorite zone of regional metamorphism'. Although many workers identified chlorite, sericite and, locally, biotite within the meta-sediments, the exact grade of metamorphism is rarely mentioned and Woodland's account represents one of the few specific references in which a clear indication of the metamorphic grade attained is given. The first identification of pumpellyite, a potentially significant indicator of metamorphic grade, within rocks from Wales was made by Nicholls (1959), although Reed (1895) described a mineral which he was unable to name specifically, but which appears to have been pumpellyite. Nicholls (op. cit.) described pumpellyite occurring in 'marginal sacs' in spilitic rocks

of Lower Ordovician age from Builth Wells, Mid Wales, replacing plagioclase feldspar, and suggested that it was produced as a result of extensive Ca-Mg-Fe metasomatism. This view was later refuted by Raam et al. (1969), who observed authigenic pumpellyite in the associated sediments and subsequently by Coombs (1974), who attributed the mineral assemblage to prehnite-pumpellyite facies metamorphism. This latter view is endorsed by the author, as will be discussed below (section 7.5.4.). Jenkins and Ball (1964) described detrital pumpellyite in Snowdonian soils. They located the source of the pumpellyite in the dolerites and gabbros in the Conway Valley area, although no inference as to its origin was made. Examination by the author of material collected from this same area by Drs. Floyd and Roach has similarly revealed the presence of minor pumpellyite. Rast (1969) realized the significance of prehnite and pumpellyite in the igneous rocks of Wales, but erroneously suggested that they were the product of zeolite facies metamorphism. As explained elsewhere, evidence suggests that the grade was somewhat higher than this. Roach (1969) reported the presence of amphibole, prehnite, epidote, and stilpnomelane from the St. David's Head and Carn Llidi Intrusions. Initially, these were thought to be of deuteric origin, but now (Roach, pers. comm.) are considered to be partly metamorphic. Bloxam and Price (1961) recorded the presence of stilpnomelane from the Dolgelly area, Mid Wales and suggested it was the result of low-grade metamorphism in the chlorite sub-zone one. Ridgeway (1971) identified various mineral assemblages in dolerites from the Aran Mountains area, in Mid Wales. These included prehnite, pumpellyite, epidote, actinolite, sericite, stilpnomelane, zoisite, clinozoisite, albite, and sphene. He suggested (op. cit. p. 178) that these were produced as a result of burial metamorphism, and recognized

two zones, one containing prehnite-pumpellyite facies assemblages, and the other greenschist facies assemblages. He suggested that the transformation from one to the other was produced as a result of increased overburden. Clearly, a small number of separate recordings of critical minerals and mineral assemblages have been made, but no overall correlations, with a view to determining the metamorphic grade or grades present within this part of the British Caledonides, have been attempted.

There is clear evidence of considerable deformation especially within the more pelitic units of the Lower Palaeozoic rocks of this region. A pervasive slaty cleavage is commonly developed within the pelitic rocks, whilst the more competent horizons may show the presence of a weak fracture-type cleavage. The deformation itself was variable in intensity over the paratectonic Caledonides. Recently, Roberts (1967) and Fitches (1972) have identified three separate periods of deformation in the Lower Palaeozoic rocks of Wales. These deformation episodes were probably end-Silurian in age, and were accompanied by considerable mineral reconstitution as a result of increased temperature and pressure conditions. This reconstitution is identified in the pelitic rocks by the formation of muscovite mica, as can be clearly seen for example in the study area within pelitic sediments from Porth Maen Melyn (sample 512), which are of probable Lower Llanvirn age. Recently, an attempt has been made to identify the grade of metamorphism based upon the degree of illite crystallinity (Weaver, 1960; Kubler, 1964; Weber, 1972 etc.). This method employs the measurement of the shape of the illite peak recorded by x-ray diffractrometry. However, the

basic meta-igneous rocks offer the greatest possibilities for interpretation of metamorphic grade based upon mineral reconstitution. As a result of initially high contents of Ca, Al, Fe, and Si in these rocks secondary phases, particularly hydrated calcium-aluminium silicates, are abundantly developed and it is this group of minerals in particular which appear to be most useful in determining the facies of metamorphism attained at low grades. Unfortunately, basic igneous rocks are not universally developed in Wales, and large areas of country, particularly those where post-Caradocian strata are exposed, are devoid of basic igneous rocks. Thus, it may be possible that the best results will be obtained by determining the illite crystallinity of the sediments within areas containing basic igneous rocks and utilising these results in comparison with illite crystallinity data from areas which lack basic igneous rocks.

It is considered here that the Ca-Al silicate phases developed within the basic igneous rocks of the Fishguard area, and described in Chapter 4, are metamorphic in origin. However, all of these phases may also be developed in low pressure, hydrothermal systems. Indeed, both pumpellyite and epidote have been observed in hydrothermally altered rocks from Iceland (Sigvaldasson, 1962) and all the phases, including actinolite, have been reported from hydrothermally altered basalts dredged and drilled from the ocean floor (see for example Cann, 1969; Miyashiro et al., 1971). However, the timing of alteration will be discussed more fully below.

## 7.2. MINERAL ASSEMBLAGES

The following secondary minerals were identified within the basic igneous rocks of the Fishguard area; chlorite, sphene, albite;



epidote, pumpellyite, prehnite, white mica, actinolite, calcite, stilpnomelane, blue-green hornblende, and brown amphibole. These phases will be discussed following a brief account of the mineral assemblages commonly present. A more detailed account of their mineral chemistry has already been given in Chapter 4.

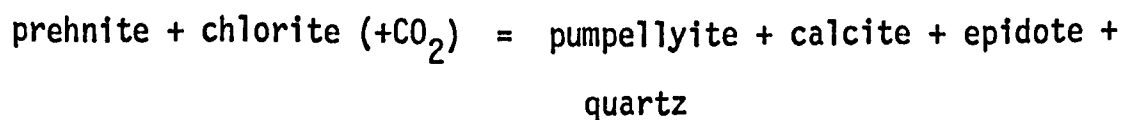
Chlorite and sphene are ubiquitously developed, and thus are present in all assemblages described here. Albite is generally present, although in some rocks, a more calcic plagioclase is preserved. However this generally only occurs in the intrusive rocks, with the pillowed and massive flows showing completely albitized feldspars.

A problem encountered in listing mineral assemblages is the scale over which minerals are considered to be in equilibrium with each other. Zen (1974) discussed this problem at length, stating that ideally only grains in contact with each other and showing no evidence for reaction should be considered to be in equilibrium, a line followed later by Kawachi (1975). However, by geometrical constraints, this limits assemblages to about three phases at the most. Zen (1974) thus lists assemblages seen over the scale of about 1mm of a thin section, and which show no obvious signs of reaction between mineral pairs. Nakajima et al. (1977), in contrast, use the whole field of one thin section. This latter approach is also used in the present study, although the strict constraints obtained by other workers from mineral compositions determined by microprobe analyses cannot be applied here.

Assemblages recorded are listed in Appendix 3. The most common assemblage is chlorite-sphene-epidote-albite, whilst chlorite-sphene-epidote-albite-pumpellyite, and chlorite-sphene-albite-pumpellyite are

also common. When calcite is particularly abundant, chlorite pseudomorphs the original ferromagnesian phase, but no calcium-aluminium silicates are developed. Specimen SB15, a highly vesiculated lava from Lower Fishguard Harbour, is a good example showing such a case. A very common association identified on a local scale in many rocks is chlorite-epidote. From its occurrence in certain hyaloclastites, it appears that this assemblage possibly represents the alteration product of glass. This association is also found however in vesicles in lavas, as well as in interstitial areas in some of the gabbroic bodies. The assemblage is clearly in equilibrium as the epidote crystals show a faceted form (see Fig. 49). If the assemblage has resulted from the alteration of glass then a considerable loss of silica and alkalis has occurred during hydration. In contrast, iron, manganese, magnesium, and calcium contents may possibly be representative of original values.

Spatial variations in the mineral assemblages are observable within the Pen Caer region. Figure 191 shows the distribution of pumpellyite and prehnite within the lava pile of the Strumble Head Volcanic Formation and basic units of the Goodwick Volcanic Formation. Two zones are seen, namely a pumpellyite-prehnite bearing zone (zone 1) and a pumpellyite-bearing, prehnite-free zone (zone 2). Zone 2 rocks are characterized by abundant epidote and it is possible that prehnite disappeared as the result of the following reaction



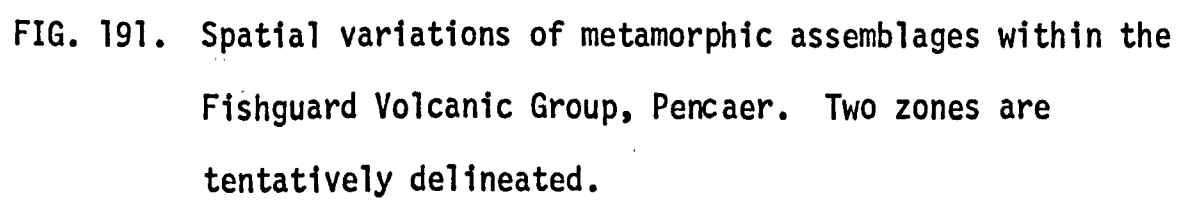
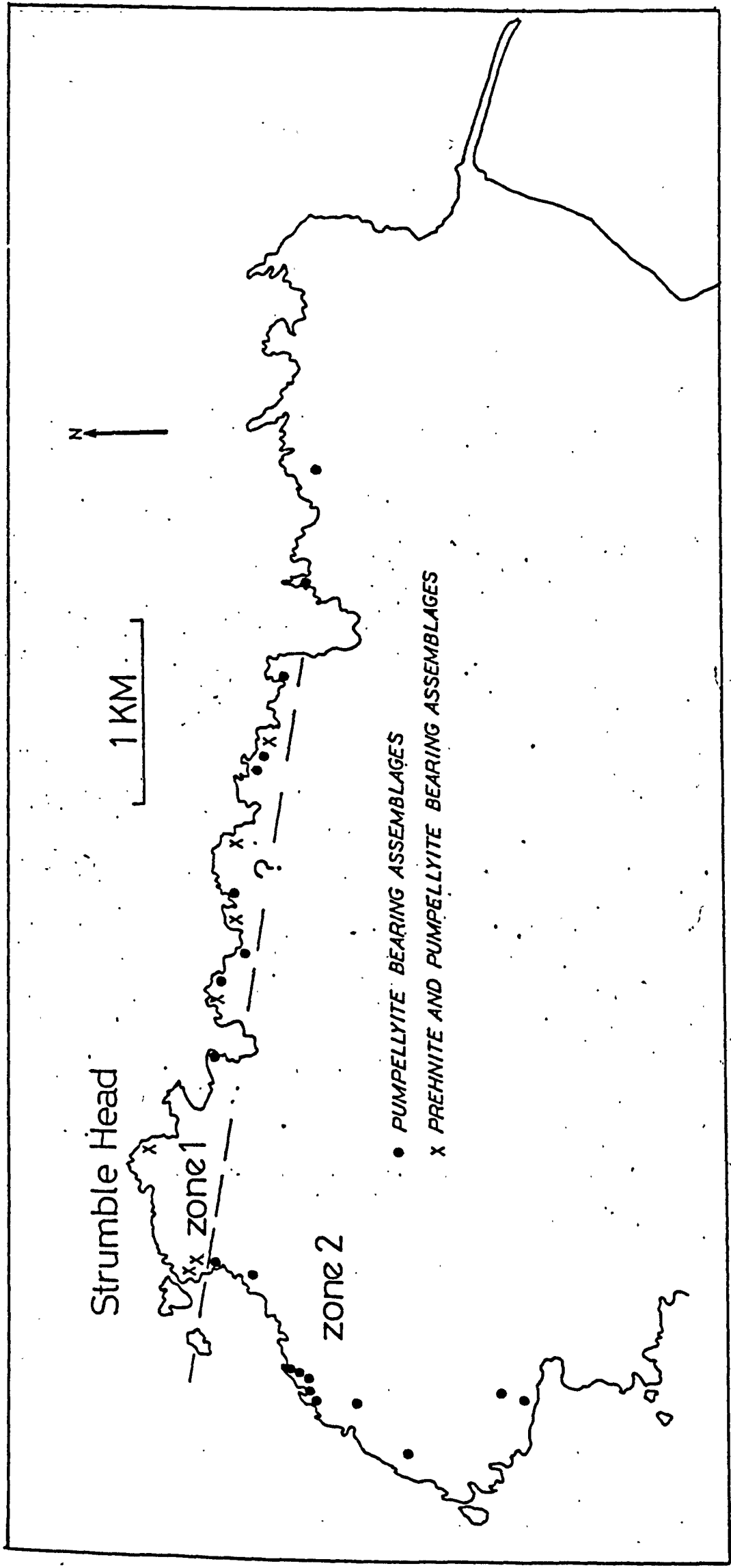
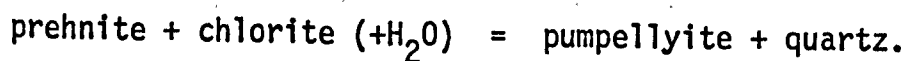


**FIG. 191. Spatial variations of metamorphic assemblages within the Fishguard Volcanic Group, Pencaer. Two zones are tentatively delineated.**



Prehnite may also have disappeared by the reaction



Direct evidence for the latter reaction was obtained from SB9, a sample collected from close to the boundary between zones 1 and 2, near the lighthouse, at Strumble Head (GR 893412). In the same rock granular aggregates of the minerals present in the first reaction outlined above suggest that the first reaction may also have occurred. Local variations in  $\mu\text{CO}_2$  and  $\mu\text{H}_2\text{O}$  (where  $\mu$  = the chemical potential) possibly drive different reactions or phases may be fixed due to local variations in the ionic potential of  $\text{Ca}^{2+}$ ,  $\text{H}^+$ , and  $\text{Si}^{4+}$ . In the east, however, at Carregwastad Point (GR 926406), no evidence for either of the above reactions was seen, despite all the above phases being present. Chlorite and prehnite are found side by side, with no evidence of reaction.

The intrusions, which appear to represent a co-magmatic high level suite, show contrasting assemblages to those of the zones identified within the lava pile, described above. Within individual intrusions contrasting assemblages are also found, but these do not show any systematic variation. Prehnite and pumpellyite are well developed, particularly in Y Garn and Garn Fawr intrusions. One sample collected from Garn Fawr (GF 53) is almost totally composed of prehnite and pumpellyite, although rare clinopyroxene crystals testify to the rocks igneous parentage. YG 54, from Y Garn, contains a well developed prehnite-pumpellyite vein, illustrated in Figure 53.

Actinolite is present in minor amounts, generally rimming clinopyroxene. It is found in the Y Garn and Garn Gilfach intrusions, where it is colourless and has a fibrous habit. Some of the more important secondary phases identified will now be described in more detail.

### 7.3. METAMORPHIC PHASES

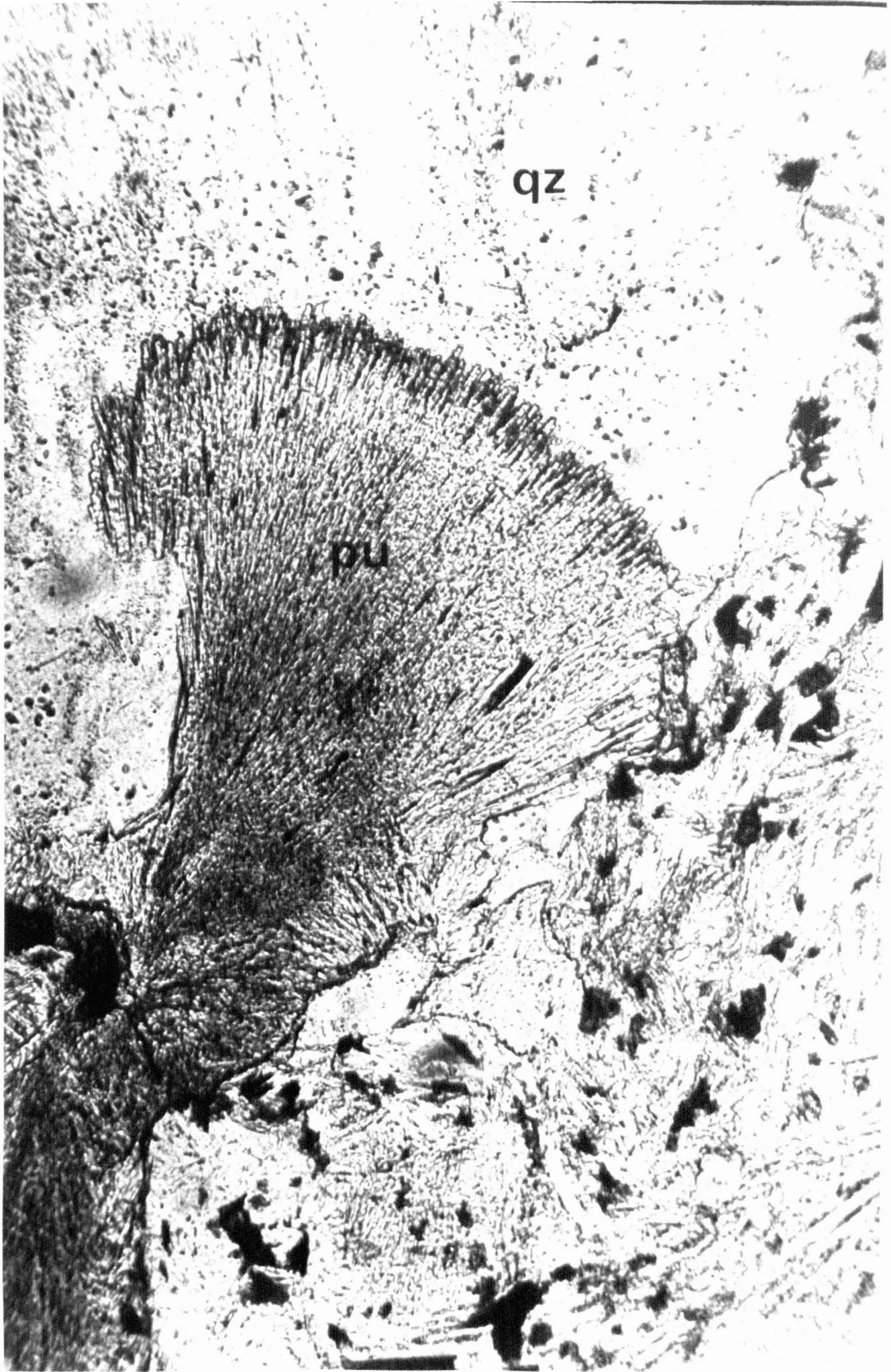
#### 7.3.1. PUMPELLYITE

Pumpellyite from the basic igneous rocks of North Pembrokeshire has been briefly described by Bevins (1978). It shows a number of contrasting occurrences, varying both in habit and optical characteristics. Generally it forms only a small percentage of the mode, although occasionally it reaches about 40%. Chemical analyses and associated mineral recalculations are presented in Appendix 2. It is most frequently found pseudomorphing plagioclase feldspar or occurring as small crystal aggregates within feldspar (Fig. 52). In this form, it probably forms up to 8 modal percent of the rock. Very rarely, it is seen marginally replacing clinopyroxene (as for example in LG2), whilst in SB9 it replaces chlorite in a reaction relationship. Occasionally, pumpellyite is found within vesicles, but this appears only to be the case where the vesicles are infilled with silica. In these cases quartz-pumpellyite intergrowths appear to be a stable assemblage, and euhedral elongate prismatic crystals of pumpellyite are found (Fig.192). Examples of pumpellyite from other low-grade metamorphic terrains and showing forms similar to those reported here have been given by Jolly and Smith (1972) and Kuniyoshi and Liou (1976). Pumpellyite is

FIG. 192. Radiating aggregate of pumpellyite associated with quartz,  
in a pillow lava from Trwyn Llwyd. Scale bar represents  
0.25mm.

qz

pu





also found associated with prehnite in veins in gabbroic rocks of the Fishguard area, for example in sample YG54 from Y Garn (see Fig. 53), whilst one sample collected from Garn Fawr (GF53) shows an almost total replacement of the primary rock texture by an intergrowth of pumpellyite and prehnite, with clinopyroxene the only relict phase seen. Commonly, however, pumpellyite is found in the groundmass, intimately associated with chlorite and epidote (Fig. 54).

As stated above, pumpellyite shows varying optical properties. Most frequently it shows strong blue-green to colourless pleochroism. This pleochroic scheme is related to a moderate iron content. Rarely, a brown or greeny-brown to colourless scheme is observed and even more rarely it is totally colourless. These variations are thought to be due to local whole-rock compositional controls, although variations on a regional scale may possibly be related to metamorphic grade. Colourless pumpellyite, identified in quartz-epidote bearing veins in the Trefgarne Volcanics of Arenig age may possibly be related to a slightly higher metamorphic grade. Seki (1961) drew attention to the low iron content of pumpellyites from glaucophane schists, whilst pumpellyites from prehnite-pumpellyite facies terrains generally have moderated iron contents, usually greater than 10%  $\text{Fe}_2\text{O}_3$  in metabasite hosts. Nakajima *et al.* (1977) recently explained in a semi-quantitative manner the decrease of  $x_{\text{Fe}}^{\text{pp}}$  and  $x_{\text{Fe}}^{\text{Ep}}$  (where  $x_{\text{Fe}^{3+}}^{\text{pp}}$  = atomic  $\text{Fe}^{3+}/(\text{Fe}^{3+} + \text{Al})$  in pumpellyite and  $x_{\text{Fe}}^{\text{Ep}}$  = atomic  $\text{Fe}^{3+}/(\text{Fe}^{3+} + \text{Al})$  in epidote) with increasing temperature.

### 7.3.2. PREHNITE

Prehnite is best developed in the upper part of the lava pile of the Strumble Head Volcanic Formation, and also within the intrusions of Llanwnda, Y Garn, and Garn Fawr. It also occurs sparingly within the Llech Dafad Intrusion. In all these occurrences, it is associated with pumpellyite. It typically occurs in large, radiating, fan shaped or bow-tie shaped aggregates, with individual elongate crystals up to 1mm in length (Fig. 55). These aggregates show low first-order polarization colours and generally exhibit a wavy, incomplete extinction. In samples SB8 and SB9 [collected from the neighbourhood of Strumble Head Lighthouse], prehnite is found infilling vesicles whilst from other localities it may be seen replacing calcic plagioclase. Rarely, it replaces glass in basic hyaloclastites. It is white in hand specimen, and in transmitted light, it is generally colourless, although occasionally, however, it has a pale brown colour, suggesting the replacement of Al by  $\text{Fe}^{3+}$ . In the lavas and intrusions, it forms up to 7 modal percent of the rock. Locally, however, as described above, it is associated with pumpellyite in veins.

### 7.3.3. EPIDOTE

Epidote is used here in a general sense, to include all members of the range clinozoisite to pistacite. It is the latter phase which is generally developed with the iron contents reflected by a strong yellow to colourless pleochroic scheme. However, colourless crystals are sometimes developed, suggesting a clinozoisitic composition. Associated with this decrease in iron is a decrease in the order of polarization colours, and those crystals which are

100

colourless in plane light generally show low first order or even anomalous interference colours. Epidote most commonly occurs as granular aggregates in the groundmass, or more rarely as discrete euhedral crystals. In many rocks, it is found as euhedral crystals associated with chlorite. The epidote generally grows from the margin of the chlorite, inwards (see Fig.49b). In the Porth Maen Melyn area, considerable Ca metasomatism appears to have occurred, as epidote pods and veins are common within the pillow lavas.

#### 7.3.4. CHLORITE

Chlorite is one of the most abundant of all the secondary phases present within the Fishguard Volcanic Group and accordingly shows many different modes of occurrence. In all of these, however, its optical properties are fairly constant, possessing dark blue or purple anomalous interference colours, with green to colourless pleochroism. Occasionally, however, dark brown anomalous interference colours are present. Microprobe analyses of a number of crystals show significant Fe-Mg variation (see Appendix 2), although most chlorites analysed are brunsvigites or pycnochlorites according to the classification of Hey (1954). Chlorite most commonly occurs in the groundmass of the lavas and intrusions. It occurs between the feldspars of rocks showing an intersertal texture, and also occurs between the feldspars of the coarse-grained intrusives, such as the Llanwnda rocks. Chlorite of similar form has been identified in samples from coarse-grained, high-level sheets drilled from the ocean floor during the Deep Sea Drilling project (e.g. Leg 30; see Stoesser, 1975), and it is thought possible that in such high-level sheets a fine-grained or glassy mesostatis may be formed. A similar conclusion is reached after inspection of sample LG6 from Llanwnda.

Here large, tabular feldspars and equant clinopyroxenes are separated by a fine-grained matrix containing hollow and skeletal feldspars, typical of crystals with rapid cooling histories. Clearly, therefore, the chlorite occurring in these areas may be after glass. In the pillow lavas, chlorite occurs in the groundmass, infilling vesicles, and replacing the former glassy crust of the pillows. Chlorite is also present as small inclusions within plagioclase feldspars and more rarely it pseudomorphs clinopyroxenes, particularly in highly carbonated rocks. In basic hyaloclastites and hyalotuffs, the glassy shards are usually replaced by chlorite, and are associated with euhedral epidote crystals. Within a number of samples collected from the intrusions, such as Y Garn and Garn Gilfach, a chlorite-like mineral shows slightly higher birefringence than normal chlorites, and is yellowy-green in colour. This is thought to be an iron-rich chlorite.

#### 7.3.5. STILPNOMELANE

Stilpnomelane is only rarely identified within the rocks of the Fishguard Volcanic Group. It occurs as thin needles forming bow-tie shaped aggregates, which are strongly pleochroic from yellow-brown to straw-yellow. It is present locally within the lavas of the Strumble Head Volcanic Formation, as well as within a number of basic intrusions. Its presence may be a response to high whole-rock Fe/Mg ratios. The pleochroic scheme suggests that it is ferristilpnomelane.

#### 7.3.6. SPHENE

Sphene, along with chlorite, is ubiquitously developed within the basic igneous rocks, and is in fact also present within the

intermediate and acidic rocks. In the basic rocks, it occurs as small spherules, composed of a granular aggregate of small crystals (Fig. 49). It shows high relief and very high birefringence. Analysis suggests that it is grothite, with considerable amounts of Fe and Al incorporated within the structure (see Appendix 2). Sphene also occurs as a replacement of the Ti-rich portions of unmixed Ti-Fe ores in some of the slow-cooled intrusive bodies (Fig. 51). Commonly, haloes of sphene are found around ore crystals in rocks where unmixing has not occurred. This suggests that titanium has been released by the ore phase during alteration, but fixed locally in association with calcium to produce sphene. Therefore titanium is in fact mobile on the very local scale (thin section scale), but immobile on the scale of a hand specimen. This mobilization and fixing no doubt accounts for the very high titanium contents recorded in the margins of some pillows (see, for example, Vallance, 1965). Sphene is abundant throughout the rocks no doubt due to the fact that this phase is the only secondary phase within the rocks which incorporates titanium. Chlorite, pumpellyite, prehnite, and epidote are all Ti-free. Considerable Ca is also readily available due to albitization of the feldspars. Only very rarely are sphenoid-shaped crystals recognized as for example in a hyaloclastite sample from the cliffs above Porth Maen (PMV3). In this rock spherulitic aggregates of sphene are also observed.

#### 7.3.7. ACTINOLITE

Actinolite is rarely seen within the lavas of the Fishguard Volcanic Group or the associated intrusions. In the Y Garn - Garn Gilfach complex a colourless amphibole showing moderate birefringence

is sparingly developed.

#### 7.3.8. BROWN AMPHIBOLE

A brown amphibole has been identified which occurs within clinopyroxene crystals in a number of rocks, particularly the intrusive rocks from Llanwnda and Y Garn. This amphibole shows moderate to low birefringence, and strong brown to colourless pleochroism. It is also found occasionally associated with chlorite in vesicles or the groundmass. It is widespread in occurrence, although forming only a very small percentage of the rock. It is also found within the dolerites of the Prescelly Hills. The origin of this phase is considered to be due to late-stage magmatic alteration.

#### 7.3.9. SERICITE

Sericitic mica is widespread throughout the basic igneous rocks of the Fishguard Volcanic Group, and a white muscovite mica is also identified within the more pelitic sedimentary rocks. Sericite in the basic rocks is found predominantly within the calcic feldspars, although it may also occur in the groundmass. Superficially, it resembles prehnite.

#### 7.3.10. ALBITE

Extensive albitization of the calcic plagioclase feldspars has taken place and occurred most probably during metamorphism. This process liberated both calcium and aluminium, which were fixed by the formation of the calcium aluminium silicates described above. However, albitization was not universally developed, and more calcic plagioclase

members are commonly preserved. In these cases, the development of secondary phases is at a minimum, for example in sample SB57, from Clegryn. Albite crystals are generally milky coloured, and contain chlorite or pumpellyite crystals within them. Twinning is less clear than in unaltered crystals, and compositional zoning is generally absent.

#### 7.4. NATURE OF METAMORPHISM

From a consideration of the mineral phases described above, it is clear that the rocks of the Fishguard area have been subjected to a low-grade metamorphic episode. Within the metabasites of the Fishguard Volcanic Group it is possible to identify the nature of this metamorphism in terms of pressure and temperature and also to suggest the nature of the fluid phase present during metamorphism. The critical phases identified are pumpellyite, prehnite and actinolite. In the volcanic pile of the Fishguard Volcanic Group, pumpellyite and prehnite are well developed, although prehnite shows a local spatial and possibly stratigraphic restriction. These rocks are thought to belong to the prehnite-pumpellyite facies of metamorphism. The prehnite-pumpellyite facies was defined by Coombs 1960, after De Roever (1947) had proposed the presence of a pumpellyite facies. It appears to be intermediate between the zeolite facies and either the greenschist facies or, at high pressures, the lawsonite-albite facies.

From an inspection of Figure 191, it can be seen that the lava pile of the Strumble Head Volcanic Formation shows two distinct zones. Zone 1 is characterized by the presence of both prehnite and pumpellyite, whilst Zone 2 possesses only pumpellyite. It is



tempting to equate this to progressive metamorphism, as Zone 1 represents the upper part of the pile, whilst Zone 2 the lower part. The disappearance of prehnite prior to pumpellyite has been observed in many orogenic belts (e.g. Coombs, 1960). However, in these cases, actinolite appeared. In the rocks of Zone 2, neither prehnite nor actinolite are seen, and the common assemblage contains abundant pumpellyite, along with epidote. Further complications to this model exist when a fuller picture of the metamorphic assemblages is examined. If the gabbros of the Llanwnda, Y Garn, and Garn Fawr region are incorporated, prehnite-pumpellyite assemblages are identified, with actinolite locally present in minor amounts.

At these low grades of metamorphism, it is important to consider the nature of the fluid phase. As most of the secondary phases are hydrated minerals, most reactions involve the introduction of water to the system, and as pumpellyite is present  $\mu\text{CO}_2$  appears for the most part to have been low (Glassley, 1974). High  $\mu\text{CO}_2$  has been suggested to favour epidote and calcite assemblages, whilst low  $\mu\text{CO}_2$  favours pumpellyite. In the cases examined here, a high  $\mu\text{CO}_2$  appears to favour calcite + chlorite + albite assemblages with pumpellyite absent. A possible cause of the variation in assemblages between the lava pile and the intrusions may be due to varying permeability to circulating fluids. The intrusions of Garn Fawr and Y Garn possess channelways or veins through which Ca-rich fluids passed. These are identified presently as prehnite-pumpellyite veins. However, the lower part of the pillow lava pile shows such veins, but the assemblage here is epidote  $\pm$  pumpellyite. Nitsch (1971)

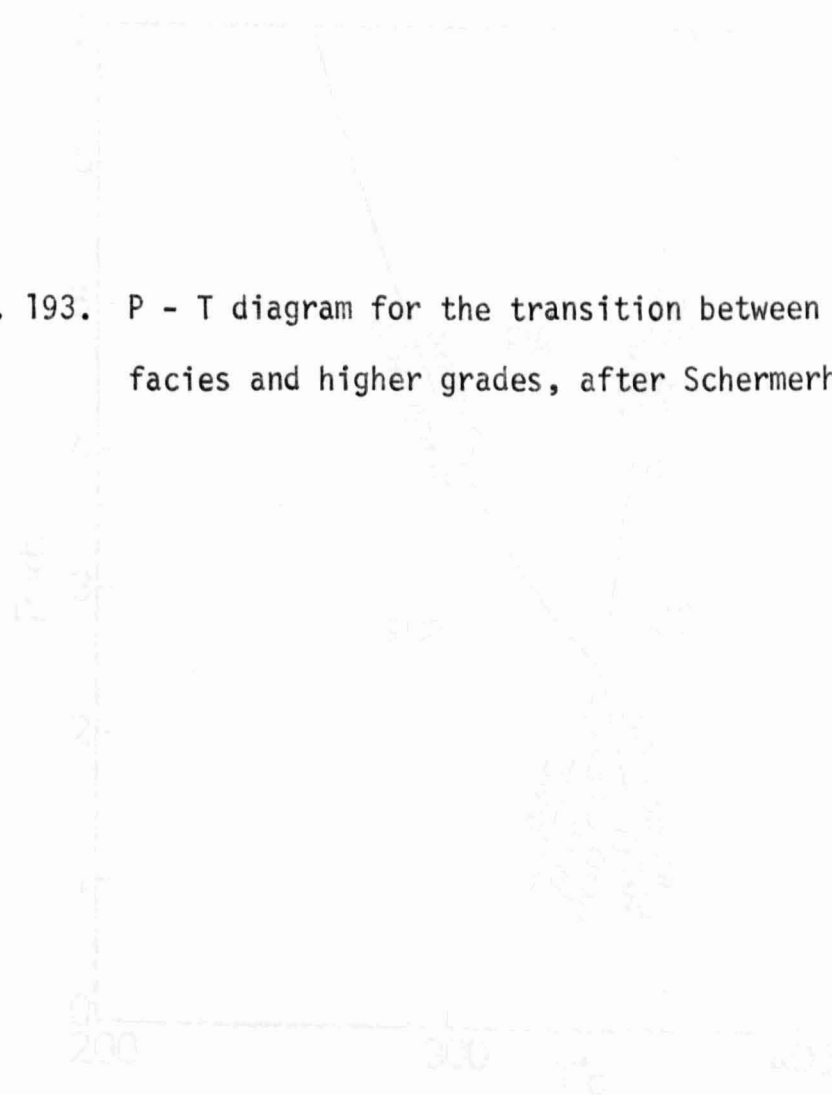


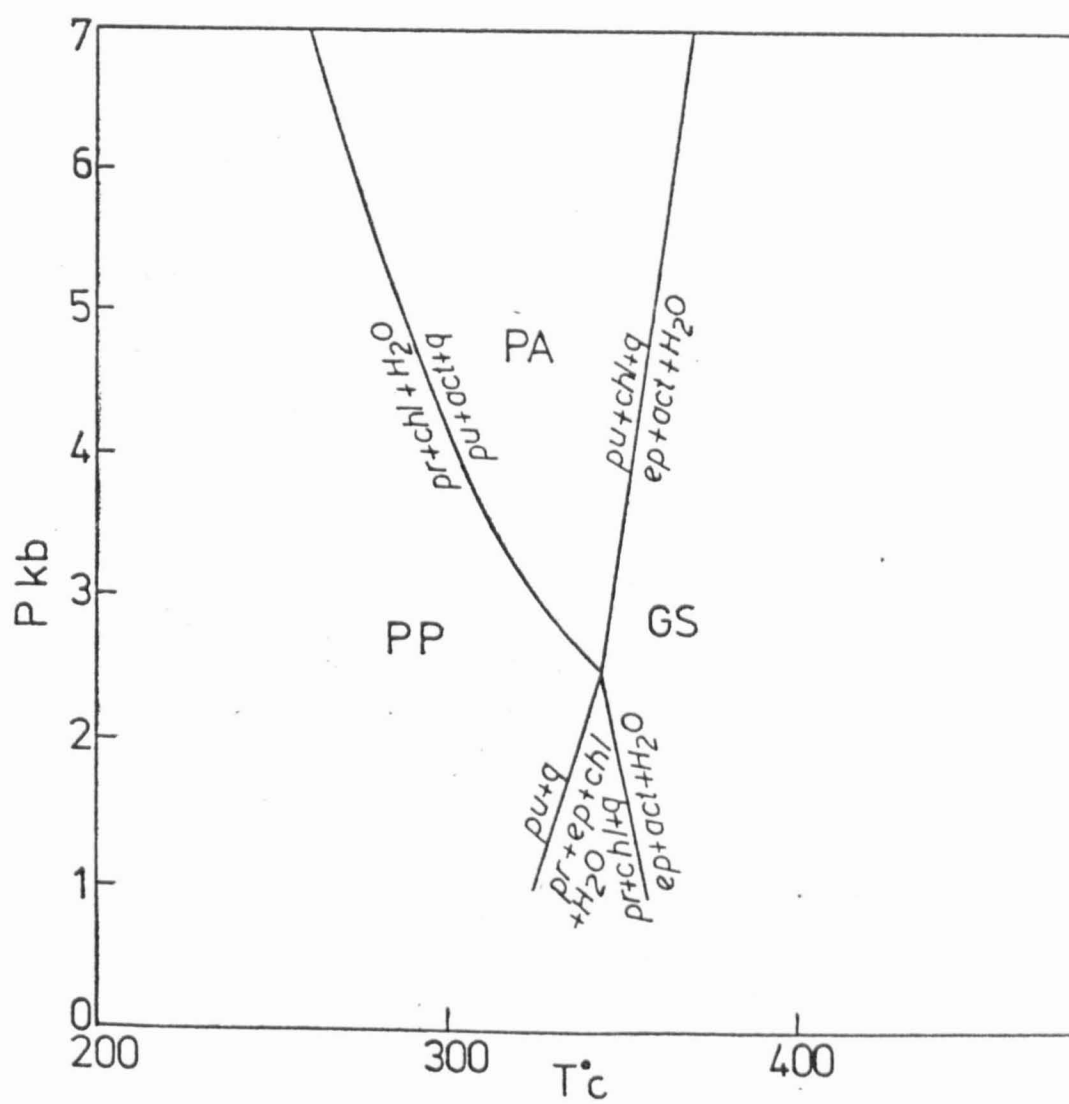
and Liou (1971) have shown that the presence of prehnite is principally temperature controlled. Possibly, therefore, local variations existed within the Fishguard Volcanic pile.

Schermerhorn (1975) observed local variations in mineral assemblages in pumpellyite-facies rocks from the Spanish Iberian Belt. He suggested that the variation may be the result of recrystallization at conditions close to an invariant point (illustrated on Fig.193). If recrystallization was in this field, then prehnite may persist into the greenschist facies. It must be remembered, however, that at this grade of metamorphism, reactions are commonly slow and, as a result, the persistence of relict phases is to be expected. Local factors, such as composition of fluid phase, may therefore obscure the more regional picture of metamorphism. Added complications are no doubt also presented by the fact that the rocks had probably undergone alteration, such as sea water-whole rock interaction, hydrothermal effects, etc. prior to metamorphism, as already discussed in Chapter 5.

Nitsch (1971) and Liou (1971) investigated the stability relations for prehnite and pumpellyite bearing assemblages. One of the most important facts to emerge from their experimental studies was that the disappearance of prehnite is largely temperature dependent, in the region of  $350^{\circ}\text{C}$ . Also observed was the fact that the appearance of actinolite is largely pressure dependant. Zen (1974) suggested the coexistence of pumpellyite and actinolite in most rocks inferred pressures exceeding 2.5kb, and temperatures of about  $300^{\circ}\text{C}$ , a feature also suggested by Figure193, after Schermerhorn (1975). Although it is difficult to estimate,

FIG. 193. P - T diagram for the transition between prehnite-pumpellyite facies and higher grades, after Schermerhorn (1975).





calculations of overburden thicknesses of the order of 6km during Caledonian deformation in Dyfed suggest that pressures in the region of 2-3kb were likely to have been operative in the Fishguard area. Thus, metamorphism in the Fishguard area appears to have been within the prehnite-pumpellyite facies, at temperatures in the range  $300^{\circ}\text{C}$ - $350^{\circ}\text{C}$ , and at pressures around 2kb. Low pressures are reinforced by the absence of lawsonite, the transition of assemblages towards greenschist facies, and also possibly by the association of prehnite with actinolite, suggesting crystallization at conditions close to the invariant point on Figure 193.

The presence of these assemblages is considered to be the result of metamorphism, although it is also accepted that all the phases present may be produced by hydrothermal alteration. However, the fact that these assemblages are not only restricted to the Fishguard area, but are developed in all the major volcanic formations of North Pembrokeshire, as well as being present in metabasites from North and Mid Wales, argues in favour of their origin by regional metamorphism. Other occurrences of these assemblages are discussed below.

#### 7.5. OTHER OCCURRENCES OF PUMPELLYITE IN SOUTH WALES

During the present study pumpellyite has been identified from a number of other occurrences in South Wales. This, together with previously reported occurrences, shows the regional development of this mineral, along with other crucial metamorphic minerals in Wales.

#### 7.5.1. PRESCALLY HILLS

Although investigations of the Prescelly Hills dolerites and associated rocks are at an early stage, preliminary petrological examinations have revealed the presence of pumpellyite, prehnite, actinolite, epidote, clinozoisite, and zoisite. These, once again, appear to show local anomalies associated with a regional grade similar to that of the Fishguard area.

#### 7.5.2. NORTH PEMBROKESHIRE COAST WEST OF LLECH DAFAD

Roach (1969) reported the presence of stilpnomelane and prehnite in the St. David's Head - Carn Llidi intrusion. Examination of other intrusions of this area has shown the occurrence of pumpellyite, prehnite, epidote, and actinolite in the intrusive rocks of this area. Pumpellyite is abundant within the Abercastle - Aberfelin intrusion, as well as within the Traeth Llyfyn intrusive sheet. Abundant pumpellyite also occurs in the basic igneous rocks of the Bishops and Clerks Islands.

#### 7.5.3. TREFFGARNE

Pumpellyite has been identified along with clinozoisite, chlorite, and quartz in alteration veins within the volcanic rocks of the Treffgarne Volcanic Series. The pumpellyite is present as small, euhedral, colourless grains, suggesting that they are iron-poor and aluminium-rich.

#### 7.5.4. SEALYHAM VOLCANICS

Pumpellyite, prehnite, and epidote veins occur within the lavas of the Sealyham Volcanics. These rocks are exposed in a number of

exposures along the southern flanks of the Prescelly Hills, suggesting that much of this ground has similarly been metamorphosed within the prehnite-pumpellyite facies. Outcrops showing the presence of pumpellyite and prehnite occur at Wallis (GR 009259), Garn Turne Rocks (GR 980273), and Carn Afr (GR 093302).

Clearly, minerals diagnostic of prehnite-pumpellyite facies metamorphism are widely developed in this part of North Pembrokeshire, suggesting that their origin is related to an event of regional aspect, and therefore not related to local hydrothermal alteration processes.

Elsewhere in Wales, pumpellyite has been described from a number of localities, as described elsewhere (see section 7.1.). During the present investigations, the presence of pumpellyite was confirmed within the lavas at Builth Wells, as well as within the dolerites of the Conway Valley area. Thus, prehnite-pumpellyite facies may be widespread throughout the Welsh paratectonic Caledonides. However, in metabasites from the Dolgelly area and the Conway Valley well formed actinolite is widespread, and stilpnomelane is also recorded (Bloxam and Price, 1961). Locally, it appears, therefore, that slightly higher grade greenschist facies rocks may be present. Only as a result of careful examination of mineral assemblages from a number of areas will a greater appreciation of the distribution of metamorphic facies in Wales be possible.

It is certain, however, that much of the so-called 'non-metamorphosed' paratectonic Caledonides of Wales has suffered prehnite-pumpellyite facies metamorphism and it is considered likely that other areas of the paratectonic Caledonides of Britain will reveal a similar history (see recent work of Oliver, 1978).

## 7.6. ATTAINMENT OF EQUILIBRIUM

Considerable evidence suggests that disequilibrium exists within the basic rocks of the Fishguard area. This is:

- (i) the presence of relict phases, sometimes surrounded by a secondary phase. Clinopyroxene is one example which is generally unaffected by alteration processes. Plagioclase feldspar, however, is more variably altered. Whilst many assemblages contain albite, the production of albite is not ubiquitous and relict Ca-rich plagioclase is locally preserved. It is considered that all plagioclase compositions from labradorite to pure albite are represented in the basic rocks of Pen Caer; and
- (ii) local variations in compositions of the secondary phases, on a local scale between crystals. This is shown by microprobe analyses of phases from different parts of the same thin section. Varying optical properties of a phase, dependant upon its mode of occurrence also suggest chemical inhomogeneities. Zoned crystals are, however, rare which is more suggestive of equilibrium conditions, albeit local. Zoned epidotes are rarely seen, although certain Prescelly Hills dolerites show epidotes with an iron-rich core, surrounded by an iron-free rim. These possibly result from progressive metamorphism.

It is difficult to apply the phase rule to the rocks in question for a number of reasons. Firstly, it is not known over what scale it is necessary to examine for equilibrium. Zen (1974) stressed that an

area no larger than 1mm should be investigated, whilst Kawachi (1975) suggests only phases in contact should be considered. Boles and Coombs (1977), however, were less rigorous, and used a scale based on a standard thin section. They neglected  $\text{Na}_2\text{O}$ ,  $\text{TiO}_2$ , and  $\text{K}_2\text{O}$ , as these were present largely in albite, sphene, and K-feldspar. This is not directly applicable to the Fishguard rocks, as K-feldspar is not identified with the metabasites. However, white-mica is a common secondary phase, and probably accounts for  $\text{K}_2\text{O}$ . Thus,  $\text{CaO}$ ,  $\text{MgO}$ ,  $\text{FeO}$ ,  $\text{Fe}_2\text{O}_3$ ,  $\text{Al}_2\text{O}_3$ ,  $\text{SiO}_2$ ,  $\text{H}_2\text{O}$ , and  $\text{CO}_2$  may be considered the initial-value components, and this allows seven-phase assemblages to exist. From the list of assemblages recognized (see Appendix 3) it can be seen that divariant equilibrium may in fact be present.

However, a more thorough investigation of chemical equilibrium between phases must await more detailed investigations of the partitioning of elements between the phases. Such studies enabled Kawachi (1975) and Brown (1967) to suggest that conditions approximating equilibrium had been attained in the pumpellyite-actinolite and greenschist facies rocks of Otago, New Zealand. Coombs et al. (1976) also identified a tendency for equilibrium to be attained in pumpellyite-actinolite facies schists from Loèche, Switzerland. Figure 161 shows a good correlation between  $\text{Fe}/(\text{Fe} + \text{Mg})$  in groundmass chlorite and  $\text{Fe}/(\text{Fe} + \text{Mg})$  in the whole rock, reflecting a certain equilibrium in the growth of chlorite.

At present, therefore, it is not possible to determine whether or not divariant equilibrium exists within the rocks of the Fishguard area. Relict phases, such as clinopyroxene and calcic



plagioclases, show that not all reactions have gone to completion, a fact also shown by the occurrence of serrated boundaries between certain secondary phases. However, the fact that the phase rule does not appear to be violated and also the presence of obvious equilibrium assemblages (e.g. chlorite-epidote intergrowths) suggest that divariant equilibrium occurs at least on a local scale.

## CHAPTER 8. INTERPRETATION OF THE FISHGUARD VOLCANIC GROUP IN A VOLCANIC ENVIRONMENT

### 8.1. INTRODUCTION

A detailed account of the lithologies of the formations comprising the Fishguard Volcanic Group was given in Chapters 2 and 3, along with some speculations regarding their origins. This having been done, it is possible to make generalisations regarding the character of this volcanic episode, and to offer suggestions as to what might be expected in contemporary analogues. This method of reconstructing palaeo-volcanic environments in ancient rocks has proved particularly useful in the exploration for mineral deposits intimately associated with volcanism, such as kuroko-type deposits. Detailed studies, such as that by Horikoshi (1969) on kuroko-type deposits of the Kosaka district of Japan, and numerous works on Canadian volcanogenic mineral deposits, allow comparisons to be made. Although the activity in the Fishguard area bears certain resemblances to the Kosaka district, there is no evidence for the associated exhalative-type of mineralization in this Welsh area. Indeed, the only evidence of contemporaneous precipitation of sulphides in these rocks is the occurrence of pyrite-bearing dark shales in the bay at Porth Maen Melyn. The pyrite occurs in layers which are concordant to the original sedimentary laminae, and it is suggested that it may have accumulated in situ.

### 8.2. ENVIRONMENT OF FORMATION OF THE FISHGUARD VOLCANIC GROUP

From an examination of Chapters 2 and 3, it can be seen that the Fishguard Volcanic Group is composed of rocks which show a wide compositional range, from basic through intermediate to acidic.

The viscosity of a magma is closely related to chemical composition, and thus a wide range of magma viscosities was prevalent during the formation of this volcanic group. The viscosity of a magma, along with certain other variables, controls the nature of vulcanism, and as a result a wide range of volcanic products are to be found in this area. The eruption of fluid, basic magma was generally quiet in nature, with little desquamation or fragmentation due to extensive vesiculation and accordingly lavas predominate. The acidic magmas, in contrast, were of a much greater viscosity and, although extensive vesiculation was not realised, abundant volcanoclastic debris was produced by the autobrecciation of the acidic magmas. These processes are discussed below in more detail. First, it is important to consider models regarding possible environments within which this activity was taking place. There is clear and plentiful evidence to show that the Fishguard Volcanic Group accumulated in a submarine environment. Firstly, the Group is directly underlain and overlain by dark pelitic sediments, which are graptolite-bearing to within a few tens of metres below the lowermost volcanics and there are graptolite-bearing pelites which are associated with the final volcanic episodes, seen at Castle Point, near Lower Fishguard Harbour (GR 962378). Within the volcanic pile, fossiliferous material is generally wanting, although an inarticulate brachiopod was identified within volcanogenic sediments near Manorwen (GR 934358). Further evidence for a subaqueous environment for the Fishguard Volcanic Group is afforded by the nature of the volcanic products themselves. The presence of pillowed lava is universally accepted as evidence for the subaqueous extrusion of lava or at least the contact of lava with wet sediments. However, pillow lavas are identified in a number of subaqueous

environments, not all of them contained within marine basins. In Iceland, pillowed lava has been described as forming where subglacial eruptions produced melting of the overlying glacier. In other cases, pillowed lava has been seen to form where lava flowed from a subaerial to a subaqueous environment, albeit a lake or the sea itself. The same may be said of hyaloclastites. The presence of hyaloclastites suggests the interaction of hot magma with relatively cold water but this may be oceanic water of the seas, or indeed lake or glacial waters. Evidence for the submarine environment lies solely upon the faunal evidence from the sediments above and below the Group. However, as there is no abrupt break in the succession, the environment may be considered to be the same as that of the sediments, i.e. submarine. The rocks of the Fishguard Volcanic Group will now be examined in terms of their composition.

Basic magma is the predominant product of this episode of vulcanism in the Fishguard-Strumble Head area, occurring both in the intrusive and extrusive form. The extrusive basic lava produced a thick pile of pillow lavas, with minor hyaloclastites, hyalotuffs and pillow breccias. As this lava pile developed, there were intrusions of basic magma as sheet-like forms within the lavas and sediments both below and within the lava pile. Where contacts between intrusive magma and the sediments are seen, flame structures are sometimes found, along with detached lobes or pillows of basic magma within the sediments. These features suggest that the sediments immediately below and within the lava sequence were still in an unconsolidated condition at the time of this emplacement and confirm

the penecontemporaneous nature of these intrusions. The period of basic magmatic activity was extensive. Basic hyalotuffs occur within the predominantly acidic Goodwick Volcanic Formation, whilst a thick basic sheet intrudes the sediments which overlie this Formation. The history is clearly complex in nature, in contrast to the simple picture of acid-basic-acid vulcanism, envisaged by Thomas and Thomas (1956).

Magma of an intermediate composition is generally restricted to an intrusive habit, although thin flows are found within the Strumble Head Volcanic Formation, and a thick (40m) rhyodacitic flow is found within the Porth Maen Melyn Volcanic Formation. This flow shows a unique pillowed form, along with the development of isolated-pillow breccias produced by desquamation of hot magma in contact with the cold sea water (Bevins and Roach, in press).

Acidic magmas gave rise to the greatest variety of products. As described in Chapter 2, the acidic magma appears to have produced extrusive rhyolitic domes on the sea floor. As these domes grew, possibly by internal expansion, a brecciated carapace was generally produced. Although predominantly produced by expansion, it is also possible that some of the breccias were produced by steam explosions as a result of sea water penetrating the fractured dome, and coming into contact with the hot magma, resulting in gaseous explosions. With expansion of the developing domes, the unconsolidated carapace material became unstable, and sloughed away under gravity. Due to the mixing of water with these slides, debris flows were generated, along with minor turbidity flows. This type of activity appears to have been common in the development of the Fishguard Volcanic Group.

Examples of such deposits are present within both the Porth Maen Melyn Volcanic Formation and the Goodwick Volcanic Formation. The important feature of the acidic magmatic activity in the Fishguard Volcanic Group is the lack of evidence for extensive vesiculation in the Fishguard area. However, in the area to the east of Fishguard there are a number of acidic volcanoclastic rocks with abundant glass shards and these are clearly the products of vesiculation.

The picture envisaged in this study contrasts with the nature of activity identified in North Wales, where many of the so-called rhyolites have subsequently been identified as ignimbrites, produced as a result of extensive magma vesiculation.

As a result of the lack of acidic magmatic activity in oceanic environments, there are relatively few accounts of subaqueous acidic volcanic activity. Indeed, recent review papers dealing with subaqueous vulcanicity (e.g. those of McBirney, 1963; Bonatti, 1970; Tazieff, 1972 etc.) deal principally with volcanic rocks of basic composition. One of the recent accounts from the DSDP reports, however, (Van der Lingen, 1973) described pumiceous volcanoclastic rocks associated with the Lord Howe Rise Rhyolites, but he suggests, in fact that the volcanic eruptions may have been subaerial with the volcanoclastic rocks described representing material transported into the marine environment. Bouma (1975) described volcanoclastic debris flow deposits from Leg 31 of DSDP, which appear similar in nature to certain of the Fishguard examples described earlier. However, other accounts of acidic vulcanicity in the submarine environment have been restricted to accounts of the development of dome-like structures as they grew to and subsequently above sea-level

(e.g. Bogoslof Island, Graham Island, etc.) or closely approximated this (e.g. Myojin Reef, Morimoto and Oosaka, 1955). As a result, accounts of subaqueous, rhyolitic activity are relatively rare and the Fishguard example allows examination and documentation of such activity. Limits to the depth of eruption of the Fishguard lavas may be placed on the fact that the basaltic flows show abundant vesicles. At high pressures in the ocean deeps, vesiculation is completely prevented. A limiting depth for vesiculation of 2,000 metres for basic magmas was calculated by McBirney (1963). Jones (1969) suggested a depth of emplacement of the Fishguard Volcanic Group basic lavas in the neritic-bathyal range (0-2,000m), rather than abyssal depths. A possible reason for the general lack of vesiculation in the Fishguard rhyolites may have been a very low volatile content. However, the fact that the rhyolites did not extensively vesiculate means that the character of vulcanism identified may well be representative of abyssal acidic vulcanism.

Evidence of reworking of the volcanic material in the Fishguard area by current action is scant, which suggests a comparatively deep water environment for the vulcanicity. Any temporary cessations in vulcanicity were followed by a return to the deposition of fine muds, which were readily disturbed by the ensuing volcanic activity. The redistribution of acidic volcanogenic debris was almost entirely the result of the generation of initially gravity-driven slides. With the incorporation of water, these, as mentioned above, turned into debris flows capable of spreading the volcanogenic material over a wide area. A similar mechanism was envisaged by Fiske and Matsuda (1964) for the origin of tuffs in the Tokiwa Formation, Japan, although in this latter case

the material was initially explosively erupted into the water column. Upon settling through the water column, an unconsolidated pile of pyroclastic material developed, which periodically slumped away due to instabilities. Although the mechanism of eruptions is different, the end-product of these two processes have similarities. Clearly, however, the Tokiwa tuffs contain pumiceous lapilli, in contrast to the Fishguard volcanoclastics. In both cases though, the spreading of material away from its source is related to secondary processes, and not to the initial eruption. As a result, thin horizons of volcanogenic material may be deposited some distance away from the centres of vulcanicity. Although this is no doubt the case in Pembrokeshire, the correlation of these horizons with their respective centres is hindered by an uncertain stratigraphy over much of the area.



## CHAPTER 9. REGIONAL ASPECTS OF VULCANICITY IN SOUTHWEST WALES

### 9.1. INTRODUCTION

During the Ordovician there is evidence of widespread vulcanicity in Wales, with episodes of activity at numerous stratigraphic levels particularly within the Arenigian, Llanvirnian and Caradocian stages. In southwest Wales Ordovician volcanic rocks are restricted to strata of Arenig and Llanvirn age.

The thickest development seen in southwest Wales is that represented by the Fishguard Volcanic Group, a part of which is described in this thesis. In this area the group reaches its maximum exposed thickness, although it must be realised that there is a considerable offshore extension of Lower Palaeozoic rocks, no doubt including rocks of the Fishguard Volcanic Group. Traced eastwards from the Strumble Head-Fishguard area, the Group thins considerably, although it can be traced as far as the Prescelly Hills. From a reconnaissance in this region it appears that extrusive rocks are restricted to lavas of rhyolitic compositions, with basic and intermediate rocks present only as high level intrusions. The igneous rocks of the Prescelly Hills area are presently under investigation (by Lees, Roach and Bevins). To the southwest of Strumble Head, doleritic intrusions of the one-pyroxene "Llanwnda" type (Roach, 1969) appear on petrological and geochemical evidence to be a part of the Fishguard suite. Clearly, therefore, this Llanvirn episode of vulcanism was of major importance, and it is relevant to consider it in a more regional context, with a view to a better understanding of

Lower Ordovician plate-tectonics. Firstly, however, a brief review of the other episodes of Ordovician volcanicity in southwest Wales will be given.

## 9.2. EPISODES OF LOWER ORDOVICIAN VULCANICITY IN SOUTHWEST WALES

One of the earliest episodes of Ordovician volcanicity to be recognized in this part of Wales is represented by the volcanic and volcanoclastic rocks at Treffgarne, some 13km south of Fishguard. Thomas and Cox (1924) described this succession and showed that it is in fault contact with Lingula Flags at its base, but is overlain conformably by the Arenig Brunel Beds. The lower part of this succession, exposed in the quarries at Treffgarne, is composed predominantly of basic to intermediate lava flows, showing varying degrees of alteration, whilst the upper part appears to be made up of volcanoclastic rocks (Bevins and Roach, in press). The lavas, although altered, show a number of features which enable their overall characteristics to be determined. They are predominantly feldspar-phyric, with large plagioclase phenocrysts or glomerophenocrystic aggregates. These feldspars have albite-oligoclase compositions, although this is no doubt a secondary composition and the presence of abundant calcite in many lavas supports this contention. Evidence of oscillatory zoning is preserved in a number of lavas, shown by undulatory extinction, as well as zones rich in inclusions. These inclusions are of chlorite, although presumably they were originally glass. The feldspars also display varying amounts of sericitic alteration. Pseudomorphs of chlorite after a pyroxene are common. Within the lava pile late-stage quartz-feldspar veins are present, whilst secondary veins bearing quartz, epidote, chlorite, and pumpellyite are also identified. Chemically these lavas appear

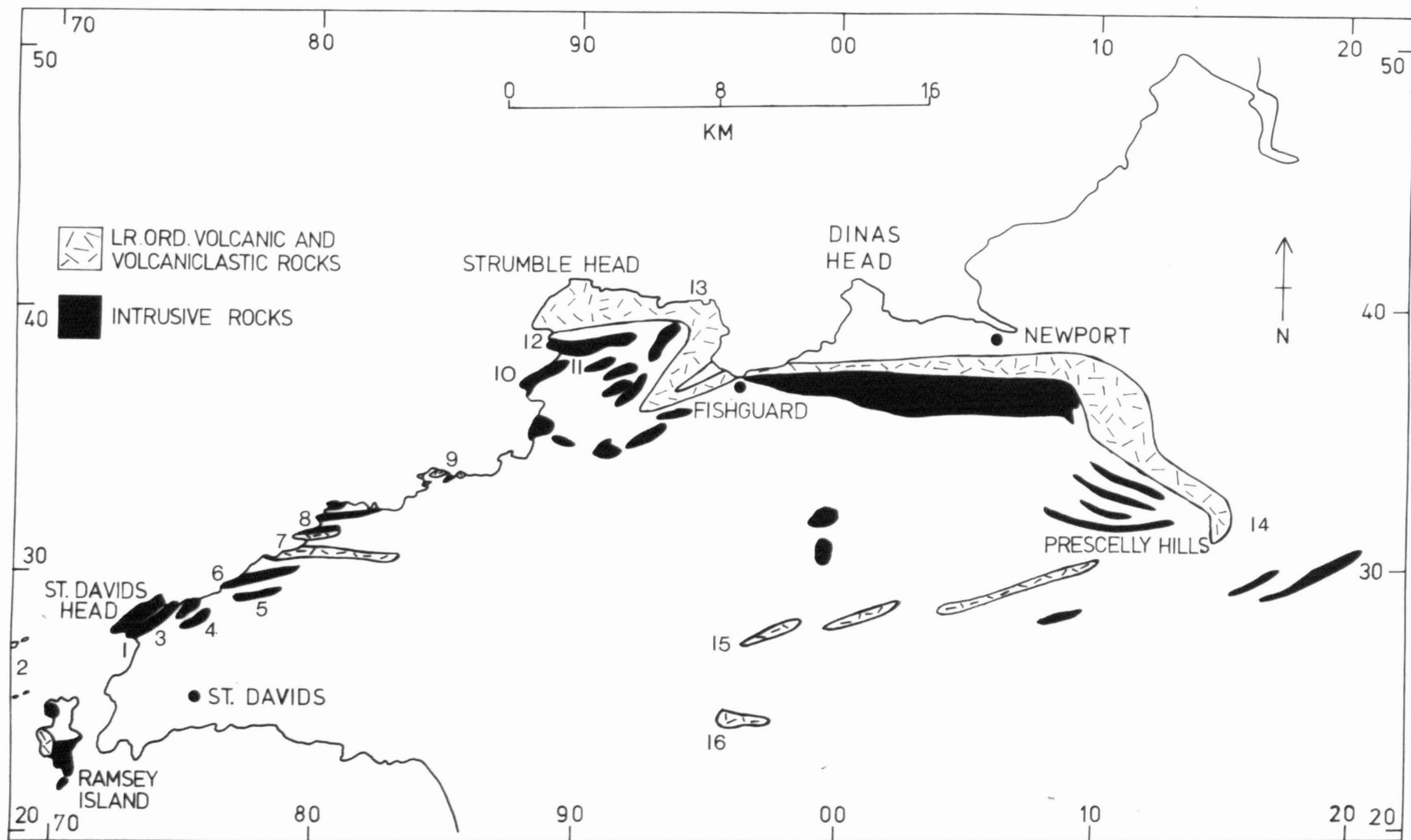
to be basaltic andesites or andesites, although the intense alteration makes the exact nature difficult to interpret. However, these lavas appear similar to the lavas of the Rhobell Volcanic Group, North Wales, described by Kokelaar (1977). The Rhobell Volcanic Group shows a variety of lavas ranging from nepheline-normative basalts to quartz-normative differentiates, and has been likened to rocks produced at modern destructive plate margin environments.

The products of a major volcanic episode are exposed on Ramsey Island (Fig.194). The succession comprises rhyolitic lavas and intrusions, volcaniclastic sandstones and siltstones in addition a slightly welded ash-flow tuff. The upper part of this succession is interbedded with shales which yield a fauna characteristic of the Didymograptus bifidus zone (Pringle, 1930), but the exact age of the lower part of this succession is, as yet, uncertain (Bevins and Roach, in press).

In early D. bifidus times there is evidence of volcanicity in the area between Wolf's Castle and Crymmyrch Arms (Fig. 194). These are the volcanics of the Sealyham Group (Evans, 1945) and are predominantly lavas, although poor exposure in the inland regions allows only a speculative interpretation and reconstruction of this volcanic episode. Their age has been variously quoted as D. murchisoni (Part, 1922, p. 320), and as basal D. bifidus (Evans, op. cit.). However, the fact that they are bleached and altered by the basic intrusive sheets of this area which are here considered to be co-eval with the Fishguard Volcanic Group, suggests that the D. murchisoni age is erroneous. The rocks are exposed in a tract of country running along the southern slopes of the Prescelly Hills,

FIG. 194. Diagrammatic sketch map of the area between Ramsey Island and the Prescelly Hills, showing the distribution of Lower Ordovician volcanic and volcanoclastic rocks, along with intrusive rocks.

Locality nos. are as follows: 1, Whitesand Bay; 2, Bishop and Clerk Islands; 3, Carn Llidi; 4, Carnedd Lleithr; 5, Pen Biri; 6, Pen Clegyr; 7, Abereiddy Bay; 8, Traeth Llyfn; 9, Abercastle; 10, Penbwchdy; 11, Garn Fawr - Garn Fechan; 12, Porth Maen Melyn; 13, Penfathach - Y Penrhryn; 14, Crymmyrch Arms; 15, Wolf's Castle; 16, Treffgarne.



and extending westwards to the Ambleston, Wallis, and Wolf's Castle area. The lavas appear to be intermediate to acid in composition, with phenocrysts, generally of plagioclase, set within a fine groundmass composed essentially of albitic plagioclase feldspars. In some of the more basic members chlorite pseudomorphs after hornblende are found. These rocks have been described as soda-trachytes and soda-rhyolites by Part (1922). An analysis of a lava from Carn Afr (GR 093303) is listed in Appendix 1. Of particular interest are the high  $\text{Al}_2\text{O}_3$  and  $\text{Na}_2\text{O}$  contents, as well as the low  $\text{K}_2\text{O}$ . The high  $\text{Al}_2\text{O}_3$  and  $\text{Na}_2\text{O}$  contents no doubt reflect the high modal proportion of albite. To what extent the alkali contents reflect original values is difficult to determine, because the rocks have been extensively altered (see below). This lava sample also shows low contents of incompatible elements, such as Y and Zr. Typically, these elements are enriched in trachytic rocks, and it there appears unlikely that this lava is the end product of fractionation of an alkali-basalt suite.

As stated above, the lavas of the Sealyham Group are considerably altered, and appear to have been metamorphosed within the prehnite-pumpellyite facies. Both of these critical minerals have been identified at a number of localities within the Sealyham Volcanic Group, for example Garn Turne Rocks (GR 980273), Carn Afr (GR 093302), and Wallis (GR 009259).

Occurring at approximately the same horizon as the Sealyham Volcanic Group (i.e. lowermost D. bifidus zone) are the Ynys Castell Ashes (Cox, 1915), exposed at Abercastle (Fig.194). This unit, which is approximately 60-70m thick, can be traced westwards from Abercastle

to Castell Coch. It appears to be composed of a sequence of subaqueous volcanoclastic deposits, probably resulting from debris and turbulent flows (Bevins and Roach, in press). Although the source of this material can not be identified with any certainty, it does not appear to have been the supposed contemporaneous activity of the Sealyham Volcanic Group, for the Abercastle Ashes contain abundant quartz crystals, which are not seen as a primary phase in the lavas of the Sealyham Volcanic Group.

In the area around Abereiddy Bay, there are extensive outcrops of volcanic rocks of Lower Ordovician age. On the north side of the bay, forming the promontory of Trwyn Castell (GRSM 793315), beds of the Llanrian Volcanic Group (Cox, 1915; Bassett, 1972) are exposed. The group, which occurs within beds of the Didymograptus bifidus zone is approximately 100m thick and composed almost entirely of subaqueous volcanoclastic deposits (Bevins and Roach, in press). These comprise crystal-lithic and crystal-vitric volcanoclastic sandstones and siltstones. Crystals are principally of feldspar and quartz, which are variably broken and fractured. The predominance of these components along with minor rhyolitic lithic clasts, suggests that the source of material was probably from nearby rhyolitic vulcanicity. In addition, the lithic clasts also contain a proportion of mudstone clasts and these appear to represent the underlying sediment which has been ripped up and incorporated into the deposits. This, along with the occurrence of sedimentary structures such as reverse grading and flame and load structures, led Bevins and Roach (in press) to suggest that these beds represent the deposits of dense, gravity-driven subaqueous flows, which were in part

turbiditic in character. Certain horizons within the sequence are fine-grained and flinty in aspect and possess near-parallel upper and lower surfaces. However, internally they are structureless and generally poor in crystals or lithic clasts. These units were interpreted by Cox (1915) as representing rhyolitic lava flows, but Bevins and Roach (in press) suggest that they possibly represent accumulations of fine, vitric dust which settled after fall through a column of water.

It thus appears that the Llanrian Volcanic Group comprises a number of volcanoclastic flow deposits which were derived from contemporaneous rhyolitic volcanicity. The site of this activity is uncertain, although it is tempting to equate these deposits with the rhyolitic volcanicity of the Fishguard area or possibly even that of Ramsey Island, both of which are, at least in part, of equivalent age.

On the south side of Abereiddy Bay, the *Didymograptus Murchisoni* Ash (Cox, 1915) is exposed. This Ash overlies sediments belonging to the *Didymograptus bifidus* zone but is in turn overlain by sediments of the *Didymograptus murchisoni* zone. This unit may be traced a considerable distance along strike to Aberdinas (GRSM 776306) and considerable facies changes may be observed. In the west the unit possesses thick, parallel-sided beds and contains abundant blocks of basic to intermediate lava, which are variably vesiculated. Traced eastwards, the unit thins and similarly the beds themselves become noticeably thinner. In addition to the lava clasts, mudstone clasts may now be observed being noticeably confined to the bases of the beds. These thin beds show fining-upward cycles



and were clearly deposited from energy flows, possibly turbiditic in aspect. The origin of the thicker beds exposed to the west is not certain, but Bevins and Roach (in press) considered that they possibly represent the accumulation of ejecta on the flanks of a submarine, pyroclastic cone. However, it is also possible that they represent the more proximal deposits of the same energy currents which were responsible for the thinner beds, seen to the east.

Thus, although this review is brief, it can be seen that volcanism was persistent throughout the Lower Ordovician in the North Pembrokehire area. The character of this volcanism appears to have changed significantly from the production of basalts and andesites of possible calc-alkaline nature in the Arenig period to basalts, basaltic andesites, dacites, and rhyolites of tholeiitic affinities in the Llanvirn. Each episode also produced considerable volcanoclastic material which was reworked in the submarine environment and deposited away from the volcanic centres, thus producing horizons rich in volcanic debris but devoid of actual lavas, such as at Abercastle and Abereiddy.

### 9.3. IMPLICATIONS OF ORDOVICIAN VULCANICITY IN SOUTHWEST WALES

A number of attempts have been made in recent years to interpret the British Caledonides in terms of a plate tectonic setting. Implicit in these models has been the evidence afforded by the chemical character of volcanic rocks from the various volcanic episodes. One of the earliest attempts at a plate tectonic reconstruction based on the petrochemistry of the volcanic rocks was that by Fitton and Hughes (1970). They suggested that during Mid-Ordovician times a southward dipping Benioff zone was responsible

for the production of tholeiitic and calc-alkaline volcanic activity in the Lake District, and essentially alkaline volcanism in Wales. This model, however, appears to be based upon erroneous information. The Rhobell Volcanic Group, recently restudied by Kokelaar (1977) has been shown to be predominantly made up of basaltic lava flows, and not andesites, as suggested by Wells (1925). The Group as a whole shows a range of lavas varying from nepheline-normative through to quartz-normative types. However, a complete differentiation suite through andesites and dacites is seen, with the former presence of rhyolites also suggested. Kokelaar (op. cit.) has suggested members of this suite were produced by pargasite-dominated fractionation and bear close analogies with rocks generated in modern subduction zone regions such as the Lesser Antilles. Fitton and Hughes (op. cit. p. 225) also state that andesites occur in the Arenig Mountains, at Builth Wells and in west Shropshire and that tholeiitic rocks are rare. The work of Dunkeley (1978) has shown that in the Aran Mountains the extensive Llanvirn volcanism is of a tholeiitic character, with basalts, basaltic andesites, and dacites. Roach (1969) described the occurrence of a large differentiated tholeiitic intrusion in North Pembrokeshire (St. David's Head - Carn Llidi), but this was erroneously described as Arenig in age by Fitton and Hughes (op. cit.). The present work has shown that the Fishguard Volcanic Group, of Llanvirn age, represents a major period of tholeiitic volcanism producing a thick basaltic pile, and associated doleritic and gabbroic sheets, with only minor amounts of andesite and dacite. The Builth Wells volcanics have been investigated by Furnes but no conclusions regarding the nature of volcanicity have been published.

It thus becomes clear that the character of Llanvirn volcanism in Mid and South Wales was predominantly tholeiitic in aspect, and not alkaline as suggested by Fitton and Hughes (op. cit.). On these grounds, along with a consideration of the Rhobell Volcanic Group, a revision of the proposed model is clearly necessary.

The picture of Ordovician volcanism in Snowdonia appears to be a little more complex. The main period of volcanism occurred in the Caradocian. Hughes (1972) suggested that these rocks were calc-alkaline in aspect, and a more recent examination by Floyd, Lees, and Roach (1976) appears to confirm this sub-alkaline, continental, calc-alkaline nature. However, the more primitive members of the suite analysed fall within the 'within-plate' and ocean-floor fields when plotted on a Pearce and Cann (1971) Ti-Zr-Y diagram. Exactly the same scatter of data is displayed by the Fishguard Volcanic Group basalt lavas and doleritic intrusions.

Jeans (1973) presented a reconstruction of the southern Caledonides, once again primarily based upon the episodes of volcanicity. He suggested that a shallow dipping Benioff zone gave rise, in Arenig times, to the volcanism of Cader Idris, Rhobell Fawr and Pembroke (presumably Treffgarne). He states that eruptions continued into the Llanvirn, but makes no reference to the change in character of the volcanic products. By Llandeilo times Jeans (op. cit.) envisaged that the zone was at a steeper angle, resulting in volcanic activity in the Lake District during the Llandeilo and Caradoc periods. In North Wales, extensive acidic vulcanism was produced as a result of crustal melting produced by a 'heat plume'.

The most sophisticated model for the British Caledonides was produced more recently by Phillips et al. (1976). For the area in question (i.e. Lake District - Wales), they propose a southward dipping subduction zone, with a volcanic arc sited over the Lake District. In their model, the Welsh Basin represents a back-arc environment.

The earliest volcanic episodes in Wales, namely Rhobell Fawr and also Treffgarne both appear to have affinities with rocks generated at modern destructive plate margins. The magmas may well have been produced by partial melting of subducted oceanic lithosphere, and is possible evidence for the operation of such a mechanism. However, by Llanvirn times this early type of vulcanism had ceased, and was replaced in Mid and South Wales by an important episode of tholeiitic volcanism. It is thought that the magmas of this episode were mantle-derived and not produced from subducted oceanic lithospheric plate, as suggested for the earlier magmas. However, it is possible that the production of these Llanvirn tholeiitic magmas may still have been related to the subduction process. It has been shown recently that at depths the descending plate sets up convective cells within the low velocity zone (Toksöz and Bird, 1977 / Due to the dip of the subduction zone, this is characteristically some distance from the trench-arc system, on the continent side. Such a convective circulation may give rise to mantle diapirs rising into the continental crust, producing a tensional environment and associated vulcanism. There is evidence that the Welsh Basin was in a tensional state during the Ordovician and thus the picture envisaged by Rast (1969) that a mantle diapir produced a tensional situation and that the associated faulting was exploited by basic magmas may be an appropriate model. In the case of the Fishguard

Volcanic Group, it appears that the basic magma differentiated to produce intermediate and acidic derivatives. However, this situation may not have existed elsewhere, and other origins for the rhyolites may be necessary. Thus the Welsh Basin may have been similar in nature to marginal basins identified today, except that continental crust was always present under this Basin and at no time separated to allow the production of oceanic crust.

## CHAPTER 10. SUMMARY AND SUGGESTIONS FOR FURTHER RESEARCH

This investigation has shown that the Fishguard Volcanic Group represents a totally subaqueous pile of volcanic and volcanoclastic rocks, with associated comagmatic high level intrusive sheets. The basic lavas of the pile display characteristics typical of activity reported from this environment, e.g. the development of pillowed lavas and hyaloclastites. The intermediate and acidic lavas display interesting features not previously described from Wales. Rhyodacite lavas, exposed at Porth Maen Melyn, show a rare development of flow tubes, along with isolated-pillow breccias. The rhyolites produced surface dome-like features on the sea floor, which were covered by a carapace of autobrecciated material. Instabilities caused the reworking of this material, and this gives valuable insights into the distribution of volcanic debris in the submarine environment where extensive vesiculation is prevented.

An investigation of the whole rock geochemistry shows that despite the pervasive alteration, original chemical characteristics are not totally obliterated. This enables the tholeiitic nature of the suite to be identified and it is thought that the intermediate and probably also the acidic rocks represent members of the same differentiation series. The generation of the various members was controlled predominantly by clinopyroxene  $\pm$  plagioclase  $\pm$  olivine in the early stage, clinopyroxene + plagioclase  $\pm$  ore in the middle stage and essentially plagioclase in the late stage.

This work thus attempts to give an overall picture of the Fishguard Volcanic Group. However, a number of lines of work remained either uncompleted or totally unpursued.

With regard to Ordovician volcanicity in South Wales, this study gives an insight into the character of one of the eruptive centres. It would be rewarding to investigate other volcanic areas in North Pembrokeshire, some of which may contain the possible lateral equivalents of the Fishguard Volcanic Group.

An investigation of the phase chemistry of the meta-basalts reveals that although other phases have been altered, the clinopyroxene is usually pristine. An illuminating picture is presented when the clinopyroxene compositions from the extrusive and intrusive rocks are compared, and it is seen that the phase chemistry appears to be controlled largely by the physical conditions of crystallization, such as rate of cooling, degree of supercooling, etc. Clinopyroxenes from the intrusive rocks show a compositional variation expected within basic rocks of a tholeiitic nature. However, the clinopyroxenes present within the extrusive rocks, which crystallized under disequilibrium conditions, show compositions normally characteristic of clinopyroxenes crystallizing from alkalic melts. The variation identified here naturally has important consequences on 'magma-typing' using clinopyroxene composition, recently suggested by Nisbet and Pearce (1977). Unfortunately, due to low-grade metamorphism, the feldspars in the Fishguard samples have been extensively altered. Thus it would be interesting to find an analagous suite of rocks in which the feldspars were also pristine. This would enable subtle changes in feldspar compositions to be detected which might be related to the clino-

pyroxene variations identified. Baragar et al. (1977) recently described similar clinopyroxenes from Leg 37 of the Deep Sea Drilling Project, and have also identified such a relationship between intrusive and extrusive suites from the Pre-Cambrian of Labrador (Baragar, pers. comm.).

The identification of pumpellyite and prehnite-bearing assemblages on a regional scale in Southwest Wales has allowed the identification of a widespread low-grade metamorphism produced during the Caledonian orogenic episode. However, local variations in assemblages, unrelated to host rock compositions, suggest the importance of more local factors, possibly fluid phase composition, ionic activity etc. An important contribution to our understanding of Caledonian metamorphism may be obtained from a wider inspection of meta-basites in North and Mid-Wales. The outcrops of Ordovician meta-basites are more limited in Mid-Wales, but prehnite-pumpellyite assemblages have been identified in this region, whilst critical assemblages have also been recognized from North Wales.



## APPENDIX 1. ANALYTICAL TECHNIQUES OF WHOLE ROCK DETERMINATIONS

Tabulated here are analyses of samples collected from the Fishguard Volcanic Group, as well as a number of samples from other Ordovician volcanic horizons in southwest Dyfed. All major elements and a number of trace elements were analysed by x-ray fluorescence techniques, although wet chemical methods were also employed. The Rare Earth Elements were analysed by neutron activation at the Universities Research Reactor, at Risley.

### 1. SAMPLE COLLECTION AND PREPARATION

A range of rock samples from the Fishguard Volcanic Group were collected in order to investigate the geochemical characteristics of the Group, and also to gain a better understanding of possible relationships between rock types of the Group. Sample sites, together with a brief petrological description, are given in Table 18 Appendix 3. Usually the freshest material was collected. Sample size naturally varied, but unless the rock was particularly coarse-grained or noticeably inhomogeneous, this was usually of the order of 1kg. In the case of collection of material from pillow lavas, samples were usually taken from the core of the pillow, where the 'freshest' material was thought to be located. A number of pillows were sampled both from the core and from the margin to study the possible chemical variations across pillow bodies. A small number of highly altered samples was collected in an attempt to understand better the nature of the alteration.

In the laboratory the samples were split into rough cubes, approximately 1-2cm across using a Denbigh fly-press rock splitter.

All weathered material, veins, etc. were removed at this stage. The split samples were then passed through a Sturtevant 2" x 5" jaw crusher which reduced the chip size to approximately 6mm. Homogenization by successive cone-and-quartering followed until one quarter (approximately 120gm weight) was selected. This quarter was then crushed in a Tema disc mill with Widia (tungsten carbide) barrel, rings and stone for 30 seconds. After further homogenization, a small sample (about 20 grams) was milled for a further 30 minutes in a Glen Creeston M280 tungsten carbide ball mill.

Major element analyses were performed on glass beads, owing the problems of sample homogeneity and matrix effects suffered by powder pellets. The beads were produced by mixing 0.4667gm of rock powder (which in most cases had been ignited to 1000<sup>0</sup>C) with 2.375gm of flux, which once again had generally been ignited. The flux used was Spectroflux 105, marketed by Johnson Matthey Chemicals Ltd., and is composed of lithium tetraborate (47.0%), lithium carbonate (36.67%) and lanthanum oxide (16.33%). The latter is added as a heavy absorber and makes the absorption coefficients of all the samples analysed in one batch relatively constant, enabling calibration curves of wide concentrations to be produced. After fusing the rock powder and flux over a meker burner, casting of the bead was performed on a brass casting plate, the liquid pressed out with an aluminium plunger. A copper ring, previously mounted onto the casting plate, acts as a binding ring to ensure durability of the bead.

Trace elements and sodium analyses were determined on pressed powder pellets. These were prepared by mixing a few drops of Mowoil N90/98 binder (produced by Hoechst Chemicals Ltd.) with 6 grams of sample by hand in an agate mortar and pestle and then subjecting this to a pressure of 25 tons per square inch for four minutes in hydraulic press in a cylindrical dye with tungsten carbide coated plattens. After baking in an oven overnight, durable discs were produced.

## 2. ANALYTICAL TECHNIQUES

### 2.1. X-RAY FLUORESCENCE

X-ray fluorescence analysis for both major and trace elements was performed on a Philips PW1212 fully automatic sequential x-ray spectrometer in the Department of Geology, at the University of Keele. A variety of x-ray generator tubes were utilized in the analyses. A Cr target tube was used for elements with atomic numbers between 11 (Na) and 23 (V), whilst those with atomic numbers greater than 23 were analysed using a tube with either a W or Mo target tube. A variety of crystals were employed for dispersion of the secondary x-rays. A  $\text{LiF}_{220}$  crystal is best suited for most heavy element analyses (except Cr, Ti, Sc, and Ca, where an  $\text{LiF}_{200}$  is superior), whereas for the lighter elements other crystals, such as PET (Si, Al, K), Ge (P), KAP (Mg), and TIAP (Na) are preferred. Full operating conditions for the analyses reported here are recorded in Table 8.

OPERATING CONDITIONS OF PHILLIPS PW 1212 X-RAY SPECTROGRAPH FOR MAJOR AND TRACE ELEMENTS REPORTED

Element	K	Ti	Si	Ca	Al	Mg	Na	P	Sc
Radiation line used	K $\alpha$	K $\alpha$	K $\alpha$	K $\alpha$	K $\alpha$	K $\alpha$	K $\alpha$	K $\alpha$	K $\alpha$
Tube	Cr	Cr	Cr	Cr	Cr	Cr	Cr	Cr	Cr
Kv	40	40	40	40	60	40	40	60	60
mA	8	8	16	8	24	35	40	24	24
Crystal	PET	LiF 200	PET	LiF 200	PET	KAP	TlAP	GE	LiF 200
Collimator	C	F	C	F	C	C	C	C	F
Counter	F	F	F	F	F	F	F	F	F
Vacuum/air path	VAC.	VAC.	VAC.	VAC.	VAC.	VAC.	VAC.	VAC.	VAC.
Method	ABS. RAT.	ABS. RAT.	ABS. RAT.	ABS. RAT.	ABS. RAT.	ABS. RAT.	ABS. RAT.	ABS. RAT.	ABS.
Time	FC	FC	FC	FC	FC	FC	FC	FC	40 sec.
Counts	$3 \times 10^4$	$3 \times 10^4$	$3 \times 10^4$	$3 \times 10^4$	$3 \times 10^4$	$3 \times 10^4$	$3 \times 10^4$	$3 \times 10^4$	
2 $\theta$ peak	50.67	86.13	109.11	113.09	144.95	43.49	55.00	141.14	97.60
2 $\theta$ BKGD (1)	52.50	88.50	112.00	115.50	138.50	46.50	56.50	144.50	95.50

TABLE 8

OPERATING CONDITIONS OF PHILLIPS PW 1212 X-RAY SPECTROGRAPH FOR MAJOR AND TRACE ELEMENTS REPORTED

Element	Rb	Sr	Y	Zr	Mo K $\alpha$ C	Ga	Zn	Cu
Radiation line used	K $\alpha$	K $\alpha$	K $\alpha$	K $\alpha$	K $\alpha$	K $\alpha$	K $\alpha$	K $\alpha$
Tube	Mo	Mo	Mo	Mo	Mo	Mo	Mo	Mo
Kv	90	90	90	90	90	90	90	90
mA	20	20	20	20	20	20	20	20
Crystal	LiF 220	LiF 220	LiF 220	LiF 220	LiF 220	LiF 220	LiF 220	LiF 220
Collimator	FINE	FINE	FINE	FINE	FINE	FINE	FINE	FINE
Counter	SCINT.	SCINT.	SCINT.	SCINT.	SCINT.	FLOW	FLOW	FLOW
Vacuum/air path	VAC.	VAC.	VAC.	VAC.	VAC.	VAC.	VAC.	VAC.
Method	ABS.	ABS.	ABS.	ABS.	ABS.	ABS. RAT.	ABS. RAT.	ABS. RAT.
Time	40 sec.	40 sec.	40 sec.	40 sec.	40 sec.	FC	FC	FC
2 $\theta$ peak	37.94	35.79	33.82	32.03	30.06	56.15	60.53	65.51
2 $\theta$ BKGD (1)	38.50	36.79	34.82	32.90		55.10	59.25	64.50
2 $\theta$ BKGD (2)	36.79	34.82	32.90	31.70		57.25		

OPERATING CONDITIONS OF PHILLIPS PW 1212 X-RAY SPECTROGRAPH FOR MAJOR AND TRACE ELEMENTS REPORTED

Element	Ce	La	Ba	Nb	Nd	Fe	Ni	Cr	Mn
Radiation line used	$L\beta_1$	$L\alpha_1$	$L\beta_2$	$K\alpha$	$L\beta_1, 4_1$	$K\alpha$	$K\alpha$	$K\alpha$	$K\alpha$
Tube	W	W	W	W	W	W	W	W	W
Kv	60	60	50	60	60	60	60	60	60
mA	32	32	40	32	32	8	32	32	32
Crystal	LiF 220	LiF 220	LiF 220	LiF 220	LiF 220	LiF 220	LiF 220	LiF 200	LiF 220
Collimator	FINE	FINE	FINE	FINE	COARSE	FINE	FINE	FINE	FINE
Counter	FLOW	FLOW	FLOW + SCINT.	SCINT.	FLOW	FLOW	FLOW	FLOW	FLOW
Vacuum/air path	VAC.	VAC.	VAC.	VAC.	VAC.	VAC.	VAC.	VAC.	VAC.
Method	ABS. RAT.	ABS. RAT.	ABS. RAT.	ABS. RAT.	ABS. RAT.	ABS. RAT.	ABS. RAT.	ABS. RAT.	ABS. RAT.
Time	FC	FC	FC	FC	FC	FC	FC	FC	FC
Counts	$10^4$	$10^4$	$10^4$	$10^4$	$10^4$	$10^4$	$10^4$	$10^4$	$3 \times 10^4$
2 $\theta$ peak	111.72	138.91	115.22	30.38	99.12	85.61	71.24	69.30	
2 $\theta$ BKGD (1)	114.00	136.00	113.75	29.75	98.10	87.50	73.50	74.50	
2 $\theta$ BKGD (2)			117.00	30.90	100.25				

An approach similar to that described by Leake et al. (1969) was used. For major elements each glass bead was run three times and the mean of these three analyses recorded. For trace elements and sodium, two cycles on each side of the pressed powder discs were made. The thickness of these discs is greater than the critical depth of penetration of x-rays and thus each side constitutes essentially duplicate samples. Counts on both peaks and backgrounds were made. The net counts (P-B) were then used, with or without additional corrections for matrix effects. Full details of this approach are given in Jenkins and de Vries (1967). Concurrent with major element determinations, pellets of a selection of international standard rock powders (Flanagan, 1974) were analysed at the same time. From their net counts a series of calibrations was constructed. The international standards used included: the U.S.G.S. standards DTS-1, PCC-1, BCR-1, W-1, AGV-1, G-2; the C.R.G.M. standard BR; the Japanese Geological Survey standard JB-1, for which values were obtained from Flanagan (1973), whilst apparent fluorescent values were obtained following an approach similar to that of Harvey et al. (1973). Inter-element corrections were made utilising the method of Norrish and Hutton (1969). Trace element calibration was achieved by running spiked internal standards, with mass absorption corrections being applied when this was deemed necessary. For Rb, Sr, Y, and Zr a method after Reynolds (1963) was followed, whereby  $\text{MoK}\alpha$  is determined, and from this an estimate of the mass absorption coefficient is made.

Tables 9 and 10 give an estimate of the precision and accuracy of the data presented here. Precision, shown by the coefficient of variation (in percentage) was determined by the use

TABLE 9

VARIANCE, STANDARD DEVIATION AND COEFFICIENT OF VARIATION OF  
ELEMENTS ANALYSED BY XRF TECHNIQUES DURING THIS STUDY

Element	Variance	Standard Deviation	Coefficient of variation 1
Sc	2.04	1.43	3.55%
Cr	15.20	3.90	1.58%
Ni	6.25	2.50	3.02%
Y	2.60	1.61	6.11%
Rb	1.58	1.26	9.78%
Sr	14.20	3.77	1.40%
Zr	20.56	4.53	4.77%
Nb	5.73	2.39	38.44%
Nd	30.91	5.56	27.62%
Ce	22.55	4.75	8.30%
La	3.85	1.96	8.41%



TABLE 10. ACCURACY OF XRF DETERMINATIONS ILLUSTRATED BY ANALYSIS OF STANDARD REFERENCE SAMPLES

	BCR-1		W-1		JB-1		BR		AGV-1		G2		NIM-N		NIM-P	
	*	+	*	+	*	+	*	+	*	+	*	+	*	+	*	+
Rb	47	46	21	21	41	41	50	45								
Sr	358	330	204	190	484	438	1443	1350								
Y	34	37	21	25												
Zr	166	190	77	105												
Cr	52	17.6	141	114	405	417	345	420	31	12.2						
Ni	13	15.8	61	76	117	139	198	270	22	18.5						
Sc	34	33	38	35	27	26			17	13	4	4	41	38	37	35
Ba	682	675	150	160	485	400	952	1050	1203	1208	1867	1870				
Nb	12.6	13.5	4.7	9.5					13.2	15	13.3	13.5				
Nd	27.1	29	11.1	15	26.7	25			25.6	39	58.2	60				
La	35	26	5	9.8	42	36	93	85	46	35			4	3	8	4
Ce	71	54	50	23	77	67			61	63			33	14	102	85

\* = Recorded during this study

+ = Recommended value from Flanagan (1973)

of a pooled variance programme adapted by D. H. M. Alderton. Accuracy is reflected by comparison of recorded international standard values with recommended values published by Flanagan (1973). Precision is generally of a high quality. Although accuracy is not always as good as desired, the analyses are internally consistent and the chemical variations seen are thought to be meaningful. Detection limits for a number of elements are quoted in Table 11. Results of these determinations are listed in Table 12.

## 2.2. WET CHEMISTRY

The various wet chemical techniques applied may be consulted in Appendix 2.

## 2.3. NEUTRON ACTIVATION ANALYSIS

A number of samples were commercially analysed for the Rare Earth Elements at the Universities Research Reactor, at Risley, using a modification of the method proposed by Graber, Lukens and MacKenzie (1970). An international standard was run concurrently with each batch analysed. The results are tabulated below (Table 13) along with an estimation of the errors involved. The samples were normalised against an average of 26 determinations on 22 individual chondrites and a composite mixture of 9 chondrites (Herrmann, 1970) (Table 14).

TABLE 11

DETECTION LIMITS IN THIS STUDY FOR A NUMBER OF TRACE ELEMENTS

	PPM
Cr	12
Ga	5
Nb	6
Ni	15
Sc	4
Rb	2
Sr	3
Y	2
Zr	6

TABLE 12. MAJOR AND TRACE ELEMENT ANALYSES OF ROCKS  
FROM THE FISHGUARD AREA

# INDEX TO WHOLE-ROCK CHEMICAL ANALYSES

<u>Sample</u>	<u>Page No.</u>	<u>Sample</u>	<u>Page No.</u>	<u>Sample</u>	<u>Page No.</u>
GF63	vi	SA8	xii	SB63	v
GG1	vi	SA9	xii	SB64	x
		SA11	xii	SB66	v
LD1	vi			SB67	v
LD2	vi	SB8	i	SB68	v
LD3	vii	SB13	xiii		
LG1	vii	SB15	i	SP2	xiv
LG2	vii	SB19	i	SP3	v
LG3	vii	SB22	i	SP62	xiv
LG4	vii	SB23	i	SP63	xiv
LG5	vii	SB25	i	SP94	vi
LG6	vii	SB26	xiv		
		SB27	i	YG1	vi
RD151	xvi	SB28	i	YG2	vi
RD154	xvi	SB30	ii		
RD155	xvi	SB31	ii	REB12	xv
RD158	xvi	SB33	ii	REB23	xv
RD165	xvi	SB34	ii	REB90	xv
RD172	xvi	SB35	ii	REB94	xi
RD175	xvii	SB37	ii	REB125	xv
RD212	xvii	SB39	ii	REB127	xv
RD225A	xvii	SB40	ii	REB153	xv
RD228A	xvii	SB41	iii	REB154	xv
RD230A	xvii	SB42	iii	REB166	vi
RD231A	xvii	SB43	iii	REB342	xi
RD229	xviii	SB44	iii	REB412	xi
RD232	xviii	SB45	iii	REB412A	xi
RD237	xviii	SB46	iii	REB413	xi
RD238A	xviii	SB47	iii	REB414	xi
RD244	xviii	SB48	iii		
RD252	xviii	SB49	iv	SBC1	viii
RD254	xix	SB50	iv	SBR1	viii
RD258B	xix	SB51	iv	SBC5	viii
RD280B	xix	SB52	xiii	SBR5	viii
RD295A	xix	SB53	iv	SBC7	viii
RD295B	xix	SB54	x	SBR7	viii
RD327	xix	SB55	x	SBC10	ix
RD328	xix	SB56	iv	SBR10	ix
		SB57	iv	SBC11	x
SA3	xi	SB58	iv	SBR11	x
SA4	xii	SB59	iv	SBC12	ix
SA5	xii	SB60	v	SBR12	ix
SA6	xii	SB61	v		
SA7	xiv	SB62	v	175S	xx

## ANALYSES OF ROCKS BELONGING TO GROUP 1, FISHGUARD VOLCANIC GROUP

## (i) IGNITED SAMPLES

Sample No.	SB8	SB15	SB19	SB22	SB23	SB25	SB27	SB28
SiO <sub>2</sub>	49.7	44.8	50.9	48.8	50.8	48.4	47.5	49.1
TiO <sub>2</sub>	1.59	2.07	2.15	2.33	2.08	1.70	1.59	2.01
Al <sub>2</sub> O <sub>3</sub>	17.1	15.5	14.7	15.4	14.8	17.1	16.7	17.0
Fe <sub>2</sub> O <sub>3</sub> *	10.13	8.66	12.57	12.41	11.19	11.72	10.62	9.39
MnO	0.17	0.32	0.18	0.18	0.20	0.21	0.16	0.16
MgO	7.99	5.86	7.27	5.07	5.73	6.79	10.15	7.33
CaO	9.16	16.33	9.83	13.02	9.73	11.23	9.11	9.56
Na <sub>2</sub> O	3.44	3.56	1.97	2.44	4.13	3.08	1.96	3.58
K <sub>2</sub> O	0.45	0.13	0.79	0.42	0.31	0.44	1.11	0.85
P <sub>2</sub> O <sub>5</sub>	0.13	0.24	0.21	0.28	0.22	0.17	0.10	0.22
Total	99.86	97.47	100.57	100.35	99.19	100.84	99.00	99.20
FeO	5.63	6.30	7.87	6.93	8.21	8.50	7.16	6.77
Loss	4.11	13.08	3.34	2.54	4.97	2.56	3.86	4.40

\* = total iron as Fe<sub>2</sub>O<sub>3</sub>

## PPM

Ba	340	n.a.	n.a.	n.a.	n.a.	n.a.	218	529
Ce	40	n.a.	n.a.	n.a.	n.a.	n.a.	n.a.	n.a.
Cr	212	75	207	115	96	240	424	301
La	2	n.a.	n.a.	n.a.	n.a.	n.a.	n.a.	n.a.
Nb	4	11	5	7	9	5	2	5
Nd	7	n.a.	11	7	n.a.	12	11	12
Ni	90	20	55	38	37	73	n.a.	n.a.
Rb	9	2	17	6	5	9	27	19
Sc	39	46	46	45	46	48	35	41
Sr	335	163	199	527	117	245	183	255
V	276	n.a.	n.a.	n.a.	n.a.	n.a.	n.a.	n.a.
Y	29	39	33	42	38	33	27	32
Zr	95	127	124	158	126	113	95	123
'f'	0.58	0.43	0.44	0.35	0.44	0.49	0.58	0.48

n.a. = not analysed

Sample No.	SB30	SB31	SB33	SB34	SB35	SB37	SB39	SB40
SiO <sub>2</sub>	49.2	51.2	62.0	50.1	49.7	50.3	51.6	52.6
TiO <sub>2</sub>	1.82	2.93	2.00	1.39	1.80	1.94	1.63	1.92
Al <sub>2</sub> O <sub>3</sub>	15.3	13.6	13.1	15.3	15.1	15.4	15.2	15.3
Fe <sub>2</sub> O <sub>3</sub> *	12.42	14.71	8.56	10.11	11.86	11.86	11.52	11.85
MnO	0.25	0.22	0.16	0.15	0.19	0.21	0.15	0.18
MgO	7.20	4.97	3.68	6.28	7.89	7.10	7.02	7.12
CaO	11.38	7.83	4.89	16.66	10.40	6.99	8.98	5.28
Na <sub>2</sub> O	2.74	3.66	4.80	0.75	2.71	3.38	3.81	4.30
K <sub>2</sub> O	0.38	0.84	0.63	0.05	0.26	1.59	0.54	0.23
P <sub>2</sub> O <sub>5</sub>	0.18	0.29	0.20	0.13	0.17	0.21	0.16	0.18
Total	100.87	100.25	100.02	100.92	100.08	98.98	100.61	98.96
FeO	8.08	10.09	5.18	5.13	7.94	9.25	8.68	8.90
Loss	3.29	2.53	1.88	4.21	3.50	2.54	4.31	3.63

\* = total iron as Fe<sub>2</sub>O<sub>3</sub>

PPM

Ba	123	296	215	n.d.	n.a.	n.a.	297	108
Ce	n.a.	n.a.	n.a.	n.a.	n.a.	n.a.	n.a.	n.a.
Cr	134	49	109	193	226	n.d.	208	57
La	n.a.	n.a.	n.a.	n.a.	n.a.	n.a.	n.a.	n.a.
Nb	5	8	7	4	7	4	4	7
Nd	21	30	15	8	n.a.	n.a.	2	22
Ni	36	16	26	55	78	22	54	22
Rb	9	14	11	2	4	23	10	5
Sc	48	43	45	43	45	40	44	41
Sr	232	224	182	399	277	345	294	202
V	355	n.a.	355	n.a.	n.a.	n.a.	n.a.	n.a.
Y	32	46	30	23	28	35	27	30
Zr	119	209	150	80	105	157	102	154
'f'	0.46	0.26	0.37	0.69	0.52	0.40	0.54	0.36

n.d. = not detected  
n.a. = not analysed

Sample No.	SB41	SB42	SB43	SB44	SB45	SB46	SB47	SB48
SiO <sub>2</sub>	54.3	51.0	51.9	46.3	53.2	47.2	49.0	47.9
TiO <sub>2</sub>	1.90	1.62	1.61	3.62	1.91	1.48	1.59	1.55
Al <sub>2</sub> O <sub>3</sub>	15.3	15.0	15.4	12.5	14.8	17.0	16.0	17.4
Fe <sub>2</sub> O <sub>3</sub> *	11.97	11.47	10.39	18.99	10.85	10.12	10.94	11.13
MnO	0.18	0.15	0.17	0.26	0.23	0.17	0.18	0.19
MgO	7.16	7.10	7.38	6.23	6.98	7.77	11.23	7.76
CaO	5.89	9.05	8.69	9.21	7.59	12.83	7.61	10.61
Na <sub>2</sub> O	3.79	3.76	3.51	2.64	2.27	2.35	1.87	2.66
K <sub>2</sub> O	0.07	0.56	1.07	0.58	1.37	0.46	0.60	1.07
P <sub>2</sub> O <sub>5</sub>	0.20	0.16	0.15	0.37	0.26	0.14	0.14	0.13
Total	100.76	99.89	100.27	100.70	99.46	99.52	99.16	100.40
FeO	9.10	8.68	8.45	10.16	8.02	6.05	6.89	7.75
Loss	4.19	3.14	2.78	2.49	3.85	3.69	6.34	4.45

\* = total iron as Fe<sub>2</sub>O<sub>3</sub>

PPM

Ba	81	283	n.a.	140	n.a.	n.a.	n.a.	n.a.
Ce	n.a.	n.a.	n.a.	n.a.	n.a.	n.a.	n.a.	n.a.
Cr	196	208	201	59	158	271	554	262
La	n.a.	n.a.	n.a.	n.a.	n.a.	n.a.	n.a.	n.a.
Nb	5	4	3	7	6	8	6	10
Nd	15	8	n.a.	21	n.a.	n.a.	n.a.	n.a.
Ni	71	54	53	32	54	198	324	171
Rb	1	10	19	8	23	8	9	25
Sc	43	44	39	60	40	39	41	39
Sr	228	294	398	225	153	354	296	191
V	n.a.	n.a.	n.a.	n.a.	n.a.	n.a.	n.a.	n.a.
Y	27	28	25	39	39	23	23	23
Zr	117	103	104	145	158	96	100	87
'f'	0.47	0.53	0.53	0.38	0.35	0.57	0.55	0.63

n.a. = not analysed



Sample No.	SB49	SB50	SB51	SB53	SB56	SB57	SB58	SB59
SiO <sub>2</sub>	50.8	46.9	46.6	51.6	52.2	51.3	52.0	53.5
TiO <sub>2</sub>	1.55	1.81	2.05	1.81	1.59	1.26	1.43	1.28
Al <sub>2</sub> O <sub>3</sub>	16.7	16.7	15.9	16.4	14.7	16.5	14.6	16.6
Fe <sub>2</sub> O <sub>3</sub> *	9.67	12.46	13.63	11.05	11.56	9.35	8.79	6.75
MnO	0.15	0.19	0.18	0.15	0.19	0.20	0.16	0.17
MgO	7.73	8.92	7.43	5.39	6.99	7.33	5.18	4.61
CaO	9.96	9.89	10.60	8.36	8.71	10.69	11.93	11.96
Na <sub>2</sub> O	2.53	1.74	2.61	4.34	2.79	2.38	3.78	3.32
K <sub>2</sub> O	0.73	0.87	0.50	0.47	1.05	0.92	0.25	0.27
P <sub>2</sub> O <sub>5</sub>	0.16	0.20	0.23	0.22	0.16	0.11	0.33	0.17
Total	99.98	99.68	99.73	99.79	99.94	100.04	98.45	98.63
FeO	6.41	8.65	8.25	6.37	6.76	6.65	6.79	4.93
Loss	4.24	4.01	3.38	3.02	2.97	2.28	8.30	7.39

\* = total iron as Fe<sub>2</sub>O<sub>3</sub>

PPM

Ba	n.a.	n.a.	n.a.	n.a.	n.a.	n.a.	n.a.	n.a.
Ce	n.a.	n.a.	n.a.	n.a.	n.a.	n.a.	n.a.	n.a.
Cr	310	251	156	164	n.d.	192	96	178
La	n.a.	n.a.	n.a.	n.a.	n.a.	n.a.	n.a.	n.a.
Nb	3	6	5	4	3	8	7	6
Nd	n.a.	n.a.	n.a.	n.a.	n.a.	n.a.	n.a.	n.a.
Ni	212	127	58	74	21	39	67	139
Rb	12	13	10	8	28	16	2	5
Sc	39	36	40	36	40	38	38	38
Sr	191	199	248	324	193	211	136	89
V	n.a.	n.a.	n.a.	n.a.	n.a.	n.a.	n.a.	n.a.
Y	24	28	30	28	27	20	58	44
Zr	94	95	119	116	100	83	195	176
'f'	0.59	0.58	0.46	0.47	0.55	0.66	0.28	0.31

n.d. = not detected

n.a. = not analysed

Sample No.	SB60	SB61	SB62	SB63	SB66	SB67	SB68	SP3
SiO <sub>2</sub>	49.2	47.9	49.0	47.1	49.7	47.9	49.3	49.8
TiO <sub>2</sub>	1.85	2.00	2.04	2.13	1.54	2.09	1.72	1.53
Al <sub>2</sub> O <sub>3</sub>	14.4	16.0	16.2	17.1	17.3	16.7	15.7	16.0
Fe <sub>2</sub> O <sub>3</sub> *	12.54	11.85	11.02	13.63	10.78	13.50	11.34	11.17
MnO	0.28	0.25	0.19	0.27	0.15	0.18	0.16	0.19
MgO	6.71	7.64	7.07	7.66	7.83	8.89	9.74	8.43
CaO	10.40	13.04	10.17	9.33	10.92	8.16	8.43	11.03
Na <sub>2</sub> O	3.65	1.68	3.10	2.48	2.70	1.48	2.65	2.61
K <sub>2</sub> O	0.08	0.25	0.42	0.46	0.30	0.99	0.31	0.41
P <sub>2</sub> O <sub>5</sub>	0.21	0.22	0.22	0.25	0.12	0.24	0.16	0.15
Total	99.32	100.83	99.43	100.41	101.34	100.13	99.51	101.32
FeO	9.61	8.94	8.39	11.78	7.08	10.15	7.77	7.59
Loss	4.64	4.36	4.42	3.30	3.88	3.97	4.34	3.40

\* = total iron as Fe<sub>2</sub>O<sub>3</sub>

PPM

Ba	n.a.	n.a.	n.a.	n.a.	n.a.	n.a.	n.a.	n.a.
Ce	n.a.	n.a.	n.a.	n.a.	n.a.	n.a.	n.a.	n.a.
Cr	151	130	145	171	359	195	214	202
La	n.a.	n.a.	n.a.	n.a.	n.a.	n.a.	n.a.	n.a.
Nb	5	8	4	3	4	7	7	2
Nd	n.a.	n.a.	n.a.	n.a.	n.a.	n.a.	n.a.	n.a.
Ni	54	58	68	64	239	68	94	75
Rb	1	4	6	6	8	17	5	7
Sc	42	38	n.a.	39	42	39	n.a.	35
Sr	151	201	379	343	238	259	295	244
V	n.a.	n.a.	n.a.	n.a.	293	n.a.	n.a.	n.a.
Y	26	31	30	32	24	32	27	28
Zr	87	110	125	128	89	120	109	107
'f'	0.63	0.50	0.44	0.43	0.62	0.46	0.50	0.51

n.a. = not analysed

Sample No.	SP94	YG1	YG2	GF63	GG1	REB166	LD1	LD2
SiO <sub>2</sub>	50.9	48.9	49.7	50.5	50.9	48.0	49.1	48.9
TiO <sub>2</sub>	1.72	1.71	1.18	1.38	1.24	1.59	1.36	1.08
Al <sub>2</sub> O <sub>3</sub>	15.2	15.9	17.2	16.6	15.9	17.5	16.5	17.5
Fe <sub>2</sub> O <sub>3</sub> *	12.20	11.50	9.72	10.52	9.37	10.60	10.76	9.35
MnO	0.23	0.21	0.18	0.19	0.17	0.17	0.18	0.16
MgO	7.28	7.72	8.04	7.49	7.92	9.86	8.74	10.01
CaO	7.44	10.22	10.51	10.70	11.74	8.79	9.60	10.44
Na <sub>2</sub> O	3.87	2.61	2.07	2.50	2.72	1.99	2.90	1.97
K <sub>2</sub> O	0.25	0.80	0.68	1.09	0.82	0.70	0.26	0.79
P <sub>2</sub> O <sub>5</sub>	0.19	0.14	0.11	0.12	0.14	0.13	0.14	0.11
Total	99.28	99.71	99.39	101.09	100.92	99.33	99.54	100.31
FeO	9.02	8.46	6.44	6.76	6.31	7.86	7.18	6.89
Loss	2.98	3.50	3.57	2.69	2.54	4.57	3.94	1.26

\* = total iron as Fe<sub>2</sub>O<sub>3</sub>

#### PPM

Ba	n.a.	n.a.	n.a.	n.a.	n.a.	135	n.a.	n.a.
Ce	n.a.	n.a.	n.a.	n.a.	n.a.	n.a.	n.a.	n.a.
Cr	172	233	196	251	434	319	220	233
La	n.a.	n.a.	n.a.	n.a.	n.a.	n.a.	n.a.	n.a.
Nb	1	16	5	7	7	4	2	6
Nd	n.a.	n.a.	n.a.	n.a.	n.a.	12	n.a.	n.a.
Ni	57	66	160	61	64	121	93	223
Rb	n.a.	15	12	28	16	10	6	21
Sc	41	42	30	37	43	40	40	32
Sr	n.a.	280	213	190	283	282	309	285
V	n.a.	n.a.	n.a.	n.a.	n.a.	n.a.	n.a.	n.a.
Y	n.a.	22	18	21	19	23	20	15
Zr	n.a.	73	64	82	77	101	72	55
'f'	-	0.75	0.90	0.67	0.71	0.54	0.76	1.00

n.a. = not analysed

Sample No.	LD3	LG1	LG2	LG3	LG4	LG5	LG6
SiO <sub>2</sub>	49.2	50.3	53.4	50.9	50.1	50.1	51.0
TiO <sub>2</sub>	1.10	1.41	1.32	1.57	1.43	1.91	2.87
Al <sub>2</sub> O <sub>3</sub>	17.7	15.0	15.8	16.3	15.3	14.6	13.4
Fe <sub>2</sub> O <sub>3</sub> *	10.36	10.15	9.29	10.91	10.77	12.72	15.71
MnO	0.19	0.18	0.17	0.19	0.18	0.23	0.25
MgO	10.25	7.17	7.19	8.04	7.67	6.73	5.49
CaO	7.73	10.49	10.87	8.33	11.48	10.52	6.33
Na <sub>2</sub> O	1.84	3.87	4.28	3.51	3.17	3.33	5.02
K <sub>2</sub> O	2.25	0.38	0.29	0.65	0.50	0.43	0.21
P <sub>2</sub> O <sub>5</sub>	0.13	0.14	0.13	0.15	0.12	0.19	0.29
Total	100.75	99.09	102.74	100.55	100.72	100.76	100.57
FeO	6.14	7.59	5.96	7.74	6.57	7.16	8.97
Loss	4.24	2.84	2.73	3.10	2.64	2.68	2.50

\* = total iron as Fe<sub>2</sub>O<sub>3</sub>

PPM

Ba	n.a.	n.a.	n.a.	n.a.	n.a.	n.a.	n.a.
Ce	n.a.	n.a.	n.a.	n.a.	n.a.	n.a.	n.a.
Cr	201	37	142	196	70	20	12
La	n.a.	n.a.	n.a.	n.a.	n.a.	n.a.	n.a.
Nb	1	7	7	4	5	7	10
Nd	n.a.	n.a.	n.a.	n.a.	n.a.	n.a.	n.a.
Ni	193	43	55	62	53	34	20
Rb	39	8	6	13	12	12	4
Sc	31	46	46	35	43	45	40
Sr	503	315	156	250	185	219	89
V	n.a.	n.a.	n.a.	270	277	n.a.	379
Y	16	28	25	26	22	36	50
Zr	76	113	85	98	69	123	179
'f'	0.72	0.49	0.65	0.56	0.80	0.45	0.31

n.a. = not analysed

## (ii) UNIGNITED SAMPLES

Sample No.	SBC1	SBR1	SBC5	SBR5	SBC7	SBR7
SiO <sub>2</sub>	49.9	47.6	52.8	59.4	47.1	46.3
TiO <sub>2</sub>	1.79	1.68	2.34	2.22	1.83	1.78
Al <sub>2</sub> O <sub>3</sub>	15.2	14.2	14.3	13.8	15.9	16.0
Fe <sub>2</sub> O <sub>3</sub> *	12.26	11.74	13.72	9.68	11.32	11.66
MnO	0.24	0.24	0.24	0.14	0.19	0.20
MgO	7.39	7.00	6.96	4.40	9.29	9.31
CaO	10.33	9.91	7.40	5.58	8.98	8.88
Na <sub>2</sub> O	2.95	3.10	3.58	3.16	1.94	1.97
K <sub>2</sub> O	0.88	0.56	0.34	0.48	0.27	0.32
P <sub>2</sub> O <sub>5</sub>	0.18	0.16	0.24	0.24	0.17	0.18
Loss <sup>+</sup>	2.17	2.26	2.40	3.30	3.86	4.16
Total	103.29	98.45	104.32	102.40	100.85	100.76
FeO	8.66	8.72	9.51	6.92	8.58	7.80
* = total iron as Fe <sub>2</sub> O <sub>3</sub>						
+ = total loss on ignition						
PPM						
Ba	308	186	117	98	135	150
Ce	57	53	69	76	58	57
Cr	136	130	24	22	298	319
La	4	6	12	10	5	4
Nb	5	4	8	8	3	5
Nd	14	15	18	29	20	15
Ni	33	34	15	15	125	138
Rb	17	15	5	6	4	5
Sc	n.a.	n.a.	41	n.a.	38	38
Sr	237	253	226	221	284	279
V	n.a.	n.a.	n.a.	n.a.	n.a.	n.a.
Y	32	31	43	36	30	29
Zr	117	117	184	172	112	101
'f'	0.47	0.47	0.30	0.32	0.49	0.54

n.a. = not analysed

Sample No.	SBC10	SBR10	SBC12	SBR12
SiO <sub>2</sub>	47.5	46.9	47.0	45.6
TiO <sub>2</sub>	1.94	1.93	1.77	1.80
Al <sub>2</sub> O <sub>3</sub>	16.0	17.3	15.3	15.4
Fe <sub>2</sub> O <sub>3</sub> *	12.49	11.65	12.93	11.55
MnO	0.18	0.17	0.21	0.22
MgO	6.29	6.30	7.54	6.05
CaO	7.94	7.21	8.37	11.37
Na <sub>2</sub> O	3.38	3.59	2.28	2.37
K <sub>2</sub> O	0.38	0.25	0.43	0.52
P <sub>2</sub> O <sub>5</sub>	0.23	0.24	0.18	0.21
Loss <sup>+</sup>	3.19	4.88	4.25	5.87
Total	99.52	100.42	100.26	100.96
FeO	10.19	9.45	10.08	9.23

\* = total iron as Fe<sub>2</sub>O<sub>3</sub>

+ = total loss on ignition

#### PPM

Ba	315	352	126	177
Ce	58	52	60	48
Cr	261	179	161	148
La	2	6	6	4
Nb	5	6	4	6
Nd	10	13	15	10
Ni	110	140	62	64
Rb	5	4	8	9
Sc	47	43	38	n.a.
Sr	424	348	331	384
V	n.a.	283	n.a.	n.a.
Y	37	36	30	28
Zr	149	151	105	107
'f'	0.37	0.36	0.51	0.51

n.a. = not analysed

## ANALYSES OF ROCKS BELONGING TO GROUP 2, FISHGUARD VOLCANIC GROUP

## (i) IGNITED SAMPLES

## (ii) UNIGNITED SAMPLES

Sample No.	SB54	SB55	SB64		SBC11	SBR11
SiO <sub>2</sub>	56.5	56.2	56.4	SiO <sub>2</sub>	56.6	60.3
TiO <sub>2</sub>	2.54	1.97	1.35	TiO <sub>2</sub>	1.22	1.34
Al <sub>2</sub> O <sub>3</sub>	13.0	16.4	15.0	Al <sub>2</sub> O <sub>3</sub>	14.8	16.1
Fe <sub>2</sub> O <sub>3</sub> *	13.70	9.58	9.03	Fe <sub>2</sub> O <sub>3</sub> *	6.20	7.26
MnO	0.24	0.20	0.17	MnO	0.08	0.09
MgO	3.85	2.58	5.49	MgO	3.39	4.07
CaO	4.76	5.25	5.90	CaO	2.72	3.64
Na <sub>2</sub> O	4.50	6.81	4.71	Na <sub>2</sub> O	5.84	5.99
K <sub>2</sub> O	0.11	0.10	0.53	K <sub>2</sub> O	0.55	0.29
P <sub>2</sub> O <sub>5</sub>	0.28	0.46	0.19	P <sub>2</sub> O <sub>5</sub>	0.27	0.32
Total	99.48	99.55	98.77	Loss <sup>+</sup>	2.37	2.59
FeO	10.41	6.34	7.31	Total	94.04	101.99
Loss	2.44	1.79	3.73	FeO	5.43	5.71
* = total iron as Fe <sub>2</sub> O <sub>3</sub>				* = total iron as Fe <sub>2</sub> O <sub>3</sub>		
				+ = total loss on ignition		
PPM				PPM		
Ba	n.a.	n.a.	n.a.	Ba	530	242
Ce	n.a.	n.a.	n.a.	Ce	78	87
Cr	n.d.	n.d.	122	Cr	142	137
La	n.a.	n.a.	n.a.	La	15	15
Nb	8	14	9	Nb	10	8
Nd	n.a.	n.a.	n.a.	Nd	45	43
Ni	8	20	69	Ni	36	41
Rb	3	2	7	Rb	8	4
Sc	37	23	34	Sc	30	n.a.
Sr	116	237	154	Sr	148	130
V	318	98	n.a.	V	171	n.a.
Y	49	59	54	Y	63	67
Zr	212	218	213	Zr	249	247
'f'	0.26	0.25	0.26	'f'	0.22	0.22

n.d. = not detected

n.a. = not analysed

## ANALYSES OF ROCKS BELONGING TO GROUP 3, FISHGUARD VOLCANIC GROUP

## (i) IGNITED SAMPLES

(ii) IGNITED SAMPLES  
(ANALYSED BY WET CHEMICAL METHODS)

Sample No.	REB94	REB342	REB413	SA3	REB412	REB412A	REB414
SiO <sub>2</sub>	67.8	67.2	69.0	66.9	66.4	67.0	70.7
TiO <sub>2</sub>	1.14	1.01	1.13	1.16	1.13	1.09	1.12
Al <sub>2</sub> O <sub>3</sub>	15.7	16.1	15.4	15.9	14.4	14.5	12.5
Fe <sub>2</sub> O <sub>3</sub> *	6.53	6.79	5.31	6.71	5.92	5.60	0.47
MnO	0.15	0.16	0.10	0.16	0.20	0.23	n.d.
MgO	1.27	1.27	1.16	1.10	1.35	1.25	0.24
CaO	2.88	0.51	1.28	3.01	1.51	1.51	1.60
Na <sub>2</sub> O	3.55	3.73	4.43	3.67	4.44	4.36	1.43
K <sub>2</sub> O	1.17	3.61	2.15	0.94	3.36	3.32	11.3
P <sub>2</sub> O <sub>5</sub>	0.23	0.24	0.23	0.24	0.22	n.a.	n.a.
Total	100.42	100.62	100.19	99.79	98.93	98.86	99.36
FeO	4.51	5.11	5.21	5.44	4.99	n.a.	n.a.
Loss	2.50	2.39	1.85	2.07	1.70	1.51	0.64
* = total iron as Fe <sub>2</sub> O <sub>3</sub>							
PPM							
Ba	n.a.	n.a.	743	n.a.	871	866	2140
Ce	n.a.	n.a.	n.a.	n.a.	n.a.	n.a.	n.a.
Cr	n.d.	n.d.	17	n.a.	7	9	n.d.
La	n.a.	n.a.	n.a.	n.a.	n.a.	n.a.	n.a.
Nb	16	20	25	25	26	23	42
Nd	n.a.	n.a.	73	n.a.	65	76	64
Ni	16	20	20	n.a.	16	17	n.a.
Rb	50	90	62	36	64	65	171
Sc	25	18	22	24	24	n.a.	n.a.
Sr	327	98	204	429	183	187	200
V	141	69	116	n.a.	n.a.	n.a.	n.a.
Y	52	52	47	51	55	54	53
Zr	320	338	313	288	324	316	306

n.a. = not analysed

n.d. = not detected



## ANALYSES OF ROCKS BELONGING TO GROUP 4, FISHGUARD VOLCANIC GROUP

## (i) UNIGNITED SAMPLES

## (ii) IGNITED SAMPLES

Sample No.	SA4	SA5	SA6	SA8		SA9	SA11
SiO <sub>2</sub>	75.0	73.2	72.8	73.8	SiO <sub>2</sub>	76.4	77.3
TiO <sub>2</sub>	0.19	0.24	0.18	0.17	TiO <sub>2</sub>	0.18	0.19
Al <sub>2</sub> O <sub>3</sub>	15.1	12.0	12.7	11.2	Al <sub>2</sub> O <sub>3</sub>	14.7	12.2
Fe <sub>2</sub> O <sub>3</sub> *	0.63	2.20	0.43	1.16	Fe <sub>2</sub> O <sub>3</sub> *	0.04	0.72
MnO	0.05	0.05	0.03	0.03	MnO	0.02	0.01
MgO	0.46	0.68	0.08	0.56	MgO	0.86	0.63
CaO	0.44	0.24	0.01	0.10	CaO	0.19	0.04
Na <sub>2</sub> O	6.51	3.63	4.56	0.05	Na <sub>2</sub> O	9.39	2.44
K <sub>2</sub> O	3.30	4.44	5.04	9.00	K <sub>2</sub> O	0.12	6.56
P <sub>2</sub> O <sub>5</sub>	0.03	0.05	0.02	0.02	P <sub>2</sub> O <sub>5</sub>	0.02	0.02
Loss <sup>+</sup>	0.48	0.81	0.49	0.56	Total	101.92	100.11
Total	102.19	97.54	96.34	96.65	Loss	0.36	0.56

\* = total iron as Fe<sub>2</sub>O<sub>3</sub>\* = total iron as Fe<sub>2</sub>O<sub>3</sub>

+ = total loss on ignition

PPM					PPM		
Ba	1911	817	1008	550	Ba	n.a.	n.a.
Ce	65	57	70	70	Ce	n.a.	n.a.
Cr	n.d.	n.d.	n.d.	n.d.	Cr	n.a.	n.a.
La	26	20	21	19	La	n.a.	n.a.
Nb	36	29	33	27	Nb	24	23
Nd	81	50	106	84	Nd	n.a.	n.a.
Ni	22	19	22	19	Ni	n.a.	n.a.
Rb	39	77	94	166	Rb	2	163
Sc	n.a.	n.a.	n.a.	n.d.	Sc	n.a.	n.a.
Sr	188	63	45	35	Sr	82	42
V	n.a.	n.a.	n.a.	n.d.	V	n.a.	n.a.
Y	77	59	70	63	Y	41	59
Zr	169	203	166	169	Zr	138	163

n.a. = not analysed

n.d. = not detected

## ANALYSES OF SILICIFIED META-BASALTS FROM CARN FATHACH AREA

## (i) UNIGNITED SAMPLES

## (ii) IGNITED SAMPLES

Sample No.	SB13		SB52
SiO <sub>2</sub>	56.2	SiO <sub>2</sub>	69.6
TiO <sub>2</sub>	1.55	TiO <sub>2</sub>	1.33
Al <sub>2</sub> O <sub>3</sub>	15.4	Al <sub>2</sub> O <sub>3</sub>	13.3
Fe <sub>2</sub> O <sub>3</sub> *	9.20	Fe <sub>2</sub> O <sub>3</sub> *	4.88
MnO	0.21	MnO	0.04
MgO	3.97	MgO	2.21
CaO	5.08	CaO	2.23
Na <sub>2</sub> O	4.11	Na <sub>2</sub> O	5.45
K <sub>2</sub> O	1.46	K <sub>2</sub> O	0.18
P <sub>2</sub> O <sub>5</sub>	0.37	P <sub>2</sub> O <sub>5</sub>	0.41
Loss <sup>+</sup>	2.08	Total	99.63
Total	99.63	FeO	4.39
FeO	n.d.	Loss	1.86
* = total iron as Fe <sub>2</sub> O <sub>3</sub>		* = total iron as Fe <sub>2</sub> O <sub>3</sub>	
+ = total loss on ignition			
PPM		PPM	
Ba	630	Ba	n.a.
Ce	100	Ce	n.a.
Cr	18	Cr	1
La	16	La	n.a.
Nb	15	Nb	11
Nd	51	Nd	n.a.
Ni	21	Ni	35
Rb	22	Rb	3
Sc	56	Sc	23
Sr	305	Sr	138
V	n.a.	V	n.a.
Y	87	Y	72
Zr	553	Zr	370

n.a. = not analysed

## ANALYSES OF VOLCANICLASTIC ROCKS FROM NORTH PEMBROKESHIRE

## (i) IGNITED SAMPLES

## (ii) UNIGNITED SAMPLES

Sample No.	SB26	SP2	SP62	SP63		SA7
SiO <sub>2</sub>	73.4	76.9	80.8	79.0	SiO <sub>2</sub>	66.8
TiO <sub>2</sub>	0.41	0.50	0.13	0.13	TiO <sub>2</sub>	0.52
Al <sub>2</sub> O <sub>3</sub>	11.8	12.4	11.3	11.6	Al <sub>2</sub> O <sub>3</sub>	13.4
Fe <sub>2</sub> O <sub>3</sub> *	5.20	1.87	1.07	1.52	Fe <sub>2</sub> O <sub>3</sub> *	5.76
MnO	0.04	0.03	0.02	0.02	MnO	0.12
MgO	4.11	0.64	0.93	1.53	MgO	2.48
CaO	3.76	0.99	0.03	0.02	CaO	1.47
Na <sub>2</sub> O	0.05	2.80	4.81	2.70	Na <sub>2</sub> O	3.03
K <sub>2</sub> O	2.06	2.79	2.06	4.50	K <sub>2</sub> O	1.38
P <sub>2</sub> O <sub>5</sub>	0.05	0.07	0.01	0.02	P <sub>2</sub> O <sub>5</sub>	0.23
Total	100.88	98.99	101.16	101.04	Loss <sup>+</sup>	3.58
Loss	3.30	0.90	0.90	1.44	Total	98.77

\* = total iron as Fe<sub>2</sub>O<sub>3</sub>\* = total iron as Fe<sub>2</sub>O<sub>3</sub>

+ = total loss on ignition

PPM					PPM	
Ba	359	n.a.	1656	2602	Ba	469
Ce	n.a.	n.a.	n.a.	n.a.	Ce	136
Cr	n.d.	n.a.	n.d.	n.d.	Cr	n.d.
La	n.a.	n.a.	n.a.	n.a.	La	42
Nb	21	29	30	24	Nb	26
Nd	78	n.a.	31	n.d.	Nd	130
Ni	15	n.a.	23	19	Ni	16
Rb	57	34	15	35	Rb	27
Sc	n.a.	n.a.	n.a.	n.a.	Sc	n.a.
Sr	133	135	107	96	Sr	295
V	n.a.	n.a.	n.a.	n.a.	V	n.a.
Y	82	85	60	57	Y	88
Zr	517	553	561	576	Zr	618

n.a. = not analysed

n.d. = not detected

## ANALYSES OF LAVAS FROM OTHER AREAS OF NORTH PEMBROKESHIRE

(i) IGNITED SAMPLES

(ii) UNIGNITED SAMPLES

Sample No.	REB23	REB90		REB12	REB125	REB127	REB153	REB154
SiO <sub>2</sub>	62.7	58.4	SiO <sub>2</sub>	58.7	58.5	57.4	57.4	53.6
TiO <sub>2</sub>	0.62	0.82	TiO <sub>2</sub>	0.80	0.83	0.85	0.86	0.89
Al <sub>2</sub> O <sub>3</sub>	18.3	20.9	Al <sub>2</sub> O <sub>3</sub>	16.7	16.9	19.7	18.4	17.3
Fe <sub>2</sub> O <sub>3</sub> *	4.96	7.08	Fe <sub>2</sub> O <sub>3</sub> *	7.63	7.06	6.94	7.53	7.27
MnO	0.10	0.28	MnO	0.16	0.11	0.08	0.27	0.10
MgO	2.90	4.21	MgO	4.68	3.43	3.70	4.60	4.35
CaO	4.02	1.02	CaO	2.85	5.05	2.57	2.39	5.55
Na <sub>2</sub> O	6.76	6.68	Na <sub>2</sub> O	3.27	3.24	2.89	3.44	4.89
K <sub>2</sub> O	0.38	0.21	K <sub>2</sub> O	0.39	1.31	2.86	1.11	0.20
P <sub>2</sub> O <sub>5</sub>	0.20	0.23	P <sub>2</sub> O <sub>5</sub>	0.17	0.19	0.18	0.18	0.16
Total	100.94	99.83	Loss <sup>+</sup>	3.78	4.24	3.40	3.47	5.21
FeO	3.64	5.67	Total	99.13	100.86	100.57	99.65	99.52
Loss	2.57	3.83	FeO	1.90	1.14	1.50	1.18	1.79

\* = total iron as Fe<sub>2</sub>O<sub>3</sub>\* = total iron as Fe<sub>2</sub>O<sub>3</sub>

+ = total loss on ignition

PPM			PPM					
Ba	202	229	Ba	134	457	1163	420	56
Ce	n.a.	n.a.	Ce	n.a.	n.a.	n.a.	n.a.	n.a.
Cr	30	53	Cr	52	44	41	31	25
La	n.a.	n.a.	La	n.a.	n.a.	n.a.	n.a.	n.a.
Nb	9	5	Nb	7	7	8	6	5
Nd	19	10	Nd	43	14	17	32	17
Ni	52	67	Ni	38	45	54	55	38
Rb	3	5	Rb	8	31	62	27	5
Sc	n.a.	n.a.	Sc	n.a.	n.a.	n.a.	n.a.	n.a.
Sr	290	140	Sr	320	430	328	332	275
V	n.a.	n.a.	V	n.a.	n.a.	n.a.	n.a.	n.a.
Y	18	15	Y	21	21	28	25	19
Zr	171	145	Zr	166	192	214	205	154

n.a. = not analysed

## ANALYSES OF DOLERITES AND GABBROS FROM NORTH PEMBROKESHIRE.

## WET CHEMICAL ANALYSES ON UNIGNITED POWDERS.

MAJOR ELEMENTS SUPPLIED BY DR. R. A. ROACH; TRACE ELEMENTS AUTHOR'S OWN DETERMINATIONS.

Sample No.	RD151	RD154	RD155	RD158	RD165	RD172
SiO <sub>2</sub>	61.4	55.1	55.9	57.7	55.5	56.4
TiO <sub>2</sub>	1.60	1.06	1.21	1.26	1.02	0.96
Al <sub>2</sub> O <sub>3</sub>	14.4	15.4	15.0	14.9	15.2	15.4
Fe <sub>2</sub> O <sub>3</sub> *	9.27	8.80	8.52	8.94	8.71	8.47
MnO	0.15	0.15	0.13	0.15	0.15	0.18
MgO	2.00	5.36	4.39	3.89	5.36	6.24
CaO	3.89	7.21	9.00	5.67	7.71	7.99
Na <sub>2</sub> O	4.20	3.43	3.24	3.72	2.81	2.62
K <sub>2</sub> O	2.13	1.62	1.62	1.74	1.11	1.57
P <sub>2</sub> O <sub>5</sub>	0.24	0.13	0.16	0.17	0.15	0.14
H <sub>2</sub> O						
Total						
FeO	6.65	6.50	5.65	7.08	6.65	6.58
* = total iron as Fe <sub>2</sub> O <sub>3</sub>						
PPM						
Ba	n.a.	262	n.a.	n.a.	n.a.	n.a.
Ce	n.a.	n.a.	n.a.	n.a.	n.a.	n.a.
Cr	n.a.	n.a.	n.a.	n.a.	n.a.	n.a.
La	n.a.	n.a.	n.a.	n.a.	n.a.	n.a.
Nb	n.a.	6	n.a.	n.a.	n.a.	n.a.
Nd	n.a.	29	n.a.	n.a.	n.a.	n.a.
Ni	n.a.	n.a.	n.a.	n.a.	n.a.	n.a.
Rb	n.a.	37	n.a.	n.a.	n.a.	n.a.
Sc	n.a.	n.a.	n.a.	n.a.	n.a.	n.a.
Sr	n.a.	219	n.a.	n.a.	n.a.	n.a.
V	n.a.	n.a.	n.a.	n.a.	n.a.	n.a.
Y	n.a.	35	n.a.	n.a.	n.a.	n.a.
Zr	n.a.	133	n.a.	n.a.	n.a.	n.a.

n.a. = not analysed

Sample No.	RD175	RD212	RD225A	RD228A	RD230A	RD231A
SiO <sub>2</sub>	52.3	54.9	47.2	48.7	49.6	48.5
TiO <sub>2</sub>	0.98	0.95	1.28	1.06	1.86	1.36
Al <sub>2</sub> O <sub>3</sub>	15.4	15.2	16.4	15.8	14.3	15.2
Fe <sub>2</sub> O <sub>3</sub> *	8.96	8.49	10.87	9.95	11.72	7.15
MnO	0.15	0.25	0.23	0.18	0.25	0.23
MgO	7.03	7.53	7.89	8.49	6.66	7.89
CaO	8.00	7.99	9.75	9.49	6.70	11.5
Na <sub>2</sub> O	2.81	2.95	2.00	2.05	3.82	3.00
K <sub>2</sub> O	1.34	1.00	1.28	1.34	0.37	0.49
P <sub>2</sub> O <sub>5</sub>	0.13	0.15	0.13	0.11	0.26	0.13
H <sub>2</sub> O						
Total						
FeO	7.00	6.49	8.13	7.48	9.49	8.32

\* = total iron as Fe<sub>2</sub>O<sub>3</sub>

PPM

Ba	n.a.	n.a.	90	178	64	258
Ce	n.a.	n.a.	n.a.	n.a.	n.a.	n.a.
Cr	n.a.	n.a.	215	n.a.	42	n.a.
La	n.a.	n.a.	n.a.	n.a.	n.a.	n.a.
Nb	n.a.	n.a.	4	3	5	3
Nd	n.a.	n.a.	7	12	19	12
Ni	n.a.	n.a.	83	n.a.	36	n.a.
Rb	n.a.	n.a.	11	14	4	9
Sc	n.a.	n.a.	n.a.	n.a.	n.a.	n.a.
Sr	n.a.	n.a.	253	254	187	324
V	n.a.	n.a.	n.a.	n.a.	n.a.	n.a.
Y	n.a.	n.a.	23	19	36	22
Zr	n.a.	n.a.	88	84	121	83

n.a. = not analysed

Sample No.	RD329	RD232	RD237	RD238A	RD244	RD252
SiO <sub>2</sub>	65.0	45.8	66.7	65.4	52.3	69.6
TiO <sub>2</sub>	0.83	0.79	0.84	0.88	1.11	0.81
Al <sub>2</sub> O <sub>3</sub>	15.6	16.2	14.9	14.9	16.0	13.0
Fe <sub>2</sub> O <sub>3</sub> *	3.53	9.69	6.99	6.94	9.27	5.69
MnO	0.03	0.15	0.10	0.15	0.20	0.08
MgO	1.24	10.20	1.24	1.24	5.88	1.50
CaO	2.80	11.70	0.10	0.60	9.49	1.33
Na <sub>2</sub> O	6.30	2.15	2.81	3.14	2.43	3.57
K <sub>2</sub> O	1.62	0.65	2.92	3.89	1.11	2.19
P <sub>2</sub> O <sub>5</sub>	0.12	0.09	0.22	0.22	0.18	0.22
H <sub>2</sub> O						
Total						
FeO	2.32	7.24	5.02	5.04	5.38	4.23

\* = total iron as Fe<sub>2</sub>O<sub>3</sub>

#### PPM

Ba	n.a.	64	842	1041	190	544
Ce	n.a.	n.a.	n.a.	n.a.	n.a.	n.a.
Cr	n.a.	226	n.a.	n.d.	n.a.	n.a.
La	n.a.	n.a.	n.a.	n.a.	n.a.	n.a.
Nb	n.a.	3	20	22	7	23
Nd	n.a.	1	55	44	20	62
Ni	n.a.	188	n.a.	20	n.a.	n.a.
Rb	n.a.	21	94	106	24	69
Sc	n.a.	n.a.	n.a.	n.a.	n.a.	n.a.
Sr	n.a.	265	72	64	213	168
V	n.a.	n.a.	n.a.	n.a.	n.a.	n.a.
Y	n.a.	11	48	51	31	50
Zr	n.a.	49	328	386	111	439

n.a. = not analysed

n.d. = not detected

Sample No.	RD254	RD258B	RD280B	RD295A	RD295B	RD327	RD328
SiO <sub>2</sub>	67.6	49.6	48.0	56.4	55.4	55.1	55.0
TiO <sub>2</sub>	0.82	1.31	1.61	0.83	0.81	0.86	1.34
Al <sub>2</sub> O <sub>3</sub>	13.7	15.5	15.2	14.5	13.4	15.1	14.6
Fe <sub>2</sub> O <sub>3</sub> *	6.85	10.40	10.82	8.28	8.80	8.24	7.81
MnO	0.31	0.15	0.18	0.15	0.15	0.15	0.15
MgO	2.00	7.60	7.89	7.33	8.18	6.92	4.13
CaO	1.00	8.99	9.00	8.73	9.00	8.99	9.23
Na <sub>2</sub> O	3.19	3.09	3.19	2.91	2.15	2.95	3.09
K <sub>2</sub> O	3.61	0.65	0.43	1.28	1.11	1.06	1.51
P <sub>2</sub> O <sub>5</sub>	0.22	0.13	0.15	0.09	0.09	0.09	0.15
H <sub>2</sub> O							
Total							
FeO	5.04	7.82	8.04	6.34	6.98	6.26	5.24
* = total iron as Fe <sub>2</sub> O <sub>3</sub>							
PPM							
Ba	913	116	80	161	162	167	218
Ce	n.a.	n.a.	n.a.	n.a.	n.a.	n.a.	n.a.
Cr	n.a.	n.a.	n.a.	n.a.	n.a.	n.a.	n.a.
La	n.a.	n.a.	n.a.	n.a.	n.a.	n.a.	n.a.
Nb	21	6	4	6	4	6	6
Nd	48	4	10	20	15	20	25
Ni	n.a.	n.a.	n.a.	n.a.	n.a.	n.a.	n.a.
Rb	105	17	9	29	n.a.	20	n.a.
Sc	n.a.	n.a.	n.a.	n.a.	n.a.	n.a.	n.a.
Sr	67	193	373	181	n.a.	210	n.a.
V	n.a.	n.a.	n.a.	n.a.	n.a.	n.a.	n.a.
Y	52	23	31	29	n.a.	38	n.a.
Zr	306	104	112	95	n.a.	92	n.a.

n.a. = not analysed



ANALYSIS OF SPHERULE FROM MATRIX OF ISOLATED-PILLOW BRECCIA,  
PORTH MAEN MELYN

(WET CHEMICAL ANALYSIS OF IGNITED POWDER)

---

Sample No.	175S
------------	------

---

SiO <sub>2</sub>	66.3
------------------	------

TiO <sub>2</sub>	1.13
------------------	------

Al <sub>2</sub> O <sub>3</sub>	13.4
--------------------------------	------

Fe <sub>2</sub> O <sub>3</sub> *	5.23
----------------------------------	------

MnO	0.01
-----	------

MgO	2.25
-----	------

CaO	0.94
-----	------

Na <sub>2</sub> O	1.75
-------------------	------

K <sub>2</sub> O	7.70
------------------	------

H <sub>2</sub> O+	1.94
-------------------	------

P <sub>2</sub> O <sub>5</sub>	n.d.
-------------------------------	------

Total	100.65
-------	--------

Loss	1.73
------	------

\* = total iron as Fe<sub>2</sub>O<sub>3</sub>

PPM

Ba	2107
----	------

Ce	n.a.
----	------

Cr	3
----	---

La	n.a.
----	------

Nb	21
----	----

Nd	32
----	----

Ni	17
----	----

Rb	136
----	-----

Sc	n.a.
----	------

Sr	158
----	-----

V	n.a.
---	------

Y	47
---	----

Zr	295
----	-----

---

n.a. = not analysed

TABLE 13

Analyses of Rare Earth Elements

Sample	SB30 <sup>1</sup>	REB412 <sup>1</sup>	BCR-1 <sup>1</sup>	SB31 <sup>2</sup>	SA6 <sup>2</sup>	BCR-1 <sup>2</sup>
La	9.3±0.3	48.91±0.9	26.48±0.5	16.1±0.2	40.1±0.6	24.1±0.7
Ce	23.78±3	96.12±3	59.46±2	36.6±1.2	97±4	55.5±1.8
Pr	2.5±0.9	11±2	8.0±1.5	5.4±0.5	13.6±1.1	6.2±1.1
Nd	15±4	53±2	34±4	26.1±1.2	45.3±1.3	27.5±0.8
Sm	5.7±0.1	10.7±0.2	8.0±0.1	6.4±0.6	8.3±1.0	6.6±0.3
Eu	1.74±0.04	2.04±0.03	2.19±0.05	2.11±0.03	0.76±0.02	1.92±0.03
Gd	7.08±0.9	9.84±5	8.17±1.2	7.5±0.7	11.0±0.7	7.0±0.6
Tb	0.94±0.10	1.45±0.06	1.07±0.05	1.3±0.1	1.73±0.07	1.05±0.04
Dy	6.2±0.4	9.5±0.4	7.2±0.5	9.3±0.3	11.4±0.4	6.9±0.3
Ho	1.1±0.2	1.6±0.1	1.0±0.1	1.5±0.1	2.0±0.1	1.2±0.1
Er	4.7±1.3	7.0±2.9	3.92±1.3	6.4±0.5	8.3±0.4	3.9±0.3
Tm	<0.3	<0.54	<0.4	1.2±0.2	1.54±0.14	0.73±0.08
Yb	3.0±0.2	5.6±0.2	3.7±0.2	5.6±0.4	7.3±0.2	3.4±0.1
Lu	0.47±0.04	0.83±0.02	0.56±0.02	0.84±0.04	1.18±0.03	0.52±0.02

1, 2 refer to sample batches

TABLE 14

AVERAGE OF 22 CHONDRITES AND A COMPOSITE MIXTURE OF 9 CHONDRITES  
(FROM HERRMANN, 1970)

Element	PPM
La	0.32
Ce	0.94
Pr	0.12
Nd	0.60
Sm	0.20
Eu	0.073
Gd	0.31
Tb	0.05
Dy	0.31
Ho	0.073
Er	0.21
Tm	0.033
Yb	0.19
Lu	0.031

## APPENDIX 2. ANALYTICAL TECHNIQUES OF MINERAL DETERMINATIONS

### 1. MICROPROBE ANALYSIS

Analyses of a number of the mineral phases present within the metabasites were performed by Mr. F. Wilkinson and Dr. G. Rowbotham on a Geoscan Mark II Microprobe at the University of Manchester. It was operated at an accelerating voltage of 15kv and a current of  $3.5 \times 10^{-8}$  amps. An energy dispersive system was used for detection and measurement with calibration against metals, oxides, and silicates. Recalculations for minerals other than clinopyroxene were performed by the author. An estimate of the precision and accuracy of this method may be obtained from Dunham and Wilkinson (1978).

Clinopyroxenes from four gabbros were obtained by magnetic separation and the use of heavy liquids and were analysed for trace elements by emission spectrograph techniques. These results are presented in Table 16.

Phengitic muscovite from sample 210, an isolated-pillow breccia from Porth Maen Melyn, was separated and analysed by wet chemical methods in the Research Geochemistry Laboratory, University of Keele, under the supervision of Mr. D. W. Emley. The results of this analysis are listed in Table 17. A standard method of classical analysis is used in this laboratory and follows that of Bennett and Reed (1971, p. 43). It involves the fusion of the powdered sample by mixing with 3g of fusion mixture (an equimolecular mixture of sodium carbonate and potassium carbonate), and 0.4g boric acid. This is heated at  $1200^{\circ}\text{C}$  for 15 minutes. The glass produced is dissolved in hydrochloric acid and from the resulting solution silica is removed by coagulation with

polyethylene oxide and determined gravimetrically after hydrofluoric acid treatment. The residue is then fused with potassium pyrosulphate and the solution is made up to volume. Aliquots from this stock solution are used for  $\text{Fe}_2\text{O}_3$ ,  $\text{TiO}_2$ ,  $\text{MnO}$ ,  $\text{P}_2\text{O}_5$  (by colourimetric techniques),  $\text{CaO}$ ,  $\text{MgO}$  (by volumetric techniques) and  $\text{Al}_2\text{O}_3$  (by gravimetric techniques).  $\text{Na}_2\text{O}$  and  $\text{K}_2\text{O}$  are determined by flame emission techniques on a separate solution.  $\text{FeO}$  values were obtained volumetrically using potassium dichromate.

TABLE 15. LIST OF MINERAL ANALYSES DETERMINED BY  
ELECTRON MICROPROBE ANALYSIS

# INDEX TO MINERAL CHEMICAL ANALYSES

## CLINOPYROXENE

<u>Sample</u>	<u>Page No.</u>
LD3	xiii-xiv
LG4	ix-x
LG6	i-v
LG7	xi-xii
SB13	xvii
SB23	xxxii
SB27	xxxii-xxxiii
SB31	xviii
SB49	xxviii-xxx
SB55	viii-ix
SB60	xxii-xxiii
SB63	xxiii-xxvii
YG54	vi-vii
SBC1	xviii-xxi
SBC5	xv-xvii

## STILPNOMELANE

<u>Sample</u>	<u>Page No.</u>
SB55	xxxiv

## PUMPELLYITE

<u>Sample</u>	<u>Page No.</u>
SB55	xxxv
YG54	xxxv

## EPIDOTE

<u>Sample</u>	<u>Page No.</u>
SBC1	xxxvi
LD3	xxxvi

## FELDSPAR

<u>Sample</u>	<u>Page No.</u>
SB23	xxxvii
SB27	xxxvii
SBC10	xxxvii

## SPHENE

<u>Sample</u>	<u>Page No.</u>
SB63	xxxviii

## AMPHIBOLE

<u>Sample</u>	<u>Page No.</u>
LD3	xxxix-xxxx

## CHLORITE

<u>Sample</u>	<u>Page No.</u>
LD3	xxxxi-xxxxii
LG4	xxxxi
SB23	xxxxi
SB48	xxxxii
SB55	xxxxi

## PREHNITE

<u>Sample</u>	<u>Page No.</u>
YG54	xxxxiii

Intrusions

Sample	LG6	LG6	LG6	LG6	LG6
SiO <sub>2</sub>	50.59	51.76	51.91	51.59	51.96
TiO <sub>2</sub>	0.89	0.80	0.80	0.85	0.79
Al <sub>2</sub> O <sub>3</sub>	1.32	1.57	1.47	1.52	1.56
FeO*	11.77	11.78	12.40	12.05	12.51
MnO	0.42	n.d.	0.39	0.38	0.30
MgO	14.60	14.91	14.54	14.77	14.68
Cr <sub>2</sub> O <sub>3</sub>	n.a.	n.a.	n.a.	n.a.	n.a.
CaO	17.90	18.39	18.50	18.35	18.64
Na <sub>2</sub> O	0.32	n.d.	n.d.	0.34	n.d.
Total	97.81	99.21	100.01	99.85	100.44

## Recalculation on the basis of 6 oxygens

Si	1.942	1.950	1.949	1.940	1.944
Al <sup>4</sup>	0.058	0.050	0.051	0.060	0.056
Σ <sub>tet</sub>	2.000	2.000	2.000	2.000	2.000
Al <sup>6</sup>	0.002	0.020	0.014	0.007	0.013
Fe	0.378	0.372	0.390	0.379	0.392
Mg	0.836	0.838	0.814	0.829	0.819
Mn	0.014	-	0.013	0.013	0.010
Ti	0.026	0.023	0.023	0.024	0.023
Cr	-	-	-	-	-
Σ <sub>oct</sub>	1.256	1.253	1.254	1.252	1.257
Ca	0.737	0.743	0.745	0.740	0.748
Na	0.025	-	-	0.025	-
Total cations	4.018	3.996	3.999	4.017	4.005

\* = Total iron as FeO

n.a. = not analysed for

n.d. = not detected



Sample	LG6	LG6	LG6	LG6	LG6	LG6
SiO <sub>2</sub>	51.81	51.86	51.35	50.38	51.73	51.79
TiO <sub>2</sub>	0.98	0.82	0.94	1.73	0.79	0.78
Al <sub>2</sub> O <sub>3</sub>	1.67	1.88	1.99	2.63	1.59	1.74
FeO*	12.18	12.11	12.02	8.83	13.85	16.63
MnO	0.27	0.41	0.28	n.d.	0.54	0.41
MgO	14.96	15.27	15.31	13.95	14.08	14.87
Cr <sub>2</sub> O <sub>3</sub>	n.a.	n.a.	n.a.	n.a.	n.a.	n.a.
CaO	18.21	18.16	18.15	22.13	18.06	17.47
Na <sub>2</sub> O	0.40	0.50	0.32	0.37	0.34	0.00
Total	100.48	101.01	100.36	100.02	100.98	100.69
Si	1.935	1.928	1.920	1.887	1.938	1.937
Al <sup>4</sup>	0.065	0.072	0.080	0.113	0.062	0.063
Σ tet	2.000	2.000	2.000	2.000	2.000	2.000
Al <sup>6</sup>	0.008	0.011	0.008	0.004	0.008	0.014
Fe	0.381	0.377	0.376	0.277	0.434	0.427
Mg	0.833	0.847	0.853	0.779	0.787	0.829
Mn	0.009	0.013	0.009	-	0.018	0.014
Ti	0.028	0.023	0.027	0.049	0.023	0.022
Cr	-	-	-	-	-	-
Σ oct	1.259	1.271	1.273	1.109	1.270	1.306
Ca	0.729	0.724	0.727	0.888	0.725	0.700
Na	0.030	0.037	0.024	0.027	0.025	-
Total cations	4.018	4.032	4.004	4.024	4.020	4.006

\* = Total iron as FeO

n.a. = not analysed for

n.d. = not detected

Sample	LG6	LG6	LG6	LG6	LG6	LG6
SiO <sub>2</sub>	51.11	50.83	50.54	51.01	51.13	51.16
TiO <sub>2</sub>	1.18	0.97	0.92	0.94	1.21	0.88
Al <sub>2</sub> O <sub>3</sub>	1.77	2.48	2.32	2.02	2.14	1.58
FeO*	12.33	11.04	10.80	11.18	10.61	12.59
MnO	0.45	0.38	0.21	0.23	0.26	0.32
MgO	15.04	15.04	14.78	14.53	14.92	14.49
Cr <sub>2</sub> O <sub>3</sub>	n.a.	n.a.	n.a.	n.a.	n.a.	n.a.
CaO	17.21	18.43	18.97	19.00	19.30	17.79
Na <sub>2</sub> O	n.d.	n.d.	n.d.	n.d.	n.d.	n.d.
Total	99.09	99.17	98.54	98.91	99.57	98.81
Si	1.933	1.916	1.918	1.930	1.919	1.944
Al <sup>4</sup>	0.067	0.084	0.082	0.070	0.081	0.056
Σtet	2.000	2.000	2.000	2.000	2.000	2.000
Al <sup>6</sup>	0.012	0.027	0.022	0.020	0.014	0.015
Fe	0.390	0.349	0.343	0.354	0.333	0.401
Mg	0.848	0.845	0.837	0.820	0.835	0.821
Mn	0.015	0.013	0.007	0.007	0.008	0.011
Ti	0.034	0.028	0.027	0.027	0.035	0.026
Cr	-	-	-	-	-	-
Σoct	1.299	1.262	1.236	1.228	1.225	1.274
Ca	0.698	0.744	0.772	0.771	0.777	0.725
Na	-	-	-	-	-	-
Total cations	3.997	4.006	4.008	3.999	4.002	3.999

\* = Total iron as FeO  
n.a. = not analysed for  
n.d. = not detected

Sample	LG6	LG6	LG6	LG6	LG6	LG6
SiO <sub>2</sub>	51.15	51.92	51.17	50.74	50.99	50.33
TiO <sub>2</sub>	0.87	0.67	0.80	0.85	0.81	0.76
Al <sub>2</sub> O <sub>3</sub>	1.55	1.69	1.14	1.86	1.01	1.09
FeO*	12.96	10.69	14.61	11.34	14.67	15.10
MnO	0.41	0.30	0.45	0.29	0.59	0.38
MgO	14.74	16.19	14.63	14.90	13.65	13.07
Cr <sub>2</sub> O <sub>3</sub>	n.a.	n.a.	n.a.	n.a.	n.a.	n.a.
CaO	17.64	18.57	16.10	18.61	17.51	17.37
Na <sub>2</sub> O	0.39	0.31	n.d.	0.34	n.d.	n.d.
Total	99.71	100.34	98.90	98.93	99.23	98.10
Si	1.933	1.931	1.953	1.924	1.951	1.952
Al <sup>4</sup>	0.067	0.069	0.047	0.076	0.046	0.048
Σtet	2.000	2.000	2.000	2.000	1.997	2.000
Al <sup>6</sup>	0.002	0.005	0.005	0.007	-	0.002
Fe	0.410	0.333	0.467	0.360	0.470	0.490
Mg	0.831	0.898	0.833	0.842	0.779	0.756
Mn	0.013	0.009	0.015	0.009	0.019	0.013
Ti	0.025	0.019	0.024	0.025	0.024	0.023
Cr	-	-	-	-	-	-
Σoct	1.281	1.264	1.344	1.243	1.292	1.284
Ca	0.715	0.741	0.659	0.756	0.718	0.722
Na	0.029	0.023	-	0.026	-	-
Total cations	4.025	4.028	4.003	4.025	4.007	4.006

\* = Total iron as FeO  
n.a. = not analysed for  
n.d. = not detected

Sample	LG6	LG6	LG6	LG6	LG6	LG6
SiO <sub>2</sub>	49.98	50.89	51.21	51.49	51.59	51.72
TiO <sub>2</sub>	0.87	0.68	0.91	0.93	1.20	0.61
Al <sub>2</sub> O <sub>3</sub>	1.53	1.01	1.26	1.45	1.85	1.10
FeO*	11.72	16.87	13.61	12.60	12.51	15.48
MnO	0.30	0.48	0.35	0.45	0.23	0.46
MgO	14.33	12.57	14.09	14.43	14.68	13.39
Cr <sub>2</sub> O <sub>3</sub>	n.a.	n.a.	n.a.	n.a.	n.a.	n.a.
CaO	17.96	16.84	18.42	18.83	18.63	17.71
Na <sub>2</sub> O	n.d.	0.42	n.d.	n.d.	n.d.	n.d.
Total	96.69	99.76	99.85	100.18	100.69	100.47
Si	1.940	1.954	1.940	1.937	1.926	1.957
Al <sup>4</sup>	0.060	0.046	0.057	0.063	0.074	0.043
Σtet	2.000	2.000	1.997	2.000	2.000	2.000
Al <sup>6</sup>	0.010	-	-	0.001	0.007	0.007
Fe	0.381	0.542	0.432	0.397	0.391	0.490
Mg	0.829	0.720	0.796	0.809	0.817	0.756
Mn	0.011	0.016	0.012	0.015	0.007	0.015
Ti	0.026	0.020	0.026	0.027	0.034	0.018
Cr	-	-	-	-	-	-
Σoct	1.257	1.298	1.266	1.249	1.256	1.286
Ca	0.747	0.693	0.748	0.759	0.745	0.718
Na	-	0.032	-	-	-	-
Total cations	4.004	4.023	4.011	4.008	4.001	4.004

\* = Total iron as FeO  
n.a. = not analysed for  
n.d. = not detected

Sample	YG54	YG54	YG54	YG54	YG54	YG54	YG54
SiO <sub>2</sub>	51.13	51.67	51.34	50.92	50.73	51.80	51.31
TiO <sub>2</sub>	0.93	0.77	1.00	0.89	0.87	0.92	0.92
Al <sub>2</sub> O <sub>3</sub>	2.07	2.12	3.10	3.01	3.08	2.49	2.56
FeO*	8.77	9.06	8.81	9.11	9.55	8.84	8.75
MnO	0.27	n.d.	n.d.	0.35	n.d.	n.d.	n.d.
MgO	14.49	14.64	14.63	14.62	14.55	14.90	14.70
Cr <sub>2</sub> O <sub>3</sub>	n.d.	n.d.	0.21	n.d.	n.d.	0.22	n.d.
CaO	20.68	20.55	20.90	21.23	21.13	21.47	21.36
Na <sub>2</sub> O	n.d.	n.d.	n.d.	0.31	n.d.	n.d.	0.39
Total	98.34	98.81	99.99	100.44	99.91	100.64	99.99
Si	1.934	1.942	1.907	1.895	1.896	1.915	1.912
Al <sup>4</sup>	0.066	0.058	0.093	0.105	0.104	0.085	0.088
Σtet	2.000	2.000	2.000	2.000	2.000	2.000	2.000
Al <sup>6</sup>	0.026	0.036	0.043	0.027	0.032	0.024	0.025
Fe	0.278	0.285	0.274	0.283	0.298	0.273	0.273
Mg	0.817	0.820	0.810	0.811	0.811	0.822	0.816
Mn	0.008	-	-	0.011	-	-	-
Ti	0.026	0.022	0.028	0.025	0.024	0.025	0.026
Cr	-	-	0.006	-	-	0.006	-
Σoct	1.155	1.163	1.161	1.157	1.165	1.150	1.140
Ca	0.838	0.827	0.132	0.846	0.846	0.851	0.853
Na	-	-	-	0.022	-	-	0.028
Total cations	3.993	3.990	3.993	4.025	4.011	4.001	4.021

\* = Total iron as FeO

n.d. = not detected

Sample	YG54	YG54	YG54	YG54	YG54	YG54	YG54	YG54
SiO <sub>2</sub>	50.56	52.35	52.30	51.32	51.67	51.49	51.20	51.89
TiO <sub>2</sub>	1.10	0.70	0.54	0.90	1.02	1.00	1.09	0.92
Al <sub>2</sub> O <sub>3</sub>	3.03	1.34	1.46	2.82	3.14	2.92	2.66	2.41
FeO*	9.44	11.92	11.33	9.40	8.24	8.86	9.27	9.08
MnO	n.d.	0.30	0.33	n.d.	0.27	n.d.	0.40	n.d.
MgO	14.15	13.82	13.90	14.40	15.27	14.55	14.77	14.83
Cr <sub>2</sub> O <sub>3</sub>	n.d.	n.d.	n.d.	n.d.	n.d.	n.d.	n.d.	n.d.
CaO	21.32	19.25	20.28	21.13	21.03	21.14	21.12	21.04
Na <sub>2</sub> O	n.d.	n.d.	n.d.	n.d.	n.d.	n.d.	n.d.	n.d.
Total	99.60	99.68	100.14	99.97	100.64	99.96	100.51	100.17
Si	1.896	1.968	1.959	1.913	1.904	1.914	1.902	1.926
Al <sup>4</sup>	0.104	0.032	0.041	0.087	0.096	0.086	0.098	0.074
Σtet	2.000	2.000	2.000	2.000	2.000	2.000	2.000	2.000
Al <sup>6</sup>	0.030	0.027	0.024	0.037	0.040	0.042	0.019	0.031
Fe	0.296	0.375	0.355	0.293	0.254	0.276	0.288	0.282
Mg	0.791	0.775	0.776	0.800	0.839	0.806	0.818	0.820
Mn	-	0.010	0.010	-	0.008	-	0.013	-
Ti	0.031	0.020	0.015	0.025	0.028	0.028	0.031	0.026
Cr	-	-	-	-	-	-	-	-
Σoct	1.148	1.207	1.180	1.155	1.169	1.152	1.169	1.159
Ca	0.857	0.776	0.814	0.844	0.830	0.842	0.841	0.837
Na	-	-	-	-	-	-	-	-
Total cations	4.005	3.983	3.994	3.999	3.999	3.994	4.010	3.996

\* = Total iron as FeO  
n.d. = not detected

Sample	SB55	SB55	SB55	SB55	SB55	SB55	SB55	SB55
SiO <sub>2</sub>	52.21	52.13	52.03	51.49	51.92	51.78	50.30	51.76
TiO <sub>2</sub>	0.43	0.47	0.61	0.50	0.55	0.51	0.59	0.60
Al <sub>2</sub> O <sub>3</sub>	0.74	0.78	0.97	0.76	0.79	0.86	0.64	0.87
FeO*	13.81	14.33	13.84	14.18	14.80	13.92	18.10	13.91
MnO	0.53	0.61	0.56	0.39	0.43	0.48	0.59	0.51
MgO	12.65	12.30	12.64	12.21	11.94	12.60	9.77	12.24
Cr <sub>2</sub> O <sub>3</sub>	n.d.	n.d.	n.d.	n.d.	n.d.	n.d.	n.d.	n.d.
CaO	19.33	19.27	18.95	19.15	19.10	19.46	18.42	19.43
Na <sub>2</sub> O	n.d.	n.d.	n.d.	n.d.	n.d.	n.d.	n.d.	n.d.
Total	99.70	99.89	99.60	98.68	99.53	99.61	98.41	99.32
Si	1.983	1.982	1.977	1.981	1.983	1.972	1.982	1.977
Al <sup>4</sup>	0.017	0.018	0.023	0.019	0.017	0.028	0.018	0.023
Σtet	2.000	2.000	2.000	2.000	2.000	2.000	2.000	2.000
Al <sup>6</sup>	0.016	0.017	0.020	0.015	0.018	0.010	0.012	0.016
Fe	0.439	0.455	0.440	0.456	0.473	0.443	0.597	0.444
Mg	0.717	0.697	0.716	0.700	0.680	0.716	0.574	0.697
Mn	0.017	0.020	0.018	0.013	0.014	0.015	0.020	0.017
Ti	0.012	0.014	0.018	0.014	0.016	0.015	0.012	0.017
Cr	-	-	-	-	-	-	-	-
Σoct	1.201	1.203	1.212	1.198	1.201	1.189	1.195	1.191
Ca	0.787	0.785	0.772	0.789	0.782	0.794	0.778	0.795
Na	-	-	-	-	-	-	-	-
Total cations	3.988	3.988	3.984	3.987	3.983	3.983	3.973	3.986

\* = Total iron as FeO

n.d. = not detected

Sample	SB55	SB55	LG4	LG4	LG4	LG4	LG4	LG4
SiO <sub>2</sub>	50.94	51.47	52.30	52.60	52.84	51.94	51.75	51.97
TiO <sub>2</sub>	0.40	0.41	0.72	0.59	0.52	0.86	0.84	0.74
Al <sub>2</sub> O <sub>3</sub>	0.49	0.77	1.72	2.09	2.06	1.43	2.16	1.94
FeO*	17.65	15.89	8.37	6.66	7.45	10.60	9.86	7.92
MnO	0.69	0.58	n.d.	n.d.	0.31	0.37	n.d.	0.23
MgO	10.70	11.26	15.81	16.49	15.84	14.71	14.93	15.76
Cr <sub>2</sub> O <sub>3</sub>	n.d.	n.d.	n.a.	n.a.	n.a.	n.a.	n.a.	n.a.
CaO	18.52	18.89	20.98	21.96	21.54	19.82	20.46	21.09
Na <sub>2</sub> O	n.d.	n.d.	n.d.	n.d.	n.d.	n.d.	n.d.	n.d.
Total	99.39	99.27	99.90	100.39	100.56	99.83	100.00	99.65
Si	1.978	1.983	1.940	1.931	1.942	1.947	1.929	1.932
Al <sup>4</sup>	0.022	0.017	0.060	0.069	0.058	0.053	0.071	0.068
Σtet	2.000	2.000	2.000	2.000	2.000	2.000	2.000	2.000
Al <sup>6</sup>	0.001	0.018	0.015	0.021	0.031	0.010	0.024	0.017
Fe	0.573	0.512	0.260	0.205	0.229	0.332	0.307	0.246
Mg	0.619	0.647	0.874	0.902	0.868	0.822	0.830	0.873
Mn	0.023	0.019	-	-	0.010	0.012	-	0.007
Ti	0.012	0.012	0.020	0.016	0.014	0.024	0.023	0.021
Cr	-	-	-	-	-	-	-	-
Σoct	1.228	1.208	1.169	1.144	1.152	1.200	1.184	1.164
Ca	0.771	0.780	0.834	0.864	0.848	0.796	0.817	0.840
Na	-	-	-	-	-	-	-	-
Total cations	3.999	3.988	4.003	4.008	4.000	3.996	4.001	4.004

\* = Total iron as FeO

n.a. = not analysed for

n.d. = not detected



Sample	LG4	LG4	LG4	LG4	LG4	LG4	LG4
SiO <sub>2</sub>	52.60	51.64	52.58	52.83	52.15	52.28	52.49
TiO <sub>2</sub>	0.68	0.80	0.60	0.64	0.76	0.75	0.47
Al <sub>2</sub> O <sub>3</sub>	2.01	1.99	2.10	2.38	1.55	2.65	2.16
FeO*	7.27	10.18	6.80	6.93	10.25	6.98	6.64
MnO	n.d.	0.28	0.27	0.24	0.31	0.25	n.d.
MgO	16.23	14.77	16.07	16.54	14.57	16.20	16.12
Cr <sub>2</sub> O <sub>3</sub>	n.a.	n.a.	n.a.	n.a.	n.a.	n.a.	n.a.
CaO	21.63	20.53	21.85	21.57	20.34	21.34	21.45
Na <sub>2</sub> O	0.32	n.d.	n.d.	n.d.	0.34	n.d.	n.d.
Total	100.74	100.19	100.27	101.13	100.27	100.45	99.33
Si	1.930	1.927	1.935	1.926	1.945	1.919	1.943
Al <sup>4</sup>	0.070	0.073	0.065	0.074	0.055	0.081	0.057
Σtet	2.000	2.000	2.000	2.000	2.000	2.000	2.000
Al <sup>6</sup>	0.017	0.014	0.026	0.028	0.013	0.034	0.037
Fe	0.223	0.318	0.209	0.211	0.320	0.214	0.205
Mg	0.888	0.822	0.881	0.899	0.810	0.886	0.890
Mn	-	0.009	0.008	0.007	0.010	0.008	-
Ti	0.019	0.022	0.017	0.018	0.021	0.021	0.013
Cr	-	-	-	-	-	-	-
Σoct	1.147	1.185	1.141	1.163	1.174	1.163	1.145
Ca	0.850	0.821	0.861	0.842	0.813	0.840	0.851
Na	0.023	-	-	-	0.024	-	-
Total cation	4.020	4.006	4.002	4.005	4.011	4.003	3.996

\* = Total iron as FeO  
n.a. = not analysed for  
n.d. = not detected

Sample	LG4	LG7	LG7	LG7	LG7	LG7	LG7	LG7
SiO <sub>2</sub>	51.64	52.74	52.52	52.98	53.22	52.28	53.16	52.94
TiO <sub>2</sub>	0.96	0.63	0.51	0.53	0.52	0.75	0.44	0.67
Al <sub>2</sub> O <sub>3</sub>	1.80	2.02	2.12	2.07	2.02	2.97	2.06	2.17
FeO*	9.54	7.23	6.84	7.06	6.52	7.58	7.23	7.37
MnO	0.25	n.d.	n.d.	n.d.	n.d.	n.d.	n.d.	n.d.
MgO	14.63	16.12	15.91	16.61	16.14	15.97	16.38	16.25
Cr <sub>2</sub> O <sub>3</sub>	n.a.	n.d.	n.d.	n.d.	n.a.	n.a.	n.a.	n.a.
CaO	20.67	21.67	21.68	21.96	21.83	21.12	21.86	21.21
Na <sub>2</sub> O	n.d.	n.d.	n.d.	n.d.	n.d.	n.d.	n.d.	0.31
Total	99.49	100.41	99.58	101.21	100.25	100.67	101.13	100.92
Si	1.936	1.938	1.943	1.931	1.951	1.916	1.939	1.935
Al <sup>4</sup>	0.064	0.062	0.057	0.069	0.049	0.084	0.061	0.065
Σtet	2.000	2.000	2.000	2.000	2.000	2.000	2.000	2.000
Al <sup>6</sup>	0.015	0.026	0.036	0.020	0.038	0.044	0.027	0.029
Fe	0.299	0.222	0.211	0.215	0.200	0.232	0.221	0.225
Mg	0.817	0.883	0.877	0.902	0.882	0.872	0.891	0.885
Mn	0.008	-	-	-	-	-	-	-
Ti	0.027	0.018	0.014	0.014	0.014	0.021	0.012	0.019
Cr	-	-	-	-	-	-	-	-
Σoct	1.166	1.149	1.138	1.151	1.134	1.169	1.151	1.158
Ca	0.831	0.853	0.859	0.858	0.857	0.829	0.854	0.831
Na	-	-	-	-	-	-	-	-
Total cations	3.997	4.002	3.997	4.009	3.991	3.998	4.005	3.989

\* = Total iron as FeO

n.a. = not analysed for

n.d. = not detected

Sample	LG7	LG7	LG7	LG7	LG7	LG7	LG7
SiO <sub>2</sub>	52.68	52.83	51.25	53.36	53.01	53.31	52.86
TiO <sub>2</sub>	0.60	0.50	0.57	0.46	0.58	0.66	0.55
Al <sub>2</sub> O <sub>3</sub>	2.03	2.22	3.97	2.17	2.28	2.09	2.20
FeO*	7.95	7.41	13.63	6.66	6.77	7.54	7.31
MnO	0.28	0.22	0.35	n.d.	n.d.	n.d.	0.22
MgO	15.81	15.76	13.56	16.61	16.34	16.30	16.38
Cr <sub>2</sub> O <sub>3</sub>	n.a.	n.a.	n.a.	n.a.	n.a.	n.a.	n.a.
CaO	21.50	21.62	15.03	22.07	21.70	21.74	22.11
Na <sub>2</sub> O	n.d.	n.d.	n.d.	n.d.	n.d.	n.d.	n.d.
Total	100.85	100.56	97.36	101.33	100.68	101.64	101.13
Si	1.935	1.940	1.942	1.938	1.937	1.936	1.924
Al <sup>4</sup>	0.065	0.060	0.058	0.062	0.063	0.064	0.076
Σ tet	2.000	2.000	2.000	2.000	2.000	2.000	2.000
Al <sup>6</sup>	0.023	0.036	0.119	0.031	0.035	0.026	0.018
Fe	0.244	0.228	0.432	0.202	0.207	0.229	0.222
Mg	0.865	0.863	0.765	0.890	0.890	0.882	0.889
Mn	0.009	0.007	0.011	-	-	-	0.007
Ti	0.017	0.014	0.016	0.013	0.016	0.018	0.015
Cr	-	-	-	-	-	-	-
Σ oct	1.158	1.148	1.343	1.145	1.148	1.155	1.151
Ca	0.846	0.851	0.610	0.859	0.850	0.846	0.862
Na	-	-	-	-	-	-	-
Total cations	4.004	3.999	3.953	4.004	3.998	4.001	4.013

\* = Total iron as FeO

n.a. = not analysed for

n.d. = not detected

Sample	LD3	LD3	LD3	LD3	LD3	LD3	LD3
SiO <sub>2</sub>	50.54	50.64	51.86	51.55	51.64	51.35	51.68
TiO <sub>2</sub>	1.35	1.35	0.84	0.75	0.72	0.73	0.76
Al <sub>2</sub> O <sub>3</sub>	2.37	2.52	1.57	2.58	2.57	2.71	2.59
FeO*	9.24	9.58	9.19	6.82	6.69	6.95	6.97
MnO	0.23	n.d.	0.34	0.24	n.d.	0.18	n.d.
MgO	14.48	14.62	15.52	15.77	16.06	16.07	15.48
Cr <sub>2</sub> O <sub>3</sub>	n.d.	n.d.	n.d.	n.d.	n.d.	0.20	n.d.
CaO	20.79	20.98	20.55	21.79	21.77	21.78	21.88
Na <sub>2</sub> O	n.d.	n.d.	0.32	0.33	0.35	0.32	n.d.
Total	99.00	99.69	100.19	99.83	99.80	100.29	99.36
Si	1.906	1.899	1.931	1.911	1.912	1.898	1.921
Al <sup>4</sup>	0.094	0.101	0.069	0.089	0.088	0.102	0.079
Σtet	2.000	2.000	2.000	2.000	2.000	2.000	2.000
Al <sup>6</sup>	0.012	0.011	-	0.024	0.025	0.016	0.035
Fe	0.292	0.301	0.287	0.212	0.208	0.215	0.217
Mg	0.815	0.818	0.862	0.872	0.886	0.886	0.858
Mn	0.007	-	0.011	0.008	-	0.006	-
Ti	0.039	0.039	0.024	0.021	0.021	0.021	0.022
Cr	-	-	-	-	-	0.006	-
Σoct	1.165	1.169	1.184	1.137	1.140	1.150	1.132
Ca	0.841	0.843	0.820	0.866	0.864	0.863	0.872
Na	-	-	0.023	0.024	0.026	0.023	-
Total cations	4.006	4.012	4.027	4.037	4.030	4.036	4.004

\* = Total iron as FeO  
n.d. = not detected

Sample	LD3	LD3	LD3	LD3
SiO <sub>2</sub>	50.68	50.22	51.10	51.24
TiO <sub>2</sub>	1.56	1.52	1.37	1.45
Al <sub>2</sub> O <sub>3</sub>	2.80	2.65	2.76	2.80
FeO*	9.04	8.71	8.90	8.72
MnO	0.19	n.d.	n.d.	n.d.
MgO	14.78	14.67	14.95	15.02
Cr <sub>2</sub> O <sub>3</sub>	n.d.	0.20	n.d.	n.d.
CaO	21.28	21.24	21.30	21.21
Na <sub>2</sub> O	0.30	n.d.	0.42	0.44
Total	100.63	99.21	100.80	101.08
Si	1.883	1.889	1.892	1.893
Al <sup>4</sup>	0.117	0.111	0.108	0.107
Σtet	2.000	2.000	2.000	2.000
Al <sup>6</sup>	0.006	0.007	0.013	0.016
Fe	0.281	0.274	0.276	0.270
Mg	0.819	0.823	0.825	0.827
Mn	0.006	-	-	-
Ti	0.044	0.044	0.039	0.041
Cr	-	0.006	-	-
Σoct	1.156	1.154	1.153	1.144
Ca	0.848	0.857	0.845	0.840
Na	0.022	-	0.031	0.032
Total cations	4.026	4.011	4.029	4.016

\* = Total iron as FeO

n.d. = not detected

Lavas

Sample	SBC5	SBC5	SBC5	SBC5	SBC5	SBC5	SBC5	SBC5
SiO <sub>2</sub>	49.17	48.96	49.27	50.07	49.34	49.60	48.53	50.18
TiO <sub>2</sub>	1.71	1.84	1.57	1.59	1.83	1.52	1.69	1.82
Al <sub>2</sub> O <sub>3</sub>	4.41	4.66	4.90	3.97	4.94	4.27	5.07	3.91
FeO*	10.88	12.26	10.06	10.61	10.89	11.92	15.89	12.58
MnO	0.34	n.d.	n.d.	0.22	0.39	0.36	0.54	0.49
MgO	14.02	13.32	13.99	15.70	14.90	14.09	11.07	15.30
Cr <sub>2</sub> O <sub>3</sub>	n.d.	n.d.	n.d.	n.d.	n.d.	n.d.	n.d.	n.d.
CaO	19.50	19.25	19.85	17.28	17.50	18.48	16.13	16.33
Na <sub>2</sub> O	n.d.	0.39	0.30	n.d.	0.34	n.d.	0.45	n.d.
Total	100.03	100.68	99.94	99.44	100.13	100.24	99.37	100.61
Si	1.845	1.836	1.843	1.871	1.840	1.859	1.860	1.867
Al <sup>4</sup>	0.155	0.164	0.157	0.129	0.160	0.141	0.140	0.133
Σ tet	2.000	2.000	2.000	2.000	2.000	2.000	2.000	2.000
Al <sup>6</sup>	0.040	0.042	0.059	0.046	0.057	0.048	0.089	0.039
Fe	0.341	0.385	0.315	0.332	0.339	0.374	0.509	0.391
Mg	0.784	0.744	0.780	0.875	0.828	0.787	0.632	0.848
Mn	0.011	-	-	0.007	0.012	0.012	0.017	0.016
Ti	0.048	0.052	0.044	0.045	0.051	0.043	0.049	0.051
Cr	-	-	-	-	-	-	-	-
Σ oct	1.224	1.223	1.198	1.305	1.287	1.264	1.296	1.345
Ca	0.784	0.773	0.796	0.692	0.699	0.742	0.663	0.651
Na	-	0.029	0.021	-	0.025	-	0.034	-
Total cations	4.008	4.025	4.015	3.997	4.011	4.006	3.993	3.996

\* = Total iron as FeO

n.d. = not detected

Sample	SBC5	SBC5	SBC5	SBC5	SBC5	SBC5	SBC5	SBC5
SiO <sub>2</sub>	48.30	48.56	50.31	49.37	48.97	50.66	50.91	52.07
TiO <sub>2</sub>	2.41	1.99	1.49	1.63	1.55	1.11	1.03	1.05
Al <sub>2</sub> O <sub>3</sub>	4.57	5.40	3.92	4.32	4.76	3.65	3.19	3.17
FeO*	13.72	11.42	11.06	11.96	10.14	9.86	10.00	11.19
MnO	0.31	0.36	0.22	0.44	0.25	0.29	0.35	0.41
MgO	12.76	14.94	15.17	12.93	13.76	14.31	15.78	17.16
Cr <sub>2</sub> O <sub>3</sub>	n.d.	n.d.	0.21	n.d.	n.d.	n.d.	n.d.	n.d.
CaO	17.42	16.95	17.42	19.43	20.35	20.07	16.47	15.54
Na <sub>2</sub> O	n.d.	n.d.	n.d.	0.33	0.31	n.d.	n.d.	n.d.
Total	99.49	99.62	99.80	100.41	100.09	99.95	97.73	100.59
Si	1.837	1.821	1.878	1.856	1.837	1.891	1.913	1.914
Al <sup>4</sup>	0.163	0.179	0.122	0.144	0.163	0.109	0.087	0.086
Σtet	2.000	2.000	2.000	2.000	2.000	2.000	2.000	2.000
Al <sup>6</sup>	0.042	0.060	0.050	0.047	0.047	0.052	0.054	0.051
Fe	0.436	0.358	0.345	0.376	0.318	0.308	0.346	0.344
Mg	0.723	0.836	0.844	0.725	0.769	0.796	0.884	0.940
Mn	0.010	0.011	0.007	0.014	0.008	0.009	0.011	0.013
Ti	0.069	0.056	0.042	0.046	0.044	0.031	0.029	0.029
Cr	-	-	0.006	-	-	-	-	-
Σoct	1.280	1.321	1.294	1.208	1.186	1.196	1.324	1.377
Ca	0.710	0.681	0.697	0.783	0.818	0.803	0.663	0.612
Na	-	-	-	0.024	0.023	-	-	-
Total cations	3.990	4.002	3.991	4.015	4.027	3.999	3.987	3.989

\* = Total iron as FeO

n.d. = not detected

Sample	SBC5	SBC5	SBC5	SBC5	SB13	SB13	SB13
SiO <sub>2</sub>	50.84	50.37	49.29	49.00	50.16	49.85	51.33
TiO <sub>2</sub>	1.31	1.54	1.66	1.42	0.82	1.19	0.94
Al <sub>2</sub> O <sub>3</sub>	3.49	3.99	3.48	3.42	2.03	2.19	1.89
FeO*	10.43	9.91	10.52	10.15	11.69	11.53	13.28
MnO	0.25	n.d.	0.22	0.37	0.39	0.46	0.45
MgO	15.07	14.85	13.56	14.15	14.29	15.08	15.11
Cr <sub>2</sub> O <sub>3</sub>	n.d.	n.d.	n.d.	n.d.	n.d.	0.26	n.d.
CaO	19.76	19.73	19.35	19.02	18.61	17.61	15.98
Na <sub>2</sub> O	0.42	0.43	0.47	n.d.	n.d.	n.d.	n.d.
Total	101.57	100.82	98.55	97.53	97.99	98.17	98.98
Si	1.874	1.865	1.877	1.880	1.924	1.905	1.943
Al <sup>4</sup>	0.136	0.135	0.123	0.120	0.076	0.095	0.057
Σtet	2.000	2.000	2.000	2.000	2.000	2.000	2.000
Al <sup>6</sup>	0.016	0.040	0.034	0.035	0.016	0.004	0.028
Fe	0.322	0.307	0.335	0.326	0.375	0.369	0.421
Mg	0.829	0.820	0.770	0.810	0.817	0.859	0.853
Mn	0.008	-	0.007	0.012	0.013	0.015	0.015
Ti	0.037	0.043	0.048	0.041	0.024	0.035	0.027
Cr	-	-	-	-	-	0.008	-
Σoct	1.212	1.210	1.194	1.224	1.245	1.290	1.344
Ca	0.781	0.783	0.790	0.782	0.765	0.721	0.649
Na	0.030	0.031	0.035	-	-	-	-
Total cations	4.023	4.024	4.019	4.006	4.010	4.011	3.993

\* = Total iron as FeO

n.d. = not detected



Sample	SB31	SB31	SB31	SB31	SB31	SBC1	SBC1	SBC1
SiO <sub>2</sub>	49.46	49.34	49.84	49.41	49.99	49.60	48.73	50.20
TiO <sub>2</sub>	1.54	1.93	1.10	1.68	1.85	0.51	1.86	1.19
Al <sub>2</sub> O <sub>3</sub>	3.61	4.37	3.35	3.51	2.97	5.87	5.62	5.25
FeO*	10.17	12.21	11.35	12.01	11.66	12.66	8.58	10.75
MnO	n.d.	0.24	0.26	0.24	0.28	0.55	n.d.	0.33
MgO	14.63	13.50	14.10	15.88	14.82	14.27	14.20	15.93
Cr <sub>2</sub> O <sub>3</sub>	n.a.	n.a.	n.a.	n.a.	n.a.	n.d.	n.d.	n.d.
CaO	19.52	20.06	19.63	16.64	18.73	14.34	20.00	15.53
Na <sub>2</sub> O	n.d.	0.34	n.d.	0.29	n.d.	n.d.	n.d.	n.d.
Total	98.93	101.99	99.63	99.66	100.30	97.80	98.99	99.18
Si	1.868	1.831	1.881	1.858	1.873	1.883	1.828	1.869
Al <sup>4</sup>	0.132	0.169	0.119	0.142	0.127	0.117	0.172	0.131
Σtet	2.000	2.000	2.000	2.000	2.000	2.000	2.000	2.000
Al <sup>6</sup>	0.029	0.022	0.030	0.013	0.004	0.146	0.077	0.099
Fe	0.321	0.379	0.358	0.378	0.365	0.402	0.269	0.335
Mg	0.824	0.747	0.793	0.890	0.828	0.807	0.794	0.884
Mn	-	0.007	0.008	0.008	0.009	0.018	n.d.	0.010
Ti	0.044	0.054	0.031	0.048	0.052	0.015	0.052	0.033
Cr	-	-	-	-	-	-	-	-
Σoct	1.218	1.209	1.220	1.337	1.258	1.388	1.192	1.361
Ca	0.790	0.798	0.794	0.670	0.752	0.583	0.804	0.620
Na	-	0.024	-	0.021	-	-	-	-
Total cations	4.008	4.031	4.014	4.028	4.010	3.971	3.996	3.981

\* = Total iron as FeO

n.a. = not analysed for

n.d. = not detected

Sample	SBC1	SBC1	SBC1	SBC1	SBC1	SBC1	SBC1	SBC1
SiO <sub>2</sub>	48.69	49.94	51.05	48.75	50.07	49.76	49.54	47.75
TiO <sub>2</sub>	1.87	1.11	0.84	1.88	1.10	1.68	1.05	1.83
Al <sub>2</sub> O <sub>3</sub>	5.77	4.44	2.55	6.06	4.75	4.72	3.22	5.58
FeO*	9.94	10.44	17.12	10.28	9.91	8.97	13.11	10.69
MnO	n.d.	n.d.	0.50	0.34	n.d.	0.28	0.36	n.d.
MgO	14.65	14.89	12.26	14.73	15.13	14.84	14.34	13.42
Cr <sub>2</sub> O <sub>3</sub>	0.21	n.d.	n.d.	n.d.	n.d.	0.27	n.d.	n.d.
CaO	18.14	18.41	16.52	16.92	18.79	19.14	16.09	19.96
Na <sub>2</sub> O	n.d.	n.d.	0.30	n.d.	n.d.	n.d.	n.d.	0.37
Total	99.27	99.23	101.14	98.96	99.75	99.56	100.71	99.60
Si	1.823	1.872	1.928	1.828	1.864	1.854	1.903	1.804
Al <sup>4</sup>	0.177	0.128	0.072	0.172	0.136	0.146	0.097	0.196
Σtet	2.000	2.000	2.000	2.000	2.000	2.000	2.000	2.000
Al <sup>6</sup>	0.078	0.068	0.041	0.096	0.072	0.061	0.049	0.053
Fe	0.311	0.327	0.541	0.322	0.309	0.280	0.421	0.338
Mg	0.818	0.832	0.690	0.823	0.839	0.824	0.821	0.756
Mn	-	-	0.016	0.011	-	0.009	0.012	-
Ti	0.053	0.031	0.024	0.053	0.031	0.047	0.030	0.052
Cr	0.006	-	-	-	-	0.008	-	-
Σoct	1.266	1.258	1.312	1.305	1.251	1.229	1.333	1.199
Ca	0.728	0.739	0.668	0.680	0.750	0.764	0.662	0.808
Na	-	-	0.022	-	-	-	-	0.027
Total cations	3.994	3.997	4.002	3.985	4.001	3.993	3.995	4.034

\* = Total iron as FeO

n.d. = not detected

Sample	SBC1	SBC1	SBC1	SBC1	SBC1	SBC1	SBC1	SBC1
SiO <sub>2</sub>	48.83	47.86	47.69	47.15	48.83	49.06	49.47	48.71
TiO <sub>2</sub>	1.05	2.06	2.24	2.18	1.76	1.58	1.53	1.99
Al <sub>2</sub> O <sub>3</sub>	3.91	5.64	4.98	6.49	6.84	5.29	5.30	5.98
FeO*	11.51	10.25	11.07	9.68	11.64	10.57	9.22	9.35
MnO	n.d.	0.29	0.26	0.29	0.30	0.25	n.d.	n.d.
MgO	12.16	12.66	11.06	12.71	10.39	14.14	13.92	13.92
Cr <sub>2</sub> O <sub>3</sub>	0.24	0.23	n.d.	n.d.	n.d.	n.d.	0.25	n.d.
CaO	20.69	20.17	20.48	20.75	18.17	19.04	19.76	19.30
Na <sub>2</sub> O	n.d.	n.d.	0.31	n.d.	1.05	n.d.	n.d.	n.d.
Total	98.39	99.16	98.09	99.25	98.98	99.93	99.45	99.25
Si	1.874	1.813	1.837	1.784	1.850	1.836	1.849	1.824
Al <sup>4</sup>	0.126	0.187	0.163	0.216	0.150	0.164	0.151	0.176
Σtet	2.000	2.000	2.000	2.000	2.000	2.000	2.000	2.000
Al <sup>6</sup>	0.051	0.065	0.063	0.073	0.155	0.069	0.082	0.088
Fe	0.369	0.325	0.356	0.306	0.369	0.331	0.288	0.293
Mg	0.696	0.715	0.635	0.717	0.587	0.788	0.775	0.777
Mn	-	0.009	0.008	0.009	0.010	0.008	-	-
Ti	0.030	0.059	0.065	0.062	0.050	0.044	0.043	0.056
Cr	0.007	0.007	-	-	-	-	0.007	-
Σoct	1.103	1.180	1.127	1.167	1.171	1.240	1.195	1.214
Ca	0.851	0.819	0.845	0.841	0.738	0.763	0.791	0.774
Na	-	-	0.023	-	0.077	-	-	-
Σ cations	3.954	3.999	3.995	4.008	3.986	4.003	3.986	3.988

\* = Total iron as FeO

n.d. = not detected

Sample	SBC1	SBC1	SBC1	SBC1	SBC1	SBC1	SBC1	SBC1
SiO <sub>2</sub>	49.02	49.47	49.58	48.91	49.41	50.25	49.54	48.93
TiO <sub>2</sub>	1.90	1.14	1.93	1.72	1.41	1.50	1.53	1.53
Al <sub>2</sub> O <sub>3</sub>	5.32	3.93	4.98	4.72	4.25	3.93	5.05	4.87
FeO*	10.17	10.89	10.00	9.77	10.91	10.99	9.59	11.08
MnO	n.d.	0.42	0.30	0.33	0.35	0.26	0.30	0.31
MgO	14.91	12.81	14.18	13.79	13.37	13.70	14.12	13.89
Cr <sub>2</sub> O <sub>3</sub>	0.21	0.23	n.d.	n.d.	n.d.	n.d.	n.d.	n.d.
CaO	17.50	20.08	18.89	18.84	19.30	19.46	19.42	18.37
Na <sub>2</sub> O	n.d.	n.d.	n.d.	n.d.	n.d.	n.d.	n.d.	n.d.
Total	99.03	98.97	99.46	98.08	99.00	100.09	99.55	98.98
Si	1.838	1.879	1.849	1.858	1.870	1.880	1.853	1.850
Al <sup>4</sup>	0.162	0.121	0.151	0.142	0.130	0.120	0.147	0.150
Σtet	2.000	2.000	2.000	2.000	2.000	2.000	2.000	2.000
Al <sup>6</sup>	0.073	0.055	0.068	0.069	0.060	0.053	0.075	0.067
Fe	0.319	0.346	0.312	0.311	0.345	0.344	0.300	0.350
Mg	0.833	0.725	0.788	0.781	0.755	0.764	0.787	0.788
Mn	-	0.013	0.009	0.010	0.011	0.008	0.009	0.010
Ti	0.054	0.033	0.054	0.049	0.040	0.042	0.043	0.044
Cr	0.006	0.007	-	-	-	-	-	-
Σoct	1.285	1.179	1.231	1.220	1.211	1.211	1.214	1.259
Ca	0.703	0.817	0.755	0.767	0.783	0.780	0.778	0.744
Na	-	-	-	-	-	-	-	-
Σ cations	3.988	3.996	3.986	3.987	3.994	3.991	3.992	4.003

\* = Total iron as FeO

n.d. = not detected

Sample	SB60	SB60	SB60	SB60	SB60	SB60	SB60	SB60
SiO <sub>2</sub>	48.46	47.47	46.96	45.40	48.94	48.11	47.46	49.96
TiO <sub>2</sub>	2.64	2.33	2.72	3.26	1.93	2.20	2.84	1.83
Al <sub>2</sub> O <sub>3</sub>	5.77	5.69	5.86	6.88	4.32	5.17	5.28	4.42
FeO*	11.56	11.25	11.74	10.86	10.25	11.32	10.66	9.98
MnO	0.27	n.d.	0.28	n.d.	0.34	0.32	0.28	n.d.
MgO	10.48	11.23	11.22	10.99	12.72	11.79	11.84	13.36
Cr <sub>2</sub> O <sub>3</sub>	n.d.	0.22	0.21	n.d.	0.24	0.32	0.25	0.23
CaO	20.87	21.67	20.96	21.24	21.40	21.03	21.78	21.93
Na <sub>2</sub> O	n.d.	n.d.	n.d.	n.d.	0.30	0.34	n.d.	n.d.
Total	100.05	99.86	100.95	98.63	100.44	100.60	100.39	101.71
Si	1.829	1.801	1.785	1.745	1.838	1.813	1.791	1.845
Al <sup>4</sup>	0.171	0.199	0.215	0.255	0.162	0.187	0.209	0.155
Σtet	2.000	2.000	2.000	2.000	2.000	2.000	2.000	2.000
Al <sup>6</sup>	0.084	0.055	0.048	0.057	0.029	0.043	0.026	0.037
Fe	0.365	0.357	0.373	0.349	0.322	0.357	0.336	0.308
Mg	0.589	0.635	0.635	0.630	0.712	0.662	0.666	0.735
Mn	0.009	-	0.009	-	0.011	0.010	0.009	-
Ti	0.075	0.067	0.078	0.094	0.055	0.062	0.081	0.051
Cr	-	0.006	0.006	-	0.007	0.009	0.007	0.007
Σoct	1.122	1.120	1.149	1.130	1.136	1.143	1.125	1.138
Ca	0.844	0.881	0.854	0.875	0.861	0.849	0.881	0.867
Na	-	-	-	-	0.022	0.025	-	-
Σ cations	3.964	4.001	4.003	4.005	4.019	4.017	4.006	4.005

\* = Total iron as FeO

n.d. = not detected

Sample	SB60	SB60	SB60	SB63	SB63	SB63	SB63	SB63
SiO <sub>2</sub>	47.51	47.00	47.83	47.28	45.05	45.41	46.39	46.17
TiO <sub>2</sub>	2.48	2.85	2.96	2.50	3.32	3.15	2.62	3.15
Al <sub>2</sub> O <sub>3</sub>	5.77	5.77	3.71	5.76	5.57	5.71	5.33	5.94
FeO*	11.29	11.93	15.25	9.79	14.40	13.92	13.39	12.81
MnO	0.22	0.27	0.43	n.d.	0.33	0.39	0.31	n.d.
MgO	11.46	11.38	10.32	12.14	9.03	9.21	10.09	10.20
Cr <sub>2</sub> O <sub>3</sub>	0.21	0.21	n.d.	0.34	n.d.	n.d.	n.d.	n.d.
CaO	21.99	21.73	19.35	21.45	20.73	21.26	21.06	21.95
Na <sub>2</sub> O	0.35	n.d.	n.d.	n.d.	0.37	0.30	0.39	0.31
Total	101.28	101.14	99.85	99.26	99.80	99.35	99.58	100.53
Si	1.784	1.771	1.841	1.793	1.763	1.764	1.789	1.761
Al <sup>4</sup>	0.216	0.229	0.159	0.217	0.237	0.236	0.211	0.239
Σtet	2.000	2.000	2.000	2.000	2.000	2.000	2.000	2.000
Al <sup>6</sup>	0.039	0.027	0.009	0.041	0.020	0.026	0.031	0.028
Fe	0.354	0.376	0.491	0.311	0.471	0.452	0.432	0.409
Mg	0.642	0.639	0.592	0.686	0.527	0.533	0.580	0.580
Mn	0.007	0.009	0.014	-	0.011	0.013	0.010	-
Ti	0.070	0.081	0.086	0.071	0.098	0.092	0.076	0.090
Cr	0.006	0.006	-	0.010	-	-	-	-
Σoct	1.118	1.138	1.192	1.119	1.127	1.116	1.129	1.107
Ca	0.885	0.877	0.798	0.872	0.869	0.885	0.870	0.897
Na	0.025	-	-	-	0.028	0.023	0.029	0.023
Σ cations	4.028	4.015	3.990	3.991	4.024	4.024	4.028	4.027

\* = Total iron as FeO

n.d. = not detected

Sample	SB63	SB63	SB63	SB63	SB63	SB63	SB63	SB63
SiO <sub>2</sub>	46.55	45.28	44.61	48.03	46.82	46.82	46.20	46.72
TiO <sub>2</sub>	2.83	3.66	4.28	2.08	3.33	2.77	3.32	2.65
Al <sub>2</sub> O <sub>3</sub>	6.08	6.01	6.66	5.95	6.44	5.68	5.60	6.27
FeO*	11.73	12.61	13.35	11.31	11.80	12.72	14.74	11.33
MnO	n.d.	0.24	0.33	0.31	0.34	0.25	0.23	0.23
MgO	10.53	9.84	9.62	9.20	9.74	10.38	9.18	11.29
Cr <sub>2</sub> O <sub>3</sub>	0.24	n.d.	n.d.	n.d.	n.d.	n.d.	n.d.	n.d.
CaO	21.90	21.47	21.26	21.20	21.34	22.27	20.94	21.86
Na <sub>2</sub> O	0.31	0.43	0.37	1.33	0.32	0.37	0.36	0.41
Total	100.27	99.54	100.48	99.41	100.13	101.26	100.57	100.76
Si	1.771	1.747	1.712	1.834	1.777	1.774	1.774	1.765
Al <sup>4</sup>	0.229	0.253	0.288	0.166	0.223	0.226	0.226	0.235
Σtet	2.000	2.000	2.000	2.000	2.000	2.000	2.000	2.000
Al <sup>6</sup>	0.044	0.020	0.013	0.102	0.065	0.028	0.027	0.044
Fe	0.373	0.407	0.428	0.361	0.374	0.403	0.473	0.358
Mg	0.598	0.566	0.550	0.523	0.551	0.586	0.525	0.635
Mn	-	0.008	0.011	0.010	0.011	0.008	0.008	0.007
Ti	0.081	0.106	0.124	0.060	0.095	0.079	0.096	0.075
Cr	0.007	-	-	-	-	-	-	-
Σoct	1.103	1.107	1.126	1.056	1.096	1.104	1.129	1.119
Ca	0.893	0.887	0.874	0.867	0.868	0.904	0.862	0.885
Na	0.023	0.032	0.027	0.098	0.023	0.027	0.027	0.030
Σ cations	4.019	4.026	4.027	4.021	3.987	4.035	4.018	4.034

\* = Total iron as FeO

n.d. = not detected

Sample	SB63	SB63	SB63	SB63	SB63	SB63	SB63	SB63
SiO <sub>2</sub>	46.60	47.05	46.50	46.61	46.72	47.03	46.44	48.23
TiO <sub>2</sub>	2.68	3.18	3.28	2.92	2.88	2.99	3.10	2.41
Al <sub>2</sub> O <sub>3</sub>	6.10	4.28	4.84	5.13	5.75	5.92	6.06	3.49
FeO*	11.50	15.44	13.49	12.51	11.52	11.77	11.54	13.33
MnO	0.31	0.31	0.44	n.d.	0.23	n.d.	n.d.	0.36
MgO	10.77	8.99	9.61	10.05	10.74	11.06	10.79	11.46
Cr <sub>2</sub> O <sub>3</sub>	n.d.	0.21	0.29	n.d.	n.d.	n.d.	n.d.	n.d.
CaO	22.09	20.83	21.55	22.00	22.09	22.21	22.14	21.04
Na <sub>2</sub> O	n.d.	0.30	0.36	n.d.	0.33	0.38	n.d.	0.35
Total	100.05	100.59	100.36	99.22	100.23	101.36	100.07	100.67
Si	1.774	1.811	1.785	1.796	1.777	1.769	1.767	1.835
Al <sup>4</sup>	0.226	0.189	0.215	0.204	0.223	0.231	0.233	0.157
Σtet	2.000	2.000	2.000	2.000	2.000	2.000	2.000	1.992
Al <sup>6</sup>	0.048	0.005	0.004	0.029	0.035	0.031	0.039	-
Fe	0.366	0.497	0.433	0.403	0.366	0.370	0.367	0.424
Mg	0.611	0.516	0.550	0.577	0.609	0.620	0.612	0.650
Mn	0.010	0.010	0.014	-	0.007	-	-	0.012
Ti	0.077	0.092	0.095	0.085	0.082	0.085	0.089	0.069
Cr	-	0.006	0.009	-	-	-	-	-
Σoct	1.112	1.126	1.105	1.094	1.099	1.106	1.107	1.155
Ca	0.901	0.859	0.887	0.908	0.900	0.895	0.902	0.858
Na	-	0.022	0.027	-	0.025	0.028	-	0.025
Σ cations	4.013	4.007	4.019	4.002	4.024	4.029	4.009	4.030

\* = Total iron as FeO

n.d. = not detected



Sample	SB63	SB63	SB63	SB63	SB63	SB63	SB63	SB63
SiO <sub>2</sub>	47.47	46.13	46.24	46.71	45.62	44.41	46.02	45.71
TiO <sub>2</sub>	2.47	3.54	3.65	3.20	3.85	3.93	2.73	3.14
Al <sub>2</sub> O <sub>3</sub>	5.10	4.53	5.27	4.90	5.43	5.91	7.88	7.70
FeO*	10.48	14.63	14.55	13.55	13.41	13.89	10.08	10.06
MnO	n.d.	0.32	n.d.	0.27	0.26	0.25	n.d.	n.d.
MgO	11.66	10.15	10.12	10.48	10.18	9.87	11.45	11.55
Cr <sub>2</sub> O <sub>3</sub>	0.52	n.a.	n.a.	n.a.	n.a.	n.a.	n.a.	n.a.
CaO	21.85	20.61	20.33	21.26	21.46	20.89	22.16	21.75
Na <sub>2</sub> O	n.d.	0.42	0.36	0.32	0.35	0.35	n.d.	n.d.
Total	99.55	100.33	100.52	100.69	100.56	100.00	100.32	99.91
Si	1.804	1.778	1.771	1.783	1.749	1.726	1.734	1.729
Al <sup>4</sup>	0.196	0.206	0.229	0.217	0.246	0.271	0.266	0.271
Σtet	2.000	1.984	2.000	2.000	1.995	1.997	2.000	2.000
Al <sup>6</sup>	0.033	-	0.009	0.004	-	-	0.084	0.073
Fe	0.333	0.472	0.467	0.433	0.430	0.452	0.318	0.319
Mg	0.661	0.583	0.578	0.597	0.582	0.572	0.643	0.652
Mn	-	0.011	-	0.009	0.008	0.008	-	-
Ti	0.071	0.103	0.106	0.092	0.111	0.115	0.077	0.089
Cr	0.016	-	-	-	-	-	-	-
Σoct	1.114	1.169	1.160	1.135	1.131	1.147	1.122	1.133
Ca	0.890	0.851	0.835	0.870	0.882	0.870	0.895	0.882
Na	-	0.032	0.027	0.024	0.027	0.027	-	-
Σ cations	4.004	4.036	4.022	4.029	4.035	4.041	4.017	4.015

\* = Total iron as FeO

n.a. = not analysed for

n.d. = not detected

Sample	SB63	SB63	SB63	SB63
SiO <sub>2</sub>	45.75	45.95	45.71	45.69
TiO <sub>2</sub>	3.00	3.08	3.66	3.38
Al <sub>2</sub> O <sub>3</sub>	7.11	6.92	5.53	5.14
FeO*	9.91	11.66	11.47	13.18
MnO	n.d.	0.34	0.21	0.26
MgO	11.99	10.99	10.76	10.31
Cr <sub>2</sub> O <sub>3</sub>	n.a.	n.a.	n.a.	n.a.
CaO	21.65	21.40	21.75	21.50
Na <sub>2</sub> O	0.34	n.d.	n.d.	0.33
Total	99.75	100.26	99.09	99.79
Si	1.735	1.744	1.761	1.763
Al <sup>4</sup>	0.265	0.256	0.239	0.234
Σtet	2.000	2.000	2.000	1.997
Al <sup>6</sup>	0.053	0.054	0.012	-
Fe	0.315	0.371	0.370	0.426
Mg	0.678	0.622	0.618	0.594
Mn	-	0.011	0.007	0.008
Ti	0.086	0.088	0.107	0.098
Cr	-	-	-	-
Σoct	1.132	1.146	1.114	1.126
Ca	0.880	0.870	0.898	0.889
Na	0.025	-	-	0.025
Σ cations	4.037	4.016	4.012	4.037

\* = Total iron as FeO

n.a. = not analysed for

n.d. = not detected

Sample	SB49	SB49	SB49	SB49	SB49	SB49	SB49	SB49
SiO <sub>2</sub>	48.21	48.91	49.17	51.64	48.29	46.37	48.25	46.37
TiO <sub>2</sub>	2.70	2.08	1.86	1.53	2.60	3.20	2.47	3.31
Al <sub>2</sub> O <sub>3</sub>	3.43	3.13	2.93	3.36	3.25	4.82	2.44	4.86
FeO*	13.94	13.45	13.40	13.00	14.66	12.18	17.04	12.55
MnO	0.35	0.41	0.25	0.22	0.41	0.26	0.41	n.d.
MgO	11.56	11.83	12.26	11.85	11.31	10.81	10.10	10.48
Cr <sub>2</sub> O <sub>3</sub>	n.a.	n.a.	n.a.	n.a.	n.a.	n.a.	n.a.	n.a.
CaO	19.85	19.98	19.47	16.60	19.17	21.39	19.44	21.44
Na <sub>2</sub> O	0.42	0.32	0.31	0.33	n.d.	0.40	0.35	n.d.
Total	100.46	100.11	99.75	98.53	99.69	99.43	100.50	99.01
Si	1.838	1.865	1.877	1.957	1.855	1.785	1.864	1.791
Al <sup>4</sup>	0.155	0.135	0.123	0.043	0.145	0.215	0.111	0.219
Σtet	1.993	2.000	2.000	2.000	2.000	2.000	1.975	2.000
Al <sup>6</sup>	-	0.006	0.009	0.108	0.003	0.004	-	0.003
Fe	0.445	0.429	0.428	0.413	0.471	0.392	0.551	0.406
Mg	0.657	0.673	0.698	0.670	0.648	0.621	0.582	0.604
Mn	0.012	0.014	0.008	0.007	0.014	0.009	0.014	-
Ti	0.077	0.060	0.054	0.044	0.075	0.093	0.072	0.096
Cr	-	-	-	-	-	-	-	-
Σoct	1.191	1.182	1.197	1.242	1.211	1.119	1.219	1.109
Ca	0.811	0.816	0.797	0.674	0.789	0.883	0.805	0.887
Na	0.031	0.024	0.024	0.025	-	0.030	0.027	-
Σ cations	4.026	4.022	4.018	3.941	4.000	4.032	4.026	3.996

\* = Total iron as FeO

n.a. = not analysed for

n.d. = not detected

Sample	SB49	SB49	SB49	SB49	SB49	SB49	SB49	SB49
SiO <sub>2</sub>	47.61	46.51	46.88	47.87	47.11	49.53	49.05	49.38
TiO <sub>2</sub>	2.77	3.00	2.90	2.51	2.68	1.85	1.87	1.87
Al <sub>2</sub> O <sub>3</sub>	4.64	4.83	4.63	4.24	3.60	3.37	3.97	2.78
FeO*	12.16	11.93	11.94	12.13	15.69	11.90	11.91	13.18
MnO	0.20	0.22	0.34	0.29	0.34	0.27	0.31	0.28
MgO	10.94	10.70	10.98	11.96	10.73	12.62	12.40	11.67
Cr <sub>2</sub> O <sub>3</sub>	n.a.	n.a.	n.a.	n.a.	n.a.	n.a.	n.a.	n.a.
CaO	21.61	21.27	21.50	20.16	18.54	20.50	19.83	20.04
Na <sub>2</sub> O	0.39	0.33	n.d.	0.31	0.37	0.33	0.45	0.33
Total	100.32	98.89	99.17	99.47	99.06	100.37	99.79	99.53
Si	1.811	1.797	1.804	1.828	1.833	1.869	1.859	1.888
Al <sup>4</sup>	0.189	0.203	0.196	0.172	0.166	0.131	0.141	0.112
Σtet	2.000	2.000	2.000	2.000	1.999	2.000	2.000	2.000
Al <sup>6</sup>	0.019	0.017	0.014	0.019	-	0.019	0.037	0.014
Fe	0.387	0.386	0.385	0.388	0.511	0.376	0.378	0.422
Mg	0.621	0.617	0.630	0.681	0.622	0.710	0.701	0.665
Mn	0.006	0.007	0.012	0.009	0.012	0.009	0.011	0.009
Ti	0.079	0.087	0.084	0.072	0.079	0.053	0.054	0.054
Cr	-	-	-	-	-	-	-	-
Σoct	1.112	1.114	1.125	1.169	1.224	1.167	1.181	1.164
Ca	0.881	0.881	0.886	0.825	0.773	0.829	0.806	0.821
Na	0.029	0.026	-	0.023	0.029	0.025	0.034	0.025
Σ cations	4.022	4.021	4.011	4.017	4.025	4.021	4.021	4.010

\* = Total iron as FeO

n.a. = not analysed for

n.d. = not detected

Sample	SB49	SB49	SB49	SB49	SB49
SiO <sub>2</sub>	48.77	46.88	47.91	45.44	48.96
TiO <sub>2</sub>	1.90	2.54	2.65	1.38	2.38
Al <sub>2</sub> O <sub>3</sub>	3.39	4.30	3.41	3.23	3.10
FeO*	12.45	12.31	14.68	18.83	16.66
MnO	0.28	0.21	0.31	0.29	0.30
MgO	12.46	11.44	11.04	7.87	10.28
Cr <sub>2</sub> O <sub>3</sub>	n.a	n.a.	n.a.	n.a.	n.a.
CaO	20.47	20.94	19.58	17.68	18.91
Na <sub>2</sub> O	n.d.	n.d.	0.35	1.23	0.60
Total	99.72	99.62	99.93	95.95	99.49
Si	1.853	1.813	1.841	1.859	1.867
Al <sup>4</sup>	0.147	0.187	0.155	0.141	0.133
Σtet	2.000	2.000	1.996	2.000	2.000
Al <sup>6</sup>	0.005	0.010	-	0.015	0.007
Fe	0.397	0.399	0.472	0.645	0.532
Mg	0.708	0.660	0.633	0.481	0.585
Mn	0.009	0.007	0.011	0.010	0.010
Ti	0.055	0.074	0.077	0.043	0.068
Cr	-	-	-	-	-
Σoct	1.174	1.150	1.193	1.194	1.202
Ca	0.836	0.868	0.806	0.775	0.773
Na	-	-	0.027	0.098	0.045
Σ cations	4.010	4.018	4.022	4.067	4.020

\* = Total iron as FeO

n.a. = not analysed for

n.d. = not detected

Sample	SB23	SB23	SB23	SB23	SB23	SB23	SB23	SB23
SiO <sub>2</sub>	52.05	49.18	48.64	48.01	48.45	51.81	49.02	49.15
TiO <sub>2</sub>	0.53	1.48	1.58	0.89	2.00	0.66	1.72	1.85
Al <sub>2</sub> O <sub>3</sub>	2.27	4.65	4.25	4.85	3.85	2.33	4.81	4.89
FeO*	9.76	8.30	10.48	9.72	11.36	8.46	8.33	8.41
MnO	0.23	0.25	0.32	0.37	0.26	0.33	n.d.	0.26
MgO	16.87	15.01	13.54	15.04	13.58	17.01	14.55	14.41
Cr <sub>2</sub> O <sub>3</sub>	n.a.	n.a.	n.a.	n.a.	n.a.	n.a.	n.a.	n.a.
CaO	18.05	20.28	19.94	18.97	20.14	18.79	21.29	21.26
Na <sub>2</sub> O	n.d.	0.35	0.31	n.d.	n.d.	n.d.	n.d.	n.d.
Total	99.76	99.50	99.06	97.88	99.64	99.39	99.72	100.23
Si	1.931	1.840	1.846	1.833	1.837	1.924	1.831	1.829
Al <sup>4</sup>	0.069	0.160	0.154	0.167	0.163	0.076	0.169	0.171
Σtet	2.000	2.000	2.000	2.000	2.000	2.000	2.000	2.000
Al <sup>6</sup>	0.030	0.045	0.036	0.051	0.009	0.026	0.043	0.044
Fe	0.303	0.260	0.333	0.310	0.360	0.263	0.260	0.052
Mg	0.933	0.837	0.766	0.856	0.767	0.942	0.810	0.799
Mn	0.007	0.008	0.010	0.012	0.008	0.010	-	0.008
Ti	0.015	0.042	0.045	0.026	0.057	0.018	0.048	0.052
Cr	-	-	-	-	-	-	-	-
Σoct	1.288	1.192	1.190	1.255	1.201	1.259	1.161	1.155
Ca	0.717	0.813	0.811	0.776	0.818	0.748	0.852	0.848
Na	-	0.025	0.023	-	-	-	-	-
Total cations	4.005	4.030	4.024	4.031	4.019	4.007	4.013	4.003

\* = Total iron as FeO

n.a. = not analysed for

n.d. = not detected

# High-level Intrusive Sheets within the Volcanic Pile

Sample	SB27	SB27	SB27	SB27	SB27	SB27
SiO <sub>2</sub>	46.98	50.09	47.55	49.00	49.52	48.81
TiO <sub>2</sub>	1.86	1.80	2.21	2.45	1.45	1.88
Al <sub>2</sub> O <sub>3</sub>	4.44	4.09	5.45	4.28	3.70	4.16
FeO*	9.24	9.56	8.79	10.47	10.09	8.44
MnO	n.d.	n.d.	0.31	0.26	0.28	n.d.
MgO	12.44	13.57	12.80	13.10	12.63	13.49
Cr <sub>2</sub> O <sub>3</sub>	n.a.	n.a.	n.a.	n.a.	n.a.	n.a.
CaO	20.66	21.75	21.84	22.03	21.44	22.36
Na <sub>2</sub> O	n.d.	0.30	0.30	0.32	n.d.	0.30
Total	95.62	101.16	99.25	101.91	99.31	99.44
Si	1.842	1.856	1.801	1.819	1.878	1.839
Al <sup>4</sup>	0.158	0.144	0.199	0.181	0.122	0.161
Σtet	2.000	2.000	2.000	2.000	2.000	2.000
Al <sup>6</sup>	0.047	0.035	0.044	0.006	0.043	0.024
Fe	0.303	0.296	0.279	0.325	0.320	0.266
Mg	0.727	0.749	0.723	0.724	0.714	0.758
Mn	-	-	0.010	0.008	0.009	-
Ti	0.055	0.050	0.063	0.068	0.041	0.053
Cr	-	-	-	-	-	-
Σ oct	1.132	1.130	1.119	1.131	1.127	1.101
Ca	0.868	0.863	0.886	0.876	0.871	0.903
Na	-	0.021	0.022	0.023	-	0.022
Total cations	4.000	4.014	4.027	4.030	3.998	4.026

\* = Total iron as FeO

n.a. = not analysed for

n.d. = not detected

Sample	SB27	SB27	SB27
SiO <sub>2</sub>	48.03	47.60	47.49
TiO <sub>2</sub>	1.99	2.08	2.36
Al <sub>2</sub> O <sub>3</sub>	4.21	4.66	4.30
FeO*	9.34	8.90	10.19
MnO	n.d.	0.24	n.d.
MgO	12.92	13.11	12.75
Cr <sub>2</sub> O <sub>3</sub>	n.a.	n.a.	n.a.
CaO	20.98	21.60	20.93
Na <sub>2</sub> O	0.36	0.36	0.31
Total	97.83	98.55	98.33

Si	1.843	1.816	1.822
Al <sup>4</sup>	0.157	0.184	0.178
Σtet	2.000	2.000	2.000
Al <sup>6</sup>	0.033	0.025	0.017
Fe	0.300	0.284	0.327
Mg	0.739	0.745	0.729
Mn	-	0.008	-
Ti	0.057	0.060	0.068
Cr	-	-	-
Σoct	1.129	1.122	1.141
Ca	0.863	0.883	0.860
Na	0.027	0.027	0.023
Total cations	4.019	4.032	4.024

\* = Total iron as FeO

n.a. = not analysed for

n.d. = not detected



Stilpnomelane Analyses

Sample	SB55	SB55
SiO <sub>2</sub>	46.92	47.09
TiO <sub>2</sub>	n.d.	n.d.
Al <sub>2</sub> O <sub>3</sub>	6.10	5.45
Fe <sub>2</sub> O <sub>3</sub> <sup>+</sup>	28.24	29.38
MnO	0.66	0.69
MgO	5.67	5.45
CaO	n.d.	n.d.
Na <sub>2</sub> O	n.d.	n.d.
K <sub>2</sub> O	2.94	2.29
Total	90.53	90.35

Recalculation on the basis of 8 Si cations

Si	8.00	8.00	Sites Z
Σ	8.00	8.00	
Al	1.23	1.20	X, Y
Ti	-	-	
Fe <sup>3+</sup>	3.62	3.75	
Mn	0.09	0.10	
Mg	1.44	1.38	
Σ	6.38	6.43	
Ca	-	-	W
Na	-	-	
K	0.63	0.49	
Σ	0.63	0.49	

+ = Total iron as Fe<sub>2</sub>O<sub>3</sub>

n.d. = not detected

Sample	SB55	SB55	YG54	YG54	SB55
SiO <sub>2</sub>	36.95	36.33	35.79	37.08	31.04
TiO <sub>2</sub>	n.d.	n.d.	n.d.	n.d.	n.d.
Al <sub>2</sub> O <sub>3</sub>	20.76	19.35	22.35	22.55	19.35
FeO*	9.97	11.16	9.65	8.31	22.72
MnO	n.d.	n.d.	n.d.	n.d.	n.d.
MgO	1.88	1.43	1.31	1.52	5.19
CaO	23.33	23.00	22.34	23.28	12.02
Na <sub>2</sub> O	n.d.	n.d.	n.d.	n.d.	n.d.
K <sub>2</sub> O	n.d.	n.d.	n.d.	n.d.	n.d.
Total	92.89	91.27	91.44	92.74	90.62

Recalculation on the basis of 16 cations

Si	6.06	6.10	6.01	6.07	) Sites Z
Al	4.00	3.83	4.00	4.00	
Fe <sup>3+</sup>	-	0.17	-	-	
Σ	4.00	4.00	4.00	4.00	) Y
Al	0.01	-	0.28	0.35	
Fe	1.36	1.40	1.36	1.14	
Mg	0.46	0.36	0.33	0.37	) X
Σ	1.83	1.76	1.97	1.86	
Ca	4.10	4.14	4.02	4.08	
					W

\* = Total iron as FeO  
n.d. = not detected

Sample	SBC1	LD3	LD3	LD3	LD3	LD3
SiO <sub>2</sub>	38.21	37.80	38.24	38.36	38.13	37.93
TiO <sub>2</sub>	n.d.	n.d.	n.d.	n.d.	n.d.	n.d.
Al <sub>2</sub> O <sub>3</sub>	23.01	25.97	25.28	26.29	26.23	26.52
Fe <sub>2</sub> O <sub>3</sub> <sup>+</sup>	12.49	9.38	10.31	9.90	9.32	9.17
MnO	n.d.	n.d.	n.d.	n.d.	0.19	n.d.
MgO	n.d.	n.d.	n.d.	n.d.	n.d.	n.d.
CaO	23.86	24.26	24.29	24.07	24.21	23.81
Na <sub>2</sub> O	n.d.	n.d.	n.d.	n.d.	n.d.	n.d.
K <sub>2</sub> O	n.d.	n.d.	n.d.	n.d.	n.d.	n.d.
Total	97.57	97.41	98.12	98.62	98.08	97.43

## Recalculation on the basis of 8 cations

Si	3.05	2.98	3.00	2.99	2.99	2.99	Sites Z
Σ	3.05	2.98	3.00	2.99	2.99	2.99	
Al	2.16	2.41	2.34	2.41	2.42	2.46	Y
Fe <sup>3+</sup>	0.75	0.55	0.61	0.58	0.55	0.54	
Σ	2.91	2.96	2.95	2.99	2.97	3.00	
Ca	2.04	2.05	2.05	2.01	2.03	2.01	W
Σ	2.04	2.05	2.05	2.01	2.03	2.01	
Total	8.00	7.99	8.00	7.99	7.99	8.00	

+ = Total iron as Fe<sub>2</sub>O<sub>3</sub>

n.d. = not detected

Sample	SBC10	SB27	SB27	SB23
SiO <sub>2</sub>	66.20	60.33	59.51	69.02
TiO <sub>2</sub>	n.d.	n.d.	n.d.	n.d.
Al <sub>2</sub> O <sub>3</sub>	21.51	24.30	25.77	19.97
FeO*	n.d.	n.d.	0.72	n.d.
MnO	n.d.	n.d.	n.d.	n.d.
MgO	n.d.	n.d.	n.d.	n.d.
CaO	2.45	5.99	7.89	0.24
Na <sub>2</sub> O	10.20	7.94	7.07	11.77
K <sub>2</sub> O	n.d.	0.16	n.d.	n.d.
Total	100.36	98.72	100.96	101.00

## Recalculation on the basis of 8 oxygens

Si	2.895	2.708	2.638	2.984
Al	1.109	1.286	1.346	1.018
Fe	-	-	0.027	-
Ca	0.115	0.288	0.375	0.011
Na	0.865	0.691	0.608	0.987
K	-	0.009	-	-
Σ	4.984	4.982	4.994	5.000
Ab	88	70	62	99
An	12	29	38	1
Or	0	1	0	0

\* = Total iron as FeO

n.d. = not detected

Sphene Analysis

Sample	SB63
$\text{SiO}_2$	31.89
$\text{TiO}_2$	31.93
$\text{Al}_2\text{O}_3$	4.41
$\text{Fe}_2\text{O}_3^+$	1.08
MnO	n.d.
MgO	n.d.
CaO	29.42
$\text{Na}_2\text{O}$	n.d.
$\text{K}_2\text{O}$	n.d.
Total	98.73

Recalculation on the basis of 4 Si cations

		Sites
Si	4.00	Z
$\Sigma$	4.00	
Al	0.65	
Ti	2.99	) Y
$\text{Fe}^{3+}$	0.11	
$\Sigma$	3.75	
Ca	3.90	X
$\Sigma$	3.90	

+ = Total iron as  $\text{Fe}_2\text{O}_3$ 

n.d. = not detected

Amphibole Analyses

Sample	LD3	LD3	LD3	LD3	LD3	LD3	LD3
SiO <sub>2</sub>	48.32	47.91	47.31	46.55	45.18	43.76	45.34
TiO <sub>2</sub>	0.26	n.d.	0.31	0.39	0.32	0.20	0.22
Al <sub>2</sub> O <sub>3</sub>	5.69	6.20	8.41	7.84	9.35	11.15	8.30
FeO*	15.05	20.34	16.15	16.79	17.54	16.72	17.78
MnO	0.27	0.23	0.25	n.d.	0.20	0.30	n.d.
MgO	15.67	10.74	13.39	12.27	12.33	13.47	13.76
Cr <sub>2</sub> O <sub>3</sub>	0.17	n.d.	n.d.	n.d.	n.d.	n.d.	n.d.
CaO	8.67	10.93	9.58	10.91	10.15	7.91	9.62
Na <sub>2</sub> O	0.41	0.37	1.23	1.23	1.11	0.99	0.54
K <sub>2</sub> O	n.d.	0.15	n.d.	n.d.	n.d.	0.11	n.d.
Total	94.51	96.87	96.63	95.98	96.18	94.61	95.56
Recalculation on the basis of 23 oxygens							
Si	7.256	7.247	7.017	7.009	6.812	6.651	6.866
Al <sup>4</sup>	0.644	0.753	0.983	0.991	1.188	1.349	1.134
Al <sup>6</sup>	0.064	0.147	0.487	0.401	0.674	0.648	0.347
Ti	0.030	-	0.035	0.045	0.037	0.024	0.025
Fe	1.891	2.561	2.003	2.115	2.212	2.125	2.253
Mn	0.034	0.030	0.032	-	0.026	0.039	-
Mg	3.509	2.421	2.961	2.754	2.771	1.997	3.105
Cr	0.021	-	-	-	-	-	-
Ca	1.396	1.772	1.523	1.760	1.640	1.288	1.561
Na	0.119	0.108	0.353	0.360	0.325	0.291	0.159
K	-	0.030	-	-	-	0.021	-
Σ cations	14.964	15.069	15.394	15.435	15.685	14.433	15.450

\* = Total iron as FeO

n.d. = not detected

Amphibole Analyses (cont'd.)

Sample	LD3	LD3	LD3	LD3	LD3	LD3	LD3	LD3
SiO <sub>2</sub>	46.43	45.13	47.86	46.08	45.32	45.69	45.93	45.27
TiO <sub>2</sub>	0.27	0.33	n.d.	0.27	0.24	0.52	0.36	n.d.
Al <sub>2</sub> O <sub>3</sub>	9.11	9.97	6.59	8.23	8.53	9.18	9.09	10.25
FeO*	16.70	17.92	18.30	18.06	17.99	16.78	16.95	20.27
MnO	0.25	n.d.	0.38	0.29	0.20	n.d.	n.d.	0.26
MgO	12.59	12.03	13.09	12.69	12.41	12.37	11.82	11.01
Cr <sub>2</sub> O <sub>3</sub>	n.d.	n.d.	n.d.	n.d.	n.d.	n.d.	n.d.	n.d.
CaO	10.58	9.99	9.45	9.93	9.73	10.47	10.93	9.09
Na <sub>2</sub> O	1.62	1.26	0.50	1.04	1.08	1.19	1.13	1.28
K <sub>2</sub> O	0.10	n.d.	n.d.	n.d.	n.d.	0.10	0.11	n.d.
Total	97.65	96.63	96.17	96.59	95.50	96.30	96.32	97.43
Si	6.877	6.775	7.189	6.923	6.891	6.856	6.898	6.796
Al <sup>4</sup>	1.123	1.225	0.811	1.077	1.109	1.144	1.102	1.204
Al <sup>6</sup>	0.468	0.539	0.355	0.381	0.420	0.480	0.508	0.610
Ti	0.031	0.038	-	0.031	0.028	0.059	0.041	-
Fe	2.069	2.250	2.299	2.270	2.287	2.106	2.129	2.544
Mn	0.031	-	0.049	0.038	0.027	-	-	0.034
Mg	2.780	2.692	2.932	2.842	2.813	2.767	2.647	2.464
Cr	-	-	-	-	-	-	-	-
Ca	1.679	1.608	1.521	1.609	1.585	1.683	1.759	1.462
Na	0.465	0.366	0.147	0.303	0.319	0.348	0.329	0.372
K	0.020	-	-	-	-	0.020	0.022	-
Σ cations	15.543	15.493	15.303	15.474	15.479	15.463	15.435	15.486

\* = Total iron as FeO

n.d. = not detected

Chlorite Analyses

Sample	SB23	LG4	SB55	SB55	LD3
SiO <sub>2</sub>	26.71	26.88	26.44	26.31	29.83
TiO <sub>2</sub>	n.d.	n.d.	n.d.	n.d.	n.d.
Al <sub>2</sub> O <sub>3</sub>	15.92	18.56	16.43	17.43	16.03
FeO*	30.50	23.66	33.67	33.74	18.29
MnO	0.36	0.38	0.31	0.27	0.19
MgO	12.66	15.83	9.64	9.44	22.46
CaO	n.d.	0.16	n.d.	n.d.	n.d.
Na <sub>2</sub> O	n.d.	n.d.	n.d.	n.d.	n.d.
K <sub>2</sub> O	n.d.	n.d.	n.d.	n.d.	n.d.
Total	86.15	85.47	86.49	87.19	86.80

Recalculation on the basis of 36 (O, OH) with 20 O and 16 OH

Si	5.92	5.77	5.94	5.85	6.10
Al <sup>4</sup>	2.08	2.23	2.06	2.15	1.90
Σ	8.00	8.00	8.00	8.00	8.00
Al	2.08	2.46	2.29	2.42	1.96
Fe <sup>2+</sup>	5.66	4.25	6.32	6.27	3.13
Mn	0.07	0.07	0.06	0.05	0.03
Mg	4.18	5.06	3.23	3.13	6.84
Ca	-	0.04	-	-	-
Σ	11.99	12.08	12.00	12.02	11.96

Name, after classification of Hey (1954)

Brunsvigite Pycnochlorite Brunsvigite Brunsvigite Pycnochlorite

\* = Total iron as FeO

n.d. = not detected



Chlorite Analyses (cont'd.)

Sample	LD3	LD3	LD3	SB48	SB48
SiO <sub>2</sub>	30.39	29.37	28.38	29.32	28.00
TiO <sub>2</sub>	n.d.	n.d.	n.d.	n.d.	n.d.
Al <sub>2</sub> O <sub>3</sub>	15.20	16.33	17.64	16.08	17.93
FeO*	17.65	18.51	20.38	20.11	21.63
MnO	0.28	0.27	0.34	0.24	0.26
MgO	22.33	21.24	19.72	20.75	19.35
CaO	n.d.	n.d.	n.d.	0.15	0.11
Na <sub>2</sub> O	n.d.	n.d.	n.d.	n.d.	n.d.
K <sub>2</sub> O	n.d.	n.d.	n.d.	n.d.	n.d.
Total	85.85	85.72	86.46	86.65	87.28
Si	6.26	6.09	5.90	6.07	5.81
Al <sup>4</sup>	1.74	1.91	2.10	1.93	2.19
Σ	8.00	8.00	8.00	8.00	8.00
Al	1.95	2.08	2.22	2.00	2.19
Fe <sup>2+</sup>	3.04	3.21	3.54	3.48	3.75
Mn	0.05	0.05	0.07	0.04	0.05
Mg	6.85	6.57	6.11	6.41	5.98
Ca	-	-	n.d.	0.03	0.02
Σ	11.99	11.91	11.94	11.96	11.99

Diabantite Pycnochlorite PycnochloritePycnochloritePycnochlorite

\* = Total iron as FeO

n.d. = not detected

Prehnite analyses

Sample	YG54	YG54	YG54	YG54	YG54	YG54	YG54	YG54
SiO <sub>2</sub>	42.76	43.27	43.45	43.01	42.41	43.42	43.67	43.46
TiO <sub>2</sub>	n.d.	n.d.	n.d.	n.d.	n.d.	n.d.	n.d.	n.d.
Al <sub>2</sub> O <sub>3</sub>	22.45	22.28	22.24	23.26	23.00	23.25	22.23	22.15
Fe <sub>2</sub> O <sub>3</sub> <sup>+</sup>	2.48	2.75	3.13	2.99	3.14	2.85	2.78	3.20
MnO	n.d.	n.d.	n.d.	n.d.	n.d.	n.d.	n.d.	n.d.
MgO	n.d.	n.d.	n.d.	0.29	0.37	0.27	n.d.	n.d.
CaO	27.21	27.26	27.28	26.92	26.51	27.15	27.63	27.56
Na <sub>2</sub> O	n.d.	n.d.	n.d.	n.d.	n.d.	n.d.	n.d.	n.d.
K <sub>2</sub> O	n.d.	n.d.	n.d.	n.d.	n.d.	n.d.	n.d.	n.d.
Total	94.89	95.61	96.11	96.50	95.42	96.97	96.31	96.36

## Recalculation on the basis of 22 oxygens

Si	5.99	6.02	6.01	6.00	5.91	5.95	6.03	6.00
Al	0.01	-	-	-	0.09	0.05	-	-
Σ	6.00	6.02	6.01	6.00	6.00	6.00	6.03	6.00
Al	3.69	3.65	3.63	3.66	3.69	3.70	3.62	3.61
Fe <sup>3+</sup>	0.26	0.29	0.33	0.29	0.33	0.29	0.29	0.33
Mg	-	-	-	0.06	0.08	0.06	-	-
Ca	4.08	4.06	4.04	4.02	3.96	3.98	4.09	4.08
Σ	8.03	8.00	8.00	8.03	8.06	8.03	8.00	8.02

+ = Total iron as Fe<sub>2</sub>O<sub>3</sub>

n.d. = not detected

TABLE 16

TRACE ELEMENT CONTENTS OF CLINOPYROXENES DETERMINED BY EMISSION  
SPECTROGRAPHY

Sample	GF63	LG2	LG4	LG6
Element				
Sc	115	122	114	134
Cr	480	355	194	113
Y	29	33	34	45
V	400	412	412	430
Sr	80	50	101	23
Cu	60	55	75	61
Ni	66	63	57	33
Co	56	44	62	65

Sample	175S
$\text{SiO}_2$	50.3
$\text{TiO}_2$	1.40
$\text{Al}_2\text{O}_3$	21.3
$\text{FeO}$	3.60
$\text{Fe}_2\text{O}_3$	4.50
$\text{MnO}$	n.d.
$\text{MgO}$	3.13
$\text{CaO}$	1.72
$\text{Na}_2\text{O}$	1.09
$\text{K}_2\text{O}$	6.62
$\text{P}_2\text{O}_5$	n.d.
$\text{H}_2\text{O}^+$	4.94
Total	98.60

Recalculation on the basis of 22 oxygens  
Sites

Si	7.08	)	Z
Al	0.92	)	
$\Sigma$	8.00	)	
Al	2.61	)	Y
$\text{Fe}^{3+}$	0.48	)	
$\text{Fe}^{2+}$	0.42	)	
Mg	0.66	)	
$\Sigma$	4.17	)	
Na	0.30	)	X
K	1.19	)	
$\Sigma$	1.49	)	

n.d. = not detected

## APPENDIX 3. SAMPLE DETAILS.

Listed below are grid reference localities and brief petrographical descriptions (where available) of samples investigated for whole-rock chemical analyses.

All this material and other samples mentioned in the text are stored at the University of Keele and may be consulted upon request.

TABLE 18

SBC1	SM88613939	Pillowed lava. Tabular plagioclase and clinopyroxene with secondary chlorite.
SBR1	SM88613939	Pillowed lava. Fine grained tabular plagioclase feldspar with intersertal clinopyroxene.
SBC5	SM88704047	Pillowed lava. Microphenocrysts of clinopyroxene within groundmass of spherulitic clinopyroxene and plagioclase.
SBR5	SM88704047	Pillowed lava. Spherulitic plagioclase, with secondary calcite, chlorite, and quartz.
SBC7	SM89404090	Pillowed lava.
SBR7	SM89404090	Pillowed lava. Skeletal plagioclase feldspar, with dendritic, purple-coloured clinopyroxene. Vesicles of chlorite.
SB8	SM89384119	Massive intrusive sheet.
SBC10	SM89554136	Pillowed lava. Skeletal plagioclase with dendritic, purple-coloured, clinopyroxene.
SBR10	SM89554136	Pillowed lava. Hollow, skeletal plagioclase with dendritic, purple-coloured clinopyroxene. Vesicles filled with calcite and clinopyroxene.

SBC11	SM90554098	Pillowed lava.
SBR11	SM90554098	Pillowed lava.
SBC12	SM90874100	Pillowed lava. Tabular plagioclase with abundant purple-coloured tabular and skeletal clinopyroxene.
SBR12	SM90874100	Pillowed lava. Tabular plagioclase and clinopyroxene with chlorite.
SB13	SM93814033	Lava. Sparse clinopyroxene and plagioclase microphenocrysts in plagiophyric groundmass. Large siliceous nodules present.
SB15	SM95953742	Pillowed lava. Plagiophyric lava, containing abundant calcite and altered mafic minerals.
SB19	SM88794063	Massive ?intrusive sheet.
SB22	SM88804068	Massive intrusive sheet. Subhedral clinopyroxene associated within tabular plagioclase. Epidote abundant.
SB23	SM88824070	Pillowed lava. Tabular plagioclase and subhedral to subophitic clinopyroxene. Chlorite and calcite present.
SB25	SM88894070	Massive, non-pillowed lava. Branching, skeletal clinopyroxene abundant. Plagioclase altered. Pumpellyite common.
SB27	SM89264082	Massive, intrusive sheet. Altered, tabular plagioclase feldspar with skeletal, coloured clinopyroxene. Chlorite abundant.

SB28	SM89384110	Massive, intrusive sheet. Subophitic clinopyroxene and plagioclase. Accessory ore and secondary chlorite and calcite.
SB30	SM88643946	Pillowed lava. Tabular, skeletal clinopyroxene and plagioclase. Secondary pumpellyite.
SB31	SB88253970	Pillowed lava. Zoned clinopyroxene and plagioclase microphenocrysts set in groundmass of spherulitic clinopyroxene and plagioclase. Skeletal ore. Minor chlorite.
SB33	SM88113971	Massive lava. Tabular plagioclase feldspar with intersertal clinopyroxene. Secondary chlorite.
SB34	SM88564040	Pillowed lava. Tabular clinopyroxene, with minor plagioclase. Secondary chlorite and pumpellyite.
SB35	SM88604030	Massive lava. Aphanitic rock, with subhedral clinopyroxene and tabular plagioclase. Vesicles with prehnite. Secondary pumpellyite also present.
SB37	SM88404020	Pillowed lava. Tabular plagioclase feldspar, with intersertal clinopyroxene. Chlorite also present.
SB39	SM88364011	Massive lava. Subhedral clinopyroxene and tabular plagioclase. Minor chlorite and pumpellyite.
SB40	SM88283998	Pillowed lava. Plagioclase rich lava, with intersertal clinopyroxene. Calcite present.
SB41	SM89804135	Pillowed lava.
SB42	SM89864139	Intrusive sheet. Subhedral to subophitic clinopyroxene with plagioclase. Minor ore.

SB43	SM89864141	Intrusive sheet. Subhedral clinopyroxene and tabular plagioclase with minor chlorite.
SB44	SM96163758	Intrusive sheet. Subhedral clinopyroxene and tabular plagioclase feldspar. Abundant ore.
SB45	SM92714023	Non pillowed lava. Subophitic clinopyroxene and altered plagioclase. Secondary chlorite and abundant pumpellyite.
SB46	SM93124046	Massive lava. Tabular plagioclase and clinopyroxene with secondary epidote.
SB47	SM93114042	Pillowed lava. Highly altered, tabular plagioclase, with intersertal clinopyroxene. Thin chlorite veins common.
SB48	SM93304046	Pillowed lava. Plagioclase phenocrysts set in groundmass of skeletal plagioclase and dendritic clinopyroxene. Vesicles with calcite and clinopyroxene common.
SB49	SM93594030	Pillowed lava. Tabular plagioclase and purple clinopyroxene, commonly skeletal.
SB50	SM93604031	Intrusive sheet. Subophitic clinopyroxene and tabular altered plagioclase. Epidotes, with minor chlorite.
SB51	SM93804033	Intrusive sheet. Tabular, subophitic clinopyroxene, and plagioclase. Abundant epidote and chlorite.
SB52	SM93894041	Massive lava. Plagiophyric lava, with plagioclase phenocrysts. Epidote common.



SB53	SM93934040	Intrusive sheet. Subophitic clinopyroxene with tabular plagioclase. Abundant secondary epidote.
SB54	SM92803545	Intrusive sheet. Large, euhedral clinopyroxene and plagioclase crystals set in finer grained feldspathic groundmass. Ore present.
SB55	SM89253513	Intrusive sheet. Large tabular plagioclase crystals, with intersertal clinopyroxene. Apatite and skeletal ore are accessory phases. Pumpellyite and chlorite also present.
SB56	SM91853499	Intrusive sheet. Tabular clinopyroxene and altered plagioclase. Accessory skeletal ore. Abundant epidote and chlorite.
SB57	SM91813496	Intrusive sheet. Euhedral to subophitic clinopyroxene, with tabular plagioclase.
SB58	SM91014096	Pillowed lava. Spherulitic plagioclase and clinopyroxene. Abundant calcite.
SB59	SM91194080	Intrusive sheet. Tabular plagioclase with minor clinopyroxene. Abundant calcite.
SB60	SM91304090	Pillowed lava. Texture variable. In part, plagioclase with intersertal clinopyroxene; elsewhere, large, skeletal clinopyroxene and minor plagioclase.
SB61	SM91304090	Intrusive sheet. Tabular, skeletal clinopyroxene, with plagioclase. Prehnite and chlorite abundant.
SB62	SM91764088	Intrusive sheet. Tabular, skeletal clinopyroxene, with plagioclase. Prehnite and chlorite present.

SB63	SM91754081	Pillowed lava. Skeletal, branching clinopyroxene with minor feldspar and chlorite. Certain areas dominated by large clinopyroxene crystals.
SB64	SM91794070	Intrusive sheet. Tabular plagioclase, with subhedral to intersertal clinopyroxene. Calcite and chlorite present.
SB66	SM92234070	Pillowed lava. Aphyric lava. Plagioclase and clinopyroxene in groundmass, with secondary quartz and chlorite.
SB67	SM92124072	Intrusive sheet. Subophitic clinopyroxene, with altered plagioclase. Secondary chlorite present.
SB68	SM92624049	Intrusive sheet. Tabular plagioclase with subhedral clinopyroxene. Chlorite and epidote present.
LG1	SM93243936	From large intrusion. Euhedral clinopyroxene with tabular plagioclase. Chlorite and minor pumpellyite present.
LG2	SM93283932	From large intrusion. Euhedral clinopyroxene with tabular, altered plagioclase. Chlorite and epidote.
LG3	SM93323921	From large intrusion. Subophitic clinopyroxene and altered plagioclase. Chlorite and pumpellyite common.
LG4	SM93353926	From large intrusion. Euhedral clinopyroxene; altered plagioclase with minor epidote and chlorite.

LG5	SM93393925	From large intrusion. Euhedral clinopyroxenes with tabular altered feldspars. Skeletal ore and secondary chlorite and epidote.
LG6	SM93403923	From large intrusion. Tabular plagioclase and clinopyroxene crystals, with abundant ore. Certain areas show skeletal plagioclase with chlorite.
LD1	SM88243558	From large intrusion. Ophitic clinopyroxene and altered plagioclase. Minor secondary chlorite.
LD2	SM88243561	From large intrusion. Ophitic clinopyroxene and altered plagioclase. Secondary amphibole.
LD3	SM88243568	From large intrusion. Ophitic clinopyroxene and altered plagioclase. Secondary amphibole, chlorite and prehnite.
REB166	SM92244063	Intrusive sheet. Tabular albitized plagioclase, with subophitic clinopyroxene. Chlorite present.
YG1	SM91603907	From large intrusion. Subophitic clinopyroxene and plagioclase. Chlorite and minor prehnite.
YG2	SM91613916	From large intrusion. Ophitic texture. Clinopyroxene, minor ore altered plagioclase. Chlorite.
SP3	SM88684059	Intrusive sheet.
SP94	SM94854060	From large intrusion. Tabular plagioclase with intersertal, subhedral clinopyroxene. Chlorite in groundmass.
GG1	SM91023907	From large intrusion. Euhedral clinopyroxene, altered plagioclase and chlorite.

GF63	SM9004395	From large intrusion.
SA4	SM94084053	From rhyolite flow. Plagioclase phenocrysts contained within recrystallized quartz-feldspathic groundmass.
SA5	SM88823933	From rhyolite flow. Recrystallized lava showing snowflake texture and microphenocrysts.
SA6	SM94683857	Flow banded rhyolite flow.
SA8	SM92433783	Dark rhyolite flow. Fine-grained intergrowth of quartz and feldspar with snowflake structure. Polygranular aggregates of coarse-grained quartz present.
SA9	SM94504047	From rhyolite flow. Phenocrysts of feldspar within a fine-grained quartz-feldspar groundmass. Micropoilitic aggregates of quartz and feldspar present.
SA11	SM90583945	From rhyolite flow. Fine-grained intergrowth of quartz and feldspar with snowflake texture. Cut by quartz and epidote veins.
SA3	SM88723938	Massive lava. Rare glomeroporphyritic plagioclase in siliceous, recrystallized groundmass.
REB94	SM88703935	Massive lava. Fine-grained, microlitic plagioclase feldspars with chloritic pseudomorphs after ?clinopyroxene.
REB412	SM88523933	From pillow in isolated pillow breccia.
REB413	SM88523933	From pillow in isolated pillow breccia.

REB414	SM88523935	Thin unit above lavas. Siliceous, recrystallized lava showing perlitic texture and altered, corroded phenocrysts.
REB342	SM88383770	From large intrusion. Sparsely feldspar porphyritic. Groundmass of tabular feldspar and quartz with chlorite and biotite.
REB412A	SM88523933	Pillow in isolated pillow breccia.
SP2	SM88704058	Thin, bedded siliceous horizon.
SP62	SM79243153	?volcaniclastic rock. Recrystallized quartzo-feldspathic groundmass, containing rare, large, quartz and feldspar crystals.
SP63	SM79263153	?volcaniclastic.
SEALYHAM VOLCANICS		
REB23	SN093303	Massive lava.
ABERCASTLE		
REB90	SM855339	?intrusive sheet.
TREFFGARNE VOLCANICS		
REB12	SM960233	Massive lava. Plagioclase feldspar phenocrysts with chloritic pseudomorphs after pyroxene, in felted feldspathic groundmass.
REB125	SM960233	Massive lava.
REB127	SM960233	Massive lava. Phenocrysts of plagioclase in sericitized groundmass. Rare ore crystals.

REB153	SM960233	Massive lava. Phenocrysts of plagioclase and chlorite after pyroxene in partly sericitized feldspathic groundmass.
REB154	SM960233	Massive lava. Plagioclase feldspar phenocrysts with chloritic pseudomorphs after pyroxene, in felted feldspathic groundmass. Epidote present.
SB26	SM89274082	Basic volcanoclastic. Abundant sericite and quartz with pumpellyite also common.
SA7	SM96123741	Crystal-lithic ash-flow tuff.

LOCALITIES AND BRIEF SAMPLE DESCRIPTIONS (AFTER ROACH, UNPUBLISHED DATA)

RD151	Carnedd Leithr.	Granophyric diorite.
RD154	Carnedd Leithr.	Microdiorite.
RD155	Carnedd Leithr.	Microdiorite.
RD158	Carnedd Leithr.	Microdiorite.
RD165	Carnedd Leithr.	Microdiorite.
RD172	Maes-y-Mynydd.	Microdiorite.
RD175	Maes-y-Mynydd.	Microdiorite.
RD212	Maes-y-Mynydd.	Microdiorite.
RD225A	Abercastle-Aberfelin.	Gabbro.
RD228A	Abercastle-Aberfelin.	Gabbro.
RD230A	Abercastle-Aberfelin.	Gabbro.
RD231A	Abercastle-Aberfelin.	Gabbro.
RD232	Llech Dafad.	Gabbro.
RD237	Penbwchdy.	Microgranophyre.
RD238A	Penbwchdy.	Microgranophyre.
RD244	Garngilfach.	Dioritic-gabbro.
RD252	Garnfechan.	Microgranophyre.
RD254	Garn Fechan.	Microgranophyre.
RD258B	Garn Fawr.	Gabbro.
RD280B	Mynydd Dinas.	Gabbro.
RD295A	Pen Biri.	Microdiorite.
RD295B	Pen Biri.	Microdiorite.
RD327	Pen Biri.	Microdiorite.

LISTED IN TABLE 19 ARE SECONDARY ASSEMBLAGES WITHIN BASIC IGNEOUS  
ROCKS OF THE FISHGUARD AREA.



## SECONDARY ASSEMBLAGES WITHIN IGNEOUS ROCKS OF THE FISHGUARD AREA

TABLE 19

Sample	chlorite	sphene	white mica	prehnite	pumpellyite	actinolite	epidote	quartz	stilpnomelane	albitized feldspar	calcite
SB25	✓	✓	✓		✓		✓			✓	
SB30	✓	✓			✓		✓	✓		✓	
SB68	✓	✓			✓	✓	✓			✓	✓
SB66B	✓	✓	✓		✓		✓	✓		✓	✓
SB9	✓	✓	✓	✓	✓		✓	✓		✓	✓ M
SB33	✓	✓					✓	✓		✓	
SB31	✓							✓		✓	
SB23	✓	✓	✓		✓		✓	✓		✓	✓
SB61	✓	✓		✓				✓		✓	✓
SB27	✓	✓	✓		✓	✓				✓	
YG56	✓	✓		✓	✓		✓			✓	
LL59	✓	✓				✓ M	✓			✓	
SB39	✓	✓			✓		✓	✓		✓	
SB15	✓	✓								✓	✓
SB46	✓	✓			✓		✓	✓		✓	✓
SB65	✓	✓	✓				✓	✓		✓	✓
SB22	✓	✓			✓		✓	✓		✓	
SB37	✓	✓	✓							✓	
SB53	✓	✓				✓	✓			✓	✓ M
SB51	✓	✓			✓		✓			✓	

M = present in minor amounts

Sample	chlorite	spene	white mica	prehnite	pumpellyite	actinolite	epidote	quartz	stilpnomelane	albitized feldspar	calcite
SB62	✓	✓		✓	✓					✓	✓
SB45	✓	✓	✓				✓	✓			✓
SB66A	✓	✓	✓		✓		✓	✓			✓
SB35	✓	✓			✓		✓				✓
SB28	✓	✓	✓		✓						✓
SB58	✓	✓			✓ M			✓			✓
SB50	✓	✓	✓				✓	✓			
SB56	✓	✓	✓			✓ M	✓	✓			
YG53A	✓	✓				✓	✓			✓	
YG1	✓	✓		✓			✓	✓		✓	
GF51	✓	✓		✓	✓					✓	
YG58	✓	✓	✓			✓	✓	✓		✓	
LL61	✓	✓	✓			✓	✓	✓		✓	✓
LL60	✓	✓	✓				✓	✓		✓	✓ M
LD1	✓	✓			✓		✓			✓	
LG7	✓	✓	✓		✓		✓	✓		✓	
SB13	✓							✓		✓	
SB52	✓	✓					✓	✓		✓	
SB42	✓	✓									
GG1	✓	✓	✓		✓		✓	✓		✓	

M = present in minor amounts

Sample	chlorite	spheue	white mica	prehnite	pumpellyite	actinolite	epidote	quartz	stilpnomelane	albitized feldspar	calcite
GF53		✓		✓	✓						
GF50	✓	✓		✓	✓		✓	✓		✓	
202	✓	✓					✓		✓		✓
253	✓	✓									
GF52	✓	✓				✓		✓			
SB47	✓	✓	✓				✓			✓	✓
SB40	✓	✓					✓			✓	✓
LL62	✓	✓	✓				✓	✓		✓	
REB166	✓	✓	✓	✓	✓		✓	✓		✓	
172	✓	✓			✓		✓	✓			✓
SB43	✓	✓		✓	✓					✓	
SB20	✓	✓						✓		✓	✓
SB59	✓	✓			✓					✓	✓
SB67	✓	✓	✓		✓			✓		✓	
SP94	✓	✓					✓ M			✓	✓ M
482	✓	✓			✓		✓	✓		✓	
LL57	✓	✓	✓				✓	✓		✓	
LD2	✓	✓		✓						✓	
LG4	✓	✓	✓				✓	✓		✓	
LG5	✓	✓					✓	✓			

M = present in minor amounts

Sample	chlorite	sphene	white mica	prehnite	pumpellyite	actinolite	epidote	quartz	stilpnomelane	albitized feldspar	calcite
SBR11	✓	✓			✓			✓			
YG54	✓	✓		✓	✓			✓			
SB64	✓	✓						✓		✓	✓
LG65	✓	✓					✓				✓
SB57	✓	✓	✓					✓		✓	
SB44	✓	✓	✓				✓	✓		✓	
286	✓	✓	✓					✓		✓	
LG2	✓	✓		✓	✓		✓			✓	
LG3	✓	✓	✓					✓			
YG2	✓		✓		✓	✓	✓			✓	

## REFERENCES

- ALBAREDE, F., 1976. Some trace element relationships among liquid and solid phases during the course of fractional crystallization of magmas. *Geochim. cosmochim. Acta*, v. 40, p. 667-673.
- ALLÈGRE, C. J., and MINSTER, J. F., 1978. Quantitative models of trace element behaviour in magmatic processes. *Earth Planet. Sci. Lett.*, v. 38, p. 1-25.
- ALLÈGRE, C. J., TREUIL, M., MINSTER, J. F., MINSTER, B., and ALBAREDE, F., 1977. Systematic use of trace elements in igneous processes, I. Fractional crystallization processes in volcanic suites. *Contr. Miner. Petrology*, v. 60, p. 57-75.
- AMSTUTZ, G. C., 1948. Lavaströme im Glarner Freiberg. *Leben und Umwelt*, p. 90-94.
- AMSTUTZ, G. C., 1950. Kupfererze in den Spilitischen laven des Glarner-Verrucano. *Schweiz. Min. Petr. Mitt.*, v. 30, p. 182-191.
- AMSTUTZ, G. C., 1968. Spilites and spilitic rocks. *In* H. H. Hess and A. Poldervaart (Eds.). *The Poldervaart treatise on rocks of basaltic composition*. Inter-science (Wiley), New York, p. 737-753.
- AMSTUTZ, G. C., 1974. (Ed.). *Spilites and spilitic rocks*. Springer Verlag, pp. 482.
- ANDERSON, A. T., and GREENLAND, L. P., 1969. Phosphorous fractionation as a quantitative indicator of crystallization differentiation of basaltic liquids. *Geochim. cosmochim. Acta*, v. 33, p. 493-505.
- ANDERSON Jr., J. E., 1969. Development of snowflake texture in a welded tuff, Davis Mountains, Texas. *Geol. Soc. Am. Bull.*, v. 80, p. 2075-2080.

- ANKETELL, J. M., 1963. The geology of the Llangranog district, southwest Cardiganshire. Unpublished Ph.D. thesis, Queen's University, Belfast.
- ARCULUS, R. J., 1973. Recent submarine pillow lavas in the Catania area, eastern Sicily. *Phil. Trans. R. Soc. Lond. (A)*, v. 274, p. 153-162.
- BARAGAR, W. R. A., PLANT, A. G., PRINGLE, G. J., and SCHAN, M., 1977. Petrology and alteration of selected units of Mid-Atlantic Ridge basalts sampled from sites 332 and 335, DSDP. *Can. J. Earth Sci.*, v. 14, p. 837-874.
- BARBERI, F., BIZOVAR, H., and VARET, J., 1971. Nature of the clinopyroxene and iron enrichment in alkalic and transitional basaltic magmas. *Contr. Miner. Petrology*, v. 33, p. 93-107.
- BARBERI, F., FERRARA, G., SANTACROCE, R., TREUIL, M., and VARET, J., 1975. A transitional basalt-pantellerite sequence of fractional crystallization, the Boina Centre (Afar Rift, Ethiopia). *J. Petrology*, v. 16, p. 22-56.
- BASSETT, D. A., 1972. Wales. In Williams, A., et al. (Eds.). A correlation of Ordovician rocks in the British Isles. *Geol. Soc. Lond. Spec. Rep.*, 3, p. 14-39.
- BATES, D. E. B., 1969. Some early Arenig brachiopods and trilobites from Wales. *Bull. Br. Mus. nat. Hist. (Geol.)*, v. 18, p. 1-28.
- BENNETT, H., and REED, R. A., 1971. Chemical methods of silicate analysis. Academic Press, London.
- BENSON, W. N., 1915. Spilite lavas and radiolarian rocks in New South Wales. *Geol. Mag.*, v. 60, p. 17-21.

- BEVINS, R. E., 1978. Pumpellyite-bearing basic igneous rocks from the Lower Ordovician of North Pembrokeshire. *Miner. Mag.*, v. 42, p. 81-83.
- BEVINS, R. E., and ROACH, R. A. (in press). Early Ordovician volcanism in Dyfed, S. Wales. In Harris, A. L., et al. (Eds.). *The Caledonides of the British Isles - Reviewed*. Geol. Soc. Lond.
- BEVINS, R. E., and ROACH, R. A. (in press). Pillow lava and isolated-pillow breccia of rhyodacitic composition from the Fishguard Volcanic Group, Lower Ordovician, S.W. Wales, United Kingdom. *J. Geol.*
- BISHOP, D. G., 1972. Progressive metamorphism from prehnite-pumpellyite facies to greenschist facies in the Darnsey Pass area, Otago, New Zealand. *Geol. Soc. Am. Bull.*, v. 83, p. 3177-3198.
- BLOXAM, T. W., and PRICE, N. B., 1961. Stilpnomelane in North Wales. *Nature*, v. 190, p. 525-526.
- BOLES, J. R., and COOMBS, D. S., 1975. Mineral reactions in zeolitic Triassic tuff, Hokonui Hills, New Zealand. *Geol. Soc. Am. Bull.*, v. 86, p. 163-173.
- BOLES, J. R., and COOMBS, D. S., 1977. Zeolite facies alteration of sandstones in the Southland Syncline, New Zealand. *Am. J. Sci.*, v. 277, p. 982-1012.
- BONNATTI, E., 1970. Deep sea volcanism. *Naturwissenschaften*, v. 57, p. 379-384.
- BOUGAULT, H., 1977. First transition series elements: Fractional crystallization and partial melting. In Aumento, F., Melson, W. G., et al., *Initial Reports of the Deep Sea Drilling Project, Volume 37*, Washington (U.S. Government Printing Office), p. 539-546.

- BOUMA, A. H., 1975. Sedimentary structures of Phillipine Sea and Sea of Japan Sediments, DSDP Leg 31. In Karig, D. E., Ingle, J. C., Jr., et al., 1975. Initial Reports of the Deep Sea Drilling Project, Volume 31, Washington (U.S. Government Printing Office), p. 471-488.
- BROMLEY, A. V., 1965. Intrusive quartz latites in the Blaenan Ffestiniog area, Merioneth. *Geol. J.*, v. 4, p. 247-256.
- BROWN, E. H., 1967. The greenschist facies in part of Eastern Otago, New Zealand. *Contr. Miner. Petrology*, v. 14, p. 259-292.
- BRUHN, R. L., STERN, C. R., and DE WIT, M. J., 1978. Field and geochemical data bearing on the development of a Mesozoic volcano-tectonic rift zone and back arc basin in southernmost South America. *Earth planet. Sci. Lett.*, v. 41, p. 32-46.
- BRYAN, W. B., 1972. Morphology of quench crystals in submarine basalts. *J. geophys. Res.*, v. 77, p. 5812-5819.
- BYERLY, G., MELSON, W. G., and VOGT, P. R., 1976. Rhyodacites, andesites, ferro-basalts, and ocean tholeiites from the Galapagos Spreading Center. *Earth planet. Sci. Lett.*, v. 30, p. 215-221.
- CANN, J. R., 1969. Spilites from the Carlsberg Ridge, Indian Ocean. *J. Petrology*, v. 10, p. 1-19.
- CANN, J. R., 1970. Rb, Sr, Y, Zr, and Nb in some ocean floor basaltic rocks. *Earth planet. Sci. Lett.*, v. 10, p. 7-11.
- CANN, J. R., 1971. Metamorphic rocks from Palmer Ridge. *Phil. Trans. R. Soc. Lond.*, v. 268, p. 605-617.



- CARLISLE, D., 1963. Pillow breccias and their aquagene tuffs, Quadra Island, British Columbia. *J. Geol.*, v. 71, p. 48-71.
- CARMICHAEL, I. S. E., 1964. The petrology of Thingmuli, a Tertiary volcano in Eastern Iceland. *J. Petrology*, v. 5, p. 95-131.
- CARMICHAEL, I. S. E., TURNER, F. J., and VERHOOGEN, J., 1974. *Igneous petrology*. McGraw-Hill Book Co.
- CHAUVEL, J-J., 1973. Matériaux pour la connaissance des minéraux du groupe des stilpnomélanes. *Bull. Soc. géol. Minér. Bretagne*, v. 5, p. 51-91.
- COISH, R. A., 1977. Ocean floor metamorphism in the Betts Cove Ophiolite, Newfoundland. *Contr. Miner. Petrology*, v. 60, p. 255-270.
- COOMBS, D. S., 1960. Lower grade mineral facies in New Zealand. *Rep. Int. Geol. Congr. 21st Session, Norden, Pt. XIII*, p. 339-351.
- COOMBS, D. S., 1974. On the mineral facies of spilitic rocks and their genesis. *In* Amstutz, G. C. (Ed.), *Spilites and spilitic rocks*. Springer Verlag.
- COOMBS, D. S., NAKAMURA, Y., and VUAGNAT, M., 1976. Pumpellyite-actinolite facies schists of the Taveyanne Formation near Loèche, Valais, Switzerland. *J. Petrology*, v. 17, p. 440-471.
- COX, A. H., 1915. The geology of the district between Abereiddy and Abercastle. *Q. J. geol. Soc. Lond.*, v. 71, p. 273-340.

- COX, A. H., 1930. Preliminary note on the geological structure of Pen Caer and Strumble Head, Pembrokeshire. *Proc. geol. Ass.*, v. 41, p. 274-289.
- COX, A. H., GREEN, J. F. N., JONES, O. T., and PRINGLE, J., 1930a. The geology of the St. David's District, Pembrokeshire. *Proc. geol. Ass.*, v. 41, p. 241-273.
- COX, A. H., GREEN, J. F. N., JONES, O. T., and PRINGLE, J., 1930b. The St. David's District. Report of the summer field meeting, 1930. *Proc. geol. Ass.*, v. 41, p. 412-438.
- COX, A. H., and JONES, O. T., 1914. Pillow lavas in North and South Wales. *Rep. Br. Ass. Advmt. Sci. 1913* (Birmingham), p. 495.
- CRISTOFILINI, R., GIROLAMO, P. DI., STANZIONE, D., 1973. Caratteri genetici e mineralogici di ialoclastiti dell'Altopiano Ibleo (Sicilia) e dell'Isola di Procida (Campania). *Soc. Italiana Mineralogia e Petrologia Milano*, v. XXIX, p. 497-552.
- DAVIES, E. R., 1936. The geology of the Fishguard and Newport districts, North Pembrokeshire. Unpublished M.Sc. thesis, University of Wales.
- DAVIES, R. G., 1958. The Cader Idris granophyre and its associated rock. *Q. J. geol. Soc. Lond.*, v. 115, p. 189-216.
- DE ROEVER, W. P., 1947. Igneous and metamorphic rocks in eastern central Celebes. In Geological explorations in the island of Celebes under the leadership of H. A. Brouwer. Amsterdam: North Holland Publ. Co., p. 65-173.

- DOBSON, M. R., EVANS, W. E., and WHITTINGTON, R., 1973. The geology of the South Irish Sea. Rep. Inst. geol. Sci. No. 73/11.
- DONALDSON, C. H., USSELMAN, T. M., WILLIAMS, R. J., and LOFGREN, G. E., 1975. Experimental modelling of the cooling history of Apollo 12 olivine basalts. Proc. Lunar Sci. Conf. 6th, p. 843-869.
- DUNHAM, A. C., and WILKINSON, F. C. F., 1978. Accuracy, precision and detection limits of energy-dispersive electron microprobe analyses of silicates. X-ray Spectrom., v. 7, p. 50-56.
- DUNKELEY, P. N., 1978. The geology of the SW Arans with particular reference to the igneous history. Unpublished Ph.D. thesis, University of Wales.
- EALLES, H. V., and ROBEY, J., Van A., 1976. Differentiation of tholeiitic karroo magma at Birds River, South Africa. Contr. Miner. Petrology, v. 56, p. 101-117.
- ELSDEN, J. V., 1905. On the igneous rocks occurring between St. David's Head and Strumble Head, Pembrokeshire. Q. J. geol. Soc. Lond., v. 61, p. 579-607.
- ELSDEN, J. V., 1908. The St. David's Head 'Rock Series', Pembrokeshire. Q. J. geol. Soc., Lond., v. 64, p. 273-296.
- ERNST, W. G., SEKI, Y., ONUKI, H., and GILBERT, M. C., 1970. Comparative study of low-grade metamorphism in the California Coast Ranges and the outer metamorphic belt of Japan. Mem. geol. Soc. Am., 124.

- EVANS, W. D., 1945. The geology of the Prescelly Hills, north Pembrokeshire. *Q. J. geol. Soc. Lond.*, v. 101, p. 89-107.
- EVANS, W. D., 1948. The Cambrian-Ordovician junction, Whitesand Bay, Pembrokeshire. *Geol. Mag.*, v. 85, p. 110-112.
- EWART, A., OVERSBY, V. M., and MATEEN, A., 1977. Petrology and isotope geochemistry of Tertiary lavas from the northern flank of the Tweed Volcano, Southeastern Queensland. *J. Petrology*, v. 18, p. 73-113.
- EWART, A., TAYLOR, S. R., and CAPP, A. C., 1968. Trace and minor element geochemistry of the rhyolitic volcanic rocks, Central North Island, New Zealand. *Cont. Mineral. Petrol.*, v. 18, p. 76-104.
- FAWCETT, J. J., and YODER, H. S., 1966. Phase relationships of chlorites in the system  $\text{MgO-Al}_2\text{O}_3\text{-SiO}_2\text{-H}_2\text{O}$ . *Am. Mineral.*, v. 51, p. 353-380.
- FERRARA, G., and TREUIL, M., 1974. Petrological implications of trace element and Sr Isotope distributions in Basalt-Pantellerite Series. *Bull. Volc.*, v. 38, p. 548-574.
- FETTES, D. J., GRAHAM, C. M., SASSI, F. P., and SCOLARI, A., 1976. The basal spacing of potassic white micas and facies series variation across the Caledonides. *Scott. J. Geol.*, v. 12, p. 227-236.
- FISHER, R. V., 1961. Proposed classification of volcanoclastic sediments and rocks. *Geol. Soc. Am. Bull.*, v. 72, p. 1409-1414.
- FISKE, R. S., 1963. Subaqueous pyroclastic flows in the Ohanapecosh Formation, Washington. *Geol. Soc. Am. Bull.*, v. 74, p. 391-406.

- FISKE, R. S., and MATSUDA, J., 1964. Submarine equivalents of ash flows in the Tokiwa Formation, Japan. *Am. J. Sci.*, v. 262, p. 76-106.
- FITCHES, W. R., 1972. Polyphase deformation structures in the Welsh Caledonides near Aberystwyth. *Geol. Mag.*, v. 109, p. 149-155.
- FITTON, J. G., and HUGHES, D. J., 1970. Volcanism and plate tectonics in the British Ordovician. *Earth planet. Sci. Lett.*, v. 8, p. 223-228.
- FLANAGHAN, F. J., 1973. 1972-values for international geochemical reference standards. *Geochim. cosmochim. Acta*, v. 37, p. 1189-1200.
- FLANAGHAN, F. J., 1974. Reference samples for the earth sciences. *Geochim. cosmochim. Acta*, v. 38, p. 1731-1744.
- FLOWER, M. F. J., ROBINSON, P. T., SCHMINCKE, H-U., and OHNMACHT, W., 1977. Magma fractionation systems beneath the Mid-Atlantic Ridge at 36°-37°N. *Contrib. Mineral. Petrology*, v. 64, p. 167-195.
- FLOYD, P. A., 1976. Geochemical variation within the greenstones of S.W. England. *J. Petrology*, v. 17, p. 522-545.
- FLOYD, P. A., 1977. Rare earth element mobility and geochemical characterisation of spilitic rocks. *Nature*, v. 269, p. 134-137.
- FLOYD, P. A., LEES, G. J., and ROACH, R. A., 1976. Basic intrusions in the Ordovician of North Wales - geochemical data and tectonic setting. *Proc. geol. Ass.*, v. 87, p. 389-400.

- FLOYD, P. A., and WINCHESTER, J. A., 1975. Magma type and tectonic setting discrimination using immobile elements. *Earth planet. Sci. Lett.*, v. 27, p. 211-218.
- FLOYD, P. A., and WINCHESTER, J. A., 1978. Identification and discrimination of altered and metamorphosed volcanic rocks using immobile elements. *Chem. Geol.*, v. 21, p. 291-306.
- FOSTER, M. D., 1962. Interpretation of the composition and a classification of the chlorites. *U.S. Geol. Surv. Prof. Paper 414-A*, 33p.
- FOUQUÉ, F., 1879. *Santorin et ses éruptions*. Paris.
- FRANKLIN, J. M., 1976. Role of laharc breccia in the genesis of volcanogenic massive sulphide deposits. *Geol. Surv. Can. Paper 76-1A*, p. 293-300.
- FREY, F. A., BRYAN, W. B., and THOMPSON, G., 1974. Atlantic Ocean floor: Geochemistry and petrology of basalts from Legs 2 and 3 of the Deep Sea Drilling Project. *J. geophys. Res.*, v. 79, p. 5507-5527.
- FURNES, H., 1972. Metahyaloclastite breccias associated with Ordovician pillow lavas in the Solund area, W. Norway. *Norsk geol. Tidsskr.*, v. 52, p. 385-407.
- FURNES, H., 1974. Structural and metamorphic history of the Lower Palaeozoic meta-volcanics and associated sediments in the Solund area, Sogn. *Norsk geol. Unders.*, v. 302, p. 33-74.

- FURNES, H., 1975. Experimental palagonitization of basaltic glasses of varied composition. *Contr. Miner. Petrology*, v. 50, p. 105-113.
- FURNES, H., SKJERLIE, F. J., and TYSSELAND, M., 1976. Plate tectonic model based on greenstone geochemistry in the late Precambrian-Lower Palaeozoic in the Solund-Staufjorden areas, West Norway. *Norsk geol. Tidsskr.*, v. 56, p. 161-186.
- GAST, P. W., 1968. Trace element fractionation and the origin of tholeiitic and alkaline magma types. *Geochim. cosmochim. Acta*, v. 32, p. 1057-1086.
- GEORGE, T. N., 1970. *British Regional Geology. South Wales. Third edition.* Inst. of Geol. Sci. H.M.S.O. London, i-xii, 1-152.
- GIBB, F. G. F., 1973. The zoned clinopyroxenes of the Shiant Isles Sill, Scotland. *J. Petrology*, v. 14, p. 203-230.
- GLASSLEY, W. E., 1974. A model for phase equilibria in the prehnite-pumpellyite facies. *Contr. Miner. Petrology*, v. 43, p. 317-332.
- GLASSLEY, W. E., 1975. Low variance phase relationships in a prehnite-pumpellyite facies terrain. *Lithos*, v. 8, p. 69-76.
- GRABER, F. H., LUKENS, H. R., and MACKENZIE, J. K., 1970. Neutron activation analysis determination of all 14 stable rare-earth elements with group separation and Ge(Li) spectrometry. *J. Radioanalytical Chem.*, v. 4, p. 229-239.
- GREEN, J. F. N., 1908. The geological structure of the St. David's area. *Q. J. geol. Soc. Lond.*, v. 64, p. 363-383.

- GREEN, D. H., 1970. The origin of basaltic and nephelinitic magmas. Trans. Leicester Lit. Phil. Soc., v. 64, p. 26-54.
- GÜVEN, N., 1971. The crystal structure of 2M phengite and 2M muscovite. Zeits. Krist., v. 134, p. 196-212.
- HAMPTON, M. A., 1972. The role of subaqueous debris flow in generating turbidity currents. J. Sed. Petrology, v. 42, p. 775-793.
- HANSON, G. N., 1978. The application of trace elements to the petrogenesis of igneous rocks of granitic composition. Earth planet. Sci. Lett., v. 38, p. 26-43.
- HART, R. A., 1970. Chemical exchange between sea-water and deep ocean basalts. Earth planet. Sci. Lett., v. 9, p. 269-279.
- HART, R. A., 1973. A model for chemical exchange in the basalt - sea-water system of oceanic layer II. Can. J. Earth Sci., v. 10, p. 199-216.
- HART, S. R., 1969. K, Rb, Cs contents and K/Rb, K/Cs ratio of fresh and altered submarine basalts. Earth planet. Sci. Lett., v. 6, p. 295-303.
- HARVEY, P. K., TAYLOR, D. M., HENDRY, R. D., and BANCROFT, F., 1973. An accurate fusion method for the analysis of rocks and chemically related materials by x-ray fluorescence spectrometry. X-Ray Spectry., v. 2, p. 33-44.
- HATTORI, H., SUGISAKI, R., and TAKANA, T., 1972. Nature of hydration in Japanese Palaeozoic geosynclinal basalt. Earth planet. Sci. Lett., v. 15, p. 271-285.
- HELLMAN, P. L., and HENDERSON, P., 1977. Are rare earths mobile during spilitization? Nature, v. 267, p. 38-40.



- HENDERSON, J. F., 1953. On the formation of pillow lavas and breccias. R. Soc. Can. Trans. 3rd ser. sect. 4, v. 47, p. 23-32.
- HERRMANN, A. G., 1970. Yttrium and Lanthanides. In Wedepohl, K. H. (Ed.). Handbook of geochemistry, vol. II/2, 39, 57-71 B-0. Berlin-Heidelberg-New York: Springer Verlag.
- HEY, M. H., 1954. A new review of the chlorites. Miner. Mag., v. 30, p. 277-292.
- HICKS, H., 1884. On the Precambrian rocks of Pembrokehire with especial reference to the St. David's district. Q. J. geol. Soc. Lond., v. 40, p. 507-547.
- HONNOREZ, J., 1961. Sur l'origine des hyaloclastites. Bull. Soc. Belg. Géol., v. 70, p. 407-412.
- HONNOREZ, J., and KIRST, P., 1975. Submarine basaltic volcanism: Morphometric parameters for discriminating hyaloclastites from hyalotuffs. Bull. Volc., v. 39, p. 441-465.
- HORIKOSHI, E., 1969. Volcanic activity related to the formation of the Kuroko-type deposits in the Kosaka district, Japan. Mineral. Deposita, v. 4, p. 321-345.
- HUGHES, C. J., and MALPAS, J. G., 1971. Metasomatism in the Late Precambrian Bull Arm Formation in southeastern Newfoundland: recognition and implications. Proc. Geol. Ass. Can., v. 24, p. 85-93.
- HUGHES, D. J., 1972. The petrochemistry of the Ordovician igneous rocks of the Welsh Basin - a review. Proc. geol. Soc. Lond., v. 128, p. 418.

- IWASAKI, M., 1963. Metamorphic rocks of the Kotu-Bizan area, eastern Shikoku. *J. Fac. Sci. Tokyo Univ., Sect. II*, v. 15, p. 1-90.
- JACKOBSSON, S. P., 1972. On the consolidation and palagonitization of the tephra of the Surtsey volcanic island, Iceland. *Surtsey Prog. Rep.*, VI, p. 7-8.
- JAGGAR, T. A., 1908. The evolution of Bogoslof Volcano. *Bull. Am. Geogr. Soc.*, v. 40, p. 385-400.
- JAMES, D. M. D., 1975. Caradoc turbidites at Poppit Sands (Pembrokeshire), Wales. *Geol. Mag.*, v. 112, p. 295-304.
- JEANS, P. J. F., 1973. Plate tectonic reconstruction of the southern Caledonides of Great Britain. *Nature*, v. 245, p. 120-122.
- JENKINS, D. A., and BALL, D. F., 1964. Pumpellyite in Snowdonian soils and rocks. *Miner. Mag.*, v. 33, p. 1093-1096.
- JENKINS, R., and DE VRIES, J. L., 1967. Practical x-ray spectrometry. MacMillan, London, pp. 109.
- JOLLY, W. T., and SMITH, R. E., 1972. Degradation and metamorphic differentiation of the Keweenawan tholeiitic lavas of northern Michigan, U.S.A. *J. Petrology*, v. 13, p. 273-309.
- JONES, J. G., 1968. Pillow lava and pahoehoe. *J. Geol.*, v. 76, p. 485-488.
- JONES, J. G., 1969. Pillow lavas as depth indicators. *Am. J. Sci.*, v. 267, p. 181-195.
- JONES, O. T., 1940. Some Lower Palaeozoic contacts in Pembrokeshire. *Geol. Mag.*, v. 77, p. 405-409.
- JOHNSTON, W. E. Q., 1969. Pillow lava and pahoehoe: A discussion. *J. Geol.*, v. 77, p. 730-732.

- KAWACHI, Y., 1975. Pumpellyite-actinolite and contiguous facies metamorphism in part of Upper Wakatipu District, South Island, New Zealand. *N.Z.J. of Geol. Geophys.*, v. 18, p. 401-441.
- KOKELAAR, B. P., 1977. The igneous history of the Rhobell Fawr area, Merioneth, North Wales. Unpublished Ph.D. thesis, University of Wales.
- KUBLER, B., 1964. Les argiles, indicateurs de métamorphisme. *Rev. Inst. Fr. Pétrole.*, v. 19, p. 1093-1112.
- KUNIYOSHI, S., and LIOU, J. G., 1976. Contact metamorphism of the Karmutsen volcanics, Vancouver Island, British Columbia. *J. Petrology*, v. 17, p. 73-99.
- KUSHIRO, I., 1960. Si-Al relation in clinopyroxenes from igneous rocks. *Am. J. Sci.*, v. 258, p. 548-554.
- KUSHIRO, I., 1962. Clinopyroxene solid solutions, pt. 1, The  $\text{CaAl}_2\text{SiO}_6$  component. *Jap. J. Geol. Geog.*, v. 33, p. 213-220.
- KUSHIRO, I., 1973. Partial melting of garnet-lherzolites from kimberlite at high pressures. In Nixon, P. H. (Ed.), *Lesotho Kimberlites*. Lesotho Nat. Development Corp., p. 294-299.
- LEAKE, B. E., HENDRY, G. L., KEMP, A., PLANT, A. G., HARVEY, P. K., WILSON, J. R., COATS, J. S., AUCOTT, J. W., LUNEL, T., and HOWARTH, R. J., 1969. The chemical analysis of rock powders by automatic x-ray fluorescence. *Chem. Geol.* v. 5, p. 7-86.
- LE BAS, M. J., 1962. The role of aluminium in igneous clinopyroxenes with relation to their parentage. *Am. J. Sci.*, v. 260, p. 267-288.

- LIU, J. G., 1971. Synthesis and stability relations of prehnite,  $\text{Ca}_2\text{Al}_2\text{Si}_3\text{O}_{10}(\text{OH})_2$ . *Am. Mineral.*, v. 56, p. 507-531.
- LIPPLE, S. L., 1972. Silica-rich pillow lavas near Soansville, Marble Bar 1 : 250000 sheet. *Annual Rep. W. Aust. Geol. Surv.*, p. 52-57.
- LOFGREN, G., 1970. Experimental devitrification rate of rhyolite glass. *Geol. Soc. Am. Bull.*, v. 81, p. 553-560.
- LOFGREN, G., 1974. An experimental study of plagioclase crystal morphology: Isothermal crystallization. *Am. J. Sci.*, v. 274, p. 243-273.
- LOFGREN, G., DONALDSON, C. H., WILLIAMS, R. J., MULLINS, JR., O., and USSELMAN, T. M., 1974. Experimentally reproduced textures and mineral chemistry of Apollo 15 quartz normative basalts. *Proc. Lunar Sci. Conf. 5th*, v. 1, p. 549-567.
- MACDONALD, G. A., 1972. *Volcanoes*. Englewood Cliffs, New Jersey. Prentice Hall. 510 pp.
- MACDONALD, G. A., and KATSURA, T., 1964. Chemical composition of Hawaiian lavas. *J. Petrology*, v. 5, p. 82-133.
- MANSON, V., 1968. Geochemistry of basaltic rocks: Major elements. In Hess and Poldervaart (Eds.), *Basalts - the Poldervaart treatise of rocks of basaltic composition*. Interscience, New York, v. 1, p. 215-269.
- MATTHEWS, D. H., 1971. Altered basalts from Swallow Bank, an abyssal hill in the NE Atlantic and from a nearby seamount. *Phil. Trans. R. Soc. Lond.*, v. 268, p. 551-571.

- MATTLEY, C. A., and WILSON, T. S., 1946. The Harlech Dome north of the Barmouth estuary. *Q. J. geol. Soc. Lond.*, v. 102, p. 1-40.
- McBIRNEY, A. R., 1963. Deep-sea volcanism. *Bull. volc.*, v. 26, p. 453-469.
- MELSON, W. G., 1973. Basaltic glasses from the Deep Sea Drilling Project. Chemical characteristics, compositions of alteration products and fission track "ages". *EOS Am. Geophys. Union Trans.*, v. 54, p. 1011-1014.
- MELSON, W. G., and VAN ANDEL, T. H., 1966. Metamorphism in the mid-Atlantic Ridge, 22°N latitude. *Marine Geol.*, v. 4, p. 165-186.
- MELSON, W. G., THOMPSON, G., and VAN ANDEL, T. H., 1968. Volcanism and metamorphism in the Mid-Atlantic Ridge, 22°N Latitude. *J. geophys. Res.*, v. 73, p. 5925-5941.
- MENZIES, M., 1976. Rare earth geochemistry of fused ophiolitic and alpine lherzolites - I. Othris, Lanzo, and Troodos. *Geochim. cosmochim. Acta*, v. 40, p. 645-656.
- MEVEL, C., 1975. Les zonations chimiques dans les pillow-lavas spilittiques du Chenaillet et des Gets (Alpes françaises). *Pétrologie*, v. 1, p. 319-333.
- MEVEL, C., and VELDE, D., 1976. Clinopyroxenes in Mesozoic pillow lavas from the French Alps: Influence of cooling rate on compositional trends. *Earth planet. Sci. Lett.*, v. 32, p. 158-164.
- MINSTER, J. F., MINSTER, J. B., TREUIL, M., and ALLEGRE, C. J., 1977. Systematic use of trace elements in igneous processes. Part II. Inverse problem of the fractional crystallization process in volcanic suites. *Contr. Miner. Petrology*, v. 61, p. 49-77.

- MIYASHIRO, A., SHIDO, F., and EWING, M., 1971. Metamorphism in the Mid-Atlantic Ridge near 24° and 30°N. *Phil. Trans. R. Soc. Lond. Ser. A*, v. 268, p. 589-603.
- MOORE, J. G., 1965. Petrology of deep-sea basalt near Hawaii. *Am. J. Sci.*, v. 263, p. 40-52.
- MOORE, J. G., 1966. Rate of palagonitization of submarine basalt adjacent to Hawaii. *U.S. geol. Surv. Prof. Paper* 550D, D163-171.
- MOORE, J. G., 1970. Pillow lava in a historic lava flow from Hualalai volcano, Hawaii. *J. Geol.* v. 78, p. 239-243.
- MOORE, J. G., 1975. Mechanism of formation of pillow lava. *Amer. Scientist*, v. 63, p. 269-277.
- MOORE, J. G., CRISTOFILINI, R., and LO GUIDICE, A., 1971. Development of pillows on the submarine extension of recent lava flows, Mount Etna, Sicily. *U.S. geol. Surv. Prof. Paper* 750-c, c89-97.
- MOORE, J. G., PHILLIPS, R. L., GRIGG, R. W., PETERSON, D. W., and SWANSON, D. A., 1973. Flow of lava into the sea 1969-1971, Kilauea Volcano, Hawaii. *Geol. Soc. Am. Bull.*, v. 84, p. 537-546.
- MORIMOTO, R., and OSSAKA, J., 1955. The 1952-1953 submarine eruption of the Myojin Reef near the Bayonnaise rocks, Japan. (1). *Earth Res. Inst. Bull.*, v. 33, p. 221-250.
- MORRE-BIOT, N., 1970. *Pétrologie des formations volcanologiques de Permo-Carbonifère du nord de la France*. *Annls. scient. Univ. Besançon, Sér. 3, Geol.*, v. 10, 148 pp.

- MUIR, I. E., and TILLEY, C. E., 1964. Iron enrichment and pyroxene fractionation trends in tholeiites. *Geol. J.*, v. 4, p. 143-156.
- MYERS, J., 1950. Note on the age of rocks on the east side of Newport Bay, Pembrokeshire. *Geol. Mag.*, v. 87, p. 263-264.
- NAKAJIMA, T., BANNO, S., and SUKUI, T., 1977. Relations leading to the disappearance of pumpellyite in low-grade metamorphic rocks of the Sanbagawa Metamorphic belt in Central Shikoku. *J. Petrology*, v. 18, p. 263-284.
- NASH, W. P. and WILKINSON, J. F. G., 1970. Shonkin Sag Laccolith, Montana. I. Mafic minerals and estimates of pressure, oxygen fugacity and silica activity. *Contr. Miner. Petrology*, v. 25, p. 241-269.
- NAYUDU, Y. R., 1962. Submarine eruptions of basalts and the problems of palagonitization. *Int. symp. of volcanology, Japan, 1962.* (Abstracts).
- NICHOLLS, G. D., 1959. Autometasomatism in the Lower Spilites of the Builth Volcanic Series. *Q. J. geol. Soc. Lond.*, v. 114, p. 137-162.
- NISBET, E. G., and PEARCE, J. A., 1977. Clinopyroxene composition in mafic lavas from different tectonic settings. *Contr. Miner. Petrology*, v. 63, p. 149-160.
- NITSCH, K. H., 1971. Stabilitätsbeziehungen von Prehnit und pumpellyithaltigen paragenesen. *Contr. Miner. Petrology*, v. 30, p. 240-260.

- NOBLE, D. C., 1967. Sodium, potassium and ferrous iron contents of some secondarily hydrated natural silica glasses. *Am. Mineral.*, v. 52, p. 280-286.
- NORRISH, K., and HUTTON, J. T., 1969. An accurate x-ray spectrographic method for the analysis of a wide range of geological samples. *Geochim. cosmochim. Acta*, v. 33, p. 431-453.
- O'HARA, M. J., 1977. Geochemical evolution during fractional crystallization of a periodically refilled magma chamber. *Nature*, v. 266, p. 503-507.
- O'HARA, M. J., SAUNDERS, M. J., and MERCY, E. L. P., 1975. In Ahrens, L. H., et al. (Eds.). *Physics and chemistry of the Earth*, v. 9, p. 571-604.
- OLIVER, G. J. H., 1978. Prehnite-pumpellyite facies metamorphism in County Cavan, Ireland. *Nature*, v. 274, p. 242-243.
- OWEN, T. R., BLOXAM, T. W., JONES, D. G., WALMSLEY, V. G., and WILLIAMS, B. P. J., 1971. Summer (1968) Field meeting in Pembrokeshire (South Wales). *Proc. geol. Ass.*, v. 82, p. 17-60.
- PAPIKE, J. J., CAMERON, K. L., and BALDWIN, K., 1974. Amphiboles and pyroxenes. Characterization of other than quadrilateral components and estimates of ferric iron from microprobe data (abstract). *Geol. Soc. Am. Abstr. Progm.*, v. 6, p. 1053-1054.
- PARKINSON, J., 1897. Some igneous rocks in north Pembrokeshire. *Q. J. geol. Soc. Lond.*, v. 53, p. 465-476.



- PART, G. M., 1922. Notes on the Ordovician lavas of the Mynydd Prescelly, North Pembrokeshire. *Geol. Mag.*, v. 54, p. 310-323.
- PASSAGLIA, E., and GOTTARDI, G., 1973. Crystal chemistry and nomenclature of pumpellyites and julgoldites. *Can. Miner.*, v. 12, p. 219-223.
- PEARCE, J. A., 1975. Basalt geochemistry used to investigate past tectonic environments on Cyprus. *Tectonophys.*, v. 25, p. 41-68.
- PEARCE, J. A., and CANN, J. R., 1971. Ophiolite origin investigated by discriminant analysis using Ti, Zr and Y. *Earth planet. Sci. Lett.*, v. 12, p. 339-349.
- PEARCE, J. A., and CANN, J. R., 1973. Tectonic setting of basic volcanic rocks determined using trace element analyses. *Earth planet. Sci. Lett.*, v. 19, p. 290-300.
- PEARCE, J. A., and FLOWER, M. F. J., 1977. The relative importance of petrogenetic variables in magma genesis at accreting plate margins: a preliminary investigation. *J. Geol. Soc. Lond.*, v. 134, p. 103-127.
- PEARCE, T. H., GORMAN, B. E., and BIRKETT, T. C., 1975. The  $TiO_2$ - $K_2O$ - $P_2O_5$  diagram: a method of discriminating between oceanic and non-oceanic basalts. *Earth planet. Sci. Lett.*, v. 24, p. 419-426.
- PHILLIPS, W. E. A., STILLMAN, C. J., and MURPHY, T., 1976. A Caledonian plate tectonic model. *J. geol. Soc. Lond.*, v. 132, p. 579-609.
- PICHLER, H., 1965. Acid hyaloclastites. *Bull. Volc.*, v. 28, p. 293-310.
- POLDERVAART, A., and HESS, H. H., 1951. Pyroxenes in the crystallization of basaltic magma. *J. Geol.*, v. 59, p. 472-489.

- PRINGLE, J., 1930. The geology of Ramsey Island (Pembrokeshire).  
Proc. Geol. Ass., v. 41, p. 1-31.
- RAAM, A., O'REILLY, S., and VERNON, R. H., 1969. Pumpellyite of  
deuteric origin. Am. Mineral., v. 54, p. 320-324.
- RAST, N., 1969. The relationship between Ordovician structure and  
vulcanicity in Wales. In Wood, A. (Ed.), The Pre-Cambrian  
and Lower Palaeozoic rocks of Wales. Univ. of Wales Press,  
Cardiff, p. 337-356.
- RAYLEIGH, J. W. S., 1896. Theoretical considerations respecting  
the separation of gases by diffusion and similar processes.  
Philos. Mag., v. 42, p. 493-498.
- REED, F. R. C., 1895. The geology of the country around Fishguard,  
Pembrokeshire. Q. J. geol. Soc. Lond., v. 51, p. 149-195.
- REYNOLDS, R. C., 1963. Matrix corrections in trace element analysis  
by x-ray fluorescence estimation of the mass absorption  
coefficient by Compton scattering. Am. Miner., v. 48,  
p. 1133-1143.
- RIDGEWAY, J., 1971. The stratigraphy and petrology of Ordovician  
volcanic rocks adjacent to the Bala Fault in Merionethshire.  
Unpublished Ph.D. thesis, University of Liverpool.
- RINGWOOD, A. E., 1955. The principles governing trace element  
behaviour during magmatic crystallization. Part II:  
the role of complex formation. Geochim. cosmochim. Acta,  
v. 7, p. 242-254.

- RINGWOOD, A. E., 1966. Mineralogy of the mantle. In Hurley, P. M. (Ed.), *Advances in Earth Sciences*. MIT Press, Cambridge, Mass., p. 357-399.
- RITTMANN, A., 1960. *Vulkane und ihre Tätigkeit*. 2. Aufl. 336 pp. Stuttgart.
- RITTMANN, A., 1958. Il meccanismo di formazione delle lave a pillows e dei cosiddetti tufi palagonitici. *Acad. Gioenia. Sc. Natur.*, Serie 4.
- ROACH, R. A., 1969. The composite nature of the St. David's Head and Carn Llidi intrusions of North Pembrokeshire. In Wood, A. (Ed.). *The Pre-Cambrian and Lower Palaeozoic rocks of Wales*. Univ. of Wales Press, Cardiff, p. 409-433.
- ROACH, R. A., FLOYD, P. A., and REA, W. J., 1972. The petrochemistry of the Lower Palaeozoic intrusives along the north Pembrokeshire coast. *Proc. geol. Soc. Lond.*, v. 128, p. 418-419.
- ROBERTS, B., 1967. Succession and structure in the Llwyd Mawr syncline, Caernarvon-shire, North Wales. *Geol. J.*, v. 5, p. 369-390.
- ROSENBUSCH, H., 1885. *Mikroskop. Physiogr.* 2nd edit., v. i.
- ROSENBUSCH, H., 1887. *Mikroskop. Physiogr.* 2nd edit., v. ii.
- ROWBOTHAM, G., and BEVINS, R. E., 1978. Textures and compositions of pyroxenes in basic igneous rocks of Ordovician age from North Pembrokeshire. *J. geol. Soc. Lond.*, v. 135, p. 589-590.
- SAHAMA, T. G., 1946. On the crystal chemistry of the mineral titanite. *Bull. Comm. géol. Finl.*, v. 138, p. 88-120.

- SALTERLEY, J., 1941a. Pillow lavas from the Dryden-Wabigoon area, Kenora district, Ontario. Toronto Univ. Studies, Geol. Ser., v. 46, p. 119-136.
- SALTERLEY, J., 1941b. Geology of the Dryden-Wabigoon area (Ontario). Ontario Dept. Mines 50th Ann. Rept., v. 50, pt. 2, pp. 67.
- SCEAL, J. S. C., and WEAVER, S. D., 1971. Trace element data on the origin of salic rocks from the Quaternary volcano Paka, Gregory Rift, Kenya. Earth planet. Sci. Lett., v. 12, p. 327-331.
- SCHERMERHORN, L. J. G., 1975. Pumpellyite-facies metamorphism in the Spanish pyrite belt. *Pétrologie*, v. 1, p. 71-86.
- SCHILLING, J.-G., and WINCHESTER, J. A., 1967. Rare earth fractionation and magmatic processes. In Runcorn, S. K. (Ed.). *Mantles of the earth and terrestrial planets*. Wiley, London, p. 267-283.
- SCHMINKE, H.-U., and STAUDIGEL, H., 1976. Pillow lavas on central and eastern Atlantic Islands (La Palma, Gran Canaria, Porto Santo, Santa Maria). *Bull. Soc., géol. France*, v. XVIII, p. 871-883.
- SEKI, Y., 1961. Pumpellyite in low-grade regional metamorphism. *J. Petrology*, v. 2, p. 407-423.
- SHAW, D. M., 1970. Trace element fractionation during anatexis. *Geochim. cosmochim. Acta*, v. 34, p. 237-243.
- SIGVALDASON, G. E., 1962. Epidote and related minerals in two deep geothermal drill holes, Reykjavik and Hveragerdi, Iceland. U.S. geol. Surv. Prof. Paper 450E, p. 77-79.

- SCOTT, R. B., and HAJASH, A., 1976. Initial submarine alteration of basaltic pillow lavas: A microprobe study. *Am. J. Sci.*, v. 276, p. 480-501.
- SMITH, R. E., 1967. Segregation vesicles in basaltic lava. *Am. J. Sci.*, v. 265, p. 696-713.
- SMITH, R. E., 1968. Redistribution of major elements in the alteration of some basic lavas during burial metamorphism. *J. Petrology*, v. 9, p. 191-219.
- SMITH, R. E., and SMITH, S. E., 1976. Comments on the use of Ti, Zr, Y, Sr, K, P, and Nb in classification of basaltic magmas. *Contr. Miner. Petrology*, v. 32, p. 114-120.
- SNYDER, G. L., and FRASER, G. D., 1963. Pillowed lavas, I: Intrusive layered lava pods and pillowed lavas, Unalaska Island, Alaska. *U.S. geol. Surv. prof. paper* 454-B, 23pp.
- SPOONER, E. T. C., and FYFE, W. S., 1973. Sub-seafloor metamorphism, heat and mass transfer. *Contr. Miner. Petrology*, v. 42, p. 287-304.
- STEAD, J. T. G., and WILLIAMS, B. P. J., 1971. The Cambrian of North Pembrokeshire. In Bassett, D. A., and Bassett, M. G. (Eds.). *Geological excursions in South Wales and the Forest of Dean. Geologists' Ass. South Wales Group*, p. 180-198.
- STOESER, D. B., 1975. Igneous rocks from Leg 30 of the Deep Sea Drilling Project. In Andrews, J. E., Packham, G., et al., *Initial reports of the Deep Sea Drilling Project, Volume 30*, Washington (U.S. Government Printing Office), p. 401-414.

- SURDAM, R. C., 1969. Electron microprobe study of prehnite and pumpellyite from the Karmutsen Group, Vancouver Island, British Columbia. *Am. Mineral.*, v. 54, p. 256-266.
- TAZIEFF, H., 1968. Sur le mécanisme des éruptions basaltiques sous-marines à faibles profondeurs et la genèse d'hyaloclastites associée. *Geol. Rundschau*, v. 57, p. 955-966.
- TAZIEFF, H., 1971. About the paper "Volcanic activity related to the formation of the Kuroko-type deposits in the Kosaka district, Japan". Discussion. *Mineral. Deposita*, v. 6, p. 89-90.
- TAZIEFF, H., 1972. About deep-sea volcanism. *Geol. Rundschau*, v. 61, p. 470-480.
- THOMAS, G. E., 1951. The geology of the Pencaer and Fishguard areas, North Pembrokeshire, with special reference to the pillow lava group of the Fishguard Volcanic Series. Unpublished M.Sc. thesis, Univ. of Wales.
- THOMAS, G. E., and THOMAS, T. M., 1956. The volcanic rocks of the area between Fishguard and Strumble Head, Pembrokeshire. *Q. J. geol. Soc. Lond.*, v. 112, p. 291-314.
- THOMAS, H. H., and COX, A. H., 1924. The volcanic series of Treffgarn, Roch and Ambleston (Pembrokeshire). *Q. J. geol. Soc. Lond.*, v. 122, p. 45-62.
- THOMPSON, G., 1973. A geochemical study of the low-temperature interaction of seawater and oceanic igneous rocks. *EOS Am. Geophys. Union Trans.*, v. 54, p. 1015-1019.
- TOKSOZ, M. N., and BIRD, P., 1977. Formation and evolution of marginal basins and continental plateaus. In (Eds.) Talwani, M., and Pitman III, W. C. *Island Arcs, Deep Sea Trenches and Back-Arc Basins*. American Geophysical Union, Washington, D.C., p. 379-393.

- THORPE, R. S., 1970. The origin of a Pre-Cambrian diorite-granite plutonic series from Pembrokeshire (Wales). *Geol. Mag.*, v. 107, p. 491-499.
- TORSKE, T., 1975. Snowflake texture in Ordovician rhyolite from Stord, Hordaland. *Norsk geol. Unders.*, v. 319, p. 17-27.
- TREUIL, M., and VARET, J., 1973. Critières volcanologiques, pétrologiques et géochimiques de la genèse et de la différenciation des magmas basaltiques: exemple de L'Afar. *Bull. Soc. géol. France*, v. 15, p. 506-540.
- VALLANCE, T. G., 1960. Concerning spilites. *Proc. Linn. Soc. N.S.W.*, v. 85, p. 8-52.
- VALLANCE, T. G., 1965. On the chemistry of pillow lavas and the origin of spilites. *Miner. Mag.*, v. 34, p. 471-481.
- VALLANCE, T. G., 1969. Spilites again. Some consequences of the degradation of basalts. *Proc. Linn. Soc. N.S.W.*, v. 94, p. 8-51.
- VALLANCE, T. G., 1974a. Spilitic degradation of a tholeiitic basalt. *J. Petrology*, v. 15, p. 79-96.
- VALLANCE, T. G., 1974b. Pyroxenes and the basalt-spilite relation. In Amstutz, G. C. (Ed.). *Spilites and spilitic rocks*. Springer Verlag.
- VAN DER LINGEN, G. J., 1973. The Lord Howe Rise Rhyolites. In Burns, R. E., Andrews, J. E., et al. Initial Reports of the Deep Sea Drilling Project, Volume 21. Washington, (U.S. Government Printing Office), p. 523-539.

- VON RAHDEN, H. V. R., and VON RAHDEN, M. J. E., 1972. Some aspects of the identification and characterization of <sup>0</sup>14A chlorites. Minerals. Sci. Engng., v. 4, p. 43-54.
- VUAGNAT, M., 1976. Pillow lava flows. Isolated sacks or connected tubes? Bull. volc., v. 39, p. 581-589.
- WAGER, L. R., and BROWN, G. M., 1967. Layered igneous rocks. Edinburgh: Oliver and Boyd.
- WALKER, K. R., 1969. The Palisades Sill, New Jersey: a reinvestigation. Geol. Soc. Am. spec. Paper III.
- WALTHAM, A. C., 1971. A note on the structure and succession at Abereiddy Bay, Pembrokeshire. Geol. Mag., v. 108, p. 49-52.
- WATERS, A. C., 1960. Determining direction of flow in basalts. Am. J. Sci., v. 258, p. 350-366.
- WEAVER, C. E., 1960. Possible uses of clay minerals in the search for oil. Clays and Clay Minerals, v. 8, p. 214-227.
- WEAVER, S. D., SCEAL, J. S. C., and GIBSON, I. L., 1972. Trace element data relevant to the origin of trachytic and pantelleritic lavas in the East Africa rift system. Cont. Miner. Petrology, v. 36, p. 181-194.
- WEBER, K., 1972. Notes on determination of illite crystallinity. N. Jb. Miner. Mh., v. 115, p. 267-276.
- WEILL, D. F., and DRAKE, M. J., 1973. Europium anomaly in plagioclase feldspar: experimental results and semi-quantitative model. Science, v. 180, p. 1059-1060.



- WELLS, A. K., 1925. The geology of the Rhobell Fawr district (Merioneth). Q. J. geol. Soc. Lond., v. 81, p. 463-538.
- WINCHESTER, J. A., and FLOYD, P. A., 1976. Geochemical magma type discrimination: application to altered and metamorphosed basic igneous rocks. Earth planet. Sci. Lett., v. 28, p. 459-469.
- WINCHESTER, J. A., and FLOYD, P. A., 1977. Geochemical discrimination of different magma series and their differentiation products using immobile elements. Chem. Geol., v. 20, p. 325-343.
- WICHMANN, A., 1921. Die vulkane der Sangi-Inseln. Verhandl. Kon. Akad. V. Wetensch., Amsterdam, v. 22, p. 3-52.
- WILLIAMS, T. G., 1934. The Precambrian and Lower Palaeozoic rocks of the eastern end of the St. David's Pre-Cambrian area, Pembrokeshire. Q. J. geol. Soc. Lond., v. 90, p. 32-75.
- WOOD, D. A., 1978. Major and trace element variations in the Tertiary lavas of Eastern Iceland and their significance with respect to the Iceland geochemical anomaly. J. Petrology, v. 19, p. 393-436.
- WOOD, D. A., GIBSON, I. L., and THOMPSON, R. N., 1976. Elemental mobility during zeolite facies metamorphism of the Tertiary basalts of eastern Iceland. Contr. Miner. Petrology, v. 55, p. 241-254.
- WOODLAND, A. W., 1938. Petrological studies in the Harlech Grit Series of Merionethshire. I. Metamorphic changes in the mudstones of the Manganese Shale Group. Geol. Mag., v. 75, p. 366-382.

- WRIGHT, T. L., 1974. Presentation and interpretation of chemical data for igneous rocks. *Contr. Miner. Petrology*, v. 48, p. 233-248.
- WRIGHT, T. L., and DOHERTY, P. C., 1970. A linear programming and least squares computer method for solving petrologic mixing problems. *Geol. Soc. Am. Bull.*, v. 81, p. 1995-2008.
- YAGI, K., and ONUMA, K., 1967. The join  $\text{CaMgSi}_2\text{O}_6$ - $\text{CaTiAl}_2\text{O}_6$  and its bearing on the titanaugites. *J. Fac. Sci. Hokkaido Univ. Ser. IV*, v. 13, p. 463-483.
- YODER, H. S., 1967. Spilites and serpentinites. *Carnegie Inst. Washington Year Book*, v. 65, p. 269-279.
- YODER, H. S. Jr., and TILLEY, C. E., 1962. Origin of basalt magmas: an experimental study of natural and synthetic rock systems. *J. Petrology*, v. 3, p. 342-532.
- ZEN, E-An., 1974. Prehnite- and pumpellyite-bearing mineral assemblages, west side of Appalachian metamorphic belt, Pennsylvania to Newfoundland. *J. Petrology*, v. 15, p. 197-242.



Sketch map of the Strumble Head-Fishguard region, showing localities described in the text.

